Generation and characterisation of human embryonic stem cells deficient in ZDHHC8, a gene deleted in 22q11.2 deletion syndrome

Thesis submitted for the degree of Doctor of Philosophy

School of Medicine, Cardiff University

2017

Matthieu TRIGANO

DECLARATION

This work has not been submitted in substance for any other degree or award at this or any other university or place of learning, nor is being submitted concurrently in candidature for any degree or other award.

Signed …….. (candidate) Date ……..……

STATEMENT 1

This thesis is being submitted in partial fulfilment of the requirements for the degree of PhD

Signed …….. (candidate) Date ……..……

STATEMENT 2

This thesis is the result of my own independent work/investigation, except where otherwise stated, and the thesis has not been edited by a third party beyond what is permitted by Cardiff University's Policy on the Use of Third Party Editors by Research Degree Students. Other sources are acknowledged by explicit references. The views expressed are my own.

Signed …….. (candidate) Date ……..……

STATEMENT 3

I hereby give consent for my thesis, if accepted, to be available online in the University's Open Access repository and for inter-library loan, and for the title and summary to be made available to outside organisations.

Signed …….. (candidate) Date ……..……

STATEMENT 4: PREVIOUSLY APPROVED BAR ON ACCESS

I hereby give consent for my thesis, if accepted, to be available online in the University's Open Access repository and for inter-library loans **after expiry of a bar on access previously approved by the Academic Standards & Quality Committee.**

Signed …….. (candidate) Date

….……..……

Je tiens à dédier cette thèse à mon grand-père qui nous a quitté quelque temps seulement après la soumission de ce travail. Merci beaucoup pour ton soutien et tes précieux conseils.

Acknowledgments

First and foremost, I would like to thank my supervisors, Prof Meng Li and Prof Jeremy Hall, for giving me the opportunity and providing me with support and guidance to complete my project in good condition.

I also would like to thank the whole Li lab, but more specifically to Claudia, who taught me the cell culture; Marija, who always gave me help when I needed but also provide me with valuable feedback on my thesis; a great thanks to Dani, without you I'll never have been able to do the transcriptomic analysis in the short time I had left; to Tom, thanks for your advices about many aspect on my thesis, you were always there when I had questions and you've been a great support during these three years; to Will who helped me a lot with MATLAB code but also our interesting conversation; I also would like to thank Aless who performed the experiments that aim to generate the homozygous mutant but also who generates the lentivirus vector.

I also would like to thank the core team and specifically Joanne Morgan who performed the transcriptomic experiment.

I would like to thank my family who has always supported me and without whom I wouldn't be here. To my partner, Audrey, I know it hasn't been easy for you with my mood swings and all my issue with the thesis, but you always supported me, and I am very grateful for that.

Abstract

The 22q11.2 Deletion Syndrome is caused by a deletion on the chromosome 22q11.2. Individuals carrying 22q11.2 deletion have an increased risk to develop schizophrenia and Parkinson disease. However, how this deletion leads to the development of these diseases and the specific role of the individual 22q11.2 genes remains largely unknown. In order to understand the neuronal cell types and developmental stages in which the 22q11.2 genes may function, we investigated the temporal and spatial expression profile of the genes located in the 22q11.2DS by RT-PCR. Human embryonic stem cells (hESCs) was used to generate excitatory projection neurons, cortical interneurons, GABAergic medium spiny neurons (MSN) and dopaminergic neurons. This study revealed that several genes appear to exhibit a specific temporal expression profile. Moreover, another group of genes were found to be preferentially expressed in dopaminergic neural lineage.

Within the 22q11.2 deletion region, ZDHHC8 is an interesting candidate due to its implication in the physiology and morphology of the neurons. I generated a hESCs cellular model carrying a heterozygous deletion of ZDHHC8. These cells can be induced toward cortical projection neuron fate in a comparable temporal kinetics to that of the parental control cells. However, phenotypic characterisation revealed that ZDHHC8 mutation altered the motility and the spontaneous calcium activity in ZDHHC8+/- neurons. Interestingly, transcriptomic analysis of excitatory progenitors identified altered expression of genes regulating calcium activity and axonal growth (motility). Furthermore, this study suggests that ZDHHC8 may also be involved in neuronal development, patterning and synaptic signalling.

In conclusion, this thesis provides further knowledges regarding the expression of the 22q11.2DS genes which would be valuable to guide future studies either in cellular or animal models. Furthermore, this study indicates that ZDHHC8 function is involved in several aspects of neuron development that potentially plays a role in the aetiology of 22q11.2DS.

Table of Contents

List of abbreviations

ADHD	Attention deficit hyperactivity disorder
AP5	2R-amino-5-phosphonovaleric acid
ARVCF	Armadillo repeat gene deleted in Velocardiofacial syndrome
ASD	Autism spectrum disorder
BCL11B	B-Cell CLL/Lymphoma 11B
BDNF	Brain derived neurotrophic factor
BMP	Bone morphogenetic proteins
CDC42	Cell division control protein 42 homolog
cDNA	Complementary DNA
CLDN5	Claudin 5
CNQX	6-cyano-7-nitroquinoxaline-2,3-dione
CNV	Copy number variant
COMT	Catechol-O- methyltransferase
CRIPSR	Clustered Regularly Interspaced Short Palindromic Repeats
DGCR	DiGeorge Syndrome Critical Region
DKK1	Dickkopf1
DMSO	Dimethyl sulfoxide
DPBS	Dulbecco's phosphate-buffered saline
DRD	Dopamine receptor
EDTA	Ethylenediaminetetraacetic acid
FGF8	Fibroblast growth factor 8
FRZ	Frizzled
GABA	γ-aminobutyric acid
GDNF	Glial cell-derived neurotrophic factor
GE	Ganglionic eminence
GO	Gene Ontology
GPCR	G protein–coupled receptor
GRIA	Glutamate Ionotropic Receptor AMPA Type
GRIN	Glutamate ionotropic receptor NMDA type
hESC	Human embryonic stem cells
HIRA	Histone cell cycle regulator
iCas9 hESCs	doxycycline-inducible expression of Cas9

IP	Intermediate progenitor
IPC	Intermediate progenitor cells
iPSC	Induced pluripotent stem cells
ISI	Interspike interval
KEGG	Kyoto Encyclopedia of Genes and Genomes
LCR	Low copy repeats
LGE	Lateral Ganglionic Eminence
LTD	Long term depression
LTP	Long term potentiation
mESC	Mouse embryonic stem cells
MGE	Medial Ganglionic Eminence
mGluR	metabotropic glutamate receptor
min	Minutes
ml	Millilitres
mM	Millimolar
mRNA	Messenger RNA
MSN	Medium spiny neurons
NEC	Neuroepithelial cells
NHEJ	Non-Homologous End Joining
NMDA	N-Methyl-D-aspartic acid
NPC	Neuronal progenitor cells
PCR	Polymerase chain reaction
PRODH	Proline dehydrogenase
PSD-95	Postsynaptic density protein 95
PV	Parvalbumin
RANBP1	RAN Binding Protein 1
RGC	Radial glial cells
rpm	Rotation per minute
RT-PCR	Real-time polymerase chain reaction
SEM	Standard error of mean
SHH	Sonic Hedgehog
SNP	single nucleotide polymorphism
SST	Somatostatin
SVZ	Subventricular zone

TGF-β	Transforming growth factor beta
TH	Tyrosine Hydroxylase
TXNRD2	Thioredoxin reductase 2
UFD1L	Ubiquitin recognition factor in ER associated degradation 1
UQCRC1	Ubiquinol-Cytochrome C Reductase Core Protein I
VGCC	voltage gated calcium channel
VZ	Ventricular zone
ZDHHC8	Zinc Finger DHHC-Type Containing 8

1. General Introduction

1.1. The 22q11.2 deletion syndrome

22q11.2 Deletion Syndrome (22q11.2DS) is a genetic disorder caused by a hemizygous deletion on the long arm (q) of the chromosome 22 (Rump et *al.* 2014). 22q11.2DS is the most common microdeletion in human and the second most common chromosomal disorder after down syndrome (Bassett et *al.* 1999; Swillen et *al.* 2015). Due to the wide range of disorders that arise from this mutation, 22q11.2DS is also known as DiGeorge Syndrome (DGS), Velocardiofacial Syndrome (VCFS) or CATCH-22. Table 1.1 presents a historical background associated with 22q11.2DS.

Table 1-1 Historical overview of the syndromes associated with the 22q11.2 deletion Event From Hendrik Paul De Decker and John Bernard Lawrenson, 2001(De Decker and Lawrenson 2001)

Event	Date
Congenital thymic hypoplasia associated with hypocalcaemia	1959
DiGeorge syndrome described	1992
Takao syndrome described (conotruncal anomaly face syndrome)	1996
Velocardiofacial syndrome described (Shprintzen syndrome)	1978
DiGeorge syndrome speculatively linked to chromosome 22	1981
Partial monosomy of chromosome 22 described	1982
"CATCH-22 syndrome" described	1989
Cayler syndrome associated with del22q11.2	1994

1.1.1. Genetics of 22q11.2DS

1.1.1.1. Prevalence of 22q11.2DS

This disorder is associated with a high prevalence with a range from 1 in 3000 to 1 in 6000 live births, which was estimated by the diagnosis of infants with major birth defects (Driscoll et *al.* 1993; Goodship et *al.* 1998).The disease occurs as a *de novo* mutation in 90% of the patients while it is inherited in an autosomal fashion in the remaining 22q11.2DS individuals (Carlson et *al.* 1997; Karayiorgou et *al.* 1995).

1.1.1.2. Causes of 22q11.2DS

The 22q11.2 region is unstable due to the presence of low copy repeats (LCRs). Sequence analysis of the chromosome 22 has identified four LCRs in the 3Mb deletion from LCRs A-D (Shaikh et al. 2000). These LCRs have high similarity with DNA sequences that

span other regions in the chromosome 22 which result in non-allelic crossing also called non-allelic homologous recombination (NAHR) (Colnaghi et al. 2011; L Edelmann, Pandita, and Morrow 1999). NAHRs occur during meiosis and in the case of 22q11.2 results in the appearance of copy number variant (CNV).

It was estimated that around 90% of the 22q11.2 deletion carriers have a 3Mb deletion between LCRA and D, 8% are carrying a 1.5Mb deletion between LCRA and B while the remaining 2% are carrying rare deletion that overlap the typical region (Shaikh et al. 2000).

The 3Mb deletion region contains around 46 proteins coding genes and about 90 known or predicted genes for pseudogenes and non-coding RNAs, including 7 microRNAs, MIR185, MIR1306, MIR1286, MIR3618, MIR 649, MIR4761 and MIR6816. Conversely, the 1.5Mb deletion contains around 29 proteins coding genes (McDonald-McGinn et al. 2015). Strikingly, it was demonstrated that the 1.5Mb deletion was able to recapitulate the phenotype observed in patients with the 3Mb deletion.

1.1.2. Clinical manifestations of 22q11.2DS

The clinical expression of the 22q11.2DS is extremely wide, more than 180 phenotypic representation have already been found (Demily et *al.* 2015) (Figure 1.1). The classical features include congenital heart defects, facial anomalies such as cleft palate, speech and learning difficulties and many others (Digilio et *al.* 2005). Interestingly, while the prevalence of schizophrenia in the general population is about 1%, it was shown to be about 30% in patients with 22q11.2DS, which makes this disorder the most frequent known cause of schizophrenia (Chow et *al*. 2011; Gambini 2016; Schneider et *al.* 2014). Other neuropsychiatric pathologies associated with 22q11.2DS are ASD, attention deficit hyperactivity disorder (ADHD), affective anxiety and obsessive-compulsive disorders.

In addition, it was recently reported that, at 37.10%, ADHD was the most frequent diagnosis in children with 22q11.2DS followed by ASD and schizophrenia at 12.77% and 1.97%, respectively. Conversely, at adulthood the proportion of patients with ADHD drop at 15.59% while it remains relatively constant for 22q11.2 patients with ASD at 16.10%. However, 22q11DS patients with schizophrenia drastically increase in adulthood to reach in some study 42% (Schneider et *al.* 2014).

Although these patients have higher susceptibility to develop psychosis, the mechanism by which the 22q11.2DS elevates the risk for the psychotic disorders mentioned above remains largely unknown. Nevertheless, several hypotheses might be able to explain these genetic variabilities such as 1) the breakpoint heterogeneity which corresponds to the region of the LCRs, 2) the allelic variation, 3) the multiple hit model (Jonas et *al.* 2014). The multiple hit model suggests that patients with 22q11.2DS will develop schizophrenia due to the presence of additional CNVs at other locations on the genome (Bassett et *al.* 2017; Hywel et *al.* 2013).

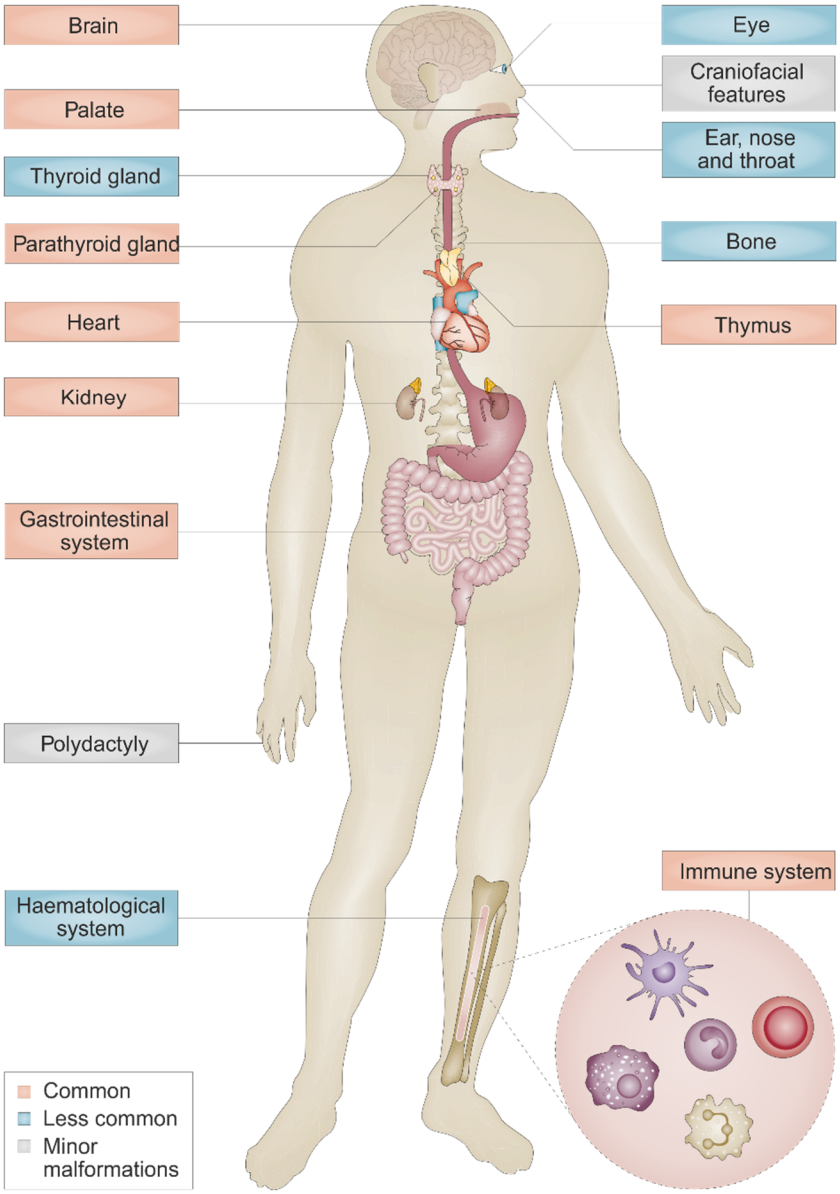

Figure 1-1 Organs affected in 22q11.2 deletion syndrome. In orange are the organs commonly affected in 22q11.2DS. In blue are the organs less affected and in grey are the minor malformation observed in patients. This schematic shows that the brain, palate, parathyroid gland, heart, kidney, gastrointestinal system, thymus and immune system are the organs commonly affected in individuals with 22q11.2DS. Less frequently, organs such as the thyroid gland, the haematological system, the eyes, the ear nose and throat and bone are affected. While minor malformation can affect the craniofacial features and also result to polydactyly in patients with 22q11.2DS. Figure adapted with permission from Springer: Nature reviews. Disease primers, McDonald-McGinn 2015 (4271450447971) Copyright (2015)

Schizophrenia

Schizophrenia is a neuropsychiatric disorder with an onset at late adolescence and early adulthood. Clinically, schizophrenia is characterized by symptoms usually classified as positive, negative and cognitive. The positive symptoms are typically associated with the psychotic symptoms (delusion, hallucination) and tend to relapse and remit. These symptoms result from an increase in the dopamine D2 receptor activation (Walter et *al.* 2009). The negative symptoms are generally chronic and associated with a decrease in motivation and social withdrawal and conversely to the positive symptoms, are due to a reduction in the activation of the dopamine D1 receptor (Walter et *al.* 2009). On the other hand, cognitive symptoms include an impairment in memory performance, attention as well as poor language ability (Moyer, Shelton, and Sweet 2015).

The dopamine hypothesis arose from the study of Jean Dealy and Pierre Deiner in 1952 in which they studied the chlorpromazine and its antipsychotic effects (Delay et *al.*, 1952). Therefore, the dopamine hypothesis stated a hyperactive dopamine transmission as the pathophysiology of schizophrenia. Because the antipsychotic drugs act on the dopamine D2 receptor, they are able to alleviate partly the positive and negative symptoms. However, post mortem examination were unable to provide evidence of an alteration of the dopamine levels or dopamine receptors, therefore it was proposed that the dopaminergic overactivity was secondary to the change of other neuronal systems (Coyle 2004; Knable et *al.* 1994). A new hypothesis, the glutamatergic hypothesis is based on the ability of anaesthetics phencyclidine (PCP) but also the ketamine to bind to N-methyl-D-aspartate (NMDA) receptors and induces schizophrenia like symptoms in healthy subjects while it worsen the positive symptoms in schizophrenic patients (Lahti et *al.* 1995; LUBY et *al.* 1962).

Thereby, the glutamate hypothesis asserts that in the cortico-striatal projection, the glutamate hypofunction produces an increase in the sensory input through facilitation of the thalamocortical circuit and thus increases the dopaminergic input (Lang et *al.* 2007). In addition to this assumption, there are the global disinhibition of the cerebral cortex which imply the loss of the tonic regulation by the GABAergic neurons (Lisman et *al.* 2008). Many studies therefore focused on the glutamate hypofunction and more particularly on the decrease inhibition by the GABAergic neurons which were observed to be related to a loss of a specific types of neurons, the parvalbumin interneurons.

1.1.3. Neurobiology of 22q11.2DS

1.1.3.1. Cognitive impairments

Children carrying 22q11.2 mutation are reported to have by average 30 points lower IQ compared to their siblings (Niarchou et *al*. 2014). Children with 22q11.2 mutation usually achieve higher scores in verbal than non-verbal task. These children have mathematical disabilities and have difficulties to compare numbers or to perform calculations (De Smedt et *al.* 2008).

Furthermore, while the ability to understand a speech is usually strong in pre-school, general language delays appears by school age (Gerdes et *al.* 1999; Scherer et *al* 1999). Studies suggest that children have problems at finding and interpreting salient spatial and temporal information, suggesting that they are less able in integrating goal relevant information (Bish et *al.* 2007; Corbetta et *al.* 2002).

Because the attention is thought to be crucial for inhibiting irrelevant information, children with 22q11.2DS are reported to have impaired sensorimotor gating (Brocki et *al.* 2004; Sobin et *al.* 2005). In addition, patients with 22q11.2DS have difficulties in identifying novel auditory stimulus when using the mismatch negativity paradigm (Cheour et *al.* 1997). Finally, children with 22q11.2DS have impaired working memory performance (Wong et *al.* 2014).

1.1.3.2. Neuroanatomical deficits

Given the impairment in cognitive function in patients with 22q11.2DS, there are good reasons to expect anatomical change in these patients. Brain of children with this deletion have a 8-10% reduction in the volume of the posterior and inferior brain regions (Simon et *al*. 2005). These reductions appear to affect white matter to greater extent than grey matter (Simon et *al.* 2005). Furthermore, it is also demonstrated that the total surface area is decreased in 22q11.2DS. On the other hand, the cortical thickness as well as the volume of the corpus callosum is increased in 22q11.2 individuals (Lin et *al.* 2017).

1.1.4. Genes located in the 1.5Mb deletion region

1.1.4.1. DGCR6

Located at the proximal part within the 22q11.2 deletion, DiGeorge Syndrome Critical Region Gene 6 (*DGCR6)* is thought to contribute to the apparition of 22q11.2DS,

however its function is still unclear (Gao et *al.* 2015). *DGCR6* was shown to have similarity with *Gonadal* (*Gdl*), a drosophila melanogaster gene of unknown function. In addition, this gene was shown to be expressed in brain, the neural tube, pharyngeal arches and the nasal process at E11.5 (Edelmann et *al.* 2001; Lindsay et *al.* 1997). DGCR6 protein is a nuclear phosphoprotein expressed in the liver, heart and skeletal muscle (Pfuhl et *al.* 2005). Interestingly, *DGCR6* was suggested to regulate *TBX1*, another gene located within the 1.5Mb deletion. Therefore *DGCR6* is postulated to be responsible for abnormalities such as heart defect which is one of the outcome of *TBX1* dysregulation (Gao et *al.* 2015). Within the brain, a study showed that DGCR6 may interact with $GABA_{B1,}$ a receptor modulating excitatory and inhibitory synapses therefore, *DGCR6* mutation might alter synaptic transmission (Zunner et *al.* 2010).

1.1.4.2. PRODH

The proline dehydrogenase (*PRODH*) is an enzyme located on the inner mitochondrial membrane that catalyses the first step of the proline degradation (Bender et *al.* 2005). In turn the product of this catabolic reaction the Δ-1-pyrroline-5-carboxylate (P5C) is a precursor of glutamate and γ-aminobutyric acid (GABA) (Jacquet et *al.* 2002). In addition to its role in the metabolism of glutamate, proline was also demonstrated to act as a co-agonist for the NMDA receptor (Zwarts et *al.* 2017). *Prodh* was further suggested to potentiate excitatory transmission of pyramidal neurons between different regions of the hippocampus (Cohen et *al.* 1997). *PRODH* deletion has been associated with an increased risk of developing schizophrenia (Willis et *al.* 2008). However a recent study failed to replicate this result and found no association between *PRODH* and the risk to develop schizophrenia (Williams et *al.* 2003). It was demonstrated that patients with 22q11.2DS have an elevated serum level of proline which can be implicated in learning impairment as well as epilepsy and schizoaffective disorders (Karayiorgou et *al.* 2004). Homozygous *Prodh* mice were observed to be viable with normal brain morphology. However behavioural assessment revealed that these mice have a sensory gating deficits (Gogos et *al.* 1999). Finally, it was demonstrated that there is an epistatic interaction between *Prodh* and *catechol-O- methyltransferase* (*Comt*).

1.1.4.3. DGCR2

DGCR2 encodes for a putative adhesion receptor. This gene is also found to be associated with schizophrenia although this result is still controversial has other study found no association with schizophrenia (Shifman et *al.* 2006; Skowronek et *al.* 2006). *DGCR2*

expression is increased in the DLPC of patients with schizophrenia relative to matched controls (Shifman et *al*. 2006). DGCR2 protein is also observed to be weakly expressed in myelinating Schwann cells but strongly expressed in dorsal root ganglia (Spiegel et *al*. 2006).

1.1.4.4. DGCR14

DGCR14 was identified as essential for early embryonic development (Wang et *al*. 2006). In situ hybridization revealed high expression in the embryo from E7 onwards with relatively higher expression in the central nervous system specifically in a sub-region of the pons (Lindsay et *al*. 1998). *DGCR14* is also associated with higher risk to develop schizophrenia in the Chinese Han population (Wang et *al*. 2006).

1.1.4.5. TSSK2

The *Testis-specific serine/threonine protein kinase 2* (*TSSK2*) is predominantly expressed in the testis. This gene was shown to be important for the formation and the function of the sperm cells. Mutation of *Tssk2* was demonstrated to cause infertility which was attributed to an impair of spermatogenesis in humans (Zhang et *al*. 2010). Real-time polymerase chain reaction (RT-PCR) carried out on different human tissue revealed that TSSK2 is also expressed in the fetal brain (Hao et *al*. 2004).

1.1.4.6. GSC2

Goosecoid Homeobox 2 (*gsc2*) was observed to be expressed in the mouse embryo during development (Wakamiya et *al*. 1998). This gene is also suggested to be expressed while neural crest are maturing and differentiating into in the pharyngeal arches (Saint-Jore et *al*. 1998). *Gsc2* was shown to be present during gastrulation at E6.5 therefore suggesting its involvement in axis formation. However knockout for *gsc2* was unable to demonstrate the presence of abnormal axis formation (Wakamiya et *al*. 1998). In addition, at E11 and postnatal day 7 (P7), *Gsc2* was shown to be robustly expressed in the interpeduncular nucleus, a region important for the generation of the hippocampal theta rhythm and also for the control of rapid eye movement (REM) (Funato et *al*. 2010). Although *Gsc2* is suggested to be present during the development its exact role is still unclear in both mouse and human.

1.1.4.7. SLC25A1

The *solute carrier family 25 member 1* (*SLC25A1*) is part of a family of nuclear encoded transporters which are encored in the inner membrane of the mitochondria. SLC25A1

protein promotes the export of citrate from the mitochondria to the cytoplasm which is thought to be crucial for the energy balance in the cell. Recessive *SLC25A1* mutation from unrelated family was demonstrated to be responsible of severe clinical phenotype which in 61% of the cases led to the death of the individual shortly after birth (Chaouch et *al*. 2014). Individuals diagnosed with *SLC25A1* mutation appeared to primarily present neuromuscular junction (NMJ) defect (Chaouch et *al*. 2014). Whole genome sequencing identified that heterozygote of two pathogenic variant of *SLC2AI* might be responsible of agenesis of the corpus callosum due to the loss of activity of the citrate transporter (Edvardson et *al*. 2013). On the other hand, knockdown in the zebrafish of *Slc25a1* was demonstrated to lead to characteristic features observed in 22q11.2DS such as proliferation defect (Napoli et *al*. 2015). Furthermore, *SLC25A1* activity is influenced by two pro-inflammatory factors, the tumor necrosis factor-α (TNFα) and interferon- γ (IFNγ), suggesting that *SLC25A1* might be central for cytokine induced inflammation signals (Infantino et *al*. 2014).

1.1.4.8. CLTCL1

The *clathrin heavy chain like 1* (*CLTCL1*) encodes for the protein CHC22 which was shown to be expressed at various level in fetal tissue. CHC22 was recently demonstrated to be required for endosomal sorting (Esk et *al*. 2010). Furthermore, it was observed that *CLTCL1* was upregulated in the developing brain suggesting that it might be important early in the patterning of the brain, conversely, in postnatal brain the level of the CHC22 protein was observed to be downregulated (Nahorski et *al*. 2015). Interestingly, knockdown of CHC22 in hESCs derived neural crest cells induces neurites outgrowth in neurons precursor cells , therefore it was concluded that the loss of CHC22 is necessary for the development (Nahorski et *al*. 2015).

1.1.4.9. HIRA

Histone cell cycle regulator (*HIRA*), also known as *DGCR1*, regulates cell cycle dependant histone transcription (Magnaghi et *al*. 1998). *Hira* was shown to be expressed in the neural crest during embryogenesis and also to interact with *Pax3*, a transcription factor important during embryonic development. Importantly, homozygous mutation of *hira* occurred to be lethal at E11 emphasizing its possible crucial function during embryogenesis (Roberts et *al*. 2002). Although the role of *HIRA* during development is thought to be important, its implication during early neurogenesis is still unknown. However, it was recently suggested that HIRA modulates the expression of β-catenin

which in turn was demonstrated to regulate neurogenesis through neuronal progenitors proliferation and differentiation (Li et *al.* 2017).

1.1.4.10. MRPL40

The *mitochondrial ribosomal protein L40* (*MRPL40*) encodes for a protein responsible of protein synthesis in the mitochondria (Devaraju et *al.* 2017). Mitochondrial ribosomes are constituted of different subunits, a small 28S and large 39S subunits. Heterozygous mice for *Mrpl40* were observed to alter the mitochondrial permeability transition pore (mPTP) which result in an abnormal control of the mitochondrial calcium at the presynaptic terminals which was shown to impair short-term plasticity. (Figure 1.2).

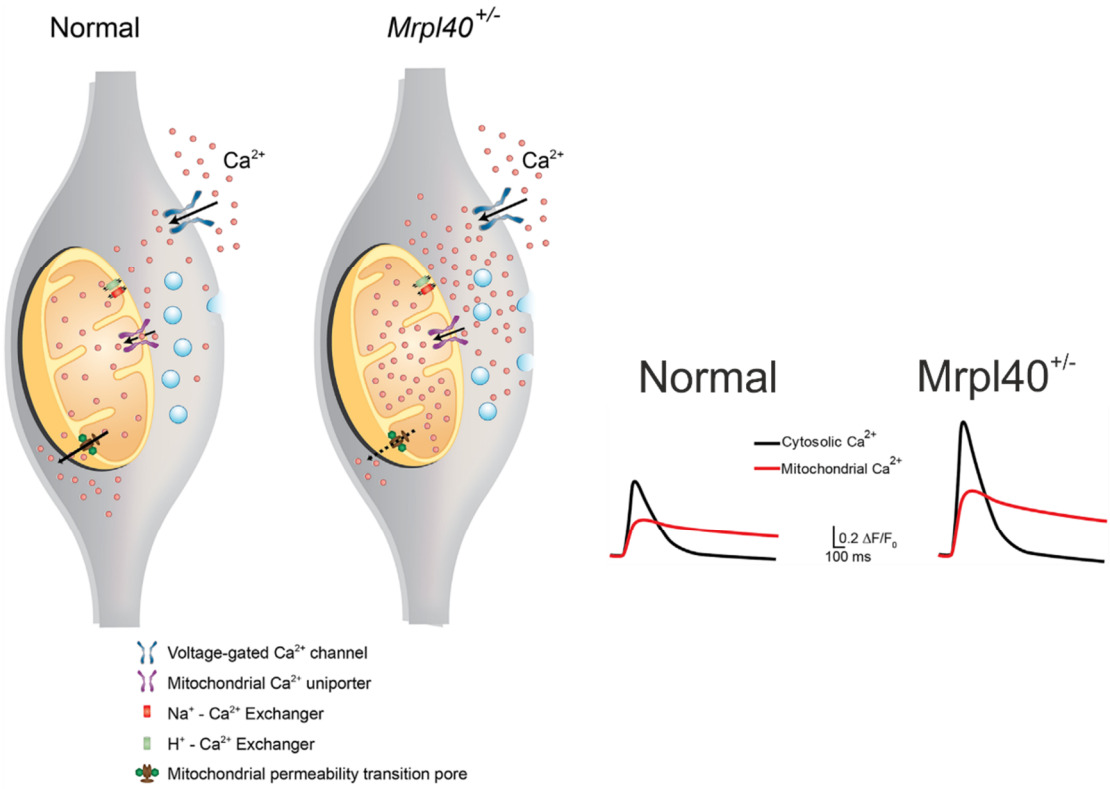

Figure 1-2 Schematic of the calcium dysregulation due to *Mrpl40*+/-. In control , the presynaptic neurons mitochondrial calcium buffering is controlled by mitochondrial uniport, the sodium-calcium and proton-calcium exchanger and also throught slow extrusion from the mitochondrial permeability transition pore. Instead, in the mutant, the slow extrusion from the mitochondrial pore is altered resulting to accumulation of calcium in the mitochondria and the presynpatic neurons, therefore creasting an increase release of vesicle of neurotransmitter. The trace represents the calcium transient in the cytosol and the mitochondira in the control and mutant. Figure adapted with permission from Springer: BioEssays : news and reviews in molecular, cellular and developmental biology, Devaraju 2017 (4296970486895) Copyright (2017).

1.1.4.11. C22ORF39

Chromosome 22 Open Reading Frame 39 (*C22ORF39*) is a protein coding gene however its function remains unknown.

1.1.4.12. UFD1L

Ubiquitin recognition factor in ER associated degradation 1 (*UFD1L*) is expressed by several tissues during embryogenesis, it encodes for a component involved in the degradation of ubiquitin fusion proteins (Mohamed et *al.* 2005). In yeast, UFD1L protein was observed to be important for the ubiquitin dependent proteolytic degradation pathway. Interestingly, mice lacking this gene was shown to die before organogenesis therefore implies an important role for this gene during embryogenesis (Yamagishi et al. 2003). *UFD1L* was also observed to be important for the development of the neural crest cells.

1.1.4.13. CDC45

Cell division cycle 45 (*CDC45*) is necessary for DNA synthesis during genome duplication as it forms the replicative DNA helicase in eukaryotes. CDC45 protein was shown to be expressed in neuronal precursors during brain development (Meechan et *al*. 2015). Although its role in 22q11.2DS appeared to be important especially during cortical development, no study was performed to investigate the function of this gene alone during brain development.

1.1.4.14. CLDN5

Claudin 5 (*CLDN5*) is part of the claudin family composed of about 26 members which are localized at the level of the tight junction (Günzel et *al.* 2013). CLDN5 protein is the most expressed claudin in endothelial tight junction in the vascular endothelium of the brain. Indeed, its defect was responsible for the alteration of the blood brain barrier (BBB), a structure particularly important to restrict the diffusion of molecules to the brain (Irudayanathan et *al*. 2016). Evidences also suggest that this gene may be involved in the vulnerability to schizophrenia (Omidinia et *al.* 2014; Sun et *al.* 2004; Wu et *al.* 2010). Mouse model homozygous for *cldn5* were observed to die at birth. While the BBB of these mice were shown to be unaffected, the selectivity of molecule inferior to 800 Dalton but not larger was affected (Nitta et *al*. 2003).

1.1.4.15. SEPT5

SEPT5 encodes for the protein SEPTIN5, which was originally identify as a GTPases required for cytokinesis. However, it was later demonstrated that SEPTIN5 is robustly expressed in the central nervous system suggesting it might have an additional role than its involvement in the cell cycle (Beites et *al.* 1999). In the mouse brain, SEPT5 was found to be localized at the presynaptic neurons where it binds to syntaxin, a SNARE (soluble NSF attachment protein receptor) protein and thus involved in the exocytosis of neurotransmitter vesicles (Asada et *al.* 2010; Beites et *al.* 1999). Furthermore, SEPT5 was observed to be a substrate of the protein PARKIN, a ring finger protein that is an E3 ubiquitin protein ligase (Choi et *al*. 2003). Mutation in *PARKIN* has been associated with familial Parkinson disease.

1.1.4.16. GP1BB

This gene was demonstrated to be part of the GPIb-V-IX system which composed the receptor for von Willebrand that mediates platelet adhesion in the blood circulation. While the main transcript of this gene is expressed in platelets and megakaryocytes, a smaller and less abundant transcript was observed to be expressed in other tissues such as the brain.

1.1.4.17. TBX1

The T-box transcription factor (*TBX1*) is a member of the family that share a common DNA binding domain, the T-box. *TBX1* was shown to be expressed during embryogenesis primarily in the pharyngeal arches which coincides with the neural crest cells migration (Chieffo et *al*. 1997). *TBX1* homozygous displays important cardiovascular, thymic, craniofacial and parathyroid defects (Ghosh et *al.* 2017; Kispert 2017). Mouse model for *TBX1* exhibits several pathologies related to the heart and facial structure abnormalities. This gene was demonstrated to be responsible of the development of the pharyngeal arch artery during development. Interestingly, the expression of *Tbx1* in the pharyngeal arches was demonstrated to overlap with *Shh* which was shown to regulate *Tbx1* (Garg et *al.* 2001). Surprisingly, a mouse model of *Trp53* which encodes for the protein p53, was demonstrated to be able to rescue the phenotype due to *Tbx1* haploinsufficiency in mice heterozygous for both genes. It was shown that the *Trp53+/-* restored the level of expression of *Gbx2*, a gene requires for aortic arch outflow in *Trp53+/-*, *Tbx1+/-*. It was also recently observed that *Tbx1+/-* mice disrupt corticogenesis due to an early

differentiation of the region that give rise to the somatosensory cortex. In addition, mouse model of *Tbx1+/-* were demonstrated to have PPI alteration.

1.1.4.18. GNB1L

GNB1L or *G Protein Subunit Beta 1 Like* encodes for a protein which contains six WD40 repeats which are known to enable the formation of heterotrimeric or multiprotein complex. This gene was shown to be expressed in the embryonic brain but in less extend in the adult brain (Sun et *al*. 2015). *GNB1L* was suggested to be associated with schizophrenia (Li et *al*. 2011; Williams et *al*. 2008), This gene is also thought to be involved in cell cycle progression, signal transduction, apoptosis and gene regulation.

1.1.4.19. C22ORF29

Chromosome 22 Open Reading Frame 29 (C22ORF39) is a gene coding protein of unknown function.

1.1.4.20. TXNRD2

Thioredoxin reductase 2 (*TXNRD2)* is part of the thioredoxin reductase family which is thought to regulate the cellular redox balance (Soerensen et *al*. 2008). *Txnrd2* encodes for a mitochondrial protein which was observed to be ubiquitously expressed in cells and tissues. The reductase activity depends on the availability of selenium due to the presence of selenocysteine residue onto the TXNRD2 protein. Furthermore, selenium was shown to be strongly retained in the brain thus its deprivation in transgenic mice was responsible to developmental and degenerative damages (Burk et *al*. 2007; Pillai et *al*. 2014). Mice specifically missing *Txnrd2* in the nervous system develop normally and do not display any histopathology alteration and have a similar lifetime than control mice. While its role in the brain is suggested to not be critical, it was demonstrated to be crucial for heart development and function (Conrad et *al*. 2004).

1.1.4.21. COMT

COMT is a key enzyme for modulating the dopamine level in the prefrontal cortex. As dopamine was demonstrated to be important for cognitive function, deficit in *comt* has been associated with psychiatric disorders (J. Chen et *al*. 2004; Tunbridge et *al*. 2007). COMT is a cytosolic enzyme present either in a soluble or membrane bound form, S-COMT or MB-COMT respectively (Harrison et *al*. 2008). Despite homozygous mouse for *Comt* showed normal basal level of dopamine, its clearance was slower suggesting a prolonged phasic activation of dopaminergic receptors. COMT has a functional

polymorphism, a valine substituted by a methionine at the codon 108 in S-COMT and 158 in for the transcript MB-COMT (Lachman et al. 1996). This is resulting to an alteration of the activity of both COMT isoforms.

1.1.4.22. ARVCF

ARVCF encodes for the ARVCF protein (Armadillo repeat gene deleted in Velocardiofacial syndrome). It is a member of the catenin family and was demonstrated to be the closest relative to the p120, a catenin (Mariner, Wang, and Reynolds 2000). The catenin family plays important role in the formation of adherents' junction by facilitating the communication between the inside and outside of cell (Sirotkin et al. 1997). Despite ARVCF is widely expressed, it was demonstrated to be present at very low amount compared to other catenins therefore suggesting that high expression is not necessary for its function or else ARVCF expression is temporally or spatially expressed (Kausalya, Phua, and Hunziker 2004). In addition, ARVCF was observed to be expressed in the ganglionic eminence (GE) during the development suggesting its involvement in cell rearrangement and migration from the GE but also a role in tangential migration towards the cortex (Ulfig and Chan 2004).

1.1.4.23. C22ORF25

Chromosome 22 open reading frame 25 is also known has *TANGO2* (Transport and Golgi organization 2). This protein was suggested to be responsible of the redistribution of the Golgi membrane into the endoplasmic reticulum in drosophila while in mice it was found to have a mitochondrial function (Kremer et al. 2016). Although is function is still unclear it was speculated that TANGO2 deficiency might be associated with an alteration of electron transfer from the FAD-dependant dehydrogenases of the respiratory chain of the mitochondria (Kremer et al. 2016).

1.1.4.24. DGCR8

DGCR8 is an RNA binding protein which is part of the microprocessor complex with Drosha in order to process long primary microRNAs (miRNA) (Petri et al. 2014). Furthermore, miRNA alteration was observed in post-mortem brain samples from individuals with schizophrenia and 22q11.2DS (Fénelon et al. 2011; Moreau et al. 2011). Analysis of heterozygous mice for *Dgcr8* resulted in perturbation of miRNAs expression which were usually reduced by 20-70%. In addition, these mice resulted in smaller

dendritic spines and tree but also exhibited working memory impairment, all of which are features also observed in patients carrying 22q11.2DS (Stark et *al.* 2008).

1.1.4.25. TRMT2A

TRNA Methyltransferase 2 Homolog A (*TRMT2A*) encodes for a protein of unknown function. However, it was suggested to act as a cell cycle regulated protein. Furthermore, this gene was associated with clinical outcome in subset of breast cancer (HER2+) (Hicks et al. 2010; Zhou et *al.* 2002).

1.1.4.26. RANBP1

RAN Binding Protein 1 (*RANBP1*) encodes for a protein responsible of nucleocytoplasmic transport. *RANBP1* messenger RNA (mRNA) was shown to be present throughout the embryo during development (Mangos et *al.* 2001). This protein is part of the Ran family, together with RANBP1, Ran and RCC1 (Regulator of chromosome exchange factor 1) form a complex important for the guidance of the mitotic spindle assembly. Indeed, RANPB1 was demonstrated to stimulate the activity of Ran GTP production which is important for the formation of this trimeric complex. Depletion of RANPB1 exhibited hyperstable spindle microtubules, disorganized microtubule asters and also defective chromosome segregation (Zhang et *al.* 2014). Furthermore, the expression of RANBP1 was shown to be misregulated in cancers (Rensen et al. 2008). In term of influence on the brain, RANBP1 was established as being important during the process of axonal injury. Indeed, upon injury, there is a local translation of RANBP1 creating a retrograde injury signalling that promotes axonal protein synthesis. Thereby RANBP1 perturbation reduces the conditioning of the neurons in response to the lesion (Pathak et *al.* 2016; Yudin et *al.* 2008). Following observation using a 22q11.2 mouse model, Paronett et *al.*, generates a homozygous knockout for *ranbp1*. Although it was demonstrated that 60% of the embryos were exencephalic, the remaining embryos showed alteration in neuronal migration. Indeed, authors observed a decrease of the layer 2/3 of the cortex (Paronett et *al.* 2015). Finally, *RANBP1* was also suggested to play a role in the development of autistic spectrum disorder (ASD) (Wenger et *al.* 2016).

1.1.4.27. ZDHHC8

ZDHHC8 encodes for a palmitoyl transferase that share a DHHC domain, the Zinc Finger DHHC-Type Containing 8 protein (ZDHHC8). This enzyme is responsible of the addition of a 16 carbons fatty acid onto a cysteine residue also known as palmitoylation. This gene

was found to palmitoylate the post synaptic density 95 PSD-95 which is an adaptor protein localised at the postsynaptic neurons (Mukai et *al*. 2015). PSD-95 is the member of the membrane associated guanylate kinase family (MAGUK). This protein is particularly important for neurons as it was demonstrated to be involved in excitatory neurons maturation (El-Husseini et *al*. 2000). Primary culture from both homozygous and heterozygous knockout for *Zdhhc8* were shown to affect dendritic arborisation (Mukai et *al*. 2008). This deficit was demonstrated to also alter the density of glutamatergic synapses which were visualized by a reduction of PSD95 and VGLUT1 puncta. ZDHHC8 deficit was shown to alter both the axonal complexity and the regulation of spine density which was established to be due to a decrease palmitoylation of cdc42palm, a CDC42 variant only expressed in the brain (Moutin et *al*. 2017; Mukai et *al*. 2015). Interestingly, by reintroducing back the full-length ZDHHC8 protein into neurons was able to recover the axonal arborisation and length in *Zdhhc8-/-*(Mukai et *al*. 2015). Furthermore, the lack of dendritic complexity and spine density was also recover upon reintroduction of ZDHHC8 in a mouse model of 22q11.2DS (Mukai et *al*. 2008).

In addition to its role in the morphology of the neurons, ZDHHC8 was also demonstrated to interact with proteins responsible of synaptic transmission. Indeed, AMPA receptor trafficking which are mediated by GRIP1b and PICK1, was altered by ZDHHC5/8 and ZDHHC8 alone respectively (Thomas et *al*. 2012, 2013). Thereby, decrease palmitoylation of PICK1 was demonstrated to impair the induction of the cerebellar long term synaptic depression (LTD) while decrease GRIP1b was observed to alter AMPA receptor trafficking.

Despite, several substrates have already been shown to be associated with ZDHHC8, it remains unknown whether they are targeted by other palmitoyl transferase. However, the Parelemmin-1 protein encoded by the gene *PALM* gene was demonstrated to be only palmitoylated by ZDHHC8 (Huang et *al*. 2009). Furthermore, ankyrin G, a protein highly enriched at the axon initial segment was observed to require to be palmitoylated by ZDHHC5/8. In an experiment, He et *al.*, reported that palmitoylation of ankyrin G by ZDHHC5/8 was necessary to its appropriate targeting to the lateral membrane of MDCK cells (He et *al.* 2014).

Recently, ZDHHC8 was observed to be localized in synaptic mitochondria of glutamatergic neurons (Maynard et *al.* 2008). This study by Maynard et *al.*, also showed the association between ZDHHC8 and Ubiquinol-Cytochrome C Reductase Core Protein I (UQCRC1) using immunofluorescence. UQCRC1 is part of the complex III of the

respiratory chain whose expression was found to be decreased in brain of schizophrenic subjects but increased in individuals with Rett-syndrome and mood disorders (Johnston-Wilson et *al*. 2000; Kriaucionis et *al*. 2006; Prabakaran et *al*. 2004). Furthermore, their study also revealed using immunocytochemistry that ZDHHC8 colocalized with Synaptophysin, a protein localized at the presynaptic site of neuron, although few puncta colocalized with parvalbumin (PV) expressing neurons they preferentially found that ZDHHC8 colocalized in glutamatergic neurons. Surprisingly, the same authors discovered that overexpression of ZDHHC8 in fibroblast was toxic upon transfection therefore leading to cell death which was shown to be likely through apoptosis. This effect was thought to be responsible by the DHHC domain of the protein (Maynard et *al.* 2008).

In addition to its palmitoyl transferase, ZDHHC8 was also identified as a modulator of G2/M phase of the cell cycle in response to DNA damage (Sudo et *al*. 2012).

Mice deficient for *Zdhhc8* were observed to have alteration in sensory gating and also open field behaviour (Mukai et *al*. 2008; Swerdlow et *al*. 2008). Furthermore, this mice were observed to have an alteration in the hippocampal medial prefrontal synchrony which is thought to also be altered in individual with 22q11.2DS (Mukai et *al*. 2015).

This thesis aims to evaluate the function of *ZDHHC8+/-* in glutamatergic neurons at the phenotypic level, and the analysis of the transcriptome of neuronal progenitors heterozygous for *ZDHHC8*.

1.1.4.28. RTN4R

Reticulon 4 receptor is also known as Nogo-66 receptor, a protein encoded by the *RTN4R* gene. RTN4R is a glycosylphosphatidylinositol (GPI)-linked protein highly expressed in the frontal cortex and also localized on the axonal membrane of the pre and post synaptic neurons (Josephson et *al.* 2002; Wang et *al.* 2002). This receptor is a crucial regulator of neurite outgrowth, indeed, the activation of RTN4R leads to the inhiation of a signalling cascade activating RhoA which ultimately inhibits axonal growth (Hsu et *al*. 2007; Sinibaldi et *al.* 2004). In addition, it was also demonstrated as being important for axon regeneration following injury (Hsu et *al*. 2007; Hunt et *al.* 2002).

1.1.4.29. DGCR6L

DGCR6L is a duplicate copy of *DGCR6*, they share 97% similarity, they only differ on only 220 residues (Chakraborty et *al*. 2012). *DGCR6L* encodes a homologous functional

copy of DGCR6, expression study identified that this gene was also expressed in fetal and adult tissue (Lisa Edelmann et al. 2001).

1.1.5. Animals model of 22q11.2DS

Several mouse models were generated to study the 22q11.2DS. The chromosome 16 in mouse harbour a syntenic region of the chromosome 22 except *CLTCL1* (Karayiorgou et *al.* 2010). As presented in Figure 1.3, these mice models of 22q11.2DS harbour different deletions which span various region (Kimber et *al.* 1999; Lindsay et *al.* 2001; Lindsay et *al.* 1999; Merscher et *al.* 2001; Mukai et *al.* 2008; Noritake et *al.* 2009; Stark et *al.* 2008). These models gave a valuable insight into the different aspects of 22q11.2DS. Indeed, they exhibited similar behavioural impairment than those observed in 22q11.2 carriers such as decrease of sensorimotor gating or prepulse inhibition (PPI) (Paylor et *al.* 2006). In addition to behavioural studies, these mice models were found to alter cortical development such as the alteration of the tangential migration of interneurons or the cortical layering which was demonstrated to be altered in 22q11.2DS (Meechan et *al.* 2015).

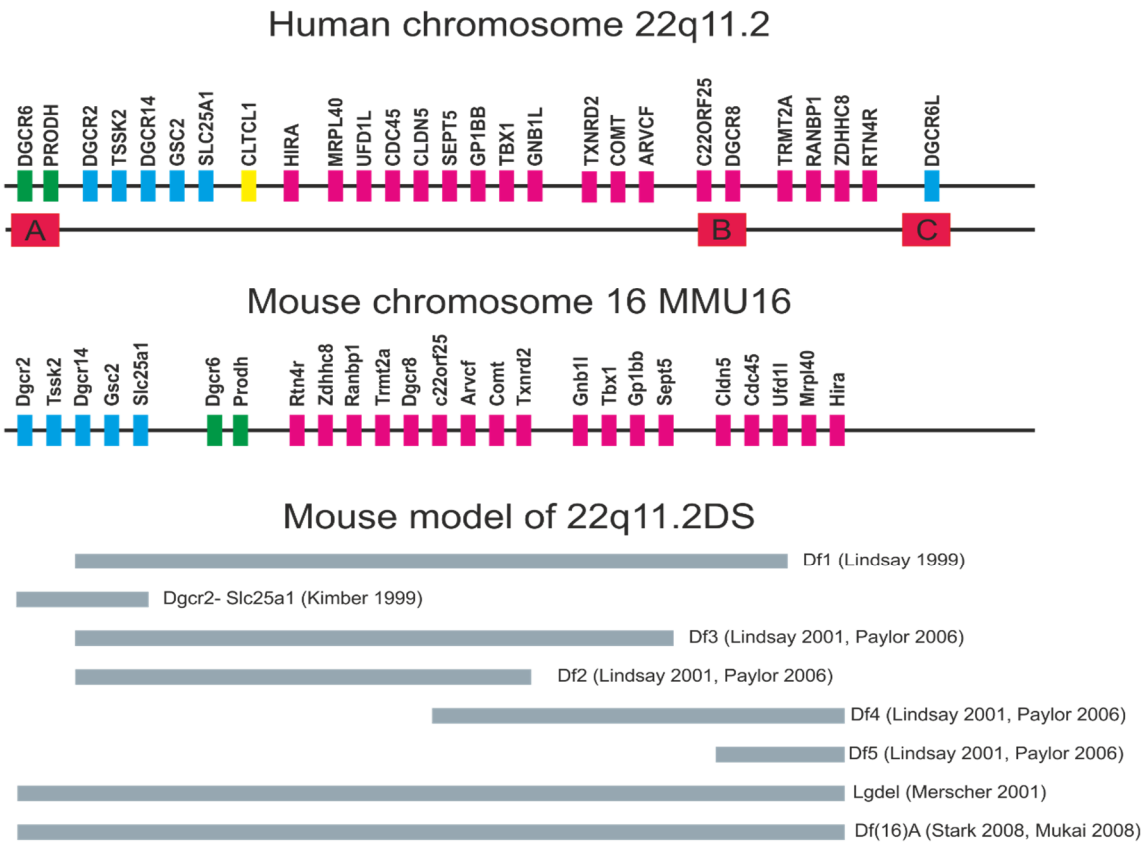

Figure 1.3 Human 1.5Mb deletion of the 22q11.2 region and the syntenic region in mouse (MMU16). Legend on next page

Figure 1-3 Human 1.5Mb deletion of the 22q11.2 region and the syntenic region in mouse (MMU16). The genes are presented in centromeric-telomeric order. This deletion is mediated by the aberrant homologous recombination of the LCRA and C, red rectangles. It is important to note that in the mouse the genes are not displayed in the same order than in human. CLTCL1 and DGCR6L are not present in the mouse (yellow boxes). The genes content of the different mouse models is depicted along with their names. Original figure adapted from Paylor & Lindsay 2006

1.1.6. 22q11.2 Duplication

Because the 22q11.2 region is predisposed to rearrangement due to the presence of multiple LCRs, both deletion and duplication can occur and may be expected in equal proportion. Only few duplications were detected however (Ensenauer et *al*. 2003). Moreover, individuals with 22q11.2 duplication have far less distinct phenotypic characteristics than those carrying the deletion. Therefore, 22q11.2 duplication are usually underdiagnosed (Yobb et *al*. 2005). Surprisingly, in a study that comprised 47005 individuals, in which they were 6882 schizophrenia case and 11255 controls, the CNV analysis revealed that 22q11.2 duplication have a protective effect against the risk to develop schizophrenia (Rees et *al*. 2014). Furthermore, 22q11.2 duplication was absent amongst the schizophrenic cases while they were 10% amongst the controls to have this CNV.

1.2. Brain development

1.2.1. Induction and patterning of the nervous system

During embryonic development, gastrulation results from the formation of the three-layered organization named, endoderm, ectoderm and mesoderm. The inner layer referred as endoderm was observed to form cells such as the lung and pancreatic cells. The middle layer, the endoderm becomes cells such as muscle, cartilage or bone cells. The outer layer also named ectoderm becomes tissues such as the epidermis as well as the nervous system. Experiments from Spemann and Hilde Mangold in which they transplanted the blastopore from an embryo to another resulted to the generation of an entire second axis including brain. Later, they discovered that this region have the capacity to promote neural induction and named the Spemann organizer or organiser (Spemann et *al.* 1924). By transplanting smaller pool of complementary DNA (cDNA) at each of its experiment, Harland managed to isolate the first morphogen NOGGIN (Smith et *al.* 1992). Indeed, in an experiment, embryos treated with UV irradiation therefore making them unable to

develop dorsal part, the injection of NOGGIN mRNA was able to restore the development of the dorsal part of the embryo (Sasai et *al*. 1994). It was later demonstrated that NOGGIN binds with high affinity to BMP2 and BMP4 therefore preventing their interaction with their receptors (Zimmerman et *al.* 1996). CHORDIN, which was isolated by DeRobertis, was demonstrated to have similar characteristics than NOGGIN (Sasai et *al*. 1994). Indeed, CHORDIN binds to BMPs therefore antagonizing the BMP signalling by preventing activation of their receptors (Piccolo et *al.* 1996). Finally, FOLLISTATIN known as activin-binding protein, was shown to be able to bind and inhibit activin therefore is involved in mesoderm differentiation. However, experiments from Hemmati-Brivanlou and Melton showed that a truncated activin receptor which is part of the TGF-β/BMP signalling was able to induce the generation of neurons at the expense of mesodermal tissue (Hemmati-Brivanlou et *al.* 1994). Therefore, FOLLISTATIN was considered as the third neural inducer. Experiments shows that without signal from the organiser, cells secret BMPs and therefore promote ectodermal cells formation. Conversely, the action of these three morphogens promotes the signalling that initiates the formation of the neural plate by inhibiting BMP and TGF-β signalling (Zimmerman et *al.*1996).

The organiser homologous structure in mammals is the node. Both structures are responsible of the simultaneous formation of the neural plate that overlie the notochord, a structure that elongates along the rostrocaudal axis and produces secreted factors in its surrounding therefore providing fate and position information. Soon after these structures form, the neural plate fold to form the neural tube in a process known as neurulation. Along the rostrocaudal and dorsoventral part of the embryo, cells are exposed to different levels of morphogens which are important for their fates. While the rostral part of the neural tube forms the telencephalon, midbrain and hindbrain, the caudal part is responsible of the formation of the spinal cord.

1.2.1.1. WNT signalling

Wnt is part of a family of secreted glycoproteins regulating several cellular behaviours during embryogenesis. Interestingly, several WNT proteins require to be palmitoylated for their function (Willert et *al.* 2003). During the development of the brain, Wnt was shown to be particularly important, the secretion of DKK1 by the organiser is crucial for the patterning of the rostrocaudal axis and the telencephalon. Indeed, DKK1 inhibits the gradient of Wnt at the rostral part of the embryo (Yamaguchi 2001). Experiments in which DKK1 is deleted result to a loss of the rostral structure, more specifically these mice lack

head and brain structure anterior to the hindbrain. Conversely, ectopic expression of DKK1 is observed to be responsible of an enlargement of the head (Mukhopadhyay et *al.* 2001). FrzB another inhibitor of Wnt contains a domain similar to the putative Wnt binding domain of the frizzled receptors. FrzB protein, that is secreted by the organiser, binds to the WNT proteins preventing them from binding to their receptors. It was later demonstrated that FrzB inhibits β-catenin signalling by biding to Wnt1 and Wnt8 which led to the formation of head larger than normal (Leyns et *al*. 1997; S. Wang et *al*. 1997). While these two inhibitors demonstrate the importance of Wnt signalling for the patterning of the rostrocaudal axis, Wnt is also associated with the establishment of the dorsoventral axis. In an experiment, Kelly et *al.*¸ demonstrated that an ectopic expression of β-catenin, a component of Wnt signalling, was associated with the formation of dorsal axis duplication in zebrafish (Ungar et *al.* 1995). In addition, Wnt signalling is also associated with the patterning of the dorsal telencephalon. Thus, overexpression of β-catenin in mouse disrupts the expression of several genes along the dorsoventral axis. Therefore, dorsal genes such as *Pax6* and *Pax7* saw their expression to be expended ventrally at the expense of progenitors with a ventral identity such as *Olig2* or *Nkx6.1*. In addition, inactivating β-catenin demonstrated that Wnt signalling was necessary to preserve dorsal identity by suppressing the expression of ventral genes (Alvarez-Medina et *al*. 2008; Backman et *al.* 2005).

Cerberus is a secreted protein expressed in the anterior endoderm. This protein was shown to inhibit both the Wnt and BMP signalling. Experiment using *Xenopus* demonstrated that Cerberus mRNA injection differs from the three neural inducers in that it induces the formation of an ectopic head but also suppresses posterior mesoderm formation (Shawlot ety *al.* 1998).

While at the neural tube stage Wnt is required for proliferation of progenitors, Wnt genes start to be expressed when the neural tube fold. Once the neural tube is closed, several *Wnt* can be detected: *Wnt1*, *Wnt3*, *Wnt3A*, *Wnt4* and *Wnt7b* are expressed in the dorsal region while *Wnt5a* and *Wnt7a* are in the ventral region (Gunhaga et *al*. 2003; Harrison-Uy et *al.* 2012).

Wnt signalling is composed of three main intracellular signalling, the canonical or WNT/β-catenin pathway, the planar cell polarity pathway and the WNT/Calcium pathway. The canonical WNT pathway involves WNT to bind its receptor Frizzled a seven-transmembrane protein that interacts with its coreceptors the low-density lipoprotein receptor related protein 5 and 6 (LRP5, 6). These coreceptors are crucial for

the canonical pathway signalling. Upon activation by WNT, the Dishevelled (DVL) is activated and induced the disassembly of the destruction complex composed of AXIN, adenomatous polyposis coli (APC) and glycogen synthase kinase 3 β (GSK3β) therefore allowing the β-catenin to be translocated into the cytoplasm and activate the target of WNT. On the other hand, in absence of WNT, β-catenin is phosphorylated by GSK3-β and therefore results to the degradation of β-catenin by the proteasome. The planar cell polarity pathway, activation of DVL induces Rho GTPases and JNK which are responsible of tissue polarity and dendritogenesis through cytoskeleton changes (Habas, Dawid et *al.* 2003). Finally, upon binding of WNT to frizzled, DVL induces calcium influx from the endoplasmic reticulum that activates the protein kinase C (PKC) as well as the calcium/calmodulin dependant kinase II (CaMKII).

1.2.1.2. Sonic Hedgehog (SHH) signalling

SHH is a protein part the Hedgehog family that is secreted by the notochord (Placzek et *al.* 1991). SHH expression is concomitant with the notochord and therefore extend from the caudal part to the rostral part of the head. While the expression of SHH in mouse and fish was observed to precede its initial expression by the floor plate, its expression in the chick coincides in the floor plate and notochord. In vivo, SHH was demonstrated to be important for telencephalic patterning and more specifically for the ventral patterning of the telencephalon. While embryos lacking SHH do not develop ventral telencephalon, ectopic expression results in the expression of floor plate markers, thus markers of ventral identity (Gaiano et *al.* 1999; Johnson et *al.* 1994). An SHH signalling gradient is necessary for the generation of different neurons type along the dorsoventral axis. Thereby, SHH along the dorsoventral axis is capable to direct different cell fates at different concentration thresholds.

Upon release from the notochord, SHH binds to its receptor Pached (PTC) and relieves the repression of the receptor on Smoothened (SMO) therefore avoids GLI truncation by inhibiting the protein kinase A. GLI proteins can then promote or repress the transcription of specific target genes (Le Dréau and Martí 2012). Conversely, in absence of SHH, the activity of SMO is inhibited by PTC. The GLI family are downstream of the SHH signalling. The GLI family is composed of three members, GLI1, GLI2 and GLI3 that are expressed in the neural tube. An incorrect expression of GLI1 mimics SHH signalling such as the induction of the floor plate but also dopaminergic and serotoninergic markers in the dorsal midbrain and hindbrain (Hynes et *al.* 1997). GLI2, that is expressed along the dorsoventral axis in the neural tube, is suggested to cooperate with GLI1 to control

cell fate (Hynes et *al*. 1997). Interestingly, GLI3 is repressed by SHH. Indeed, the gradient of GLI3 is higher in the dorsal telencephalon where the SHH gradient is the weakest (Rallu et *al.* 2002).

1.2.1.3. The transforming growth factor beta (TGF-β) signalling

TGF-β is a large family of proteins composed of two subfamilies, TGF-β, Activin and Nodal family and the bone morphogenetic proteins (BMPs) and growth and differentiation factors (GDFs) family. These proteins were demonstrated to be responsible of cell proliferation but also differentiation and cell migration.

In addition to its antagonizing role on Wnt signalling, Cerberus also inhibits nodal. Nodal is important for the formation of the floor plate thus its loss result to *Cyclop* mutant that involves an absence of the floor plate therefore resulting to important alteration of ventral forebrain development.

As previously mentioned, inhibition of the BMP signalling, mainly BMP4 by the three neural inducers is crucial for neural induction (Piccolo et *al*. 1996; Zimmerman et *al.* 1996). Experiments aiming to silence BMP2, BMP4 and BMP7 identified that the strongest dorsalization phenotype was achieved by BMP4. Furthermore, complete inactivation of these three BMPs causes complete neuralization of the ectoderm in *Xenopus*, interestingly, their reintroductions in the same embryo result to restoration of epidermal patterning (Reversade et *al.* 2005). Early during the development, the expression of NOGGIN and CHORDIN by the organiser is regulated by β-catenin which reduces BMP4 expression.

The TGF-β receptors family is composed of type I and II receptors serine threonine kinase. Upon binding of TGF-β onto its receptors, this one is phosphorylated which in turn induces the phosphorylation of the receptors activated smads (R-SMADs). Subsequently, R-SMADs form a complex with SMAD4 which is translocated into the nucleus to regulate the transcription of target genes (Derynck et *al.* 2003). R-SMADs activation through type I receptors kinase were observed to be inhibited by SMAD6 or SMAD7. SMAD6 and 7 acts by binding to the receptor therefore preventing its phosphorylation and subsequent recruitment of R-SMADs.

BMPs are secreted by the roof plate, they are important for the dorsoventral patterning of the neural tube. BMP concentration dependant mechanism is high at the dorsal part and

weak in the ventral neural tube which is in opposition with SHH thus the two-signalling pathways antagonised one another.

In vitro, it was demonstrated that the complex, TGF-β/Nodal/activin signalling was important for the pluripotency in hESCs. Thus, its inhibition was shown to induce neuroectodermal fate. Thereby in undifferentiated cells, TGF-β/Nodal/Activin are activated through SMAD2 and SMAD3 (James et al. 2005).

In this thesis, the action of NOGGIN, CHORDIN an FOLLISTATIN is mimicked in vitro by the action of the small molecule LDN193189 and SB431542 that allow the neuronal conversion of our hESCs and iPSCs culture.

1.2.2. Cerebral cortex development

During embryogenesis, the developing forebrain is divided into prosomeres along the rostrocaudal axis. The prosomere 1 is next to the mesencephalon, prosomere 2 and 3 divide the diencephalon while prosomere 4, 5 and 6 divide the telencephalon (Puelles et *al.* 2003).

The vertebrate forebrain is divided along the dorsoventral axis into the subpallial and pallial. While the pallium generates the cerebral cortex, the subpallium is composed of the GE, the lateral, medial and caudal ganglionic eminence (LGE, MGE and CGE). Therefore, the pallial and subpallial boundary, at the level of the LGE, coincides with the expression of *Pax6* dorsally and *Dlx1/2* as well as *Gsx2* ventrally. *Pax6* and *Dlx1/2* were shown to have complementary effect for the patterning of the forebrain (Yun et *al.* 2001). Due to the dorsoventral gradient of SHH, it was suggested that SHH could be responsible of the distinction between the LGE and MGE. The transcription factor, NKX2.1 is highly expressed in the MGE and give rise to cortical interneurons and striatal interneurons.

The brain is constituted of different neuronal population which are dispersed in different brain area. The most documented has been the cortical neurogenesis. The mammalian neocortex is composed of two classes of cortical neurons, the interneurons and the glutamatergic neurons which respectively makes local connection and extend axons either intracortical or to other part of the brain (Molyneaux et *al.* 2007).

1.2.2.1. Cortical Interneurons generation

Cortical interneurons release as neurotransmitter GABA, they are originated from the MGE in the subpallium (Molyneaux et *al*. 2007). Upon generation, these neurons expressed the transcriptional marker NKX2.1 whose expression is activated by SHH. However, reduction of SHH signalling was shown to reduce the proportion of NKX2.1 progenitors. In addition, mutant mice for *Nkx2*.1 exhibit a 50% reduction of cortical interneurons. Furthermore, it was observed that the MGE transforms into LGE. Interestingly, in interneurons migrating to the striatum the expression of NKX2.1 is maintained while it is downregulated for interneurons of the cortex.

The MGE primarily gives rise to PV and somatostatin interneurons (SST) whose fate depend upon the level of Shh, indeed, it was demonstrated that high level of SHH preferentially give rise to SST expressing neurons (Kelsom et *al.* 2013; Xu et *al.* 2005). These cells are then migrating tangentially in order to populate the pallium. During tangential migration, the interneurons precursors are expressing LHX6 (Figure 1.4). In mouse deficient for *LHX6*, interneurons were still shown to properly populate the pallium, however they did not express either PV or SST, while on the other hand, an increase of interneurons expressing neuropeptide Y (NPY) was observed. NPY expressing interneurons is another class of cells originating from the MGE. Once interneurons progenitors achieve their tangential migration in the pallium, they switched to radial migration and move towards the appropriate cortical layer within the cortical plate.

Another transcription factor, *SOX6* which is expressed by the MGE was shown to be important together with *LHX6* for the specification of PV and SST neurons. Mice deficient for *sox6* exhibit a strong reduction of SST neurons while PV neurons were absent (Azim et *al.* 2009; Batista-Brito et *al*. 2009).

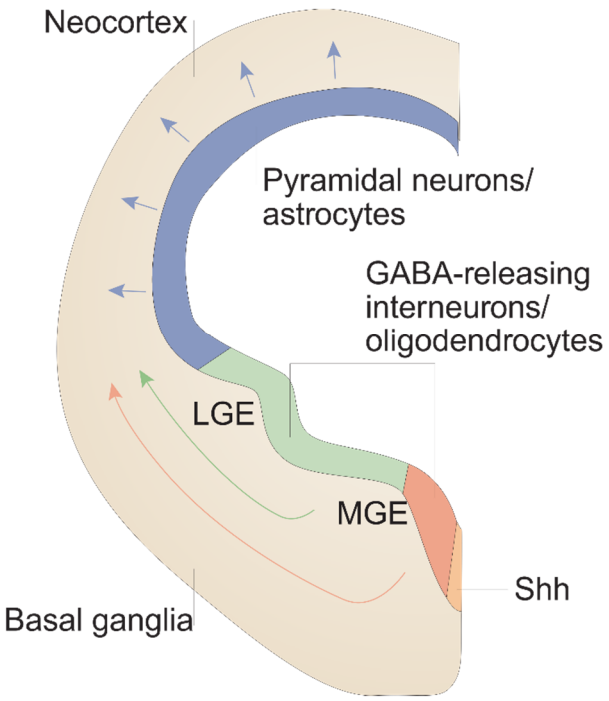

Figure 1-4 Different migration route for pyramidal or cortical interneurons. Cortical interneurons origninating from the MGE tangetially migrate towards the neocortex together with cells from the LGE respectively in orange and green. Conversely, pyramidal neurons generated in the ventricular zone of the developing pallium are migrating radially to populate the different cortical layer of the neocortex. Figure adapted with permission from Springer: Nature reviews. Neuroscience, Rowitch 2004 (4296970336434) Copyright (2004).

1.2.2.2. Cortical excitatory neurons generation

Cortical projection neurons originate from the lumen of the pallium, a region called the ventricular zone (VZ) and also from an additional proliferative layer above the VZ called the subventricular zone (SVZ). There are three different types of progenitor's present in the developing cortex, the neuroepithelial cells (NEC), the radial glial cells (RGC) and the intermediate progenitors (IP) (Figure 1.5). Initially, division is symmetrical, one NEC give rise to two NEC, this step is important to expand the proportion of multipotent cells. A transition from NEC into RGC appears following the expression of bHLH (basic helix loop helix) transcription factor form Hes (hairy/enhancer of split) family together with Fgf10 (Hatakeyama et *al*. 2004; Sahara et *al.* 2009). This transition was also observed to be dependant of Notch signalling, indeed upon binding of delta localized on a neighbouring cell to the Notch receptors, it leads to the release of the intracellular part of Notch, named Notch-ICD which once translocated into the nucleus promotes the transcription of the Hes genes (Pierfelice et *al.* 2011). The RGC have long process that extend from the ventricular wall to the pial surface. In addition to their role in the neurogenesis, RGC were also demonstrated to be important to guide neurons into their final cortical layers. At the beginning of the corticogenesis, RGCs from the VZ divide symmetrically in order to expand their population. On the other hand, at the onset of the neurogenesis, the RGCs divide asymmetrical following different modes which can be 1)

a neurogenic division which results in a self-renewing RGC and a neuron, 2) an asymmetric progenitor division of a RGC into an IP or basal radial glial cells (bRGC) and a self-renewing RGC and finally 3) gliogenic division that corresponds to the division of a RGC into a neuron and an astroglia which will be translocated away from the VZ (Kriegstein et *al.* 2006; Noctor et *al.* 2004). Additionally, another subdivision of the pallium called the outer SVZ which is absent from mouse is populated by the bRGC (Hansen et *al.* 2010). During the asymmetrical division, the bRGC can divide into a self-renewing bRGC and an IP.

Neurons constituting the cortex were shown to radially migrate in the developing cortex. The earliest neurons constitute the preplate and then further neurons constitute the cortical plate which split the preplate into the marginal zone also known as the layer I and the subplate which is localized below the layer VI. The cortex is composed of 6 layers which are generated in an inside-out manner. Thus, the early neurons are populated the deep layer (layer VI and V) while the late neurons are migrating to the upper layer (layer IV and II/III).

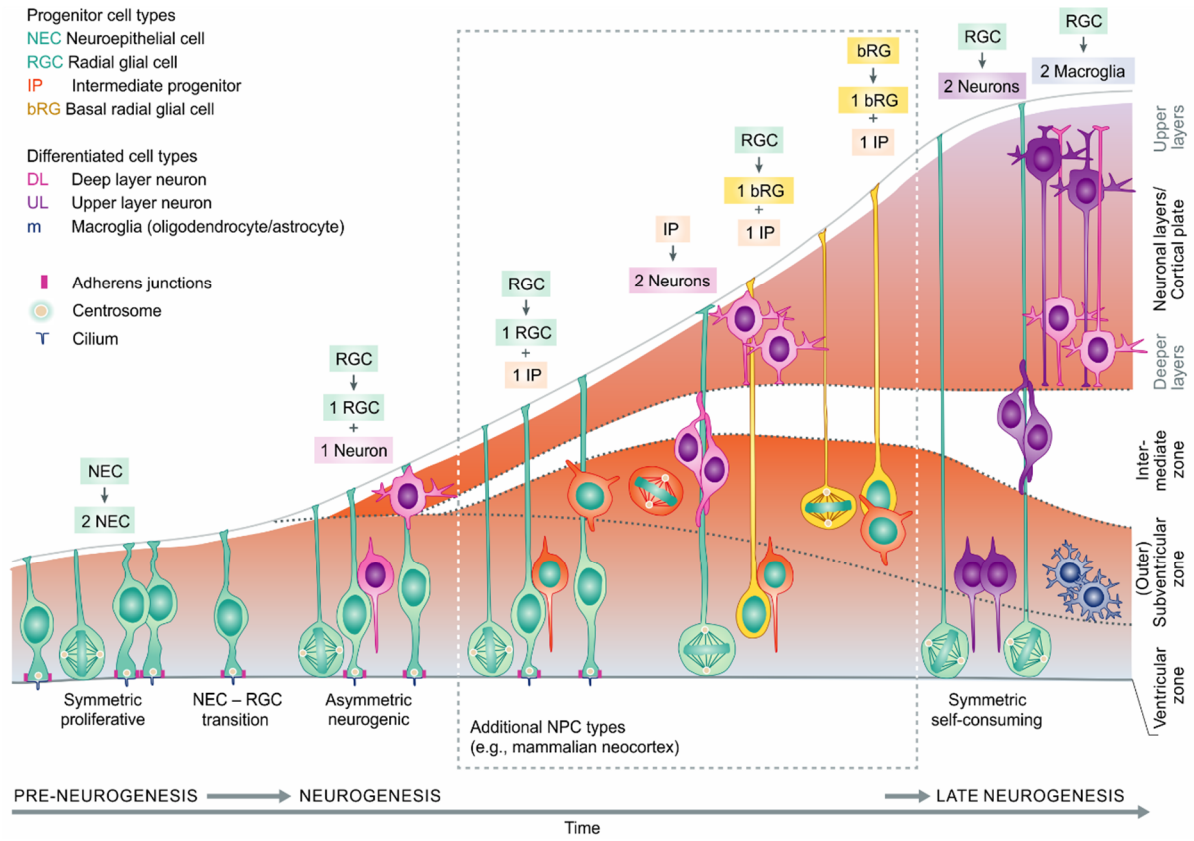

Figure 1-5 Overview of the cortical neurogenesis. The principal types of NPCs with the progeny they produce are indicated by different colors. Additional NPC types that are typically found in mammalian neocortex are indicated in the box; note that only some of the possible daughter cell outcomes are depicted. Figure adapted with permission from Springer: EMBO reports, Paridaen 2014 (4296970210648) Copyright (2014).

1.3. Disease modelling using pluripotent stem cells

The majority of studies about disease modelling have been performed using animal models or primary tissues. Although rodent primary tissues can be used routinely in laboratory, human primary tissues are limited and do not allow to study early developmental stage of a disease.

Embryonic stem cells (ESCs) have the ability to differentiate into any type of tissues of the human body. Our laboratory has the expertise to differentiate ESCs into the four-main neurons population which are excitatory projection neurons, cortical interneurons, MSN and dopaminergic neurons.

Disease modelling can be achieved either by using the novel CRISPR/Cas9 technique described in detail below or taking advantage of the novel technique of induced pluripotent stem cells (iPSCs) to study polygenic disorder which would be more difficult to generate in vitro.

1.3.1. Pluripotent stem cells

Embryonic stem cells (ESCs) are derived from the inner mass of the embryo. They have the characteristic to possess unlimited self-renewal capabilities and can thus be maintained in culture indefinitely under the right conditions. The maintenance of pluripotency is controlled by essential genes such as *Nanog*, *Oct4* (*Pou5f1*) and *Sox2*

Mouse embryonic stem cells (mESCs) were first used to explore the characteristics of these cells. In culture, mESCs require the addition of myeloid leukaemia inhibitory factor (LIF) to allow their self-renewal and proliferation. Indeed, experiments by Martins et *al.* demonstrated that upon transfer of these cells from feeder layer to gelatin, differentiation occurs (Martin 1981). Later, it was demonstrated that the addition of the recombinant LIF factor to gelatin coated mESC culture was able to maintain the cells into an undifferentiated state (Smith et *al.* 1987). It was also shown that the self-renewal property of LIF factor results from the activation of the transcription factor STAT3 (Niwa et *al.* 1998).

While human embryonic stem cells (hESCs) also originate from the inner mass of the embryo, these cells do not require LIF for self-renewal; instead, support by Fgf2, Nodal and activin is necessary for their self-renewal (Vallier et *al.* 2009). The SMAD2/3 signalling pathway is particularly important for hESC self-renewal. Indeed, SB531542

inhibit SMAD2/3 phosphorylation resulting in decrease expression of *oct3/4* (Laping et *al.* 2002).

Another type of pluripotent stem cells, the induced pluripotent stem cells (iPSCs) were discovered by Yamanaka et al. in 2006. They demonstrated that mouse fibroblasts could be reprogrammed into iPSCs by viral transduction of four transcriptional factors, *Oct3/4*, *Sox2*, *c-Myc* and *Klf4* (K. Takahashi et *al.* 2006). The following year the same authors reported the reprograming of human adult dermal fibroblast into iPSCs using the same four transcriptional factors (K. Takahashi et al. 2007). Figure 1.6 presents the ability of ESCs to differentiation into any types of tissues.

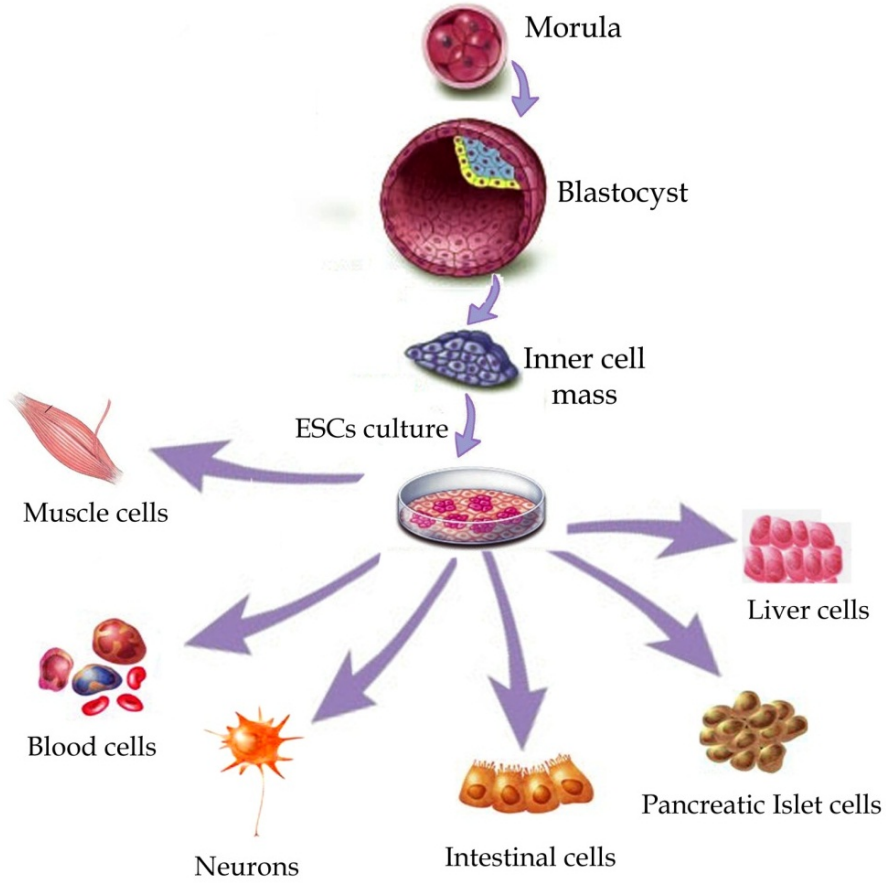

Figure 1-6 ESCs differentiation. Schematic of the potential of embryonic stem cell lines. ESCs are extraceted from the inner mass of the blastocyst. Following various treatment, they can give rise to any cell types such as muscle cells, blood cells, neurons, instestinal cells, pancreatic cells or liver cells. Picture from Meregalli et *al.*(K. Takahashi and Yamanaka 2006)

1.3.2. Genome editing using CRISPR/Cas9

The recent discovery of the CRIPSR/Cas9 technology make it possible to efficiently edit the genome of hESCs. The RNA guided clustered regularly interspaced short palindromic

repeats (CRISPR) contain several short repeats conferring immunity to bacteria and archaea. In addition, the Cas9 in an RNA guided endonuclease cleaving DNA upon recognition of the foreign DNA/RNA therefore confer protection against further infection. The CRISPR/Cas system can be classified into two mains categories which are further classified into six different categories. This classification is based respectively on the presence of multiple or a single protein effector (Cas) which carried out the interference.

The defence mechanism that convey the protection against further posterior infection is divided in three stages, 1) adaptation, 2) crRNA biogenesis and 3) target degradation. The adaptation also called protospacer acquisition enables the host to memorize the unknown genetic material that is subsequently transcribed into a crRNA which is a small guide RNAs. A duplex formed between the crRNA and a tracrRNA (trans activating CRISPR RNA) is then processed by RNase III yielding to the mature small guide RNA that once hybridized to the Cas will confer interference to avoid further infection.

The CRISPR-Cas system as we use it in the laboratory is part of the second family and derived from the bacteria *Streptococcus pyogenes*. The only requirement is a 20 nucleotides guide sequence complementary to the targeted DNA which is immediately preceded by a 5'NGG protospacer adjacent motif (PAM). These three nucleotides sequence are responsible of triggering the transition between target binding and cutting conformation of the Cas9. Upon cleavage by the Cas9, the targeted sequence undergoes one of the two pathways responsible of DNA damage repair, respectively, the error-prone Non-Homologous End Joining (NHEJ) or the high fidelity Homologous Direct Repair (HDR). NHEJ has a higher capacity of repair and cause the introduction of unpredicted insertion or deletion (INDELs) in one or two alleles that can cause frameshift in the protein coding region by the introduction of a premature STOP codon, leading to loss of function mutation. Unlike NHEJ, HDR uses a donor template similar to the targeted regions allowing integration of an exogenous DNA sequence. Although this method is used worldwide as a tool for genome editing, a major drawback is the possibility for the nuclease to cleave off-target DNA targets called off-target mutagenesis. However, the addition of two extra base pair, a guanine, was demonstrated to reduce the off-target effect (Kim et *al*. 2015). This technique was demonstrated to efficiently edit the genome to generate KO in our laboratory. Furthermore, as an example, report demonstrated the generation of hESCs line deficient for DNMT3B (Horii et *al.* 2013). More recently it was also used to correct disease such as Huntington disease or Parkinson disease(Chung et *al.*

2013; X. Xu et al. 2017). Finally, it was reported that CRISPR/Cas9 could also be used for generating microdeletion and microduplication (Tai et *al.* 2016).

1.3.3. HESCs and or iPSCs to study the development of neurons

Due to their ability to give rise to any type of tissue, hESCs and iPSCs (hPSCs) offer a powerful tool to study neuronal development. In vitro differentiation of hPSCs into neurons can be achieved either through embryoid body formation or monolayer differentiation. Cells differentiating as monolayer are exposed to the various exogenous factors relatively uniformly and exhibit more synchronous differentiation than those differentiating in embryoid bodies. Therefore, unless for addressing question that require a 3D structure, such as cortical layer specification, studies in our laboratory use monolayer differentiation as a routine.

Monolayer differentiation was first described by Chambers et *al.*, in which TGF-β and BMP inhibitor was used to convert hPSCs into neurons fate (Chambers et *al.* 2009). The molecule SB431542 (SB) was used to block the phosphorylation of ALK4, ALK5 and ALK7, therefore inhibit SMAD2/3 phosphorylation and thus inhibit the TGFβ/Activin/Nodal pathway. Thereby, dual smad inhibition by noggin and SB was demonstrated to be able to convert hPSCs into neurons. Later, noggin was replaced by LDN193189 (LDN), this molecule inhibits the BMP signalling pathway and was demonstrated in combination with SB to efficiently give rise to PAX6 positive cells, a neuroectodermal marker. Compared to dorsomorphin which is another BMP antagonist, LDN was demonstrated to be less toxic (Surmacz et *al.* 2012). Interestingly, this protocol was demonstrated by default to give rise to neurons from the dorsal telencephalon.

While neuronal conversion of hPSCs preferentially give rise to neurons from the dorsal telencephalon and therefore excitatory projection neurons, it is necessary to add further molecules to promote the generation of others neuronal population.

To generate cortical interneurons, an additional factor is necessary during the neural conversion, XAV939. This small molecule that substitute DKK1 is a WNT signalling inhibitor that simulates the degradation of β-catenin, therefore strongly increases telencephalic commitment and thereby increases the proportion of neural progenitors expressing FOXG1. Time window expression of SHH and its agonist purmorphamine promotes the induction of cells with a ventral identity expressing NKX2.1. Therefore,

progenitors with a MGE identity are expected to express protein such as NKX2.1 and FOXG1 but also OLIG2, a marker of cells originating from the MGE.

Medium spiny neurons (MSN) are primarily GABAergic projection neurons that form the striatum which is one of the nuclei of the basal ganglia. MSN originates from the LGE, a structure of the forebrain. The location of the LGE below the pallium requires the precise concentration of SHH with or without WNT inhibitor. Thereby several experiments over the years investigated the time window and concentration of WNT inhibitor and SHH that would lead to the highest proportion of dopamine and cAMP-regulated neuronal phosphoprotein (DARPP32) positive cells, a MSN marker (Aubry et *al*. 2008; Delli Carri et *al.* 2013; Ma et *al.* 2012; Nicoleau et *al.* 2013). A recent publication from our laboratory reported the generation of MSN using activin A which was demonstrated to promote the generation of neurons with an LGE identity (Arber et *al.* 2015). Therefore, following conversion into neurons, cells require the addition of activin A to obtain an LGE identity which is known to express the transcription factor *GSX2* as well as *CTIP2*.

Compared to the other three neuronal populations previously presented, dopaminergic arise from the ventral midbrain. During development, the midbrain hindbrain boundary (MHB) is formed through the repression of the transcription factor orthodenticle homolog 2 (*OTX2*) and gastrulation brain homeobox 2 (*GBX2*). The patterning of the MHB is regulated by a gradient of *WNT1* and *FGF8* respectively from the midbrain and hindbrain. It was demonstrated that brain explants at distance from the source of FGF8 was able to generate midbrain dopamine neurons (Arenas et *al.* 2015). Therefore, midbrain dopaminergic neurons induction employs both SHH and FGF8.

In this thesis, all these four neuronal types were generated in order to evaluate whether the expression of specific genes differ depending on the neuronal population.

1.3.4. Disease Modelling using iPSC

Since the discovery of iPSCs, it is now possible to study the development of neurons from individuals with genetic background associated with monogenic neurological disorders such as Huntington disease or Amyotrophic lateral sclerosis. In addition, iPSCs are particularly valuable for the study of polygenic disorders such as 22q11.2DS which

results of the haploinsufficiency of more than 30 genes or also diseases with a genetic background not yet identified.

Thereby, Brennand et *al*., report the first study modelling schizophrenia using iPSCs. They demonstrated that neurons from individuals with schizophrenia had an impaired neuronal connectivity using a modified rabies virus (Brennand et *al.* 2011; Wickersham et *al.* 2007). They also observed an alteration of the overall morphology of neurons and identified using transcriptomic analysis novel signaling pathways such as NOTCH signaling that were not previously linked to schizophrenia. Physiological assessment was performed using electrophysiology and calcium imaging, the last one will be further discussion later. This study was the first to report the use of iPSCs to study schizophrenia. However, this study uses iPSCs from patients with idiopathic schizophrenia therefore an heterogenous genetic background, because schizophrenia is a multigenic disorder the results observed in this study might differ between individuals.

Several other studies reported the use of iPSCs from Parkinson disease patients. Schöndorf et *al.*, reported the use of iPSCs from individuals with glucocerebrosidase (*GBA1*) mutation. While homozygous mutation is responsible of Gaucher syndrome, a lysosomal storage disease, heterozygous mutation of *GBA1* is associated with higher risk to develop Parkinson disease. In this study, iPSCs were differentiated into midbrain dopaminergic neurons. The dopaminergic population was further enriched using fluorescence-activated cell sorting. They examined the overall expression of key markers of midbrain dopaminergic neurons differentiation, they also observed lysosomal and autophagic defect in mutant neurons therefore emphasizing that iPSCs can replicate in vivo pathology. In addition, they also observed an impairment of the calcium homeostasis in the neurons with *GBA1* mutation.

Another study from Paşca et *al.*, used fibroblasts from individuals with Timothy syndrome which were reprogramed to obtain iPSCs. This pathology was demonstrated to cause a missense mutation in the L-type calcium channel, *CACNA1C* gene. The study investigates the development of the iPSCs into a protocol of cortical neurons precursors and neurons. They evaluated the calcium activity using Fura 2AM, a radiometric dye able to measure intracellular calcium which allow them identified calcium activity defect in neurons with Timothy syndrome mutation. Furthermore, they also performed single cell q-PCR which identified a decrease expression of lower cortical layer genes.

Several studies also evaluated neurons derived iPSCs from individuals with 22q11.2DS. In their study, Belinsky et al., used two hPSC from individual with 22q11.2DS. Their study investigated the electrophysiological and calcium imaging activity in neurons with a forebrain identify which was compared to a healthy individual. Electrophysiology and calcium imaging activity were performed simultaneously several times from day 13 to 88. No important differences were observed regarding action potential property and frequencies.

However, most study investigating iPSCs from 22q11.2DS primarily focused on transcriptomic analysis such as study from Toyoshima et *al,* as well as Lin et *al,* which investigated the transcriptome of neurons derived from individuals with 22q11.2DS.

Instead of studying the entire 22q11.2 deletion, we aimed to understand the function of one specific gene within this deletion. Therefore, we investigated its role during neuronal development using assays such as calcium imaging to determine whether the physiology of the neurons was altered in our mutant neurons.

1.3.5. Calcium Imaging a technique to assess neuronal activity in neurons derived stem cells

Calcium ion is responsible of many function in cells, such as muscle contraction but it is also involved in several steps of the cell cycles. In neurons, calcium is essential for several functions such as propagation of action potential and acts as second messenger through G protein couple receptors (GPCRs). In resting neurons, calcium concentration varies from 50 to 100nM. However, during electrical activity, this concentration can transiently rise ten or even hundred times higher (Berridge, et *al.* 2000). Overall, the calcium concentration is maintained lower enough at rest to allow a significant change without extensive energy cost during electrical activity. The calcium homeostasis is determined by the calcium efflux and influx (Figure 1.7). Calcium efflux is mediated by the plasma membrane ATPase, the sodium calcium exchanger and the endo/sarcoplasmic reticulum calcium ATPase (SERCA). Instead, the calcium influx is composed of the voltage gated calcium channel (VGCC), the ionotropic receptors (NMDA, AChR, AMPA). Finally, internal storage of calcium can be released through the ryanodine receptor or the inositol 1,4,5-trisphosphate receptor (IP_3).

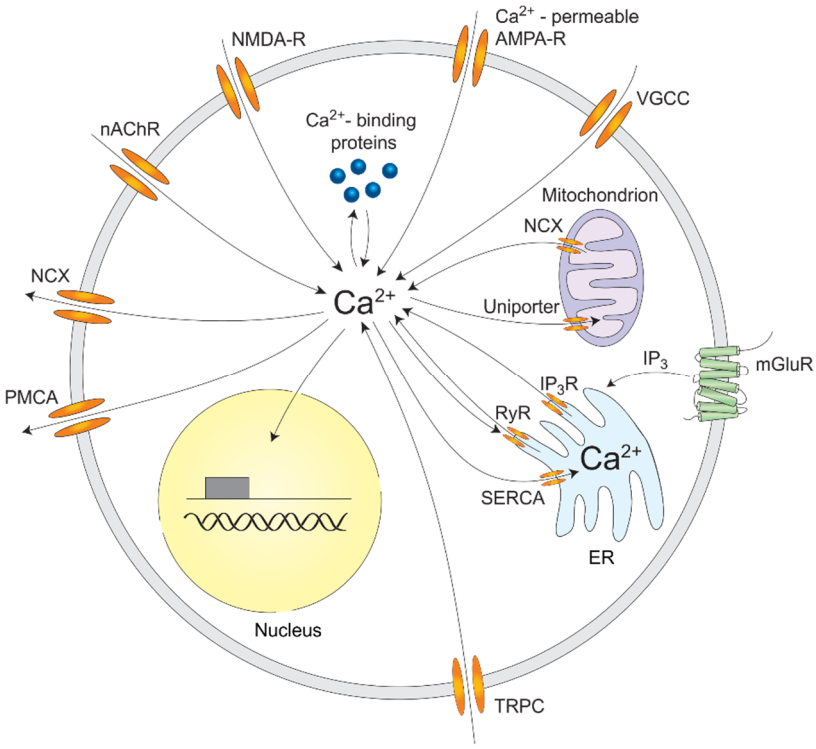

Figure 1-7 Calcium signalling in neurons. Schematic of the neurons depicting the differente available source of calcium. AMPA, NMDA, VGCC, nAChR and TRPC are source of calcium influx. IP3R, RyR are source of calcium released from the internal store. PMCA, NCX and SERCA are source of calcium efflux. Figure adapted with permission from Springer: Neuron, Grienberger 2012 (4296970017957) Copyright (2012).

The process of neurotransmitter release requires the calcium to have a dual role. First the calcium enters axons terminal through the VGCC following depolarization of the plasma membrane. Then the calcium binds to the calcium sensor synaptotagmin which is localized at the surface of the synaptic vesicle. Upon binding, synaptotagmin interact with SNAP25 and synaptobrevin (SNARE protein) which are anchored at the presynaptic membrane and allow the release of the neurotransmitter within the synaptic cleft (Mohrmann et *al.* 2013).

The plasma membrane calcium channel is comprised of four different groups which are composed of calcium influx, the VGCC, the NMDA receptors, the alpha-amino-3-hydroxy-5-methyl-4-isoxazole propionic acid-sensitive receptors (AMPARs). Calcium signalling can further be mediated through GCRPs located on the neurons, the metabotropic glutamate receptors.

Upon depolarization, the VGCCs are important to initiate the calcium signalling cascade. The VGCCs are composed of two main classes based on their thresholds of activation, the high and low voltage activated channel respectively, HVA and LVA (Catterall 2000).

The HVA can be further subdivided into four categories, the L-type composed of the $Ca_v1.1$ to $Ca_v1.4$, the P/Q type ($Ca_v2.1$), the N type ($Ca_v2.2$) and the R type ($Ca_v2.3$). The LVA instead is only composed of the T type ($Ca_v3.1$ to $Ca_v3.3$).

Amongst the L-type calcium channel, the $Ca_v1.2$ is encoded by the *CACNA1C* gene which was shown to be expressed in neuronal cell body and dendrites. This channel permits large influx of calcium that activates pathways necessary for long term potentiation (Benarroch 2010). The $Ca_v1.3$ (*CACNA1D*) is expressed by auditory hair cells (Kollmar et *al.* 1997). Overall the Ca_v1 family is important for synaptic transmission, neurotransmitter release and generation of calcium transient in dendrites (Brini et *al.* 2014).

The Ca_v2 family are present at the presynaptic membrane but also on cell body and dendrites where they are responsible for the fast neurotransmitter releases. The P/Q channel type ($Ca_v2.1$), encoded by *CACNA1A,* is expressed at the excitatory synapses but also by the Purkinje cell from the cerebellum. The N-type channel ($Ca_v2.2$), encoded by *CACNA1B,* is involved in the neurotransmission at the inhibitory neurons, but also noradrenergic and the dorsal root ganglia. Both $Ca_v2.1$ and $Ca_v2.2$ were observed to be regulated through G protein coupled (Hille 1994).

The T type channel corresponding to the LVA channel were demonstrated to be located at the soma as well as the dendrites in most brain region. It was observed that gain of function of the Ca_v3 channel was responsible of epilepsy in human and genetic mouse model (Khosravani et *al.* 2006). This family composed of three channels, $Ca_v3.1$, $Ca_v3.2$ and $Ca_v3.3$ encoded respectively by *CACNA1G*, *CANA1H* and *CANA1I.*

The calcium permeable AMPA receptor is anchored to the postsynaptic membrane. Upon binding of glutamate, different types of ions can enter into the cell through the channels pore. This receptor is responsible of the fast-synaptic transmission. AMPA receptors are permeable to sodium Na^+, potassium K^+ and also in some case calcium and zinc et *al* 2007). The AMPA receptor is an heterotetramer composed of GluA1, GluA2, GluA3 and GluA4 which are encoded by different genes known respectively as, *GRIA1*, *GRIA2*, *GRIA3* and *GRIA4.* It was reported that the AMPA receptor in the brain is mainly in the form of an heteromeric complex composed between GluA1 with GluA2 or GluA2 and GluA3 subunits (Lu et *al.* 2009). Instead, the GluA4 subunit is developmentally regulated and expressed at adult synapse (Lu et *al.* 2009). There are two forms of GluA2 subunit, a

permeable to calcium which can be either GluA2 lacking or unedited GluA2-contaning and a calcium impermeable named edited GluA2-containing. The difference between the unedited and edited is the presence of a glutamine or an arginine respectively on the GluA2 subunit at the 607 amino acids.

The NMDA receptor is localized at the postsynaptic membrane of neurons. The receptor is an heteromeric complex which is composed of either GluN1, GluN2 or GluN3 subunits. Each NMDA receptor contain at least a GluN1 subunit. The GluN2 subunit is subdivided into four, GluN2A, GluN2B, GluN2C and GluN2D. During development, the majority of NMDA receptors are composed of GluN1 and GluN2B subunits, however during postnatal development, there is a switch in subunit composition from GluN2B to GluN2A (Berridge, Lipp, and Bootman 2000). Compared to the AMPA receptor, the NMDA receptor has a high permeability for calcium which usually occur upon triggering of long term potentiation (LTP) or LTD.

Upon release of glutamate by the presynaptic neurons, the neurotransmitter binds to the AMPA receptor. Thus, the channel of the AMPA receptor opens provoking an influx of Na^+ into the postsynaptic neurons which in turn induce depolarization of the postsynaptic membrane. If the depolarization if strong enough, it removes the magnesium block on the NMDA receptor and therefore allows an influx of calcium in the postsynaptic neurons which lead to activation of several molecular pathways (Brini et *al.* 2014).

The metabotropic glutamate receptors (mGluRs) are composed of 7 transmembrane G coupled receptors. The mGluRs are classified into three categories. The group I includes mGluRs 1 and 5 and are mostly expressed at the postsynaptic membrane than the presynaptic membrane of glutamatergic neurons. The group I is couple to G_q/G_{11}, which are responsible of downstream activation of the phospholipase C and therefore induces calcium inside the cells. Often, the function of mGluR1 and mGluR5 are different depending of the neuronal population. The group I also plays an important role in fast synaptic transmission conveyed by glutamate, it also involves in the induction of LTP and LTD (Bellone et *al.* 2008; Kullmann et *al.* 2008). The group II includes the mGluR2 and 3. Conversely to the group I, the group II is couple to $G_{i/o}$ which results in the inhibition of the adenylate cyclase and thus calcium channel. The mGluR2 and mGluR3 are usually found on presynaptic membrane and inhibit neurotransmitter release at both glutamatergic and GABAergic synapses. In addition, the group II of metabotropic receptor can also be localized at the postsynaptic membrane where it induces

hyperpolarization (Muly et *al.* 2007). Also, the mGluR3 was found to be expressed by glial cells.

Finally, the group III of metabotropic receptors is composed of mGluR4, mGluR6, mGluR7 and mGluR8. Similarly to the metabotropic receptors of the group II, the group III is couple with $G_{i/o}$ and thus is also inhibiting calcium channel but also regulates potassium channels. However, it was demonstrated that group III is couple with other signalling pathways than the adenylate cyclase, such as the MAPK or the phosphatidyl inositol 3-kinase (Iacovelli et *al.* 2002). The metabotropic group III was observed to be in similar location than the group II.

Calcium indicator

Several techniques exist to record and evaluate the calcium activity in vivo and in vitro. While most of these techniques involved the loading of the calcium indicator using sharp micropipette during whole cell path clamp recording. It is currently possible to load bulk of neurons either in vivo and in vitro using dye conjugated with acetoxymethyl ester (AM). Once loaded, cells are able to remove the ester because of the presence of intracellular esterase. In addition, new generation of genetically encoded calcium indicators (GCaMP) enable to evaluate calcium activity without injection of a dye. Furthermore, they can be used to target specific neuronal population in vivo.

In this thesis, we used Fluo-4-AM, a dye derived from the Fluo-3. Fluo-4 exhibits brighter dynamic range than Fluo-3 therefore is able to detect smaller change in the calcium activity. The excitation emission of this dye ranges from 494/506 nm respectively and therefore do not necessarily require the use of a confocal microscope.

1.4. Aims

The overall aims of this thesis are:

- To investigate the temporal and spatial expression profile of the genes between LCR A and B of the 22q11.2DS in different neuronal population
- To examine the role of *ZDHHC8* during cortical excitatory projection neurons development.

The thesis is then subdivided into the three following results chapters:

1. The 22q11.2 mutation is composed of a multitude of genes whose function during brain development is not clear yet. Therefore, this study aims to explore whether genes within this mutation revealed a specific temporal and spatial expression profile through the examination of gene expression at different time points and/in different neuronal population (cortical interneurons, glutamatergic projection neurons, dopaminergic neurons and medium spiny neurons). The results would be an indication of the potential underlying function of those genes during brain development which therefore might guide which gene to study in future study.

2. In the chapter 4, I have used the novel CRISPR/Cas9 technique to generate a hESCs line deficient for *ZDHHC8* whose function will further be studied in a protocol of glutamatergic neurons differentiation. The chapter 4 also aims to investigate whether *ZDHHC8* haploinsufficiency alters the kinetics of glutamatergic neuronal differentiation and alters the expression of several key genes necessary for proper neuronal maturation. Moreover, both to elucidate its physiological role during neurons differentiation and due to its association with reduced dendritic and axonal arborisation, the motility and the spontaneous calcium activity was also investigated in neurons derived from hESC heterozygous for *ZDHHC8*.

3. Lastly, the chapter 5 investigates the transcriptome of *ZDHHC8+/-* at the neuronal progenitor level in order to determine whether heterozygous deletion of *ZDHHC8* affects signalling pathways responsible of neurons differentiation and maturation. These results were then compared to the transcriptome of progenitor cells from 22q11.2 derived hiPSC to identify if similar pathways are altered.

.

2. Materials and Methods

2.1. Cell Reprogramming

2.1.1. 22q11.2 patient

The 22q11.2 hiPSC line analysed in this PhD was recruited via clinic assessment at the National Centre for Mental Health by Professor Jeremy Hall. The individual consented to the DEFINE/ECHO and NCMH consent form. The patient is a female of 27 years old who was diagnosed with 22q11.2DS at the age of 14. She is thought to have inherited the 22q11.2 CNV from her mother who also carries a 22q11.2 mutation. She had speech and language delay during her childhood and was diagnosed with dyslexia. She also experienced delayed motor skills development. Her current medication is Aripiprazole 10mg and Fluoxetine 20mg twice a day. In terms of psychiatric disorders, the patient was diagnosed with ASD, intellectual disability as well as schizophrenia.

2.1.2. Control subject

The subject is a 27 years male who has been recruited and agreed to the NCMH participant consent form. The patient did not report any psychiatric disorders. His medical history did not mention any known disease.

2.1.3. Fibroblast reprogramming

A skin biopsy from individuals consenting to take part in the study was performed by a dermatologist and further processed by Craig Joyce. Directly after collection, the biopsy was kept in fibroblast media prior to being plated. The fibroblast media was composed of 90% DMEM (GIBCO), 10% of Fetal Bovine Serum (FBS, GIBCO), 1% of MEM Non-Essential Amino Acids Solution (Life technologies), 10mM and 0.1% of β-mercaptoethanol 55mM (Life technologies). After plating, fibroblasts were grown for a couple of passages and either frozen down or processed for reprogramming.

The CytoTune®- iPS 2.0 Sendai Reprogramming Kit (Life technologies) was used to reprogram the fibroblasts. Two days prior the transduction, the fibroblasts were replated onto two wells of a 6-well plate and kept in the fibroblast media. The day of the transduction, fibroblasts were usually at 50-80% confluency. A volume of fibroblast

medium was pre-warmed prior to harvesting cells. Cells were harvested in 0.5ml of TrypLE™ per 1 well of a 6-well plate and incubated at room temperature until cells started to detach, at which point a double volume of fibroblast medium was added to the cells to inactivate the TrypLE. A portion of cells was taken out to perform cell counts using Trypan Blue exclusion criteria. The volume of virus was calculated using the formula below.

$$\text{Volume of virus (µL)} = \frac{\text{MOI (CIU/cell)} \times \text{number of cells}}{\text{titer of virus (CIU/mL)} \times 10^{-3}\ \text{(µL/mL)}}$$

The MOI for each virus were as follow, hKOS = 5, hcMyc = 5, hKLF4 = 3. The appropriate volume of virus was added to 1ml of fibroblast medium and subsequently added into the wells. The following day, the medium was replaced with fresh solution and then changed every day until the sixth day post transduction. At day 7, a second run of transduction was performed with the hKLF4 virus using similar concentration to that in the first transduction. Fresh medium was replaced every day for the next seven days. On the fourteenth day, iPSCs colonies were picked and replated onto Matrigel coated plates in mTeSR™1 (STEMCELL). After a couple of passages, mTeSR1 was switched to TeSR™-E8™ (STEMCELL).

2.2. Cell culture

All cell cultures were maintained in an incubator (Galaxy 170R, New Brunswick) at 37°C and 5% CO_2. All cell work was performed under a laminar flow hood (Maxisafe 2020, Thermo Scientific). The cells were grown on treated plastic 6-, 12- or 24-well plates (Thermo Scientific) or glass coverslips (VWR).

2.2.1. hESCs and hiPSCs culture

Experiments were carried out using an H7 hESC, iCas9 hESC, 22q11.2 iPSC, and 900 iPSC lines. Cell culture dishes were coated with hESC qualified Matrigel (Corning). An aliquot of Matrigel was resuspended into 6ml of Nutrient Mixture F-12 (DMEM/F12, GIBCO) media then 1ml/well of the solution were added and incubated for at least 1h at 37°C. Cells were maintained in TeSR-E8 medium except where mentioned otherwise. While media was changed every day, cells were passaged as follows once reached 60 to

80% confluence. Media was aspirated and cells were washed with Dulbecco's phosphate-buffered saline (DPBS, GIBCO) and incubated with Ethylenediaminetetraacetic acid (EDTA) 0.02% (Sigma) at 37°C for up to 5 minutes. Once the EDTA was removed, the cells were manually scratched to dissociate colonies into small clusters using a serological pipette. Cell suspension was gently centrifuged at 1150 rotation per minute (rpm) for 3 minutes. Cell pellet was then resuspended in fresh medium and seeded at 1:1, 1:2 and 1:5 ratios.

2.2.2. Freezing and thawing of stem cells

Cells were passaged as mentioned in Section 2.2.1. Once centrifuged, the pellet was resuspended in a solution of TeSR™-E8™ medium containing 10% of Dimethyl sulfoxide (DMSO, Sigma) for cryoprotection. Cell suspension was transferred into a 1.5mL cryovial (Thermo Scientific) and placed into a cell freezing container which allows a slow freezing rate of -1°C/min (Bioscision) when placed at -80°C. Cells were ready to be placed in liquid nitrogen after at least 3 hours at -80°C.

Thawing cells compared to freezing needs to occur quickly to stop ice crystals from damaging the cells. Cells were transferred from liquid nitrogen straight to 37°C in a water bath. They were then resuspended in 5 volumes of DMEM-F12 and centrifuged at 1150rpm for 3 minutes in order to dilute and remove DMSO. Cells were resuspended in TeSR™-E8™ medium and seeded into a well of a 6-well plate.

2.2.3. Neuronal differentiation

To begin with neuronal differentiation, cells reaching 70-80% confluence were replated into an appropriate number of wells coated with reduced growth factor Matrigel (Corning). Cells were let to grow in stem cell media for up to two days until they reached 80% confluence. Then cells were treated accordingly depending on the protocol.

A basal neuronal medium was prepared as follow, 100 ml of DMEM-F12 + 1ml of B27 supplement 50X w/o Vitamin A (Life technologies) with 50 ml of Neurobasal (Life technologies) + 1 ml of N2 supplement 100X (Life technologies), the total volume was supplemented with 2mM of L-glutamine (Life technologies) and 1:500 MycoZap™ Plus-CL (Lonza) and 0.1mM of β-mercaptoethanol (Gibco).

2.2.3.1. Cortical projection neurons

To start cortical excitatory neuron differentiation, TeSR™-E8™ media was removed and cells were washed with DPBS. Media was replaced with the basal neuronal media supplemented with 10μM SB431542 (Tocris) and 100nM LDN (STEMCELL), a modified dual-smad inhibition protocol (Arber et al. 2015; Chambers et al. 2009) to promote neuroinduction. Every other day, half of the media was changed. Between days 9 and 10, cells were passaged onto fibronectin coated plates (15μg/ml, Millipore). In brief, manual dissociation of the cells was performed using 0.02% EDTA in a similar way to that used for stem cells (see Section 2.2.1). Cells were collected and gently homogenised in neuronal media supplemented with 10uM ROCK inhibitor (Tocris) to promote cell survival. Cells were then replated at a 2:3 ratio and half of the media was replaced every other day. At day 12, LDN and SB were removed from the basal neuronal media and media was changed every other day. About 10 days after the first passage, cells were incubated in StemPro Accutase Cell Dissociation Reagent (Thermo Fisher Scientific) for up to 10 minutes, collected and triturate with a P1000 (Eppendorf) in order to obtain a quasi-single cell solution. Cells were replated onto wells coated with a solution of poly-D-lysine (Sigma) at 0.01mg/ml and laminin (Sigma) at 10μg/ml at a density of 75000 cells/cm^2 and 125000 cells/cm^2 for calcium imaging/immunofluorescence and RNA extraction, respectively. At day 20, B27 w/o Vitamin A in the basal neuronal medium was replaced with B27 with Vitamin A and cells were every few days as needed by changing half of the media.

2.2.3.2. Cortical interneurons

For cortical interneuron differentiation, neuronal conversion was performed using basal neuronal media supplemented with 10μM SB431542, 100nM LDN, and 2μMXAV939 (Tocris) until day 9. From day 10 to day 18, 200ng/ml of Sonic Hedgehog (SHH, R&D) and 1μM purmorphamine (STEMCELLS) were added to the basal neuronal media. During the second passage, cells were split at a ratio of 1:5. From day 20, the media was supplemented with 10ng/ml of BDNF (PeproTech) and 10ng/ml of GDNF (PeproTech).

2.2.3.3. MSNs (Dr Marija Fjodorova)

For MSN differentiation, the neuronal conversion was performed in the same way as for cortical projection neurons. SB and LDN were stopped and basal neuronal media was supplemented with 25ng/ml of Activin A from day 10 onwards. During the second

passage, cells were split at a ratio of 1:1 and BDNF and GDNF were added at the same concentration as in cortical interneuron differentiation.

2.2.3.4. Dopaminergic neurons (Dr Marija Fjodorova)

Finally, for dopaminergic neuron differentiation, neuronal conversion was performed with 10μM SB431542 and 100nM LDN from day 0. From day 3 to 7, neuronal conversion media was supplemented with 1μM PD0325901 (Sigma). At day 7, LDN, SB, and PD were removed and 200ng/ml of SHH and 1μM purmorphamine were added to the basal neuronal media until day 16. During the first passage at day 9, 100ng/ml of FGF8 was also added to the neuronal media until day 16. Following the second passage at day 20, BDNF and GDNF were added to the basal neuronal media at the same concentration as in the cortical interneuron differentiation.

2.2.4. Human primary astrocyte culture

Human primary fibroblasts (Lonza) were plated onto 75ml flask without coating. Primary medium was prepared with 50ml of neurobasal supplemented with 10% FCS, 1ml of B-27, 1:500 Mycozap, and 2mM L-glutamine.

Astrocytes were passaged once confluent at a ratio of 1:3. Cells were incubated in Trypsin for 5 to 10 minutes followed by the inactivation of the enzyme with a double volume of media. Cells were gently triturated and dispensed accordingly.

2.3. Gene expression analysis

2.3.1. RNA isolation and RT-PCR from cell culture

Total RNA was isolated from cultured cells according to the protocol supplied with TRIzol reagent (Invitrogen, Life Technologies, Carlsbad, CA).

Concentration and purity of RNA samples were determined using a spectrophotometer (Eppendorf) which scans in the ultraviolet (UV). The absorbance ratio 260/280 was measured, a value above 2.0 was considered as pure.
To prevent DNA contamination, RNA samples were treated with DNase, PerfeCTa DNase I (Quanta bioscience). The reaction was designed as follow:

RNA template	1µg
10X reaction buffer	1µl
PerfeCta® DNase I (2U/ul)	1µl
RNase/DNase free water	variable
Total Volume (µl)	**10µl**

Reagents were combined in 0.2ml tubes sitting on ice. Each reaction was gently vortexed followed by a centrifugation to collect the solution at the bottom of the reaction tube. Samples were incubated at 37°C for 30minutes, then 1µl of 10X Stop buffer was added to each sample. Reactions were gently mixed and then centrifuged to collect samples at the bottom of the tube. Samples were incubated 10 minutes at 65°C. The entire reaction volume was then used as a template for the first-strand cDNA synthesis.

Total RNA was reverse transcribed with the qScript cDNA superMix (Quanta Bioscience). The reaction was performed as follow:

qScript cDNA Supermix	4µl
RNA template	2µl
RNase/DNase free water	14µl
Total Volume (µl)	20

Reagents were added to 0.2ml tubes sitting on ice. The reactions were vortexed and subsequently centrifuged in order to collect the solution at the bottom of the tube. Tubes were placed in a thermocycler, which was set up as follow:

5 minutes	25°C
30 minutes	42°C
5 minutes	85°C
Hold	4°C

Samples were then kept at -20°C until processed for RT-PCR.

2.3.2. Pre-amplification

Prior to gene expression analysis, cDNA samples from the reverse transcription were pre-amplified in order to obtain optimal cDNA concentrations for gene expression.

In a 0.2ml tube, 1µl of each 100µM stock primer was added. Final volume was adjusted to 200 µl with the DNA Suspension Buffer (10 mM Tris, pH 8.0, 0.1 mM EDTA; TEKnova, PN T0221), a full list of primers is presented in Table 2-1. When possible,

primers were designed to have a PCR product not exceeding 200bp. To prepare the reaction solution, reagents were added to a 1.5ml Eppendorf tube together with the mix of primers as presented below.

Component	Vol per reaction (µl)	Vol for 96 Reactions w/Overage (µl)
Preamp Master Mix (Fluidigm PN 100-5580)	1	105.6
Pooled Primers (500nM)	0.5	52.8
DNase free water	2.25	237.6
cDNA	1.25	
TOTAL Volume	5	-

Pre-Mix

A 96-well plate was filled in by dispersing 3.75µl of the premix. Then 1.25µl of cDNA was added into individual wells. Samples were vortexed and centrifuged at 1000g for a minute. The pre-amplification reactions were loaded into a thermocycler using parameters presented below:

Cycles	Temperature	Time
Hold	95°C	2 min
10	95°C	15 secs
	60°C	4 min
Hold	4°C	∞

Following this, samples required incubation with exonuclease I (New England Biolabs PN M0293S) to remove unincorporated primers. In total, 2µl of diluted Exonuclease I at (4U/ µl) were added to each reaction and incubated at 37°C for 30 minutes followed by 15 minutes at 80°C. The final product was diluted 1:5 in TE buffer.

Table 2-1 List of primers

GAPDH	F: acgacccctcattgacctcaact R: atatttctcgtggttcacacccat	**B-ACTIN**	F: tcaccaccacggccgagcg R: tctccttctgcatcctgtcg
MASH1	F: gtcctgtcgcccaccatctc R: ccctcccaacgccactgac	**NESTIN**	F: agcaggagaaacagggcctac R: ctctggggtcctagggaattg
NGN2	F: tcaagaagacccgtagactgaagg R: gtgagtgcccagatgtagttg	**OTX2**	F: tgccaaaaagaagacatctcca R: aagctgggctccagatagacac

TUJ1	F: acctcaaccacctggtatcg R: tgctgttcttgctctggatg	**EMX1**	F: accggaggacaaagtacaaac R: tagtcattggaggtgacatcg
FOXG1	F: tggcccatgtcgcccttcct R: gccgacgtggtgccgttgta	**EMX2**	F: gcttctaaggctggaacacg R: ccagcttctgccttttgaac
LDB1	F: cgatgtgaagatgtcagtgggctg R: atccctatccagcatggtgcc	**GSX2**	F: tcactagcacgcaactcctg R: ttttcacctgcttctccgac
NKX2.1	F: tgtgcccagagtgaagtttg R: tgtgcccagagtgaagtttg	**NKX2.2**	F: tgcctctccttctgaaccttgg R: gcgaaatctgccaccagttg
NKX6.1	F: acacgagacccacttttccg R: tgctggacttgtgcttcttcaa	**PAX6**	F: aataacctgcctatgcaaccc R: aacttgaactggaactgacacac
CALRET	F: ccttacctgcacctggccga R: ccagagcctttccttgccttc	**FOXP2**	F: aatgtgggagccatacgaag R: gcctgccttatgagagttgc
REELIN	F: atgtggaggtcgtcctagtaagc R: ggaaagtggtgtacactcgg	**SATB2**	F: caacgcaactaataatcatctccc R: gagaaagggctgagaacccg
EOMES	F: caccgccaccaaactgagat R: cgaacacattgtagtgggcag	**TBR1**	F: agcagcaagatcaaaagtgagc R: atccacagacccccctcactag
VGLUT1	F: gaaactcatgaacccccctca R: gggagatgagcagcaggtag	**VGLUT2**	F: attccatcagcagccagagt R: ttgctccatatcccatgaca
BRN4	F: taactagtaggggatcctcaccg R: tggaactgagaatgctgtagg	**CTIP2**	F: ctccgagctcaggaaagtgtc R: ctccgagctcaggaaagtgtc
EBF1	F: aatgtaagcaaggtggacgc R: tcaaggtctaagccggacac	**HELIOS**	F: acctcaggacccattctgtg R: gcaggtctctcaaaaggcac
ISL1	F: aagcgcaggaagagagactg R: ccaagagacccaggatttca	**NOLZ1**	F: acattttgcaccccgagtac R: ggagtacggcttgaaactcg
ARPP21	F: ggaagctggttgacgatgtgtc R: ggcttctgtcgttctacgcc	**CALB**	F: atcaggacggcaatggatac R: taagagcaagatccgttcgg
DARPP32	F: ggtatttttatccgtgcgcgaac R: cttcctcctctggtgaggagtg	**CHRM4**	F: acgaacgatctttgccattc R: tgttgacgtagcagagccag
DRD1	F: ttgtcatctccttggctgtg R: aggccacccagatgttacag	**PENK**	F: gctgtccaaaccagagcttc R: tctggctccatgggataaag
CRABP1	F: acttatcctgacgtttggcg R: tattggtaggggaaaagggc	**LHX6**	F: acagatctacgccagcgact R: catggtgtcgtagtggatgc
LHX8	F: ggaaacgcttcccctatttc R: tgcgaccaagagtctgtacg	**NPY**	F: cgctgcgacactacatcaac R: cagggtcttcaagccgagtt
ZCCHC12	F: aattctgtgcagctgattgc R: caggggacgaactctgaaac	**DGCR6**	F: ggagttgcccagctcattcc R: cgatgctcgttctgtaggc
PRODH	F: ctcacagcactggggagac R: ttggtgaaagaagcacctcca	**DGCR2**	F: ccaacagtaccgcaaggac R: ggccatggagtcaaacagac
DGCR14	F: tatatcgagggcctccagacg R: gcatccgttccaagtctcca	**TSSK2**	F: ggtaaggcagtgctgtggaa R: gctgtgtccttggtgtggta
GSC2	F: tgcagaaccagtatcctgacg R: ttcttgaaccagacctccacg	**SLC25A1**	F: cgcacaaataccggaacacg R: gtgcccttgtagaatgccttg
CLTCL1	F: ttcttcagcaggggcgtaag R: ttgcccgaaggtacacactc	**MRPL40**	F: gactagcgggcttctgggaa R: agacaacaatgacgctcgct
HIRA	F: cagtagtgggtctgcggaag R: tgtcgagctgttcctgacac	**C22ORF39**	F: caccactactacgtccacgg R: tctcacagagggattgctgg
UFD1L	F: aaaggttgaagaggatgaagctg R: ccctgtcagtgccagtaactaa	**CDC45**	F: tgggccatcgttggactaa R: caggacaccaacatcagtcac

CLDN5	F: tctgctggttcgccaaca R: agctcgtacttctgcgacac	**SEPT5**	F: aggacttcaagcagcaggac R: caccgtgttgctgcctataac
GP1BB	F: accacgtgggacagaactc R: tttggaagggagacgcagca	**TBX1**	F: tcgacaagctcaagctgac R: gctggtatctgtgcatggaa
GNB1L	F: gattcgcgtagcctcaggtaa R: gtgcctcggaggacaaactg	**C22ORF29**	F: ttcgcgtagcctcagattgc R: gacagggatggctgaacagg
TXNRD2	F: gccatagcaccttgcatctc R: cagggaaggcgaggatgatt	**ARVCF**	F: ggagtggttccaccaaggaaagaa R: ggtgttgaagttccggctctc
COMT	F: gtcttcctcgaccactggaa R: agtagcactgtccccttcc	**C22ORF25**	F: aacgcgtacaggctcatctt R: gctgcaggtagttggtgagt
DGCR8	F: ctgggctgttgtctccatatca R: ttgatagacgtgtcacccatcc	**TRMT2A**	F: catccccgaagccaccaa R: tctgggtcgtatgccgagta
RANBP1	F: gaccctcagtttgagccaata R: ctcagaggcaaatcggaaca	**ZDHHC8**	F: acgtggatgtgcgaggtatc R: agtggtggtcaaagtcctct
ZDHHC8-F	F: catggaccctggtgttttcc R: cgcacatccacgttcttgta	**ZDHHC8-I**	F: cagcgtctgtgacaactgtgta R: cgatgcagttgttgaccca
RTN4R	F: gcccaacccctacgatgaa R: accttgggctcattgtagca	**SHANK1**	F: ggctcctacgacagctttga R: gtaatcgctccctgggccaat
NANOG	F: gcttgccttgctttgaagca R: ttcttgactgggaccttgtc	**OCT4**	F: cgaccatctgccgctttgag R: ccccctgtcccccattccta
GLUN1	F: acaagagcatccacctgagc R: ttctctgccttggactcacg	**GLUN2A**	F: cccaagagcctcatcacgca R: agacgtcggatccttgtcagc
GLUN2B	F: tctgaccggaagatccaggg R: tccatgatgttgagcattacgg	**GAD1**	F: cgtcttcgaccccatcttcgt R: cgcagatcttgagccccagtt
CUX1	F: cttgaaagggcaaaccagag R: acctctatggcctgctccac	**PALM**	F: ctgcagcacctgaagtcca R: cgctccagcacctcaatttc
GLI1	F: tgaggcccttcaaagccc R: gtatgacttccggcacccttc	**PV**	F: aaagagtgcggatgatgtgaag R: accccaattttgccgtccc
TH	F: tgtgaaggtgtttgagacgtttg R: tcgaggcgcacgaagtact	**SST**	F: gctgctgtctgaacccaac R: cgttctcggggtgccatag
PSD95	F: cacaacctcttattcccagcac R: catggctgtggggtagtcg		

2.3.3. Gene expression using Biomark HD

In a 0.2ml tube, the SsoFast™ EvaGreen® and 20X DNA binding dye (sample pre-mix) were combined with each sample as specified in the table below. In brief, the master mix of the sample pre-mix was vortexed and centrifuged at 1000x for 10 seconds. A total of 3.3µl of pre-mix was added into individual tubes together with 2.7µl of the final product of pre-amplification. To assure correct homogenisation, samples were mixed then centrifuged at 1000g for at least 30 seconds.

Component	Volume per inlet with overage (µl)	Vol for 96.96 IFC overage
2X SsoFast EvaGreen supermix with low ROX	3	360
20X DNA binding Dye	0.3	36
Pre-amplified cDNA	2.7	
TOTAL	6	-

Sample Pre-Mix

In a 0.2ml tubes, the forward and reverse primers at 100µM were combined and mixed as follows:

Component	Vol per inlet with overage (µl)	Vol for 50 µl Stock (µl)
2X Assay Loading Reagent (PN 100-761)	3.0	25
1X DNA TE Buffer	2.7	22.5
100µM combined primers	0.3	2.5
TOTAL	6.0	50

Gene expression was carried out using the 96.96 IFC (BMK-M-96.96). Each IFC contains two accumulators that need to be filled in with a viscous fluid provided in a syringe. They were then placed into the Controller HX (Fluidigm) and the program Prime (136x) was run. Samples and primers were then loaded into their respective inlets on the IFC. Once performed, the IFC was placed back into the Controller HX and the program load mix (136x) was run. Then the IFC was inserted into the Biomark HD and was run using the program GE 96x96 PCR+Melt v2.

Data were collected with the software Biomark HD Data Collection (Fluidigm) and then processed with the Real time PCR Analysis software (Fluidigm). Once the software opened, gene expression data were loaded and a test report was generated. This test summarized the name of the chip, it also mentioned the program used for the real-time PCR and finally a screenshot of a heatmap with Ct values was generated. Each sample and primer were then manually annotated according to their position within the IFC. The quality threshold was set up as recommended by the company at 0.65. Although value below 0.65 are considered to have failed they were individually checked to determine whether or not the sample failed. Data were exported into an excel file in order to be analysed.

All qPCR data presented in this thesis are the result of one experiment with n = 3 or 2 biological replicates for cortical interneurons, glutamatergic neurons and medium spiny neurons, dopaminergic neurons respectively. Data were normalised to the reference gene β-ACTIN – and relative mRNA expression was compared to control basal conditions using the $2^{-\Delta\Delta CT}$ method.

2.4. Genome Editing

2.4.1. DNA extraction

DNA was extracted from cultured cells with a solution of lysis buffer containing; 10nM Tris, pH8.0; 50mM EDTA; 100mM NaCl; 0.5% SDS. A solution of proteinase K at 20mg/ml stock was diluted 1:100 in lysis buffer. Once the culture media was removed, cells were washed with DPBS. A volume of 500µl of lysis buffer was added into the well and left to incubate overnight at 37°C. The next day, the solution was retrieved into a 1.5ml tube together with an equal volume of 100% isopropanol. The solution was briefly vortexed and centrifuged at 12,000g for 20 minutes at 4°C. The supernatant was aspirated and the white pellet was resuspended in a solution of 70% ethanol. Again, the supernatant was removed after centrifugation, the pellet was air dried for 10 minutes and dissolved in 50µl of ddH_2O (double distilled water).

2.4.2. Estimating nucleic acid concentration

DNA concentration was estimated with the spectrophotometer using the appropriate program. The optical density was taken at 260nm, the ratio 260/280 was used to estimate the purity of the sample. A ratio between 1.8 and 2.0 was being considered as pure.

2.4.3. Detection of nucleic acids

The polymerase chain reaction (PCR) reaction was used in order to amplify specific DNA fragment. Primers were designed to match specific DNA sequence. Using a T*aq* polymerase I, the DNA fragment between a pair of primers was amplified.

PCR reaction was performed in a PCR reaction tube using the MyTaq™ DNA polymerase (BIO-21107) as described below:

PCR reaction set-up	
5x MyTaq Reaction Buffer	10µl
Template	200ng
Primers 20µM each	1µl
MyTaq DNA polymerase	1µl
ddH_2O	Up to 50µl

Samples were then transferred into a thermocycler and processed according to the following protocol:

PCR cycling conditions			
Step	**Temperature**	**Time**	**Cycles**
Initial denaturation	95°C	1min	1
Denaturation	95°C	15s	5
Annealing	60°C ramp down -1°C/cycle	15s	
Extension	72°C	10s	
Denaturation	95°C	15s	25
Annealing	55°C	15s	
Extension	72°C	10minutes	-
Hold	4°C	∞	-

2.4.4. Agarose gel electrophoresis

Visualization of PCR fragments was performed using agarose gel electrophoresis. A range between 1 to 5µg of agarose (UltraPURE, Gibco) was dissolved in 1x TAE buffer. Once melted, Safeview (G108, ABM) 1/10000 was added to allow the visualization of nucleic acids when excited at 470nm. Electrophoresis was performed in 1x TAE solution with a voltage ranging from 60 to 100 volts until desired separation of different amplicons was achieved, usually 1h. DNA was visualized using a transilluminator and pictures were acquired for further analysis.

2.4.5. Cloning

2.4.5.1. Oligo annealing

Different gRNAs were designed using the CRISPR MIT website from the Zhang lab. A list with the resulting gRNAs is presented below. The first two gRNA and two last were targeting the exon 3 and 4 respectively of the *ZDHHC8*.

gRNAs sequence (3'→5')	PAM sequence
CGTTCTTGTACAGCGGAGCC	**CGG**
CGGGCGGTAGAAGTGGCACG	**TGG**
CCCGATGCAGTTGTTGACCC	**AGG**
CGTGGTTCAGCACGTAGACC	**AGG**

Below is presented the DNA sequence which were targeted by our different gRNA together with the primers used to check for INDELs and the set of primer to evaluate the mRNA level of *ZDHHC8*. The intronic and exonic sequence were respectively represented in lower case and upper case/bold. Both sequence highlighted in grey represent the pair of primers used to check for INDELs located in intron 2 and 4. The sequence highlighted in green are representing the different gRNAs with their PAM sequence in red. Finally, the sequence in yellow represents the primers used to assess the mRNA level of *ZDHHC8*. It was noteworthy that the third gRNA and the reverse primer were partly sharing the same sequence.

tgagtggctaacttgagacagccttagggattcctggtgggtgggctggacttgggggagggattcacctgccaggaaagtcaacttcctgctcactgcctggctcctggtctgtagCGGA
TGAGGATGAGGACAAGGAGGACGACTTCCGGGCTCCGCTGTACAAGAACGTGGATGTGCGAGGTATCCAGG
TCCGCATGAAGTGGTGTGCCACGTGCCACTTCTACCGCCCGCCGCGCTGCTCCCACTGCAGCGTCTGTGACA
ACTGTGTAGAGgtgaccgccctgctgccccgcgctccccagccctgtgccacatccctgcctgccatgtgccctgatgcactgctcccgcccagGACTTTGACCA
CCACTGCCCCTGGGTCAACAACTGCATCGGGCGTCGAAACTATCGCTACTTCTTCCTGTTCCTGCTGTCACT
CAGTGCACACATGGTGGGCGTCGTGGCCTTCGGCCTGGTCTACGTGCTGAACCACGCTGAGGGGCTGGGAG
CCGCGCACACCACCATCACgtatccttggttcctgtgggcctcattgcagaggcgatgtggaccggggacacgttcac

The complementary sequence of each gRNAs was synthetized together with the specific overhangs corresponding to the BbsI restriction enzyme thus allowing their cloning within the host plasmid. The nucleotides sequence is presented in the table below with in red the overhangs. In addition, two guanine bases were added, in green. The first guanine was necessary for the U6 promoter, while the second guanine was demonstrated to reduce the off-target effect.

Target Exon	Forward 5'→ 3'	Reverse 5'→ 3'
Exon 3	CACCGGCGGGCGGTAGAAGTGGCACG	AAACCGTGCCACTTCTACCGCCCGCC
Exon 3	CACCGGCGTTCTTGTACAGCGGAGCC	AAACGGCTCCGCTGTACAAGAACGCC
Exon 4	CACCGGCCCGATGCAGTTGTTGACCC	AAACGGGTCAACAACTGCATCGGGCC
Exon 4	CACCGGCGTGGTTCAGCACGTAGACC	AAACGGTCTACGTGCTGAACCACGCC

Each pair of oligos were annealed to form a dimer. In a 0.2ml tube, 1µl of each oligo at 100µM, 1µl of 10X T4 Ligation Buffer (NEB), 6.5µl of ddH_2O and 0.5µl of T4 PNK (NEB) were added and incubated in a thermocycler with the protocol presented below.

Temperature	Time
37°C	30 min
95°C	5min
95°C ramp down to 25°C at 5°C/min	-

2.4.5.2. Multiplex CRISPR/Cas9 Construction

Two steps were necessary for the construction of the all-in-one multiplex CRISPR/Cas9. The CRISPR kit used to generate the multiplex CRISPR/Cas9 vectors(Sakuma et al. 2014) was a gift from Takashi Yamamoto (Addgene kit # 1000000054). The first step involved the cloning of the annealed oligos into four different plasmids, one pX330 Ampicillin (pX330A 1-4) resistant plasmid and three pX330 (pX330S 2, 3 and 4) resistant to spectinomycin.

Ligation of the oligonucleotides was performed in a 0.2ml PCR tubes. In four tubes, we premixed 0.2µl of 10X T4 DNA ligase buffer (NEB), 0.1µl of BbsI (NEB), 0.8µl of Quick ligase (NEB) and 0.8µl of ddH_20. Then 0.3µl of the circular plasmid at 25ng/µl together with 0.5µl of 10µM of annealed oligonucleotides were added into their respective tubes. The tubes were added to a thermocycler and 3 cycles at 37°C for 5minutes and 16°C for 10 minutes were performed and followed by an additional BbsI digestion at 37°C for an hour and inactivation at 80°C for 5 minutes.

Digestion by BbsI results to the appearance of sticky ends allowing the integration of our different gRNAs therefore our gRNAs were generated with the specific overhang sequence allowing their specific integration into the host plasmid A schematic of this process is presented below with the example of the first gRNA. The gRNA sequence with the specific overhangs is presented at the top. The bottom sequence corresponds to the region where the BbsI enzyme is cutting with the letter in red corresponding to the sticky end sequence. Once BbsI is cutting, the fragment will be removed therefore allowing the integration of our donor sequence. Interestingly, due to the specificity sequence of the overhangs, there is a unique orientation in which the donor plasmids can be ligated.

It was noteworthy that once integrated, the BbsI recognition site isn't present anymore therefore preventing it to be cut again by the enzyme. As a result, the last step of the protocol which consisted of the additional digestion was used to linearize all remaining plasmids that did not contain the donor plasmid. As only circular plasmid can be introduced into bacterial cells it increased the likelihood of obtaining a positive clone.

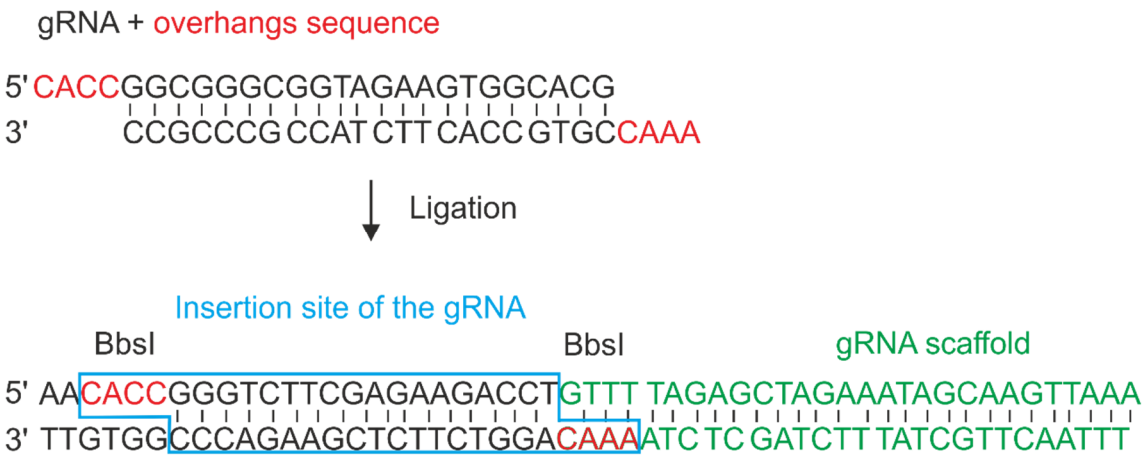

Figure 2-1 Cloning map of the gRNA into the recipient plasmid. The gRNA sequence on top in black, contain the sequence of the overhangs corresponding to the BbsI restriction enzyme. Once the BbsI enzyme cut the plasmid, we can observe that the gRNA is able to be ligated within the plasmid. Furthermore, it was noteworthy that the BbsI sequence disappeared once ligated into the recipient plasmid.

The second step of the multiplex CRISPR/Cas9 consisted of golden gate reaction which was responsible of cutting the fragment of interest and inserting them into one recipient plasmid using the BsaI enzyme. Once cutting, the enzyme induces specific overhangs sequence which are different for each plasmid (Figure 2-2). Therefore, it ensures the specificity of insertion. The golden gate reaction was performed as follow, in one tube, a solution was prepared with 100ng/µl of each spectinomycin plasmid, 50ng/µl of the ampicillin plasmid together with 2µl of 10X T4 DNA ligase buffer, 1µl of BsaI enzyme and 1µl of quick ligase. The reaction was then run using a thermocycler with the following parameters.

Cycle	Temperature	Time
25	37°C	5
	16°C	10
Hold	4°C	∞

Figure 2-2 below allows the visualisation of the cloning process during the step 2.

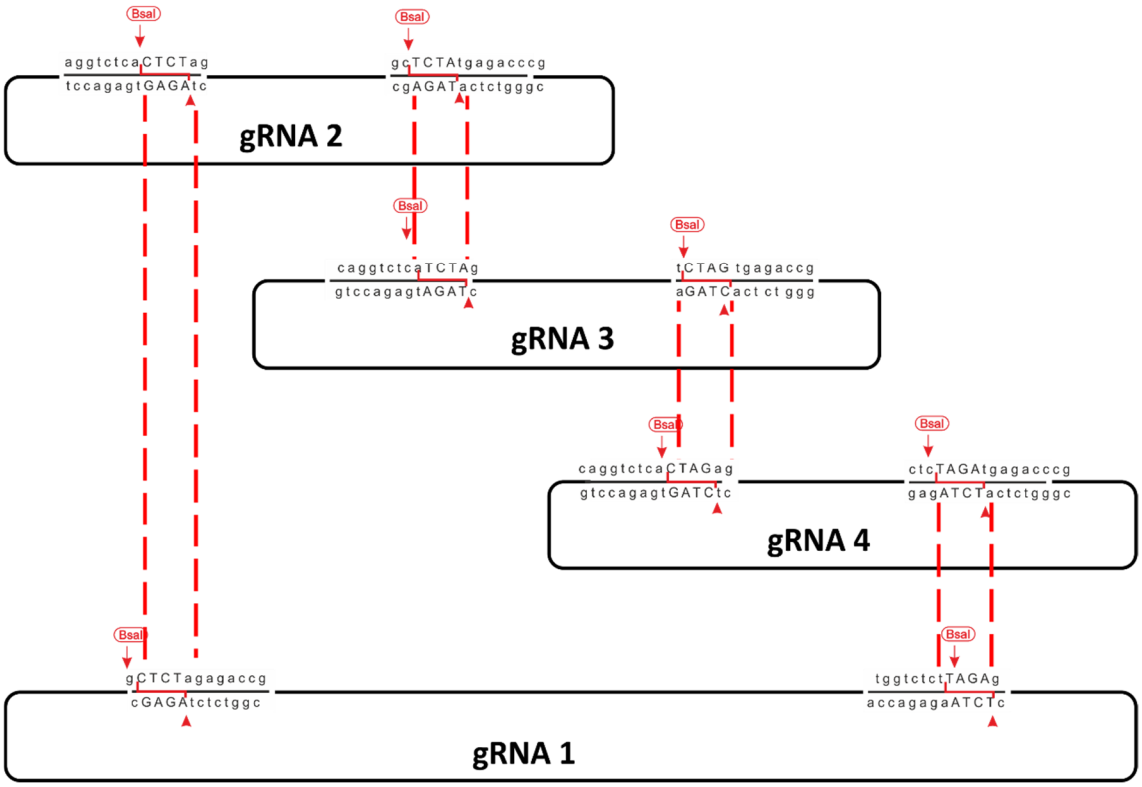

Figure 2-2 Second step of the generation of the all-in-one multiplex CRISPR/Cas9.The reaction involves the cutting of each plasmid by BsaI which generate the specific overhangs sequence allowing their ligation within the plasmid containing the gRNA 1. Digestion by BsaI generates fragment of 445bp which contained the U6 promoter, the gRNA as well as the gRNA scaffold.

2.4.5.3. Bacterial Transformation

Bacterial transformation which corresponds to the insertion of exogenous genetic material into bacterial cells was performed as follows: 1µl of each reaction were transferred to a corresponding vial of competent cells 5-alpha F'Iq Competent E. coli (C2292H, NEB) and carefully flicked to mix the bacteria with DNA. The vials were placed on ice for 30 minutes. A water bath was set up at 42°C and vials were heat shocked for exactly 30 seconds and placed on ice for 5 minutes. A volume of 950µl of SOC media provided by the manufacturer was added to each vial. They were further incubated for 1 hour at 37°C under constant agitation at 200 rotations per minutes (rpm). In the meantime, the agarose plates were warmed at 37°C to avoid condensation. Prior dispersion onto the agar plate, the vials were flicked thoroughly as well as inverted. Two different volumes, usually 50 and 75µl, were spread onto the plates and incubated overnight at 37°C.

Bacterial colonies were manually picked and transferred to a bacterial tube with 3ml of LB media and incubated overnight on the shaker at 37°C and 200rpm.

2.4.5.4. Genomic DNA extraction

2.4.5.4.1. Miniprep

From the previous step, 1.5ml of the bacterial solution was transferred into a 2ml Eppendorf tube and centrifuged at 12000g for a minute. The supernatant was removed and replaced by 200µl of solution A (25mM Tris HCl, pH8, 10mM EDTA) which was previously prepared by adding 3µl of RNAse A per ml. In addition, 200µl of lysis buffer (200mM NaOH, 1% SDS) was incubated for no longer than 5 minutes. To neutralise the lysis buffer, 240µl of solution K (5M potassium acetate, pH5.5) was added and mixed gently by inverting 5-6 times. The bacterial solution was further incubated at room temperature for 3 minutes. The bacterial solution was centrifuged at 12000g for 2 minutes allowing the protein and debris to pellet. The supernatant was carefully collected into a 1.5ml Eppendorf tube and 400µl of 100% isopropanol were added to the tubes which were subsequently vortexed in order to precipitate the DNA and left to incubate for a minute at room temperature. The DNA was pelleted by centrifugation at 14000g for a minute. Supernatant was immediately removed and replaced by 1ml of 70% ethanol and vortexed to clean the DNA pellet. Tubes were centrifuged at 14000g for a minute, the supernatant was removed and centrifuged a second time to remove the remaining ethanol. Tubes were air dried for 10minutes. Finally, 50µl of ddH_2O was added to resuspend the DNA.

2.4.5.4.2. Maxiprep

In order to perform a Maxiprep, 150ml of bacterial solution was incubated overnight at 37°C under continuous agitation. DNA extraction was performed using the HiSpeed Plasmids Kit (Qiagen, 12662) following the instructions provided by the manufacturer.

2.4.5.4.3. Plasmid Digestion

Plasmid digestion was performed using the appropriate enzymes and buffers which was suggested by the manufacturer. The usual protocol is described below and particular restriction enzymes are stated in relevant results chapters.

NEB digestion Reaction	Volume (µl)
Buffer 10X	5µl
DNA template	1µg
Restriction enzyme	0.5µl
ddH_2O	Up to 50µl

The solution was mixed and centrifuged to collect the solution at the bottom of the tube. Tubes were run using a thermocycler for 1h at 37°C. The digestion product was loaded to a 1% agarose gel and run for 1h at 80V.

2.4.5.4.4. Nucleofection

In order to integrate the all in one CRISPR/Cas9 complex, electroporation was performed using the Amaxa NucleoFector™ system (Lonza). This system was designed for the transfection of primary cells. It consists of the application of an electric pulse generating momentary pores in cell membrane thereby allowing the integration of an exogenous plasmid.

Prior to nucleofection, cells were harvested onto another well in order for them to be in their exponential growth phase. This step increases the number of cells surviving the nucleofection process.

An aliquot with 3.5µg of a neomycin resistant plasmid was mixed with 1.5µg of the multiplex CRISPR/Cas9 complex. A volume of 68µl of the P3 Primary cell 4D-nucleofector® X solution was mixed with 12µl of supplement. This solution was mixed with the plasmids and left in the incubator at 37°C.

Cells were harvested as described above (chapter 2.2.1). The cell suspension was centrifuged at 1150rpm for 3 minutes. The supernatant was discarded while the pellet was resuspended with the pre-warmed nucleofection solution and passed through a cells scrapper to obtain a quasi-single cell solution. The solution was added to the Nucleocuvette® and quickly processed in the Nucleofector using the CB-150 program. Cell suspension was divided into 6 wells of a 6-well plate in E8 medium supplemented with 1/100 of RevitaCell (Life technologies).

2.4.5.4.5. pGEM-T easy and sequencing

PCR product from the screening of positive clones were cleaned using the PCR Purification Kit (QIAquick, Qiagen) following the manufacturer protocol. Clean PCR products were ligated into the pGEM®-T Easy vector (Promega). This plasmid contains a 3'-T overhangs at the insertion site which greatly improves the ligation efficiency. Due to the presence of a restriction site and the RNA promoter T7 and SP6 it can respectively be digested or amplified. Figure 2-3 represents a map of the vector with all the different enzymes that can be used to screen for insert or for sequencing.

The pGEM-T-easy vector was used firstly to visualize single allele amplicon secondly to send those selected plasmids for sequencing.

Several plasmids for each clone were sent for sequencing. The T7 promoter was used to amplify the different ligated PCR products.

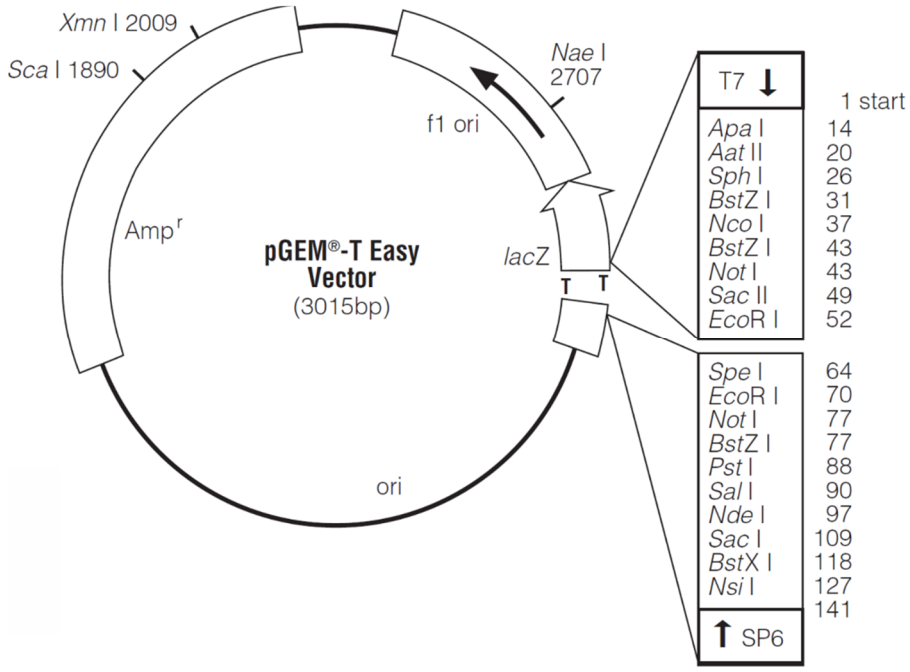

Figure 2-3 Map of the pGEM-T Easy vector. Several enzymes can be used to screen for fragment insertion. To determine whether or PCR product were inserted, we digested the plasmid with EcoRI. For sequencing, fragments were amplified using the T7 promoter.

2.5. Immunocytochemical staining

Cells in culture were washed once with PBS and subsequently fixed in a solution of 3.7% PFA for up to 15 minutes at room temperature. After two washes in PBS, fixed cells were incubated in PBS-NH_4Cl to quench the remaining aldehyde residues for 20 minutes. Cells were stored for up to three weeks at 4°C or stained immediately after the quench. For nuclear stains, cells further underwent 5 minutes of ascending and descending methanol washes in PBS (33%, 50%, 66% at 4°C, then at -20°C in 100% methanol). Fixed cells were permeabilized in a solution of PBS-T (PBS + 0.3% Triton-X100, Sigma) for 4 minutes at room temperature. The cells were incubated overnight at 4°C in PBS with 5% donkey serum (Gentaur) in which the primary antibodies were added. The following day, the cells were washed three times for 10 minutes. Secondary antibodies raised against species of the primary antibody were then added to PBS (1/200, Alexa Fluor 488, 594,

647, Life technologies) and incubated for 40 minutes at room temperature under constant agitation. Cells were counterstained with DAPI (1/3000, Life technologies) in PBS for 5 minutes at room temperature followed by three 10-minute PBS washes. Either the stained cells were covered in the culture plate with a coverslip or coverslips were transferred onto a glass slide (VWR) and mount respectively with a 20µl drop of DAKO (Life technologies). A list of primary and secondary antibodies is presented in Table 2-2.

Table 2-2 List of primary antibodies used for immunostaining

Antigen	Species	Supplier	Code	Dilution
CTIP2	rat	Abcam	ab18465	1/500
FOXA2	goat	Santa cruz	Sc6554	1/200
FOXG1	rabbit	Abcam		1/250
KI67	mouse	BD bioscience	550609	1/200
LMX1A	Guinea Pig	Custom made		1/1000
MAP2	rabbit	Millipore	AB5622	1/1000
N-CADHERIN	mouse	Invitrogen	18-0224	1/1000
NKX2.1	rabbit	Abcam	Ab40880	1/1000
OCT4	goat	Santa cruz	Sc8628	1/500
PAX6	mouse	DSHB		1/1000
PSD-95	mouse	Neuromab		1/50
SSEA3	rat	Chemicon	MAB4303	1/500
TRA1-81	mouse	Chemicon	MAB4381	1/500

Cells were imaged on a Leica DMI6000 inverted fluorescence microscope. A stack of images was acquired to obtain information from all planes. For quantification, we used a 10x objective while for synaptic proteins a 100x oil immersion objective was used.

Images were post processed in ICY (open source software for bioimage informatics). One slice from each stack was extracted for each channel then processed using histogram equalization, a plugin in ICY which allow to obtain an equal histogram. This step is crucial for the subsequent quantification performed in CellProfiler (Cell image analysis software). To count the nuclear staining, CellProfiler was setup on DAPI then the marker of interest.

2.6. Motility Assay

Motility assay was performed on neurons plated on glass coverslip. The experiment was performed at day 20 with excitatory progenitor cells. The coverslip was transferred into

a recording chamber filled with neuronal media. The chamber was temperature, CO_2 and humidity controlled (Ibidi). The recording chamber was placed under a ZEISS Axio Observer Z1 microscope with a 10x objective. Five to eight random fields of view were selected on the same coverslip. Pictures were acquired every 5 minutes for 12 hours. The recording chamber was setup at 37°C, with 90% humidity and 5% CO_2.

The images were analysed using a manual tracking plugin in Fiji. Data were then transferred to excel and analysed.

2.7. Calcium Imaging

In order to accelerate neuronal maturation of our cortical excitatory projection neurons, at day 20 - 26 of differentiation, basal neuronal media was supplemented with β-secretase inhibitors, 10μM DAPT (Sigma) and 2μM PD0332991 (Selleckchem) to synchronise cell cycles and push progenitors to a post-mitotic stage to mature. After this treatment, half of media was replaced with a mix (at 1:1 ratio) of the basal neuronal media and astrocyte-conditioned medium (ACM). At the same time, neurons were transferred to an incubator monitored at 2% oxygen. Until the end of the differentiation, the media was replaced once a week.

Neurons were loaded with 5μM Fluo-4AM (Life technologies), 0.02% Pluronic F-127 (20% in DMSO, Life technologies) and 0.01% Cremophor EL (10% in DMSO, Sigma) and incubated at 37°C in fresh media for 30 minutes. Neurons were quickly washed twice and transferred into a solution of artificial cerebrospinal fluid (aCSF), which contained (in mM): 142 NaCl, 5 KCl, 2.5 $MgCl_2$, 1 $CaCl_2$, 30 D-glucose, 10 2-[4-(2-hydroxyethyl) piperazin-1-yl] ethanesulfonic acid (HEPES) (Sigma), pH 7.4. Neurons were further incubated in the aCSF for 30 minutes at 37°C. Prior to recordings, the aCSF media was replaced with a fresh recording solution.

Calcium activity was acquired using an LED system (Rapp OptoElectronic and Lumencor) at 10Hz for 10 minutes with a final resolution of 1024*1024 pixel. From each time frame, we extracted random regions of interest of 308*308 pixels. The segmentation was performed using NeuroCa, standalone MATLAB package(Janget *al.* 2015) with the following parameters: the type of raw image, TIF; the image size, 308*308; the radius, 2-7; sensitivity, 0.9 and the frame rate at 10Hz. The segmentation files were retrieved and

run in FluoroSNNAP, a MATLAB script for the analysis of calcium activity(Patel et *al.* 2015).

The analysis generates a summary text file with values corresponding to the amplitude ($\Delta F/F_0$), the inter-spike-interval (ISI), the number of events, the rise and fall time of the spikes. All cells exhibiting no events were discarded from the analysis.

2.8. RNA sequencing

2.8.1. Sample preparation and sequencing

Heterozygous cell line for *ZDHHC8* and its isogenic control (iCas9?) as well as an iPSC line (one from each) from a 22q11.2 carriers and a healthy individual were used for this experiment. Cells were differentiated into cortical excitatory projection neurons.

At day 15, RNA samples were extracted by pooling two wells together in order to reduce the variability of the samples. In total, we extracted six RNA samples per line using the mirVana™ miRNA Isolation Kit following the protocol provided by the manufacturer. The concentration and the purity of each sample were determined using the spectrophotometer.

To accurately assess the purity of our RNA samples, they were run on a bioanalyser (CBS Cardiff University) which evaluates the integrity of the 28S and 18S ratio using the Agilent RNA 6000 Nano Kit (Agilent). RNA samples were quantified again using the Qubit RNA High Sensitivity Kit (Life technologies). To extract only the mRNA from the total RNA, the KAPA mRNA HyperPrep Kit was used and aimed to capture the poly(A) RNA. The protocol was followed according to the manufacturer recommendation and using a total of 1µg of RNA.

Prior to RNA sequencing, the library preparation was quantified using the Qubit DNA high sensitivity kit (Life technologies). The clustering and sequencing was carried out as per standard Illumina protocols, with 2 times 75bp paired-end reads on HiSeq 4000.

Except for the neuronal differentiation and RNA extraction, the sample preparation and sequencing were performed by Joanne Morgan.

2.8.2. RNA sequencing analysis

Prior to alignment of the reads, data were processed with the Trimmotic software to remove the adaptor sequences and also base pairs with a Phred lower than 30 (Bolger et *al.* 2014). FastQC was performed before and after the trimming as a quality control.

The RNAs-seq reads alignment was performed by Daniel Cabezas De la Fuente in our laboratory using a script developed by Dr Robert Andrews and Daniel Cabezas De la Fuente. Data were aligned to the reference genome hg38 with the STAR aligner software (Dobin et *al.* 2013).

The average read depth for present samples is summarised in table 2-3 below

Table 2-3. Read depth of the RNA-seq experiment

Samples	Read depth in millions reads
Cas9 (Control)	42.82
541 (ZDHHC8+/-)	47.13
900 Control	43.32
E11 (22q11.2)	46.83

After alignment, the RNA-seq data were processed in R using a script developed and tested by Daniel Cabezas De la Fuenta and Dr Robert Andrews. The script used the DEseq2 package from the Bioconductor(Love et *al.* 2014).

2.9. Statistical analysis

For cell counting analysis, the proportion of cells was calculated using different field of view from one experiment. Normality of the data was first examined. If data passed normality test, we performed a parametric t-test, unpaired t test. Conversely if they did not pass normality, we performed a nonparametric t-test, Mann-Whitney test. Statistical analysis was performed using Prism Graphpad.

Similarly, for motility assay and calcium imaging, data were first checked for normality and statistical analysis was performed accordingly.

For gene expression data, a one-way and a two-way ANOVA was conducted to test for significant differences in our samples with a post-hoc Bonferroni correction for multiple pairwise comparisons.

3. Temporal and spatial expression of the 22q11.2 genes during neuronal differentiation of hESCs.

3.1. Introduction

The 22q11.2DS is a highly penetrant mutation that affects 1/4000 live births making it the most common microdeletion in humans (Karayiorgou et *al.* 2010). Most deletions are either 3Mb or 1.5Mb, which encompass around 60 genes and 28 genes, respectively (Williams 2011). 90% of the 22q11.2 deletion cases arise by *de novo* mutation while 10% are inherited in an autosomal dominant fashion (Ellegood et *al.* 2014). Patients with 22q11.2DS are more likely to develop psychiatric disorders than the general population (Schreiner et *al*. 2013). Recent evidences have also linked 22q11.2DS with Parkinson's disease (Dufournet et *al*. 2017; Retnakaran et *al*. 2010). Although most patients commonly carry a 3Mb deletion, it has been demonstrated that the 1.5Mb deletion was responsible for the underlying pathologies, hence many studies are focusing on this specific region (Jonas et *al* 2014).

Whereas most studies on 22q11.2DS focused on the role of selected genes such as *Dgcr8*, *Tbx1*, *Comt* or *Prodh* in mouse model, the study from Maynard et al. 2003 investigated the expression profiling of all 22q11.2 genes in WT mouse. Thus, the group addressed whether genes within the 1.5Mb deletion were temporally and spatially expressed during mouse embryonic development and adulthood. Samples from either mouse brain or other organs extracted at different time points were screened against genes from the 22q11.2 small deletion. The study identified six genes that were primarily located in neurons including forebrain regions which are known to be altered in schizophrenia. Amongst the twenty-two genes tested, twelve exhibited a similar expression across the different time points from embryonic stage to adulthood. *Tmvcf*, also known as *Cldn5*, displayed an expression pattern that increased over time. Conversely, *Cdc45l* (*Cdc45*) exhibited a brain expression profile that peaked at E12 and E14. The PCR result of *Prodh2* (*Prodh*) was negative in brains at embryonic stage but increased postnatally and declined in the adult. *Tbx1* and *Wdvcf* (*Gnb1l*) exhibited expression in other tissues but not in the brain. Three genes: *Gscl* (also known as *Gsc2*), *Gpibb* (*Gp1bb*) and *Stk22b* (*Tssk2*) were found not expressed. Finally, authors examined the expression of a subset of these genes in human fetal brain, different adult brain regions and several other human tissues with similar observations to that in mice (Maynard et *al.* 2003).

Although studies have already shed light on the expression profiling and brain region specific expression of genes in the 1.5Mb deletion, the data presented lacked temporal and spatial resolution. Furthermore, microdissected brain tissue does not allow to assess differentially expressed genes in specific neuronal populations.

Neurons derived from hESCs offer a unique opportunity to understand the expression of these genes during human neural development. It is currently possible to differentiate hESCs into the major neuronal lineages present in the brain allowing the examination of the spatial and temporal expression profile of the genes present in the 1.5Mb deletion.

Aims

The aims of this chapter were to determine the temporal and cell-type specific expression of twenty-eight genes located in the 1.5Mb deletion. Due to the transcript similarity between DGCR6 and DGCR6L, only DGCR6 was studied. The specific objectives are:

1. To differentiate hESCs into glutamatergic cortical neurons, GABAergic cortical interneurons, medium spiny neurons (MSN) and dopaminergic neurons and to extract RNA samples at different time points.
2. To investigate the temporal expression profile and determine whether any genes exhibit a cell type specific expression using a high-throughput Biomark HD PCR machine.

3.2. Results

The hESCs iCas9 and H7 were differentiated using previously establish protocols into cortical excitatory projection neurons (Espuny-Camacho et *al.* 2013) , GABAergic MSN (Arber et *al.* 2015), cortical interneurons (Maroof et *al.* 2013) and midbrain dopaminergic neurons (Jaeger et *al.* 2011). All protocols were based on dual SMAD inhibition that block BMP signalling. The newly derived naïve neuroepithelial cells, largely of forebrain characteristics by default, can then be directed towards specific regional fate by appropriate morphogens. For example, SHH and/or SHH agonist purmorphamine are normally applied to ventralize forebrain progenitors into medial ganglionic fate for generating cortical interneurons. Instead addition of activin A is necessary to the differentiation into LGE progenitors that gives rise to MSNs. Finally, a MEK blocker PD0325901, SHH and FGF8 were used for generating midbrain dopaminergic neurons.

All different protocols are presented in the schematic timeline in Figure 3-1 moreover, details of the concentration for each compound are presented in 2.2.3.

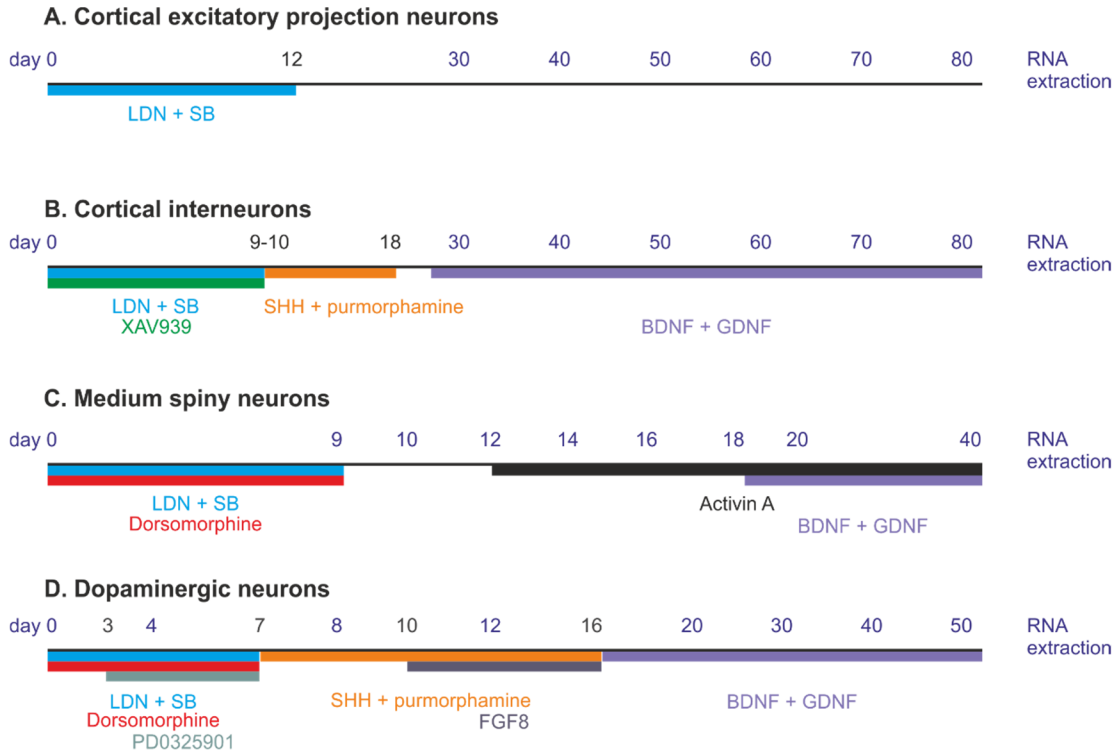

Figure 3-1 Schematic timeline of the four differentiation protocols. A, cortical excitatory projection neurons differentiation. B, cortical interneurons. C, MSN. D, dopaminergic neurons. Time points for RNA extraction are also represented in blue.

RT-PCRs were performed on 3 or 2 biological samples from one experiment using the qScript cDNA superMix as explained in chapter 2 and processed using the Biomark HD to assess the variation level of these different genes. To identify potential regulated expression, all data were firstly normalized to the housekeeping gene β-actin and compared to one common reference usually time point at day 0 when possible.

3.2.1. Neuronal Subtype differentiation from hESC

3.2.1.1. Glutamatergic neuron differentiation

To verify glutamatergic fate induction, cultures at day 15 were stained with antibody against FOXG1, a transcription factor expressed exclusively in the developing telencephalon. The majority of cells were positive for FOXG1 (Figure 3-2A), suggesting highly efficient induction of glutamatergic precursors. VGLUT1 (*SLC17A7*), PSD-95

(*DLG4*) and *GRIN1* (GLUN1) are proteins essential for excitatory synapses and hence can be used as markers for mature neurons (Figure 3-2B). As neurons matured morphologically from day 30 to 80, an increase in transcript levels of these marker genes was observed. Furthermore, we observed that during the course of differentiation the expression of these genes were significantly higher when compared to day 30 for *GRIN1* and *SLC17A7* and day 0 for *DLG4*.

In keeping with the RT-PCR observation, immunofluorescence staining confirmed the expression of the postsynaptic protein PSD-95 and microtubule associated protein 2 (MAP2) in neuronal processes (Figure 3-2C).

Together these data support the generation of glutamatergic neurons derived from hESCs.

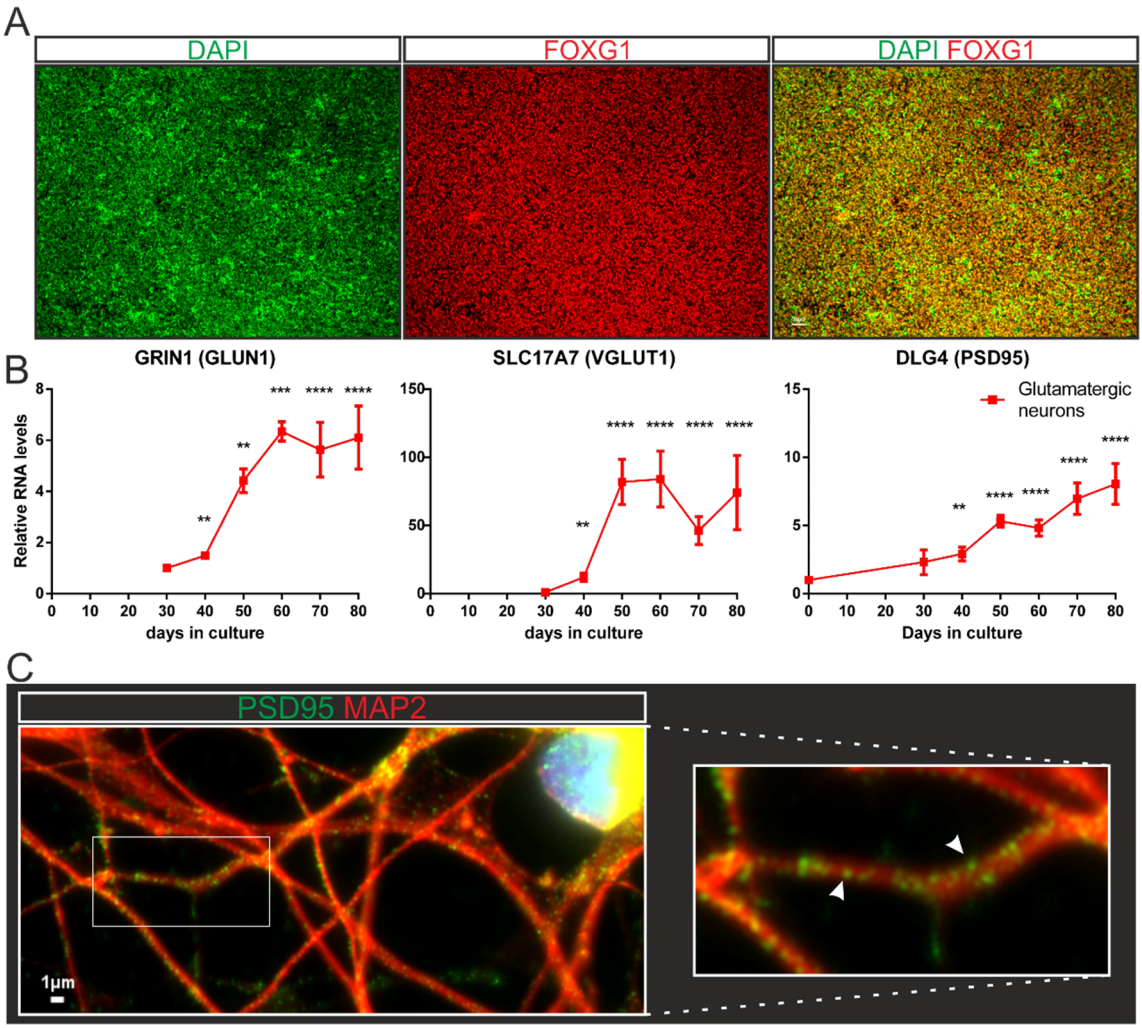

Figure 3-2 Glutamatergic precursors and mature neurons Legend on the next page.

Figure 3-2 Glutamatergic precursors and mature neurons A, immunofluorescence of glutamatergic neurons precursors at day 15 for FOXG1 (red) with DAPI counter staining, scale bar 50µm. B, Temporal expression profiling of mature neurons markers, *GRIN1*, *SLC17A7* and *DLG4*. Data were normalized against the housekeeping gene *β-actin*. Data were then compared to day 30 for *GRIN1* and *SLC17A7* while *DLG4* was compared to day 0. The levels of all three transcripts increased over time suggesting a differentiation of the precursors into mature neurons. Error bars represent mean+/-SEM with n = 3 biological replicates. Statistical analysis was performed on ΔCT value with a one-way ANOVA with Bonferroni post-hoc, **P<0.01, ***P<0.001 ****P<0.0001. C, immunofluorescence of glutamatergic neurons at day 60 stained for PSD-95 (green), MAP2 (red) and DAPI (blue). Arrowhead are pointing towards PSD-95 puncta localized on a dendrite. Pictures were acquired with an upright Leica Microscope with a 100x immersion objective, scale bar 1µm.

3.2.1.2. Cortical Interneuron differentiation

Cortical interneuron differentiation was characterized at day 20 by immunostaining for NKX2.1, a transcription factor expressed in medial ganglionic eminence (MGE), a region in the ventral forebrain that gives rise to major types of cortical interneurons. As illustrated in Figure 3-3A, a large proportion of cells were NKX2.1 positive. To further characterize those cells, the expression of key transcripts was analysed by RT-PCR (Figure 3-3B). *LHX6* is a transcription factor responsible for the tangential migration of MGE cells towards the cortex (Alifragis et *al.* 2004). An increase of this crucial gene could be detected from day 30. SST and PV are two major classes of inhibitory interneurons, generation of which was confirmed by increased expression of these two genes in the present experiment.

For this experiment, day 30 interneurons progenitors were provided by Maria Cruz Santos and re-plated onto poly-D-lysine laminin and kept in neuronal media until day 80. RNA samples were extracted every 10 days from day 30. Pictures presented below are a courtesy of Maria Cruz Santos. The above data together suggests an efficient conversion of hESCs into cortical interneurons.

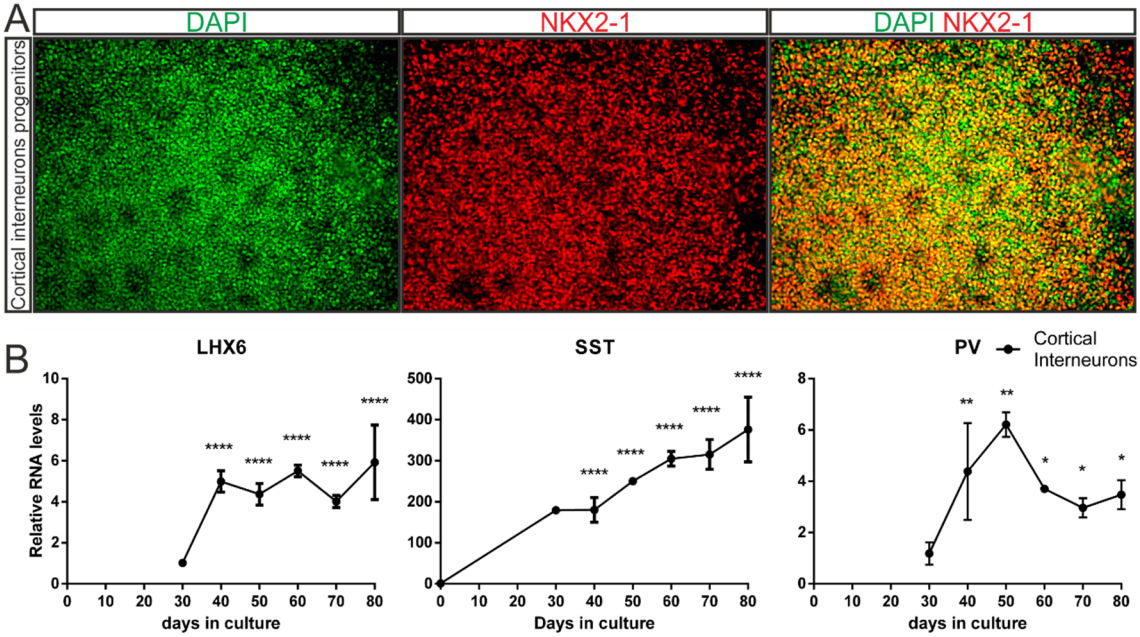

Figure 3-3 Cortical Interneuron differentiation. A, Immunofluorescence of interneuron precursors at day 20 with DAPI (green) and NKX2.1 (red) a marker of the MGE. An image was acquired using a Leica inverted microscope with a 10x objective. B, Temporal expression profiling of mature interneuron markers. The expression of *LHX6*, *SST* and *PV* were normalized to the housekeeping gene β-actin. Due to high Ct value prior day 30, the relative mRNA levels for *LHX6* and *PV* were compared to day 30. Conversely, relative mRNA level for *SST* was compared to day 0. The expression of *LHX6*, *SST* and *PV* increased over the course of the differentiation suggesting a neuronal maturation. Error bars represent mean+/-SEM with n = 3 biological replicates from one experiment. Statistical analysis was performed on ΔCT value with a one-way ANOVA with Bonferroni post-hoc, *P<0.05, **P<0.01, ****P<0.0001.

3.2.1.3. Dopaminergic neuron differentiation

Immunofluorescence using FOXA2 and LMX1A antibodies was performed at day 20 (Figure 3-4). Together, these early markers are key determinants for dopaminergic neuron identity. As illustrated in Figure 3-4A, an important proportion of cells were positive for both FOXA2 and LMXA1 suggesting an appropriate regionalisation towards a dopaminergic fate. While maturing, these neurons express the enzyme tyrosine hydroxylase (*TH*), responsible for the conversion of tyrosine into L-DOPA, a precursor of the neurotransmitter dopamine. This gene started to be expressed from day 20 and increased 11-fold at day 50 when compared to day 20 (Figure 3-4B).

RNA samples and immunofluorescences were a courtesy of Dr Marija Fjodorova.

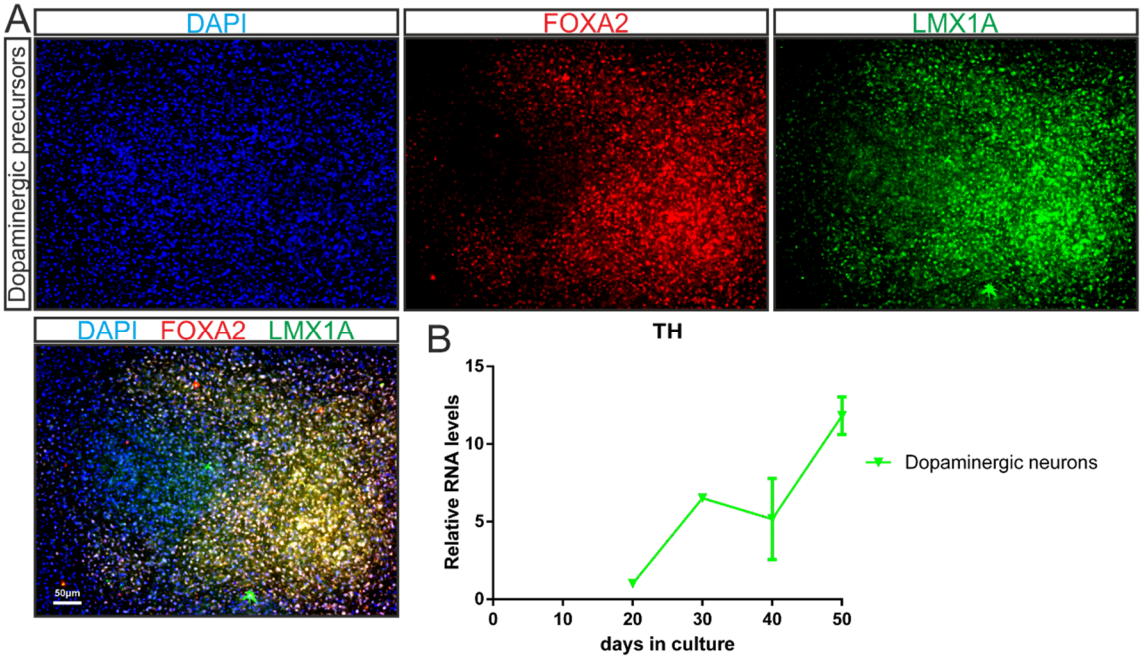

Figure 3-4 Dopaminergic neuron differentiation. A, Immunofluorescence of dopaminergic precursors at day 20 with DAPI (blue), FOXA2 (red) and LMX1A (green). Images were acquired using a Leica inverted microscope with a 20x objective, scale bar = 50µm. B, Temporal expression profiling of gene expressed by dopaminergic neurons. The expression of *TH* was normalized to the housekeeping gene β-actin and mRNA expression level was compared to day 20. Error bars represent mean+/-SEM. No statistical analysis was performed due to sample size.

3.2.1.4. MSN differentiation

GABAergic medium spiny projection neurons were characterized at day 20 using an antibody against CTIP2 (*BCL11B*) protein, a transcription factor known to be expressed by striatal progenitors in the LGE. A high proportion of cells positive for CTIP2 could be observed in day 20 cell cultures (Figure 3-5). While this protein is also expressed by glutamatergic neurons, *CTIP2* and the transcription factor *GSX2* are two genes which can be used to assess the cellular identity of the LGE. Indeed, a peak of expression of *GSX2* was detected at day 20 corresponding to the progenitor stage. *CTIP2* expression increased over the course of differentiation. During development, these progenitors are morphologically and physiologically maturing thus marker like *DRD1* can be used to evaluate the maturation stage. Dopamine receptors D1 are expressed by mature neurons from the direct pathway and an increase in expression of this gene was observed over the course of differentiation.

RNA samples and immunofluorescence were a courtesy of Dr Marija Fjodorova.

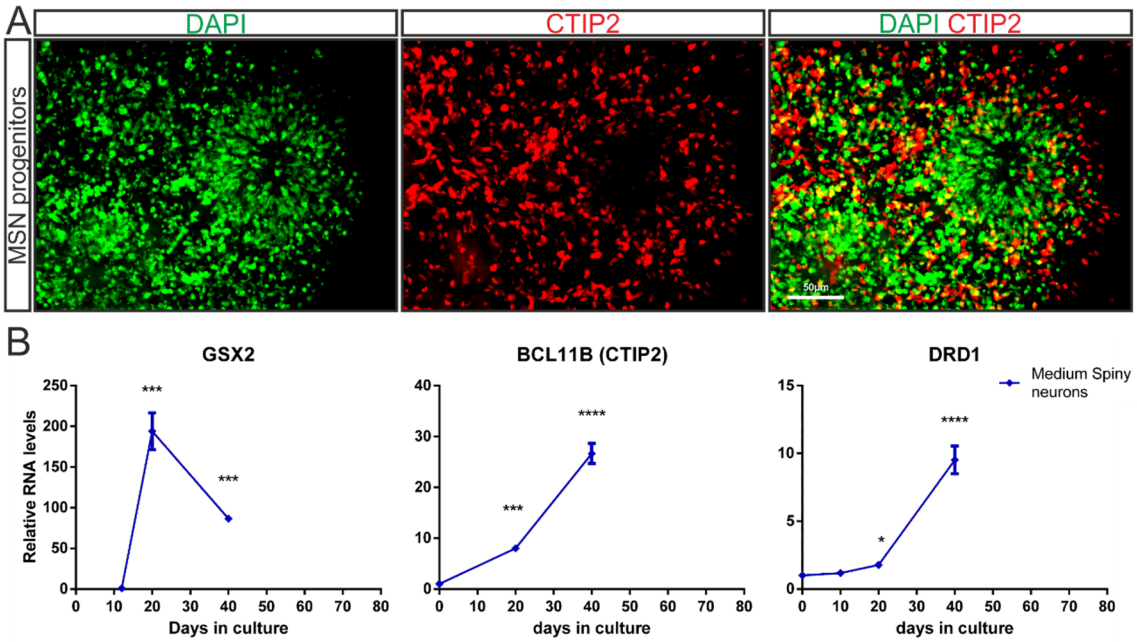

Figure 3-5 Medium Spiny Neuron differentiation. A, Immunofluorescence of MSN precursors at day 20 with DAPI (green) and CTIP2 (red) a marker of the LGE. Images were acquired using a Leica inverted microscope with a 40x objective, scale bar = 50µm. B, Temporal expression profiling of genes expressed by MSN. The expression of *GSX2*, *CTIP2* and *DRD1* was first normalized to the housekeeping gene β-actin. Relative mRNA levels for *GSX2* was compared to day 12 while it was compared to day 0 for *CTIP2* and *DRD1*. Error bars represent mean+/-SEM with n = 2 biological replicates from one experiment. Statistical analysis was attempted on the ΔCT value with a one-way ANOVA with Bonferroni post-hoc, *P<0.05, ***P<0.001, ****P<0.0001.

Taken together, these data demonstrate that four different neuronal precursor populations were properly differentiated from hESCs stage. Given the high proportion of relevant progenitor markers, cells were directed to mature glutamatergic, cortical GABAergic, striatal medium spiny and midbrain dopamine neurons.

3.2.2. Temporal expression of the 22q11 genes

First, genes were categorized according to their Ct value from high to low and not expressed. These data are presented in table 3-1 and an average Ct value of all cell lineages for each gene is shown.

Table 3-1 Average Ct value across cell lineages

Ct < 15	15 ≤ Ct ≤ 22	Ct > 22
DGCR6, DGCR2, DGCR14, SLC25A1, CLTCL1, HIRA, MRPL40, CDC45, SEPT5, C22ORF29, COMT, C22ORF25, DGCR8, TRMT2A, RANBP1, ZDHHC8	*PRODH, TSSK2, UFD1L, CLDN5, GP1BB, TBX1, ARVCF, RTN4R*	*GSC2, C22ORF39, GNB1L, TXNRD2*

Amongst the 28 genes in the 1.5Mb deletion, four had a Ct value higher than 22, eight had a Ct value between 15 and 22, while sixteen genes had a Ct value below 15.

According to the manufacturer, when samples are processed on the Biomark HD, due to the high sensibility of the equipment, they advised to discard genes with a Ct value of 22 and above. Thereby, in our experiment genes with a Ct value of 22 and above were also discarded.

Subsequent analysis investigated whether these genes exhibited a temporal expression profile and the twenty-four genes were grouped into three categories: early expression, later expression and constitutive expression.

3.2.2.1. Early expression

The expression of four genes, *HIRA, CDC45, RANBP1* and *UFD1L* showed a higher level at early stage of differentiation compared to the later stages (Figure 3-6). These genes are thought to regulate the cell cycle (Meechan et *al*. 2009). *Hira* is only weakly present in the mouse developing cortex; however, this gene is considered to be an important candidate responsible for the pathophysiology of 22q11.2DS (Maynard et *al*. 2003). *Cdc45* has been shown to be expressed in the VZ and SVZ of the mouse developing brain and is essential for the initiation of DNA replication (Maynard et *al*. 2003). Likewise, *Ranbp1* is also highly expressed in the VZ/SVZ where it controls the nucleocytoplasmic transport of proteins and nucleic acids (Maynard et *al*. 2003). Finally, *Ufd1l* has demonstrated to be restricted to the intermediate zone of the mouse developing cortex (Maynard et *al*. 2003).

Because we did not collect RNA samples prior day 30 in cortical differentiations, data were plotted on two different graphs. The first one displayed dopaminergic and MSN while the other displayed glutamatergic and cortical interneurons. The relative expression

of *CDC45* and *RANBP1* were significantly higher at day 10 and 20 in MSN and dopaminergic differentiation cultures. Although, it appeared that the relative expression of *HIRA* at day 10 and day 10-20 in MSN and dopaminergic neurons respectively was higher, data failed to reach significance. Similar result was obtained for *UFD1L* although the expression was higher in dopaminergic cultures than MSN.

The level of *HIRA, CDC45* and *RANBP1* transcript showed little change in the time windows analysed. The Ct value for these RT-QPCRs were low in both the cortical glutamatergic and interneurons samples, suggesting a high level of expression of these genes in these cells. However, *UFD1L* expression appeared to increase in cortical interneurons and decrease in glutamatergic cells as the cultures matured.

Table 3-2 below presents the results of the two-way ANOVA to compare the expression between the different cell type. Only significant data were displayed.

Table 3-2 Results of two-way ANOVA that compare difference between cell lineages

Gene	Day	Cell types	Significance
HIRA	40	Cortical Interneurons vs Dopaminergic	*
CDC45	30	Cortical interneurons vs Glutamatergic	*
	40		****
	50		****
	60		****
	80		**
	30	Cortical interneurons vs Dopaminergic	***
	40		****
	50		****
	50	Glutamatergic vs Dopaminergic	**
	40	Cortical interneurons vs MSN	***
	20	Dopaminergic vs MSN	**
RANBP1	20	Dopaminergic vs MSN	**
UFD1L	30	Cortical interneurons	**
	40		*
	70		****
	80		****
	30	Cortical interneurons vs Dopaminergic	*
	30	Glutamatergic vs Dopaminergic	****
	40		****
	40	Glutamatergic vs MSN	***

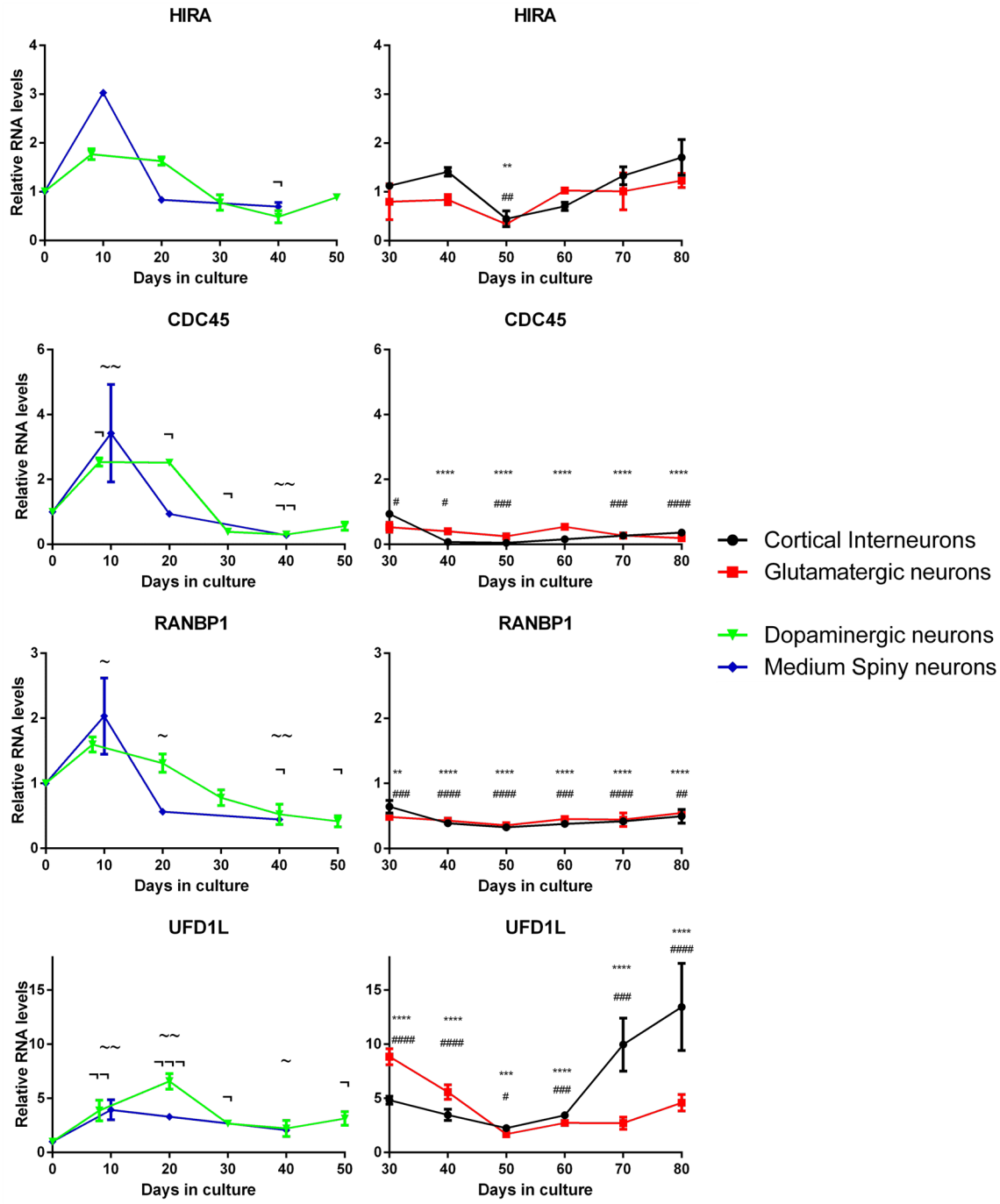

Figure 3-6 Expression profile of a subset of the 22q11.2 genes displaying an early expression pattern. A small subset of four genes in the 22q11.2 genes displayed an early expression profile. Cortical interneurons (black), glutamatergic neurons (red), dopaminergic neurons (green) and MSN (blue). Data were normalised to the housekeeping gene β-actin and compared to day 0. Error bars represent mean+/-SEM. The data presented correspond to one experiment with n = 3 biological replicates for cortical interneurons, glutamatergic neurons and n = 2 for dopaminergic and medium spiny neurons. Error bars represent +/-SEM. Statistical analysis was performed on the ΔCT value with a one-way ANOVA with Bonferroni post-hoc to compared within cell lineage the expression of each time point to day 0 with * (cortical interneurons), # (glutamatergic neurons), ¬ (dopaminergic neurons) and ~ (medium spiny neurons). *P<0.05, **P<0.01, ***P<0.001 and ****P<0.0001.

3.2.2.2. Late expression

SEPT5, *GP1BB*, *DGCR6* and *ARVCF* are four genes which displayed a later stage expression pattern (Figure 3-7). *Sept5* has been shown to be involved in the process of

exocytosis and cell division (Choi et *al.* 2003), while *Gp1bb* has a role in the formation of the platelet plugs (Kunishima et *al*. 2013). *Dgcr6* is part of the family of the DiGeorge syndrome Critical Region regrouping genes implicated in DiGeorge Syndrome. *Dgcr6* is suggested to play a role in neural crest migration (Hierck et *al*. 2004), finally *Arvcf* was shown to be involved in protein-protein interaction at adherens junction (Ulfig et *al.* 2004).

Due to high Ct value, data for *GP1BB* were normalized from day 16 for MSN and dopaminergic neurons whereas cortical interneurons and glutamatergic neurons were normalized from day 30. *ARVCF* was normalized at day 8 for dopaminergic neurons. Thus, comparison between these two groups was not possible.

As shown in Figure 3-7, transcript levels of this group increased over the course of neuronal maturation in all four differentiation cultures. All genes in this group showed their highest expression at the end of differentiation for most of the cell lineages, with the exception of *DGCR6*, which peaked at day 30 in dopaminergic neuron cultures.

Although the expression profile of *GP1BB* in glutamatergic and cortical interneurons was not obvious, an increase from day 30 to 80 was observed. A 4-fold change increase was observed in glutamatergic neurons while it was 2-fold in cortical interneurons.

Similarly to the early expression profiling, statistical analysis was performed on our data in order to determine whether different existed between the different cell type at a given time point. These data are presented in table 3.3.

Table 3-3 Results of two-way ANOVA that compare difference between cell lineages.

Gene	Day	Cell type	Significance
SEPT5	40	Cortical interneurons vs Glutamatergic	***
	60		*
	70		***
	80		****
	30	Cortical interneurons vs Dopaminergic	**
	40		**
	40	Glutamatergic vs MSN	**
	20	Dopaminergic vs MSN	**
DGCR6	80	Cortical interneurons vs Glutamatergic	**
	30	Cortical interneurons vs Dopaminergic	****
	40		**
	30	Glutamatergic vs Dopaminergic	****
	40		****
	40	Glutamatergic vs MSN	***
	40	Dopaminergic vs MSN	**
ARVCF	30	Cortical interneurons vs Dopaminergic	*
	30	Glutamatergic vs Dopaminergic	***
	20	Dopaminergic vs MSN	*

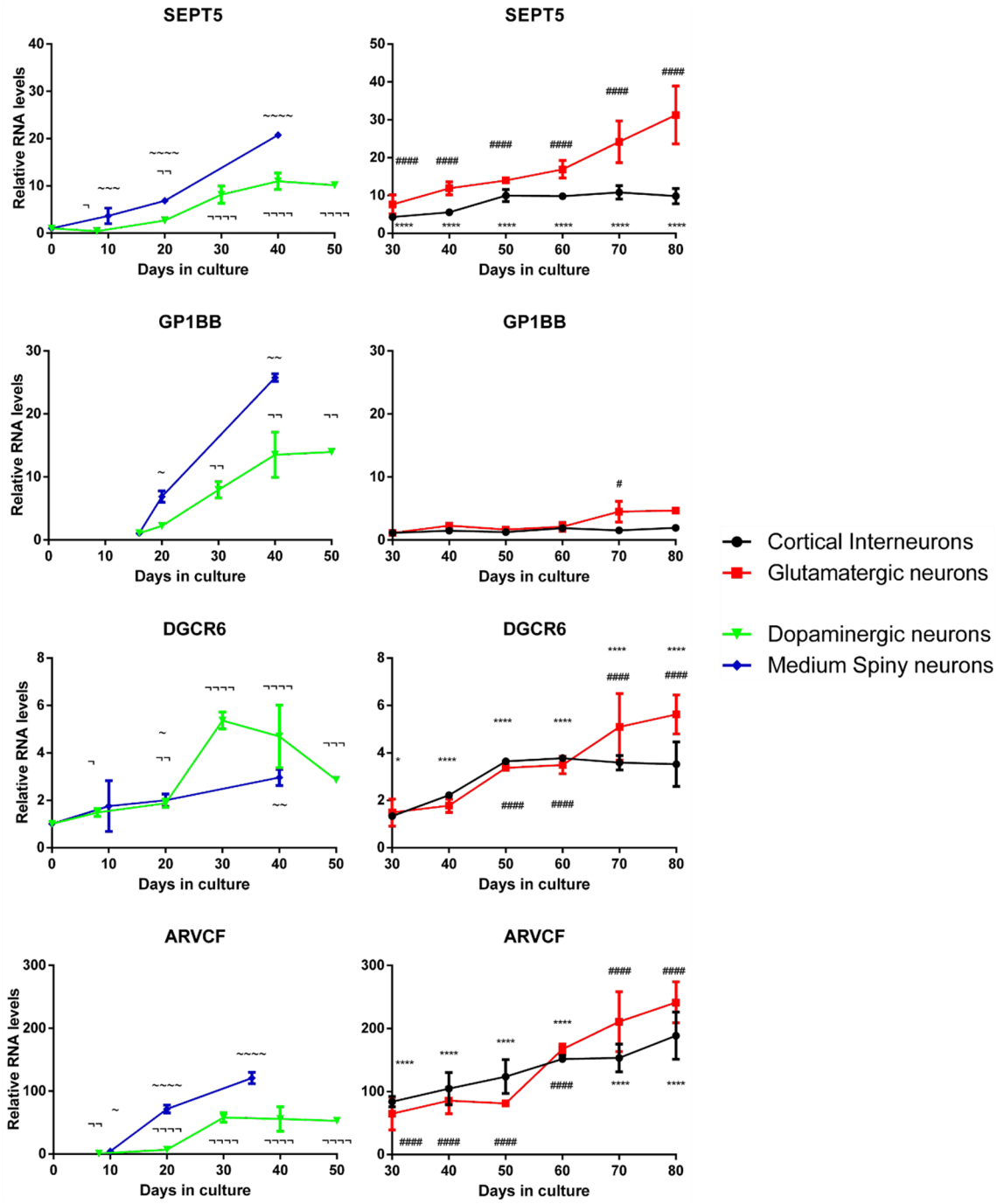

Figure 3-7 Expression profile of a subset of the 22q11.2 genes displaying a later expression pattern. Four of the 22q11.2 genes displayed an expression profile that increased along the course of differentiation. Black, red, green and blue lines represent cortical interneurons, glutamatergic neurons, dopaminergic neurons and MSNs, respectively. Data were normalised to the housekeeping gene β-actin and compared to day 0 for *SEPT5*, *DGCR6* and *ARVCF* while *GP1BB* was compared to day 16 for dopaminergic, MSN and day 30 for cortical interneurons and glutamatergic neurons. The data presented correspond to one experiment with n = 3 biological replicates for cortical interneurons, glutamatergic neurons and n = 2 for dopaminergic and medium spiny neurons. Error bars represent +/-SEM. Statistical analysis was performed on the ΔCT value with a one-way ANOVA with Bonferroni post-hoc to compared within cell lineage the expression of each time point to day 0 with * (cortical interneurons), # (glutamatergic neurons), ¬ (dopaminergic neurons) and ~ (medium spiny neurons). *P<0.05, **P<0.01, ***P<0.001 and ****P<0.0001.

3.2.2.3. Genes with no apparent temporal profile

The profiles of *PRODH, DGCR2, TSSK2, TBX1* and *COMT* did not exhibit an obvious trend. (Figure 3-8).

PRODH expression decreased during the course of MSN and dopaminergic neuron differentiation when compared to day 0. On the other hand, the transcript level remained constant at all the time points analysed for the two cortical cultures. However, the average Ct value was 16 suggesting that the transcript was present in enough quantity to be detected in these samples. *COMT* followed a similar pattern to that of *PRODH* except a very small increase during glutamatergic differentiation at day 80. DGCR2 encodes for an activity dependent adhesion protein (Kajiwara et *al*. 1996). As shown in Figure 3-8, the expression level of *DGCR2* increased slightly in all four differentiation paradigms. *TSSK2* is part of a family of serine threonine kinase that is mostly expressed in testis (Hao et *al*. 2004). Surprisingly, as illustrated in Figure 3-8, *TSSK2* expression was detected in all four lineages. The Ct value was classified as high with an average Ct of 16 across the different neuronal populations. The expression profile rose in dopaminergic neurons from day 0 until day 10 then remained steady. In MSNs, the expression kept increasing until day 50. A similar pattern was observed in cortical interneurons where the transcript levels increased from day 30 to 80. However, during glutamatergic differentiation, *TSSK2* expression appeared to drop first before it increased again from day 50 to 80.

Table 3-4 below is the result of the statistical analysis which aimed to compare difference between cell lineages at a given time point.

Table 3-4 Results of two-way ANOVA that compare difference between cell lineages

Gene	Day	Cell type	Significance
DGCR2	40	Cortical interneurons vs Glutamatergic	**
	40	Cortical interneurons vs Dopaminergic	*
PRODH	30	Cortical interneurons vs Glutamatergic	****
	40		****
	50		****
	60		****
	70		****
	80		****
	30	Cortical interneurons vs Dopaminergic	***
	50		****
	40	Glutamatergic vs Dopaminergic	**
	50		*
	40	Cortical interneurons vs MSN	***
	20	Dopaminergic vs MSN	**
	40		*

COMT	30	Cortical interneurons vs Glutamatergic	****
	40		****
	50		****
	60		****
	70		****
	80		****
	30	Cortical interneurons vs Dopaminergic	****
	40		**
	30	Glutamatergic vs Dopaminergic	**
	40		****
	50		****
	40	Cortical interneurons vs MSN	****
	20	Dopaminergic vs MSN	*
TSSK2	30	Cortical interneurons vs Glutamatergic	**
	70		*
	40	Cortical interneurons vs Dopaminergic	*
	30	Glutamatergic vs Dopaminergic	**
	50		*

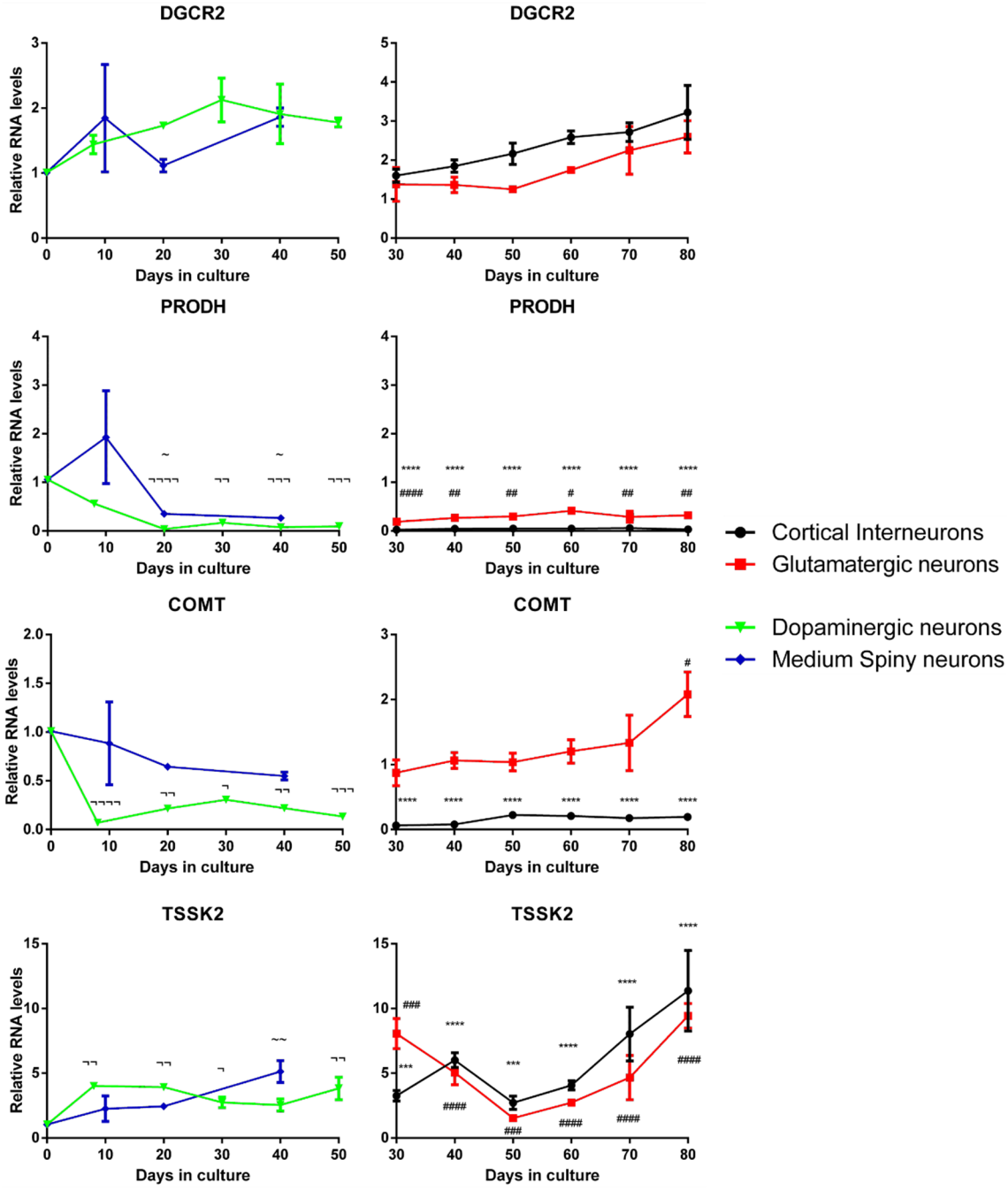

Figure 3-8 22q11.2 genes with no apparent expression profile. Five genes showed no apparent temporal profile. In black, red, green and blue are represented the cortical interneurons, glutamatergic neurons, dopaminergic neurons and MSN respectively. Data were normalised to the housekeeping gene β-actin and compared to day 0. The data presented correspond to one experiment with n = 3 biological replicates for cortical interneurons, glutamatergic neurons and n = 2 for dopaminergic and medium spiny neurons. Error bars represent +/-SEM. Statistical analysis was performed on the ΔCT value with a one-way ANOVA with Bonferroni post-hoc to compared within cell lineage the expression of each time point to day 0 with * (cortical interneurons), # (glutamatergic neurons), ¬ (dopaminergic neurons) and ~ (medium spiny neurons). *P<0.05, **P<0.01, ***P<0.001 and ****P<0.0001.

3.2.3. Subtype specific expression

In addition to temporally regulated expression, it is particularly interesting to investigate whether any of the 22q11 genes show a cell type-specific expression. Therefore, the data was next analysed from this perspective.

As shown in Figure 3-9, ten genes were identified as being preferentially expressed in a specific cell lineage. This group including *DGCR6, CLTCL1, MRPL40, CLDN5, TBX1, C22ORF29, C22ORF25, DGCR8, ZDHHC8* and *RTN4R* were selected due to their expression profile that suggested an enrichment in dopaminergic neurons. Similar to the data presented earlier, the classification was based on first a visual assessment, then confirmed by statistical analysis. Reported functions of these genes are summarized in table 3.-5.

Table 3-5 Function of the gene exhibiting cell type specific expression

Gene	Function
DGCR6	Suggested to play a role in neural crest migration
CLTCL1	Encodes for CH22 protein thought to be involved in intracellular endosomal trafficking
MRPL40	Implicated in mitochondrial translation
CLDN5	Plays a role in tight junction at the blood brain barrier
TBX1	Transcriptional regulator involved in developing process
C22ORF29	May induce apoptosis in a BH3 domain
C22ORF25	Predicted to play roles in secretory protein in the endoplasmic reticulum
DGCR8	Component of the microprocessor complex that is required to process micro RNA
ZDHHC8	Palmitoyltransferase responsible of posttranslational modification
RTN4R	Mediates axonal growth inhibition, may be involved in axonal regeneration

In order to directly compare the relative level of expression, data of all four cell types from day 20 (committed neuronal progenitors) to 50 (neurons) were included in Figure 3-9.

DGCR6 was already described above as a late expression gene, and indeed its transcript levels increased in cortical interneurons and glutamatergic neurons from day 40 onward. In addition, this gene demonstrated preferential expression in dopaminergic neurons at days 30 and 40. *TBX1* exhibited a peak of expression in dopaminergic neurons at day 30 and although it decreased thereafter, the fold change was still higher in these cultures compared to the other cell lineages. *CLTCL1*, *MRPL40*, *CLDN5*, *C22ORF29*, *C22ORF25*, *DGCR8*, *ZDHHC8* exhibited a constant expression in MSN, cortical glutamatergic and interneurons while peaking at day 30 in dopaminergic neurons. *RTN4R* followed a similar pattern of expression to the aforementioned group of genes in dopaminergic neurons, while its expression in the other lineages exhibited only a slight increase at day 50. Such enrichment of these particular genes in dopaminergic neurons may suggest that at this stage they are more important for the development of this specific category of neurons.

The result of the statistical analysis which aimed to compare whether we had different in expression between cell lineage at a given time point is presented below in table 3-6. Only significant data were presented.

Table 3-6 Results of two-way ANOVA that compare difference between cell lineages

Gene	Day	Cell Type	Significance
DGCR6	30	Cortical interneurons vs Dopaminergic	****
	40		**
	30	Glutamatergic vs Dopaminergic	****
	40		****
	40	Dopaminergic vs MSN	**
CLCTL1	30	Cortical Interneurons vs Dopaminergic	*
	40		**
	30	Glutamatergic vs Dopaminergic	****
	40		**
	50		***
	20	Dopaminergic vs MSN	**
	40		****
MRPL40	30	Cortical interneurons vs Dopaminergic	**
	30	Glutamatergic vs Dopaminergic	****
	20	Dopaminergic vs MSN	**
CLDN5	30	Cortical interneurons vs Dopaminergic	****
	40		****
	50		****
	30	Glutamatergic vs Dopaminergic	****
	40		****
	50		****
	20	Dopaminergic vs MSN	****
	40		***
TBX1	30	Glutamatergic vs Dopaminergic	*
C22orf29	30	Cortical interneurons vs Dopaminergic	***
	40		**
	30	Glutamatergic vs Dopaminergic	****
	40		****
C22orf25	30	Cortical interneurons vs Dopaminergic	**
	30	Glutamatergic vs Dopaminergic	**
	50		**
DGCR8	30	Glutamatergic vs Dopaminergic	*
	50		***
	50	Cortical interneurons vs Dopaminergic	*
ZDHHC8	30	Cortical interneurons vs Dopaminergic	*
	30	Glutamatergic vs Dopaminergic	***
RTN4R	30	Cortical interneurons vs Dopaminergic	****
	40		***
	30	Glutamatergic vs Dopaminergic	****
	40		****
	20	Dopaminergic vs MSN	*
	40		****

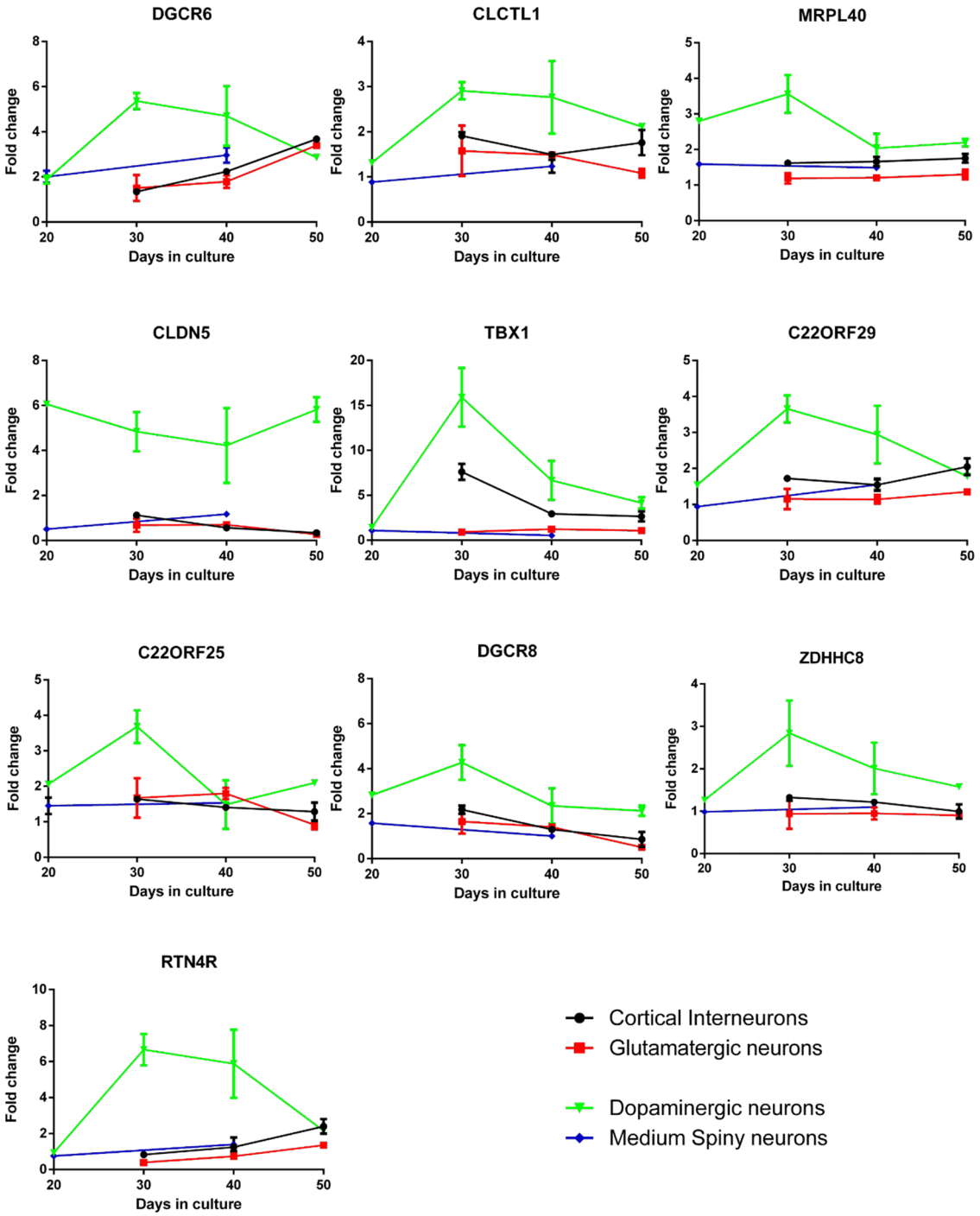

Figure 3-9 22q11.2 gene exhibiting dopaminergic enrichment. In black, red, green and blue are represented cortical interneurons, glutamatergic neurons, dopaminergic neurons and MSNs, respectively. Error bars represent +/-SEM Statistical analysis was performed on the ΔCT value with a two-way ANOVA with Bonferroni post-hoc to compared at a given time point between cell lineage, data are presented in table 10.

Finally, table 3-7 shows a summary of above analyses, specifying at what stage of differentiation 22q11.2DS genes were expressed and whether they were enriched in a specific neuronal population.

Table 3-7 Summary of the findings on the expression of 22q11.2DS gene expression. Genes were classified according to their order in the genome.

GENE LIST	Temporal profile		Cell type specific expression
	Early	Late	
DGCR6		X	Dopaminergic neurons
TSSK2			
CLTCL1			Dopaminergic neurons
MRPL40			Dopaminergic neurons
HIRA	X		
UFD1L	X		
CDC45	X		
CLDN5			Dopaminergic neurons
SEPT5			
GP1BB		X	
TBX1			Dopaminergic neurons
C22orf29			Dopaminergic neurons
ARVCF			
C22orf25			Dopaminergic neurons
DGCR8			Dopaminergic neurons
RANBP1	X		
ZDHHC8			Dopaminergic neurons
RTN4R			Dopaminergic neurons

3.3. Discussion

Previous studies in mouse brain have suggested that some of the 22q11 genes exhibited a temporally regulated expression fashion. However, little is known about the cellular identity in which specific 22q11 genes are expressed, particularly in human neurons.

This chapter investigated the temporal expression profile of the genes located in the 1.5Mb deletion of the 22q11.2DS and identified genes whose expression was enriched in a specific neuronal population. Over the twenty-eight genes present in this region, twenty-two displayed identifiable expression features. Present data suggest that *HIRA*, *CDC45*, *RANBP1* and *UFD1L*, are expressed early during hESCs neuroectodermal differentiation. Conversely, *DGCR6*, *SEPT5*, *GP1BB* and *ARVCF* are expressed later during neuronal development. Interestingly, *DGCR6*, *CLTCL1*, *MRPL40*, *CLDN5*, *TBX1*, *C22ORF29*, *C22ORF25*, *DGCR8*, *ZDHHC8* and *RTN4R* showed preferential (or enriched) expression in dopaminergic neurons.

Variation in the expression of *PRODH* and *COMT* has been shown to cause brain abnormalities and increases vulnerability to schizophrenia (Zinkstok et *al.* 2008). Furthermore, due to their implication in neuronal physiology, these two genes were

intensively studied. PRODH is a mitochondrial protein responsible for the first step of the proline catabolism that is subsequently converted into glutamate (Willis et *al*. 2008). COMT is an enzyme that degrades catecholamines like dopamine or norepinephrine (Craddock et *al.* 2006). However, as presented in the current study, expression of *COMT* and *PRODH* did not show convincing results. Except in dopaminergic neurons where levels of COMT decreased, it remained constant in other neuronal populations. Furthermore, *PRODH* expression was similar to that of *COMT* in glutamatergic and cortical interneurons while it decreased in MSN and dopaminergic neurons. Despite the level of maturity of neurons in this study, they still may not be mature enough at these stages for these two specific genes to be expressed. It was demonstrated that *PRODH* as well as *COMT* showed enrichment in adolescent brain but not in embryonic brain supporting their role later in life (Lin et *al*. 2016).

Previous studies using mouse model of 22q11.2DS identified genes in the 1.5Mb deletion which have crucial role in early stages of brain development, namely, *Cdc45, Hira, Ranbp1, Ufd1l* (Meechan et *al.* 2015; Meechan et *al*. 2009). Thus, present experiment was in accordance with these previous findings as the same genes were identified as having their peak of expression early in the process of differentiation.

The role of *RANBP1* at the first stage of neuronal differentiation is coherent with a recent study which revealed that *Ranbp1* homozygous mice showed cortical growth alteration (Paronett et *al.* 2015). Authors discovered that it was due to a disruption of the basal progenitors which in turn are responsible for the generation of the layer 2/3 projection neurons (Paronett et *al.* 2015).

Due to the function of *Ranbp1* early in cortical neurogenesis, it is very likely that despite the absence of RNA samples before day 30 in glutamatergic and cortical interneurons, one should expect to observe a similar profile to that observed in dopaminergic and MSN differentiation.

Moreover, individual homozygous knock-out of these four genes, *Cdc45, Ranbp1, Ufd1l* and *Hira* was demonstrated to be lethal, emphasizing their importance during development (Meechan et *al.* 2015).

With novel tools available for gene editing, such as CRIPSR/Cas9, it would be interesting to generate hESCs lines deficient for these genes in order to study their role over the course of human neuronal differentiation.

Tssk2 and *Gp1bb* are two genes whose expression was not detected in the mouse brain in previous studies (Maynard et *al*. 2003). *Tssk2* was shown to be mainly expressed in testis while the *Gp1bb* has been associated with platelet adhesion. However, present findings suggest that these two genes might be expressed in the brain. Indeed, *GP1BB* exhibited a profile of expression that increased along the course of differentiation in all four neuronal populations. *TSSK2* transcripts were also observed in all four neuronal lineages whereas this gene was previously shown to be absent or only weakly expressed in the brain (Li et *al*. 2011). To conclude, current data demonstrated the presence of two novels genes in differentiating human neurons, *GP1BB* and *TSSK2*. While the function of TSSK2 in the brain is still largely unknown, present study suggested that this gene may have a function in mature neurons. On the other hand, as *GP1BB* is important for platelet formation which involves secretion of granules, a recent study from Goubau et al. identified common molecular mechanism between granule trafficking in platelets and neurons (Goubau et *al*. 2013) . Thus, it would be interesting to study the role of GP1BB in mature neurons to identify whether it has a role in neuronal trafficking.

All genes that were classified as being expressed later during development in current analysis have been implicated in neuronal physiology. *Septin5* has been shown to be expressed exclusively in non-dividing cells and its role in neurons has been linked to vesicular exocytosis, an important process in neurons. *Dgcr6* has been found to interact with $GABA_{B1}$, a metabotropic receptor subunit part of the $GABA_B$ metabotropic receptor (Zunner et *al*. 2010). On the other hand, *Arvcf* has been suggested to be expressed in the MGE during development.

Thus, it can be concluded that the increase of expression of these different genes is consistent with neuronal maturation. During this process, vesicle exocytosis increases, more receptors are either secreted or sent to synapses and neurons in turn are making more connections giving rise to the network complexity.

Present analysis discovered that a subset of 10 genes from the 1.5Mb deletion exhibited an enrichment in dopaminergic neurons when compared to other neuronal populations. Although these results have not been replicated yet, it is the first time that a study revealed an enrichment of these genes in a specific neuronal population.

Dopaminergic alteration is known to be implicated in the occurrence of both Parkinson's disease and schizophrenia. Indeed, dopaminergic neurons were observed to be involved in cognitive deficits in individuals with schizophrenia. This alteration of dopamine

transmission occurs primarily in the mesolimbic brain area, but also in the amygdala and prefrontal cortex. On the other hand, Parkinson's disease occurs due to a loss of dopamine neurons from the substantia nigra pars compacta. It would thus be interesting to investigate the function of these genes in dopaminergic neurons.

In addition to the study presented in this chapter and due to the availability in our institute of iPSCs derived from individuals carrying a 22q11.2 mutation, it would be interesting to perform a similar experiment than the one presented in this chapter. This study would aim to investigate whether hemizygous deletion of the 22q11.2 genes alter their temporal profile but also determine if we would obtain similar genes enrichment than the one observed in the control experiment. This experiment therefore might explain the appearance of the subsequent neurological alteration observed in patients with 22q11.2DS.

Finally, our experiments revealed limitations regarding neurons differentiation. Indeed, genes such as *COMT* or *PRODH* are usually expressed in adolescent neurons. However, neurons derived stem cells in vitro never mature past the second trimester. Therefore, progress would be necessary to obtain neurons in vitro that would mimic older neurons in human. Recently a new media was developed by Telezhkin et *al*. 2016, named the synaptoJuice (Telezhkin et *al*. 2016). This media consists of different steps and different media composition during the course of the differentiation. Authors demonstrated that it improves the maturation of hESCs derived GABAergic neurons in vitro. Others have also investigated the composition in ions of neuronal media. The study demonstrated that the culture media usually used for neuronal differentiation is altering the electrical activity thus synaptic communication of neurons. Therefore, they designed a new media in which the ions concentration was adjusted in order to mimic physiological condition. Future studies should also consider the use of different medias when examining genes whose function appear later during development.

To summarize, the data presented in this chapter, we first confirmed that neurons derived stem cells are able to recapitulate expression features observed in mouse model of 22q11.2DS. Secondly, our analysis successfully identified genes that exhibit a specific expression profile across lineages. Indeed, our classification revealed genes with a preferential expression early or late during the development while others showed a gene specific enrichment in dopaminergic neurons when compared to the other cell lineages.

Although, the classification was exclusively based on visual assessment at first, statistical analysis was enable us to confirm our categories. To conclude, this study gives valuable insight on the potential genes associated with early and late neuronal differentiation which therefore might be responsible of the underlying pathologies in 22q11.2 carriers. In addition to these genes, we demonstrated that the cell type is also important when considering studying a gene.

4. Generation and characterization of *ZDHHC8*-deficient hESCs lines

4.1. Introduction

ZDHHC8 is a particularly interesting candidate within the 1.5Mb of 22q11.2DS due to its suggested physiological role in neurons. It is a palmitoyl acyltransferase (PAT) protein belonging to a family of 23 members that share a conserved cysteine rich domain referred to as the DHHC domain (Korycka et *al.* 2012). Protein palmitoylation (protein S-acylation) is a process which consists of 16-carbons fatty acids attached onto a cysteine residue (Chamberlain et *al.* 2015). Compared to the other lipid modification such as myristoylation or geranylgeranylation, palmitoylation is the only posttranslational lipid modification that is reversible which thus has a significant role in the control of cellular protein dynamic. Palmitoylation enhances the hydrophobicity of protein thus contributes to their membrane association, protein-protein interaction as well as their subcellular trafficking (Globa et *al*. 2017; Holland et *al.* 2017; Huang et *al.* 2005).

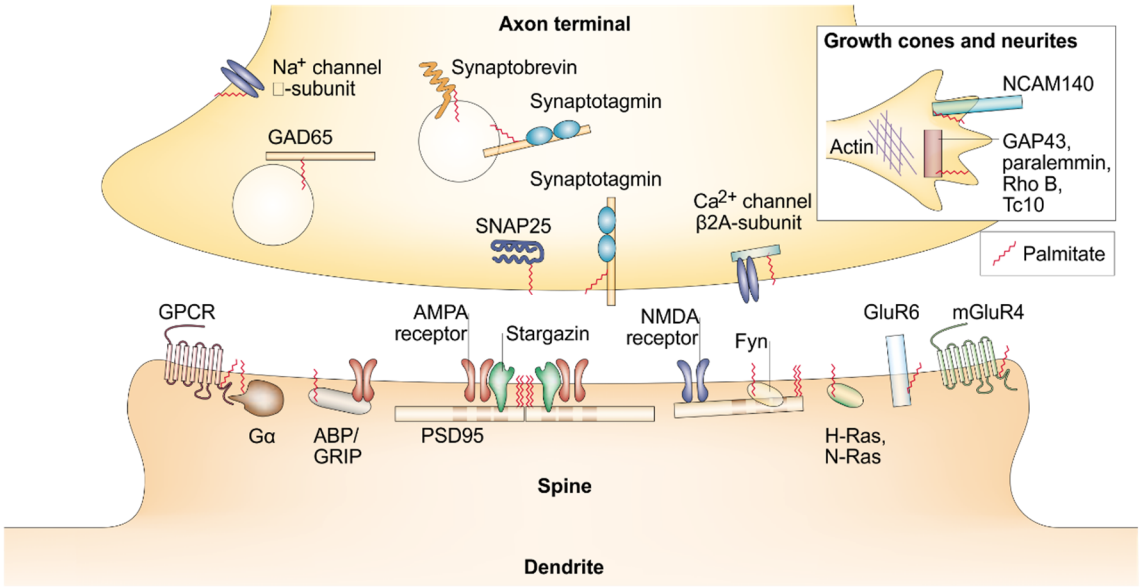

Figure 4-1 Palmitoylation of protein regulates synaptic transmission. This figure shows that several key regulators of synaptic transmission located at the pre and post-synaptic neurons require to be palmitoylated On the presynaptic side, palmitoylation is necessary for protein regulating synaptic vesicle fusion and neurotransmitter synthesis and release. We can also found ions channel. On the postsynaptic side, protein palmitoylation include protein involved in the scaffolding of receptors but also ionotropic receptors. Figure adapted with permission from Springer: Nature reviews. Neuroscience, El-Husseini 2002 (4296960901940) Copyright (2002).

Growing lines of evidence suggest that protein palmitoylation plays a central role in synaptic physiology. As illustrated in Figure 4-1 (Fukata et *al.* 2010), protein palmitoylation is suggested to be essential for the proper function of the majority of the pre- and post- synaptic proteins, as well as proteins involved in neurons development (el-Husseini et *al.* 2002).

Studies of *Zdhhc8* homozygous deficient mice have demonstrated interaction between ZDHHC8 and PSD-95, a key component of the postsynaptic density responsible for the anchoring of postsynaptic receptors as well as protein that mediates the formation and maintenance of synapses (Irie et *al.* 1997; Sheng 2001; Sheng et *al.* 2011). Previous studies have also shown that ZDHHC8 is the only palmitoylation enzyme for Paralemmin-1, a regulator of filopodia (small protrusion on dendrites that serves as precursor of spines) (Gauthier-Campbell et *al.* 2004). Thus, reduction of Paralemmin-1 palmitoylation was suggested to result in a decrease of functional synapses. Similarly, CDC42, a protein regulating actin cytoskeleton has been demonstrated to be palmitoylated by ZDHHC8. Thus, impairment of CDC42 palmitoylation results in a decrease of dendritic and axonal arborisation (Mukai et *al.* 2008, 2015; Nishimura et *al.* 2013; Wirth et *al.* 2013).

ZDHHC8 has been shown to be primarily localized in the vicinity of the nucleus and in vesicle-like clusters in the dendritic shafts (Mukai et *al.* 2004). However, a study from Maynard et *al.* 2008 observed that ZDHHC8 might also be localized in the mitochondria, which was demonstrated by its colocalization with a mitochondria specific protein UQCRC1 (Maynard et *al.* 2008; D. W. Meechan et *al.* 2011).

It is known that 30% of individuals carrying the 3Mb or 1.5Mb 22q11.2 deletion develop schizophrenia (Liu et *al.* 2002). Recently, it was also demonstrated that individuals with 22q11.2DS have an increased risk to develop Parkinson disease (Dufournet et *al.* 2017). Furthermore, several studies identified single nucleotide polymorphism (SNP) which were shown to increase the risk to develop schizophrenia, one of which is rs175174 A/G in *ZDHHC8 locus* (Chen et *al.* 2004; Mukai et *al.* 2004). This specific SNP located in the middle of the intron 4 of *ZDHHC8* gene is expected to introduce a STOP codon which is suggested to lead to a premature stop of translation. However, several other studies revealed no association with schizophrenia for this SNP (Demily et *al.* 2007; Glaser et *al.* 2006; Otani et *al.* 2005).

Neuronal migration defect was observed in patients carrying 22q11.2 mutation but also in patients developing schizophrenia (Castro et *al.* 2011; Nadarajah et *al.* 2003). Therefore, it would be interested to identify whether *ZDHHC8* alter the migration process in culture of neurons.

Dysregulated neuronal electrical activity has been identified in mouse models of 22q11.2DS (Earls et *al.* 2010). These mice exhibited an increase in their short- and long-term plasticity. Moreover, neurons presented an increase in presynaptic neurotransmitter release whilst the postsynaptic function was unaltered. This increase of neurotransmitters release was suggested to be linked to the altered calcium kinetics and upregulation of the sarco-endoplasmic reticulum calcium ATPase type 2 (SERCA2) which was observed in CA3 presynaptic terminal.

Aims

In this chapter, we investigate the role of *ZDHHC8* in cortical neuronal development using hESCs as a model. The specific objectives are:

- To generate and validate hESCs deficient for *ZDHHC8* using the CRIPSR/Cas9 technology
- To evaluate the effect of *ZDHHC8*-deficiency in cortical excitatory neuron differentiation (kinetics and expression)
- To investigate the role of *ZDHHC8* in glutamatergic progenitors and neurons using motility assay as well as calcium imaging

4.2. Results

4.2.1. Generation of *ZDHHC8* KO hESCs using CRISPR/Cas9

The all in one multiplex CRISPR/Cas9 employed to target and edit *ZDHHC8*. This method is believed to reduce the stress caused by multiple plasmids insertion and increase the cutting efficiency. Indeed, in order to efficiently target and maximize the likelihood of at least one gRNA inducing INDELs in *ZDHHC8*, we designed four gRNAs, with two targeting exon 3 and two targeting exon 4 respectively named 1, 2, 3 and 4 (Figure 4-4). The gRNAs were chosen according to their off-target score; high score closed to 100

indicated a low probability of off-target of the specific gRNA. Our gRNAs 1, 2, 3 and 4 had respectively a score of 76, 91, 85 and 88.

4.2.1.1. Construction of the multiplex CRISPR/Cas9 plasmid

To generate a stem cell lines deficient for *ZDHHC8*, I used the all-in-one multiplex CRISPR/Cas9 system. As illustrated in Figure 4-2, two steps were necessary for its construction. The first one consisted of the insertion of each gRNA into individual plasmid whereas the second step involved the assembly of each individual gRNA into the final recipient plasmid by golden gate assembly (Sakuma et *al*. 2014).

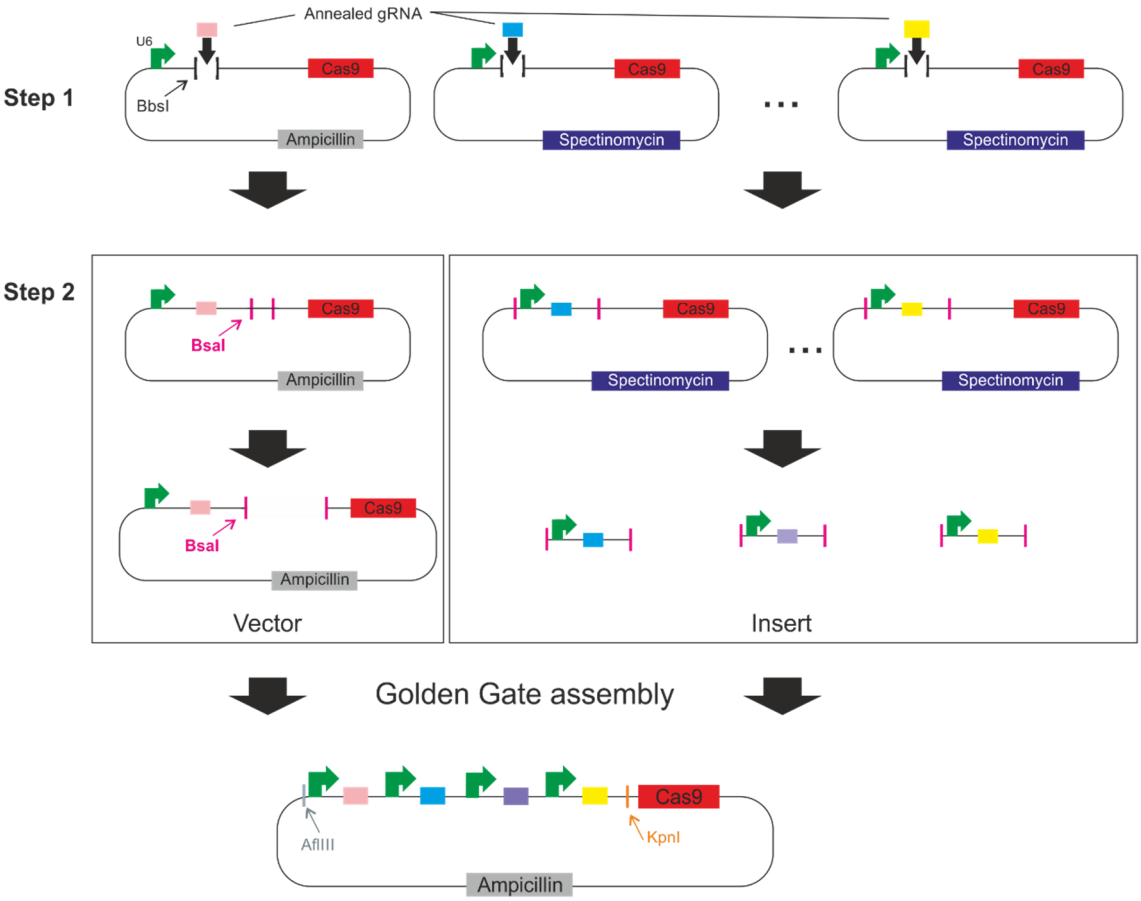

Figure 4-2 Illustration of the construction of the multiplex CRIPSR/Cas9. Two plasmids are necessary for the construction of the all-in-one CRISPR/Cas9, one ampicillin resistant plasmid in grey and three others spectinomycin resistant plasmids in purple. The Cas9 protein is represented in red. The U6 promoter in green is necessary to drive the expression of the gRNAs. The BbsI enzyme in black was used to clone the gRNAs. The presence of overhangs specific for BbsI (see 2.4.5.2) ensured the correct orientation of the gRNAs into their recipient plasmids. Moreover, once ligated, the BbsI site disappeared therefore the enzyme can be used to screen for positive clone. Instead, BsaI enzyme in pink was used for the golden gate assembly. BsaI first opens the ampicillin plasmid then cut at the restriction site on the spectinomycin plasmids (see Figure 2-2). Finally, the AflIII and KpnI enzymes in grey and orange respectively was used to control the total number of gRNA cloned following golden gate assembly. **Figure adapted from Tetsushi Sakuma et al. 2014.**

In order to determine whether each individual gRNA in step 1 were properly inserted, a double digestion using BbsI and EcoRI was performed (Figure 4-3A-D). Figure 4-3A-D illustrates the digestion pattern of the four-different gRNAs from which we have five samples for the 1st, 2nd and 4th gRNAs and four samples for the 3rd gRNA. The positive control (C+) corresponded to the expected pattern for an empty plasmid with two bands at 5255 and 3421bp.

Due to the presence of a difference resistance cassette in the 1st plasmid, ampicillin instead of spectinomycin for the remaining plasmids, the size of the 1st plasmid was larger than the others (Figure 4-3A).

Figure 4-3A, B and D, we can observe that the sample 1 of the 1st, 2nd and 4th gRNAs have a digestion product similar to the C+ thereby the gRNAs are not inserted. On the other hand, as all other samples have one digestion product at 8702bp, we concluded that they were cut by EcoRI only and therefore the gRNAs were inserted. To conclude, the first step resulted in an 80% of efficiency of insertion.

The step 2 is illustrated in Figure 4-2 and 2-2 and consisted to the golden gate reaction using the BsaI restriction enzyme that enabled to cut and insert the gRNAs of each spectinomycin plasmid into the final recipient, the ampicillin resistant plasmid. As illustrated in Figure 4-2, the BsaI site of the ampicillin plasmid is located downstream of the gRNA insertion site therefore resulting to the opening of the plasmid. On the other hand, the remaining three spectinomycin plasmids have two sites for BsaI respectively upstream and downstream of the gRNAs and gRNA scaffold which resulted to small fragments of 455bp which were then inserted into the recipient ampicillin plasmid. The reaction uses the sample 2 from each gRNA (step 1). The restriction enzymes AflIII and KpnI were used to screen and identify the number of gRNAs inserted. While an empty vector (C+) had a digestion product of 8063bp, a plasmid with 4, 3 or 2 gRNA had an additional digested product at 1790bp, 1335bp or 880bp respectively. From the 13 plasmids screened, 61% appeared to have correctly integrated the four gRNAs.

To generate the hESCs line deficient for *ZDHHC8*, we used the plasmid number 2 from the second step, Figure 4-3E.

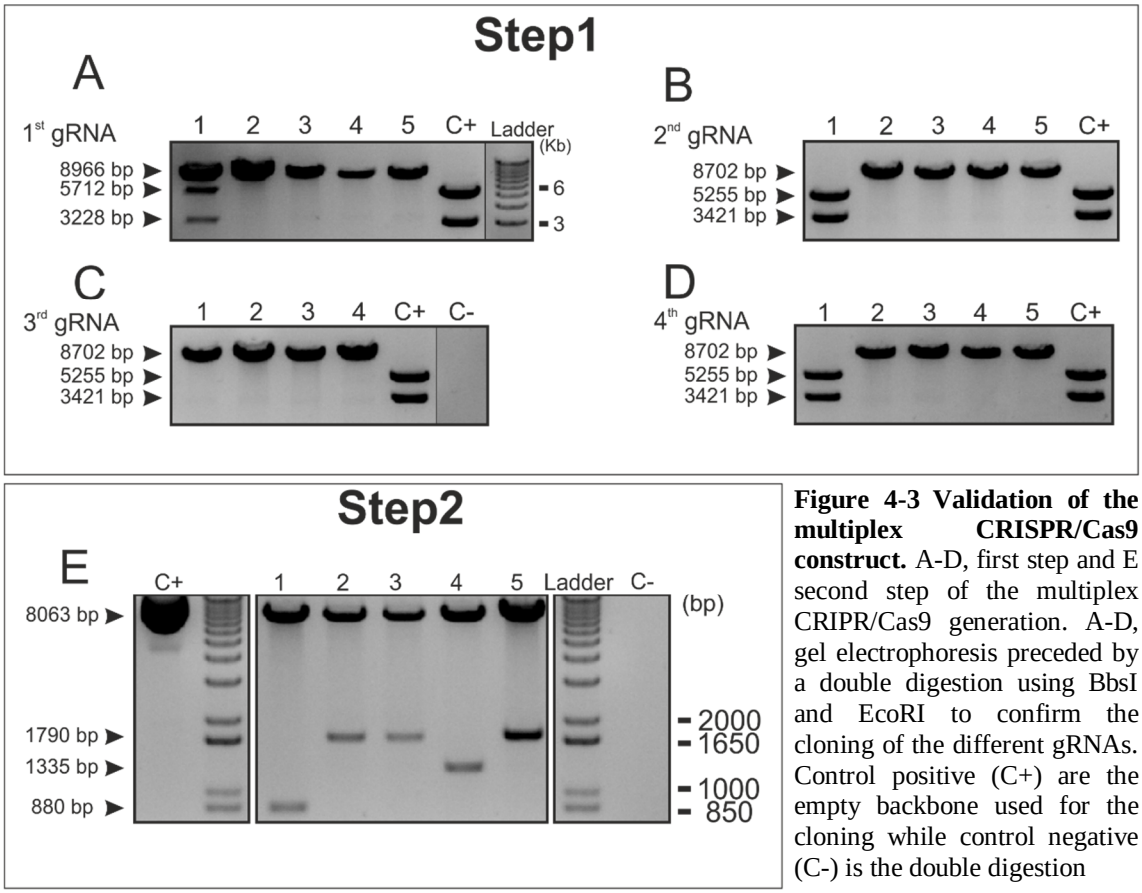

Figure 4-3 Validation of the multiplex CRISPR/Cas9 construct. A-D, first step and E second step of the multiplex CRIPR/Cas9 generation. A-D, gel electrophoresis preceded by a double digestion using BbsI and EcoRI to confirm the cloning of the different gRNAs. Control positive (C+) are the empty backbone used for the cloning while control negative (C-) is the double digestion reaction without plasmid. E, step 2 of the multiplex CRISPR/Cas, the picture represents a gel electrophoresis preceded by a double digestion by AflIII and KpnI to confirm the construction of the all-in-one CRIPSR/Cas9 by golden gate assembly. These two-restriction enzymes are flanking the region of the gRNAs. Thus, as shown, a band at 880, 1335 or 1790bp respectively correspond to a plasmid which contained 2, 3 and 4 gRNAs.

4.2.1.2. Generation of ZDHHC8-deficient hESCs

The iCas9 hESCs line was used to generate the *ZDHHC8* KO. Cells were nucleofected as described in the methods with the multiplex CRISPR/Cas9 construct along with a plasmid containing a neomycin resistant gene. Cells were cultured for five days to form individual colonies before being picked.

As shown in Figure 4-4, exon 3 and 4 of *ZDHHC8* were targeted by two gRNAs each. This particular region was chosen because it encodes the DHHC domain responsible for the enzymatic activity of ZDHHC8. Thus, frame shift mutations in this region is expected to disrupt the enzymatic activity of the protein.

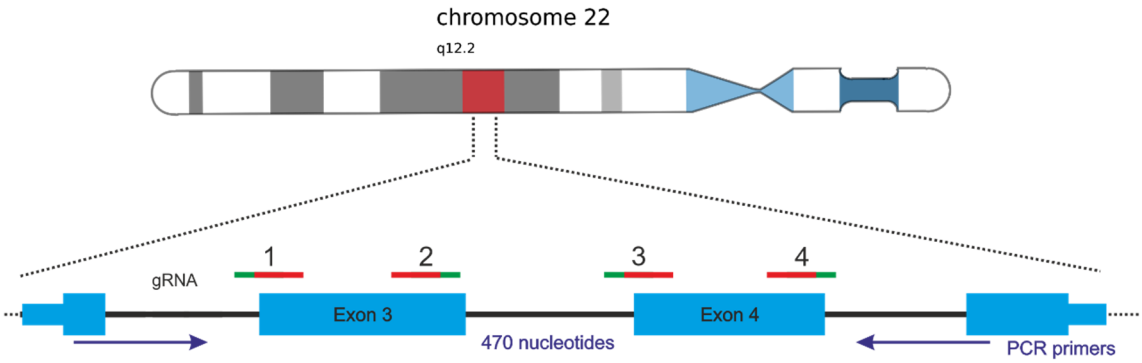

Figure 4-4 Genome editing experimental design. Exons 3 and 4 were targeted by four gRNAs respectively named 1, 2, 3 and 4. The gRNA sequence in red and the PAMs sequences in green are represented above the exon 3 and 4 in blue. One set of primers flanking the targeted region was designed to screen for INDELs in mauve. The expected PCR product was 470 baise pairs.

Genomic PCR was employed to examine whether INDELs were generated. A pair of primers was designed to encompass the four gRNAs which gave rise to a predicted 470 nucleotides amplicon in wild type allele (Figure 4-4).

Figure 4-5 illustrates an example of gel electrophoresis of the amplified PCR fragments from the parental isogenic iCas9 hESCs (C+) and four independent clones (297, 510, 539 and 541) carrying a mutation. The control amplified only one band corresponding to the predicted 470bp PCR product. On the other hand, in addition to a 470bp band, an additional amplicon of about 300bp in length was also present in clones named 297, 510, 539 and 541. This pattern suggested that these clones might be heterozygous for *ZDHHC8*. Of the 100 clones screen, 12 clones yielded an additional PCR product, all of which are around 300bp.

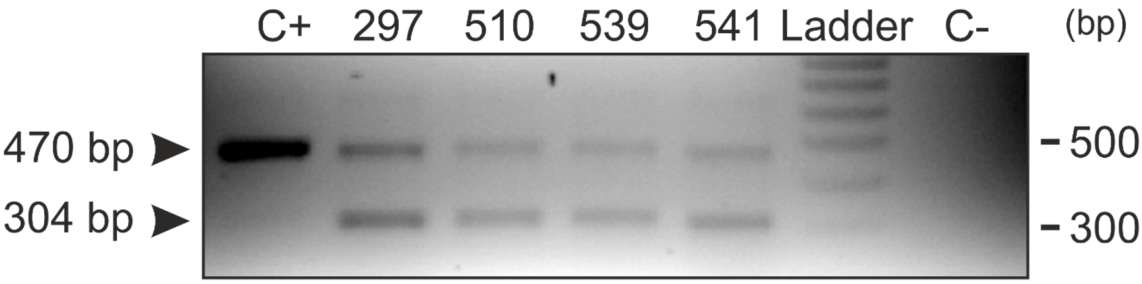

Figure 4-5 Agarose gel electrophoresis displaying screening of control iCas9 hESCs and four different clones, 297, 510, 539 and 541. The iCas9 hESCs (C+) allowed to visualize the expected amplicon size of about 470bp length. While clones 297, 510, 539 and 541 had a similar amplicon than the C+ at 470bp we observed another PCR product of 300bp length. This gel therefore implying that these clones (297, 510 539 and 541) had a potential deletion within the gDNA sequence.

PCR fragment from clones presumably heterozygous for ZDHHC8 were ligated into the pGEM-T-easy vector. Due to the presence of two different restriction sites for EcoRI flanking the cloning region, a gel electrophoresis was performed to distinguish the wildtype and mutated amplicon. The plasmids containing candidate mutant amplicons were sent for sequencing with selected wildtype controls. The result is illustrated in Figure 4-6. We observed that amongst the four-gRNAs used to target exon 3 and 4, only gRNA 2 and 3 successfully cut the DNA sequence and yielded to a deletion of 166bp length. Interestingly, the deletion was almost 100% identical between the different mutant amplicons. Furthermore, except one amplicon which had a guanine instead of an adenosine, the sequences of the WT mutant amplicons were 100% identical. The WT amplicons were also almost 100% identical except for couple of bases pairs difference at random location. In addition, in mutants and controls the WT amplicons were also similar. Overall the difference in several bases pairs was attributed to error in the sequencing process rather than mutation.

While the gDNA sequence was deleted of 166bp, the resulting mRNA sequence which contains only exons had a deletion of 83 nucleotides. This deletion was suggested to result in the appearance of a premature STOP codon and therefore a truncated protein (Figure 4-7). Figure 4-7A represents the gDNA sequence of the WT *ZDHHC8* which is composed of 11 exons. On the other hand, Figure 4-7B shows the resulting gDNA of the mutated allele of *ZDHHC8* on which we observed the disappearance of the intron 3 as well as the truncation of the exon 3 and 4. While WT full length ZDHHC8 protein is 765aa, prediction of the resulting heterozygous protein showed a truncated protein of 147aa. In addition, it appeared that the enzymatic domain of the protein, the DHHC domain is missing. Therefore, it would suggest that the palmitoylation activity would be reduced by half in the mutant.

Figure 4-6 Sequencing results of different clones. Twenty sequences were sent for sequencing, four controls together with four clones, 297, 510, 539 and 541. The sequences highlighted in yellow represent the position of the pair of primers used for the screening while in green are the location of the four-different gRNAs used to edit the *ZDHHC8* sequence. In total, we sequenced four PCR fragment for each of the clones

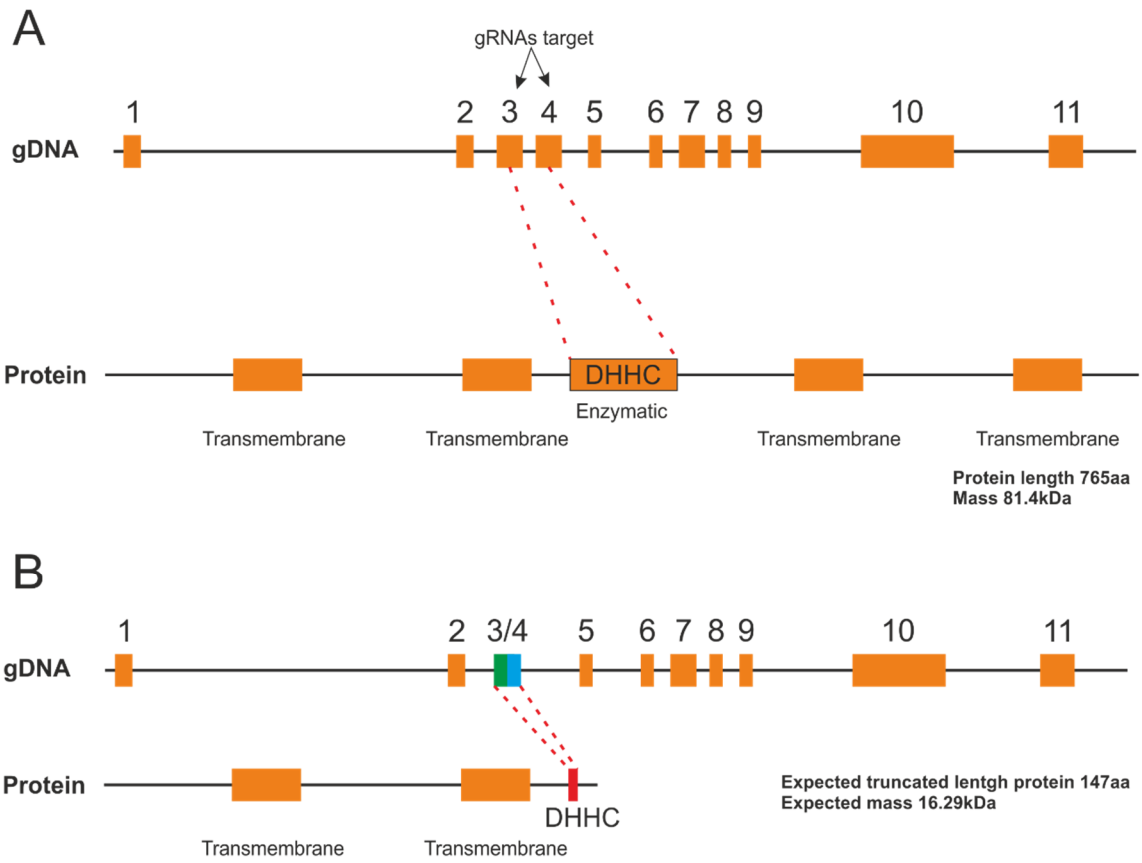

Figure 4-7 Genomic DNA and protein structure of the wild-type and heterozygous mutant for *ZDHHC8*. A, the wild-type DNA sequence encoded for 11 exons. The corresponding protein is composed of 4 transmembrane domains as well as the DHHC domain which is responsible of the palmitoyltransferase activity of the protein. The red dotted lines indicate that exon 3 and 4 are responsible of the DHHC domain translation. The wild-type full length protein is 765aa while its mass is 81.4kDa. The region targeted by the gRNA was also indicated on top of exon 3 and 4. B, in the *ZDHHC8* heterozygous mutant, we observed that the region targeted by the gRNA resulted to the disappearance of intro 3 but also the fusion of exon 3 and 4. At the protein level, this deletion is expected to give rise to a premature STOP codon resulting to a truncated protein of 147aa and a mass of 16.29kDa. The schematic demonstrated that the truncated protein is expected to have lost the DHHC domain (Red domain) therefore preventing its enzymatic activity to occur. The protein activity therefore should be reduced by half in the heterozygous mutant.

4.2.2. General phenotypic characterisation of ZDHHC8 deficient hESCs

4.2.2.1. Stem cell properties

To determine whether *ZDHHC8* heterozygous cells maintain key pluripotency properties, we examined the expression of OCT3/4, TRA1-81 and SSEA3 by immunostaining on two heterozygous (clones 297 and 541) and the parental iCas9 hESCs (Figure 4-8). OCT3/4 is a transcription factor playing a pivotal role in controlling self-renewal of embryonic stem cell, while TRA1-1 and SSEA3 are surface markers expressed by undifferentiated hESCs. As shown in Figure 4-8A and B, the majority of cells expressed OCT4, TRA1-81 and SSEA3. The proportion of cells stain positive for the different markers are similar between the control iCas9 hESCs and the two *ZDHHC8* heterozygous

lines. Therefore, the major pluripotent characteristics is preserved in *ZDHHC8*-heterozygous hESCs.

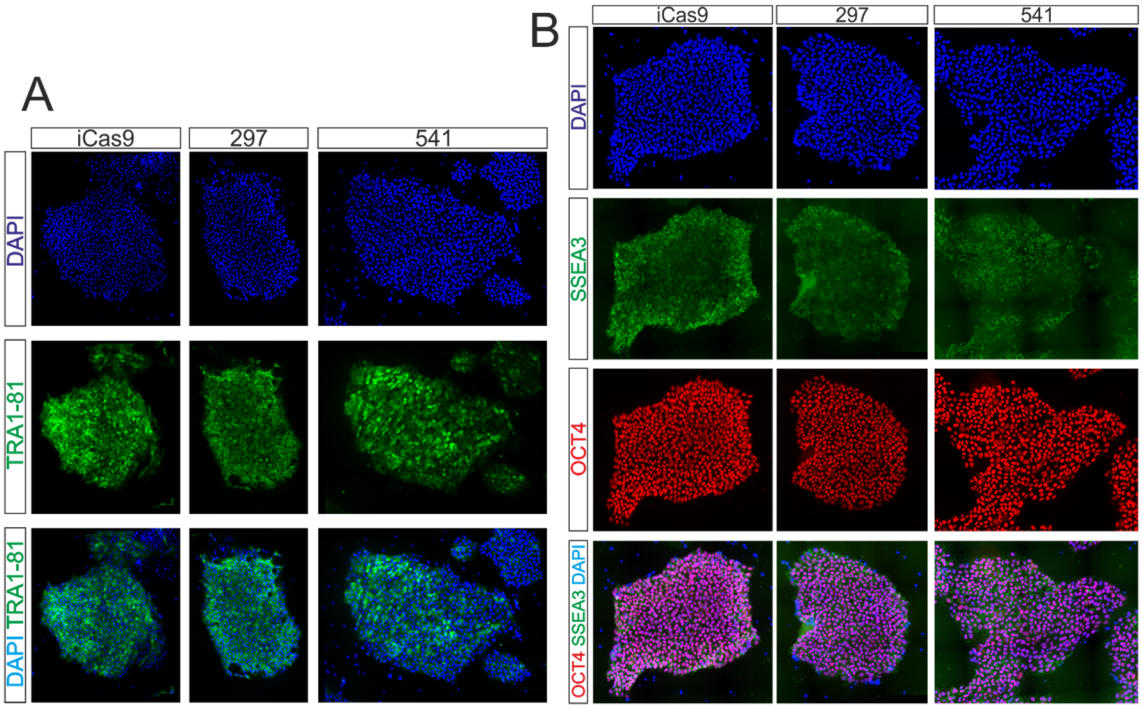

Figure 4-8 Immunofluorescence of iCas9 hESCs and two ZDHHC8+/-, 297 and 541. (A), (B) represents pictures acquire using a LEICA DMI6000B Inverted Time-lapse microscope. Those pictures are a tile scan with a magnification of 40x in order to acquire the entire colony and stained by the nuclear marker OCT3/4 and the membrane marker TRA1-81 and SSEA3. In (A), TRA1-81 is co-stained with DAPI and expressed all over the cells in all different cell line. (B), SSEA3 and OCT3/4 are co-expressed with DAPI in all cells.

In order to determine if the expression level of *ZDHHC8* was affected by the deletion, RNA was extracted from self-renewing *ZDHHC8* KO clones. One set of primers targeting the deleted exonic region was designed as illustrated in Figure 4-9 below. Thus, it was possible to assess whether the deletion in the genomic DNA (gDNA) remained at the mRNA level.

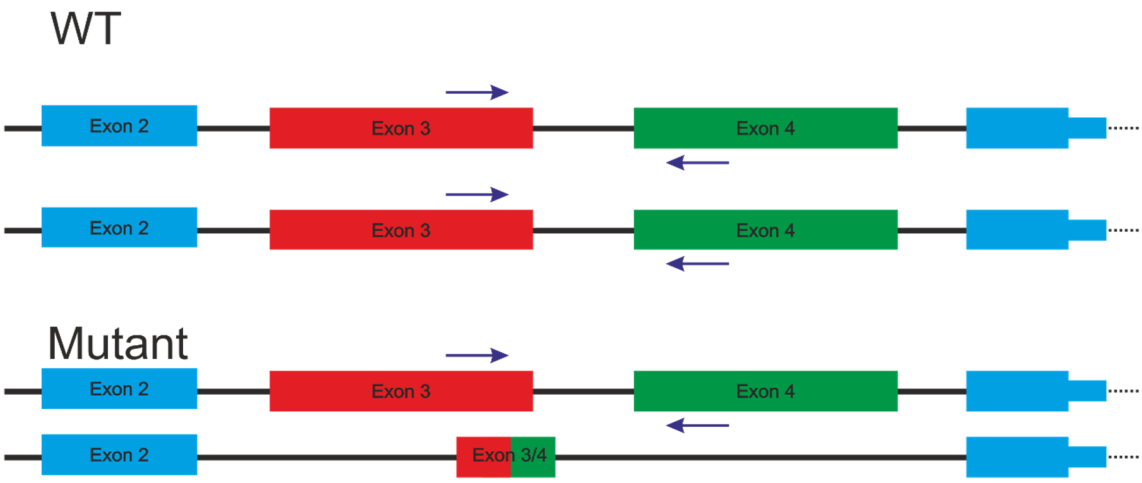

Figure 4-9 Real-time PCR screening strategy for *ZDHHC8*. One set of primer in purple was targeting the exon 3 and 4 within the deletion respectively in red and green. In WT condition, primers are targeting both allele of *ZDHHC8*. On the other hand, in the mutant condition, because the primers are targetiting the region deleted in the mutant allele of *ZDHHC8*, we are expecting to observe an expression of *ZDHHC8* which is reduced by half when compare to the control.

Figure 4-10 illustrates the relative RNA level of *ZDHHC8* in undifferentiated cells using a set of primer targeting the deleted region to assess if the deletion resulted to a decrease in the mRNA levels of *ZDHHC8*. The expression in cell line 297, 510 and 541 showed a 50% reduction of *ZDHHC8* mRNA expression. Although the clone 539 carried a similar deletion than the cell line 297, 510 and 541, the mRNA expression was unchanged.

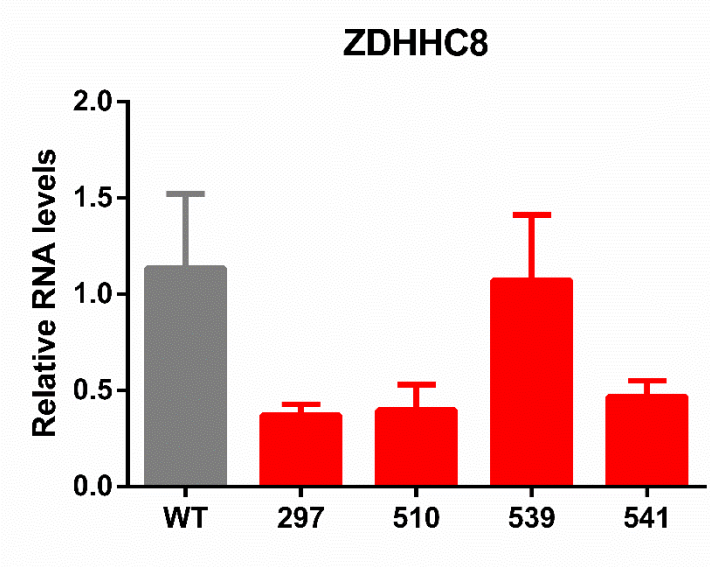

Figure 4-10 ZDHHC8 expression at the stem cells levels. Quantitavive PCR at the stem cells levels using primers for *ZDHHC8*. The primers target the region deleted in *ZDHHC8*+/-.Data were normalized to the housekeeping gene β-actin. 297, 510, 539 and 541 are four cell type that demosntrated to have a deletion between the exon 3 and 4 of the *ZDHHC8* gene. Statistical analysis using one-way ANOVA failed to demonstrated significance.

4.2.2.2. Expression of key class defining molecular markers during cortical differentiation of *ZDHHC8+/-* hESCs

Normal brain development can be 'visualised' by dynamic temporal and spatial expression of region- and cell type-specific gene markers. During pluripotent stem cell in vitro differentiation, regulated expression of these markers can be used as readout to access whether neural development is in order. To investigate whether *ZDHHC8* deletion affects the process of cortical neural differentiation, our hESCs were differentiate towards the neuroectoderm fate using dual SMAD inhibition with LDN and SB, the concentration of each compounds is shown in 2.2.3.1. Cells which are mainly of cortical excitatory neurons identity with this protocol were let to mature for the subsequent experiments. We performed a panel of immunofluorescence to evaluate the proportion of cells expressing specific markers. While we according to chapter 3, *ZDHHC8* expression was suggested to be preferentially expressed in dopaminergic neurons, experiment in chapter 3 and 4 were performed in parallel therefore we were unaware of this result at the time.

PAX6 and FOXG1 were used as markers of cortical identity (Figure 4-11). PAX6 is expressed in the neuroepithelial cells in the VZ of the developing pallium. While FOXG1 is expressed by cells in the neural plate from which the telencephalon is originating. As shown in Figure 4-11, a large proportion of cells stain positive for FOXG1 and PAX6 (Figure 4-11A and B), suggesting efficient conversion of hESCs to the forebrain fate. Moreover, we detect no difference in the proportion of PAX6+ or FOXG1+ cells between the wild-type and *ZDHHC8 +/-* cultures (Figure 4-11.C-D).

Finally, Figure 4-11E represented the temporal expression of *PAX6* in control and mutant *ZDHHC8+/-*. The expression of *PAX6* was absent from the stem cell stage. The expression profile of *PAX6* was shown to increase at day 20-30 which corresponded to the neural progenitor's cells (NPCs), while it decreased thereafter and became significantly reduced compared to day 10 from day 60 onwards. On the other hand, unlike to control, the expression of *PAX6* in *ZDHHC8+/-* showed no increases at the progenitor's stage between day 20-30. However, *PAX6* expression decreased from day 50 and become significantly reduced from day 60 onwards when compared to day10 of *ZDHHC8+/-*.

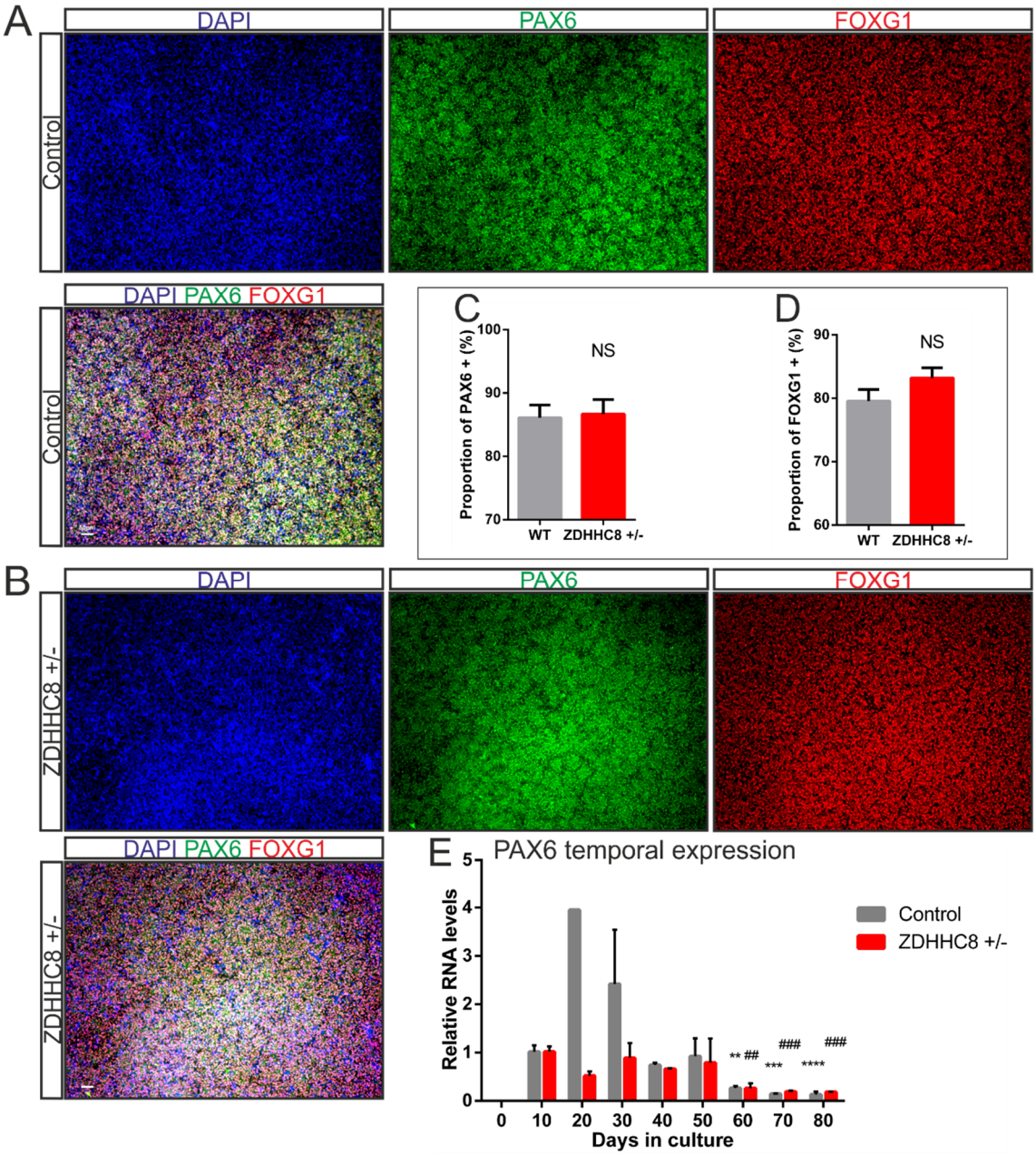

Figure 4-11 Glutamatergic precursors A-B, Immunofluorescence of control (A) and *ZDHHC8*+/- (B) glutamatergic neurons precursors at day 15 for PAX6 (green), FOXG1 (red) with DAPI counter staining, scale bar 50µm. C, quantification of FOXG1 positive cells (Control = 79.57 ± 1.820, ZDHHC8+/- = 83.19 ± 1.612, pvalue NS), two-tailed Mann and Whitney U test. D, quantification of PAX6 positive cells (Control = 86.12 ± 1.995, ZDHHC8+/- = 86.70 ± 2.298, pvalue NS), two-tailed unpaired Student's t-test. Bar chart represented the mean ± SEM. E, Temporal expression of *PAX6* gene. The data presented correspond to one experiment with n = 3 biological replicates. Data were normalised to the housekeeping gene β-actin and compared to day 10. Error bars represent +/-SEM. Statistical analysis was performed on the ΔCT value with a one-way ANOVA with Bonferroni post-hoc to compare whether for each differentiation, the expression at each time point differs from day 10 (Control and *ZDHHC8*+/-). Time point exhibiting a significant different when compared to day 10 were marked by * for control and # for *ZDHHC8*+/- (541). **P<0.01, ***P<0.001 and ****P<0.0001.

During differentiation, hESCs-derived neural epithelial cells often organize themselves in polarized structures referred to as neural rosettes. This structure has a radial arrangement that mimic the formation of the neural tube in vitro. To determine if

ZDHHC8+/- influenced the development of the neural rosette, the N-cadherin antibody which stains the apical structure of the neural rosette was used (Figure 4-12). A similar morphology and number of rosettes was observed in *ZDHHC8+/-* and control cultures, suggesting that reduced levels of *ZDHHC8* do not compromise their formation (Figure 4-12A and B). However, analysis of their area demonstrated that *ZDHHC8+/-* mutant cells have a small but significant neural rosette area ($p < 0.0001$).

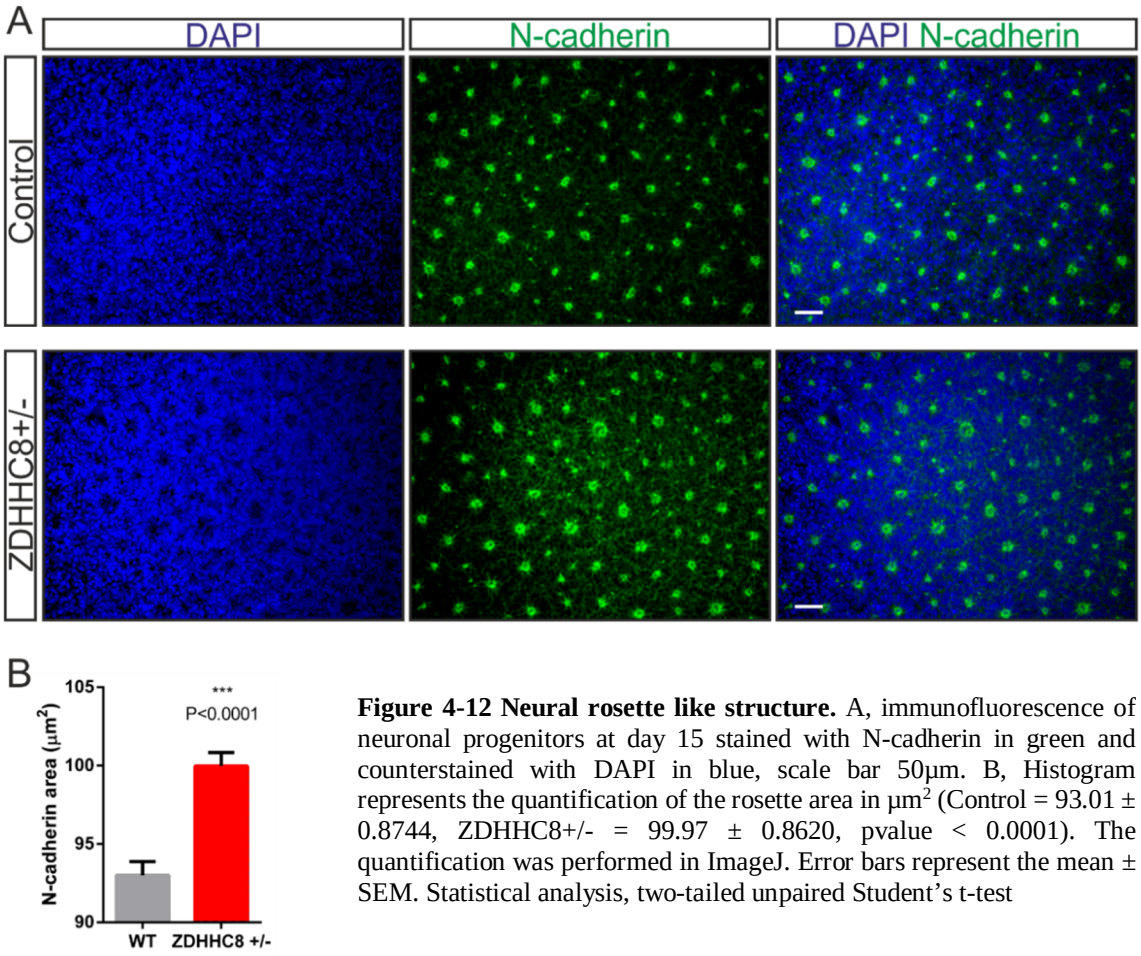

Figure 4-12 Neural rosette like structure. A, immunofluorescence of neuronal progenitors at day 15 stained with N-cadherin in green and counterstained with DAPI in blue, scale bar 50µm. B, Histogram represents the quantification of the rosette area in μm^2 (Control = 93.01 ± 0.8744, ZDHHC8+/- = 99.97 ± 0.8620, pvalue < 0.0001). The quantification was performed in ImageJ. Error bars represent the mean ± SEM. Statistical analysis, two-tailed unpaired Student's t-test

During the first ten days of differentiation, cells are transiting from pluripotent stem cells to neuroectodermal cells. At around days 10-12 of differentiation, the cultures are enriched with cycling neural progenitors. To determine whether progenitor proliferation was affected in *ZDHHC8+/-* cultures, an antibody staining for Ki67, a marker for cells in all phase of the cells cycle, was performed (Figure 4-13). Figure 4-13A displays the cells following immunostaining. Quantification of the number of positive cells demonstrated that the proportion of Ki67 positive cells in the WT was 45.71 ± 2.303 (mean ± SEM)

while it was 56.94 ± 1.679 in *ZDHHC8*+/-. Thus, these data suggested that proliferation of the neuronal progenitors were increased in *ZDHHC8*+/-.

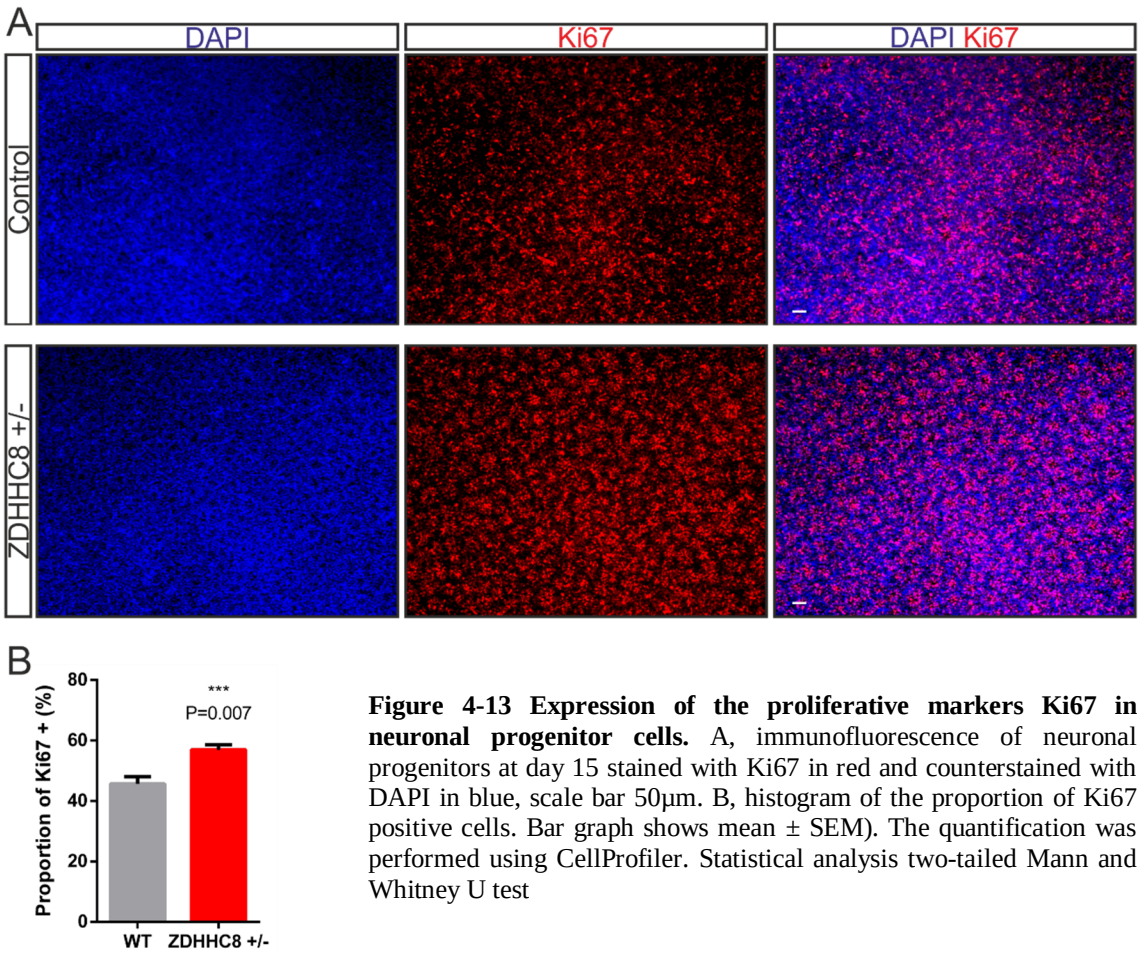

Figure 4-13 Expression of the proliferative markers Ki67 in neuronal progenitor cells. A, immunofluorescence of neuronal progenitors at day 15 stained with Ki67 in red and counterstained with DAPI in blue, scale bar 50µm. B, histogram of the proportion of Ki67 positive cells. Bar graph shows mean ± SEM). The quantification was performed using CellProfiler. Statistical analysis two-tailed Mann and Whitney U test

At day 30 of differentiation, neurons start to express proteins of the different cortical identity which start by the deep layer 5 and 6 as cortex is generated in an inside out manner. CTIP2 antibody was used to evaluate the proportion of neurons from the layer 5 (Figure 4-14A). Both control and mutant expressed CTIP2 proteins. However, quantification revealed a significant decrease of CTIP2 positive neurons in the mutant line (Figure 4-14B). Indeed, the proportion of CTIP2 in *ZDHHC8*+/- was 35.58 ± 1.653 (mean ± SEM, $P < 0.0042$) while in the control it was 45.80 ± 3.046 (mean ± SEM). Finally, we observed that the temporal expression profile of *CTIP2* (Figure 4-14) showed a peak of expression at day 30 and decreased thereafter. On the other hand, the expression of *CTIP2* increased from day 30 but remained relatively constant until day 70 and then started to decrease at day 80.

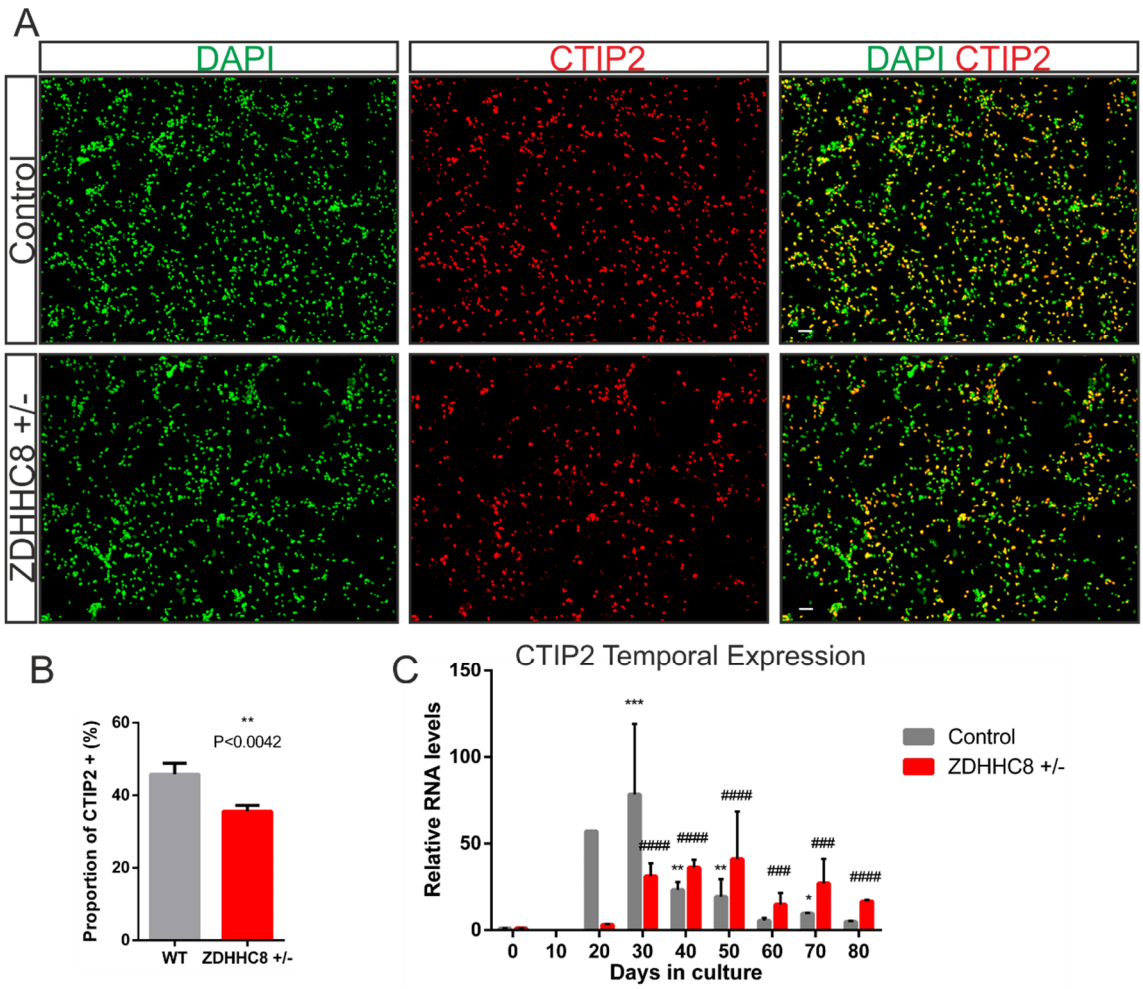

Figure 4-14 CTIP2 expression at the protein and mRNA level. A, immunofluorescence of neuronal progenitors at day 30 stained with CTIP2 in red and counterstained with DAPI in green, scale bar 50µm. B, the histogram represents the proportion of CTIP2 positive cells. Bar graph represents mean ± SEM. The quantification was performed using CellProfiler. Statistical analysis two-tailed Mann and Whitney U test. C, Temporal expression profile of CTIP2 gene. The data presented correspond to one experiment with n = 3 biological replicates. Data were normalised to the housekeeping gene β-actin and compared to day 0. Error bars represent +/-SEM. Statistical analysis was performed on the ΔCT value with a one-way ANOVA with Bonferroni post-hoc to compare whether for each differentiation (control and ZDHHC8+/-), the expression at each time point differs from day 0 (Control and ZDHHC8+/-). +/-). Time point exhibiting a significant different when compared to day 0 were marked by * for control and # for *ZDHHC8*+/- (541). The cell line used for the cortical neurons differentiation was iCas9 for the control and 541 for ZDHHC8+/-. *P<0.05, **P<0.01, ***P<0.001 and ****P<0.0001.

4.2.2.3. Gene expression analysis of *ZDHHC8*+/- hESCs derived cortical neurons

To investigate whether *ZDHHC8* heterozygous deletion affects glutamatergic neuron differentiation, we examine the expression of a panel of cortically expressed genes during the course of differentiation. RNA samples were extracted and run with the Biomark HD. Ct value above 22 were considered as not expressed and thus discarded from the analysis. The data were presented to first assess the temporal profile and therefore compared the expression to day 0. Next, we compared the expression of *ZDHHC8*+/- to the control and

therefore *ZDHHC8+/-* expression was compared to the control of the same time point. In addition, similar to chapter 3, the statistical analysis performed in this chapter are the result of one experiment with n=3 biological replicate. It was noteworthy that some time point only exhibited two biological replicates due to the presence of outliers.

Although, *ZDHHC8+/-* do not affect the expression of the pluripotency markers at the protein levels, the expression of *OCT4 (POU5F1)* is examined to determine whether *OCT4* extinction is delayed in *ZDHHC8+/-* (Figure 4-15). We observed that *OCT4* mRNA expression stopped from being expressed in both control and mutant from day 10. Furthermore, the relative level of *OCT4* at the stem cell levels was similar between *ZDHHC8+/-* and the control. Thereby, heterozygous mutation of *ZDHHC8* do not seem to alter pluripotency.

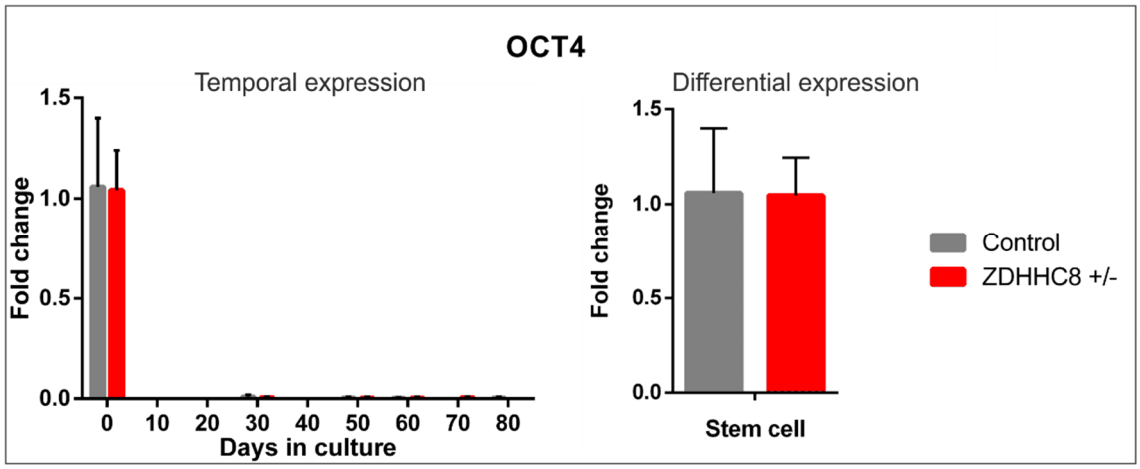

Figure 4-15 Expression of *OCT4* (*POU5F1*) during neuronal differentiation. A-B, data were first normalized to the house keeping gene β-actin. A, each time points were normalized to day 0 which was set up at 1. B, time point for *ZDHHC8* were normalized to their respective control thereby the controls time points were set up at 1. Statistical analysis revealed no difference at the stem cells levels between the control and *ZDHHC8+/-*.

4.2.2.3.1. Temporal expression profile of key markers of differentiation

In addition to the temporal expression of *PAX6* and *CTIP2*, we also investigated the profile of other key molecular markers to evaluate whether the conversion of *ZDHHC8+/-* cells into glutamatergic neurons followed a similar kinetic than the control. (Figure 4-16). These data were used to visualize the expression profile compared to day 0. Thereby, data indicated whether the expression at a given time point was different to day 0, see Figure legend. In control condition, the expression of *ZDHHC8* showed a slight increase for couple of time points while the expression in the heterozygous was constant along the course of the differentiation when compared to day 0. (Figure 4-16A). We examined the

EMX family of transcription factor, *EMX1* and *EMX2* (Figures 4.16B and C). Both genes are expressed by cells in the dorsal telencephalon however, *EMX2* is mostly expressed in the visual area of the cortex. While the *EMX1* expression rapidly decreased and remained relatively weakly expressed from day 20 to 80 when compared to day 0 in both the control and the *ZDHHC8+/-* neurons, *EMX2* expression appeared to gradually increase from day 30 to day 80. TUJ1 is a beta tubulin protein encoded by the *TUBB3* gene which is primarily expressed in neurons (Figure 4-16D). The control and the mutant neurons exhibited a similar expression profile of *TUBB3* during the course of the differentiation.

The expression of genes involved in the patterning of the cerebral cortex such as *TBR1*, *CUTL1* (CUX1) and *FOXP2* were also examined (Figures 4-16E-G). These genes were demonstrated to be expressed by cells of a specific cortical layer. *TBR1* is specifically expressed by new-born neurons from the cortical layer 6. *FOXP2* is also expressed by deep layer neurons, usually layer 5-6. *CUX1* is an upper layer marker, expressed by layer II/IV neurons. Similarly, the profile of expression of *ZDDHC8+/-* followed a similar pattern than the control for *TBR1*, *CUTL1* and *FOXP2*.

Next, we examined the temporal profile of genes that have a functional role for neurons such as genes coding for the NMDA receptors but also presynaptic genes involved in neurotransmitter transport such as VGLUTs (Figures 4-16.H-K).

In the heterozygous neurons for *ZDHHC8*, we can observe that the expression profile of *DGL4* and *GRIN2B* have a similar profile than the control (Figures 4-16H and I). The expression profile of *GRIN2A* and *SLC17A7* followed a similar trend which increase along the course of differentiation in both mutant and control. However, by day80, we observed a stronger expression of *GRIN2A* in control as well as a stronger expression of *SLC17A7* from day 50 and onwards in the control condition.

Thus, we conclude that overall, the temporal expression analysis indicated that the kinetics of the differentiation in the *ZDHHC8+/-* followed a similar profile than the control.

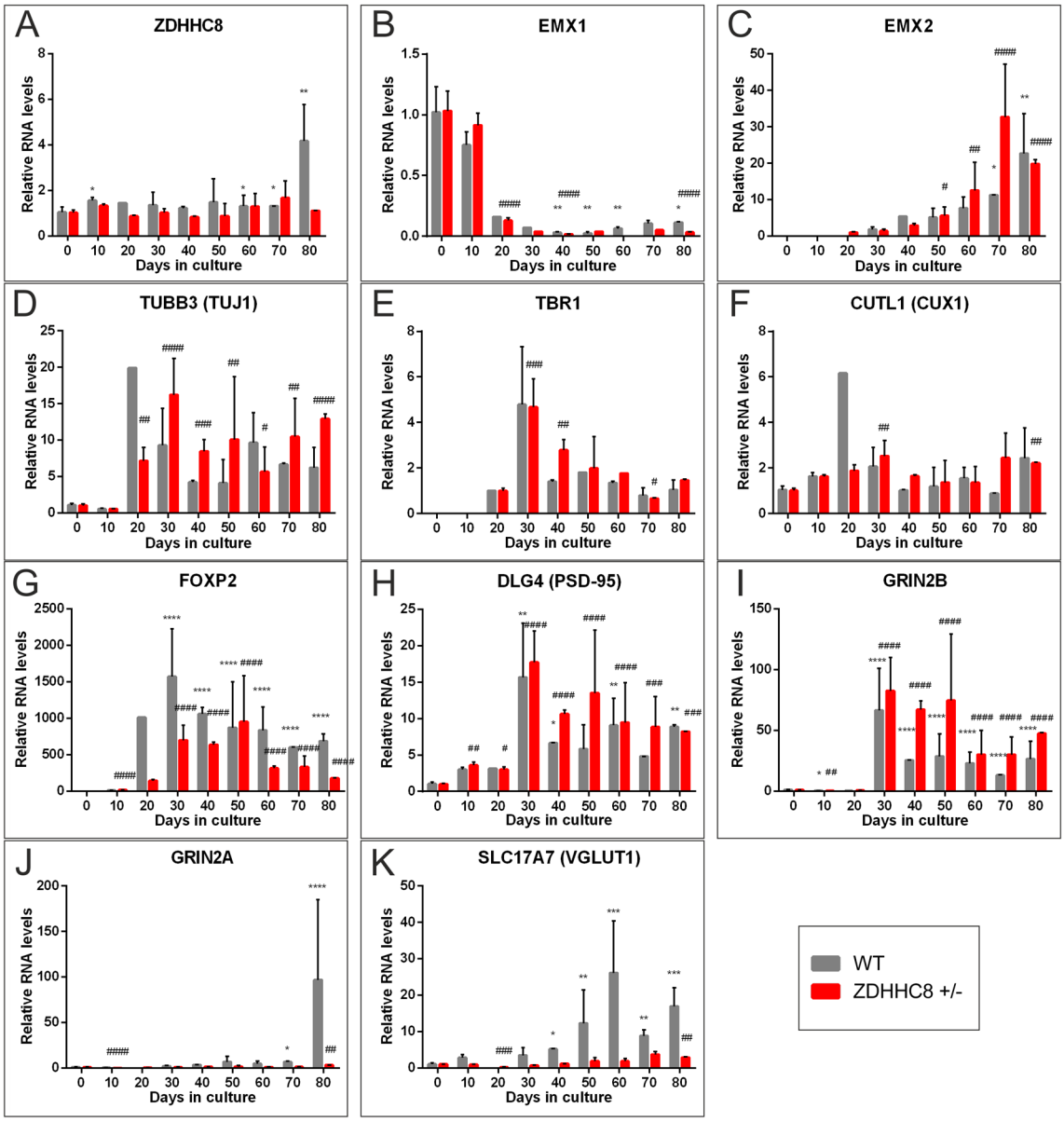

Figure 4-16 Temporal expression of key expressed gene in *ZDHHC8*+/- and the parental line. Figure legend on the next page.

4.2.2.3.2. Differential expression of key neuronal genes between control and mutant

In addition to evaluate the temporal expression, we also compared the expression of *ZDHHC8*+/- with its isogenic control to determine whether genes were found to be differentially expressed.

We investigated the expression of *PAX6* and *OTX2* (Figure 4-17B and C). We observed that the expression of *PAX6* was particularly downregulated at day 10 and 30 which correspond to the progenitor's stage (Figure 4-17B). The expression of *PAX6* remained downregulated at day 60 and 80 but in less extend than at day 10 and 30. Conversely, *OTX2* a gene expressed by forebrain and midbrain neuronal precursors, showed a strong

Figure 4-17 Temporal expression of key expressed gene in *ZDHHC8+/-* and the parental line. The control and *ZDHHC8+/-* were respectively represented in grey and red. A, *ZDHHC8*. B, *EMX1* expression was demonstrated to be significantly decreased from day 20 and onwards in both control and *ZDHHC8+/-*. At day 20 and 30 in the control and day 30, 50, 60 and 70 in *ZDHHC8+/-*, we only had one biological replicate. C, *EMX2* expression profile was significantly increased from day 50 onwards in *ZDHHC8+/-* while only significantly increased at day 70 and 80 in the control. Data in control at day 40 had one biological replicate. D, *TUBB3* (TUJ1) expression was observed to be significantly increased in *ZDHHC8+/-* from day 20 onwards when compared to day 0. Although the expression in the control appeared to be increased statistical analysis failed to reach significance. E, *TBR1* expression was significantly higher at day 30 and 40 then decreased until day 80 in *ZDHHC8+/-* when compared to day 0. While similar trend was observed in the control, statistical analysis did not reach significance as data were compared to day 30 because data at day 20 only had one biological replicate. F, *CUTL1* (CUX1) was observed to be relatively constant along the course of differentiation in control and *ZDHHC8+/-* when compared to their respective day 0. G, *FOXP2* expression was observed in both conditions to be significantly higher at day 30 then started to decrease until day 80 although data remained significantly increased when compared to day 0. H, *DLG4* (PSD-95) expression was shown to be significantly increase along the course of differentiation in both control and *ZDHHC8+/-*. I, *GRIN2B* expression was significantly increased from day 30 onwards in both control and *ZDHHC8+/-* when compared to value at day 0. J, *GRIN2A* expression showed an important and significant increase of its expression towards the end of the differentiation at day 80 in control and *ZDHHC8+/-* when compared to day 0. K, *SLC17A7* (VGLUT1) expression was observed to significantly increase along the course of differentiation in control. However, while the expression in *ZDHHC8+/-* also appeared to increase the statistical analysis failed to reach significance. The data presented correspond to one experiment with n = 3 biological replicates. Data were normalised to the housekeeping gene β-actin and compared to day 0. Error bars represent +/-SEM. Statistical analysis was performed on the ΔCT value with a one-way ANOVA with Bonferroni post-hoc to compare whether for each differentiation (control and *ZDHHC8+/-*), the expression at each time point differs from day 0 (Control and *ZDHHC8+/-*). The significance is showed using * for the control and # for *ZDHHC8+/-*. The cell line used for the cortical neurons differentiation was iCas9 for the control and 541 for *ZDHHC8+/-*. *P<0.05, **P<0.01, ***P<0.001 and ****P<0.0001.

upregulation from day 60 and day 80 while its expression was similar at earlier time point when compared to the control (Figure 4-17C). *EMX1* expression was shown to be downregulated of more than 50% in the mutant *ZDHHC8* at day 30 and 80 while similar at day 10 between control and mutant (Figure 4-17D). *EOMES* (TBR2), a transcription factor expressed by intermediate progenitor cell (IPC) also known as basal progenitors, is observed to have an expression comparable to control at day 10, however by day 30 its expression was significantly downregulated to be almost null (Figure 4-17E). Despite the strong downregulation of *EOMES* in *ZDHHC8+/-*, examination of the Ct values revealed that they were below 22 therefore the transcript of *EOMES* was present in enough proportion to be detected. *FOXP2* expression was also observed to be downregulated of about 50% in *ZDHHC8+/-* (Figure 4-17H). The expression of *TBR1* was shown to be increased at day 60 and 80 when compared to the control (Figure 4-17F). While the expression of *BCL11B* was downregulated of 50% in *ZDHHC8+/-*, at day 80 its expression was upregulated in *ZDHHC8+/-* compared to the control (Figure 4-17G). The expression of *CUTL1* did not appear to be different in *ZDHHC8+/-* (Figure 4-17I). While our differentiation protocol is thought to give rise to excitatory glutamatergic neurons, an upregulation of *GAD1* was observed at day 80 in *ZDHHC8+/-* (Figure 4-17J).

The NMDA receptor is located at postsynaptic site of the neurons. This receptor is an heterotetramer composed of four subunits. We were unable to detect the transcript of *GRIN2C* and *GRIN2D* in both control and mutant neurons. Despite the expression of *GRIN2A* was similar to the control in the mutant neurons at day 10 and 30, the expression was downregulated of almost 50% at day 60 and 80 in the mutant (Figure 4-17K).

SLC17A7 and SLC17A6 are two important genes encoding the proteins VGLUT1 and VGLU2 respectively (Figure 4-17L and 4.17M). The vesicular glutamate transporters family allows the loading of glutamate into vesicles. We observed a downregulation of *SLC17A7* from day 10 which persisted until day 80 (Figure 4-17L). Conversely, examination of SLC17A6 mRNA expression in *ZDHHC8*+/- neurons was observed to be similar to the control at day 10 and 30 while it was downregulated at day 60 and 80 (Figure 4-17M).

DLG4 encodes for PSD-95, a protein expressed at the postsynaptic membrane of the neurons which is part of the postsynaptic density (Figure 4-17N). This scaffolding protein is responsible of the anchoring of different synaptic receptors and ions channels to the membrane. The data were unable to show an alteration of *DLG4* in ZDHHC8 +/- differentiation at the mRNA levels except at day 80 which exhibited a downregulation of *DLG4* expression in *ZDHHC8*+/- neurons.

To finish, I also examined whether the expression of *ZDHHC8* was impaired during the differentiation using a similar set of primers than Figure 4-9 (Figure 4-17A). Overall, a 50% reduction of *ZDHHC8* mRNA expression at each time point was observed suggesting that the deletion was still present while undergoing neuronal differentiation.

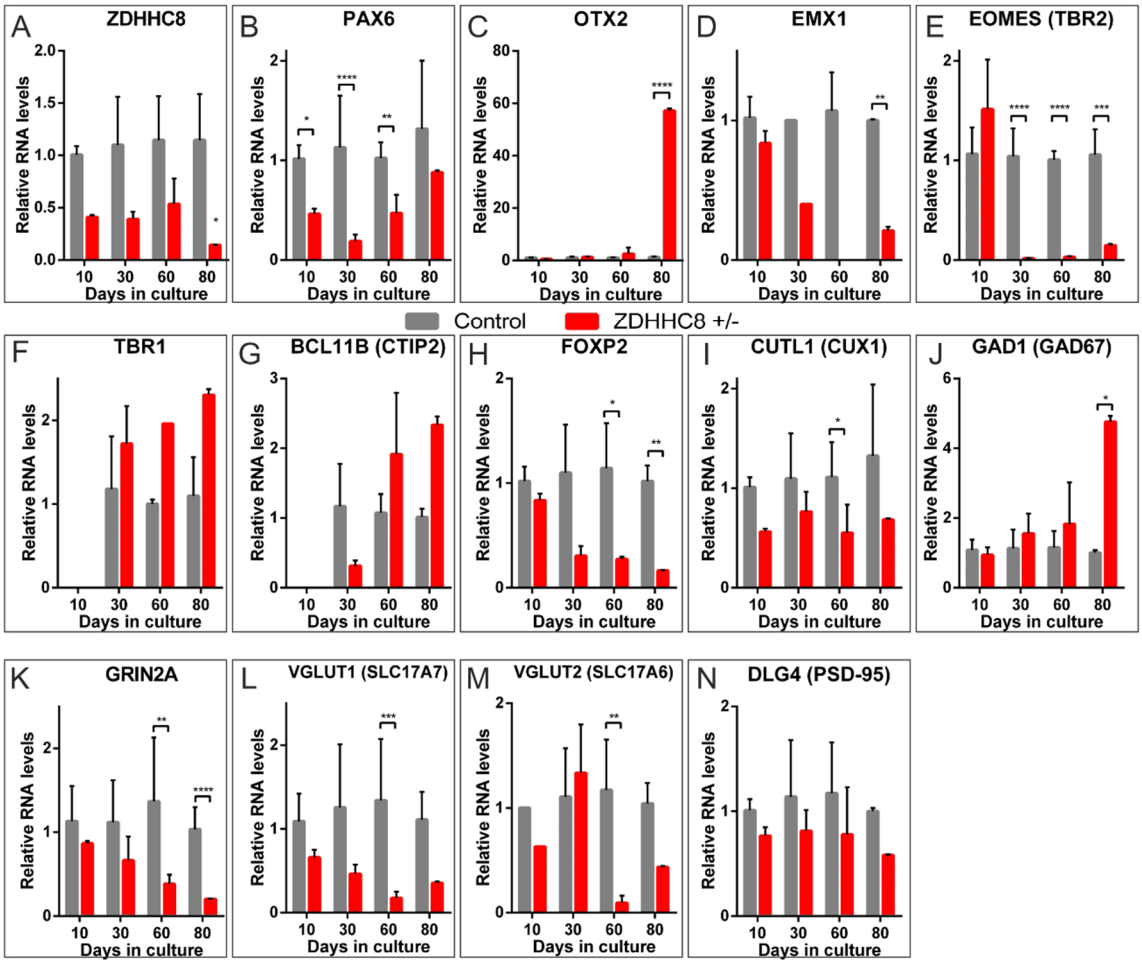

Figure 4-18 Differentially expressed genes in ZDHHC8 +/- excitatory projection neurons differentiation. WT and ZDHHC8+/- were represented in grey and red respectively. The histogram represents the mean ± SEM. A, *ZDHHC8* expression was found to be reduced in *ZDHHC8+/-* when compared to the control, however, statistical analysis only reached significance at day 80. B, *PAX6* expression was observed to be significantly reduced at day 10, 30 and 60 in *ZDHHC8+/-*. C, *OTX2* expression was strongly upregulated at day 80 in *ZDHHC8+/-*. D, *EMX1* expression was found to be downregulated at day 80 in *ZDHHC8+/-*. E, *EOMES* (TBR2) expression in *ZDHHC8+/-* was found to be significantly downregulated from day 30 onwards when compared to the control. F, *TBR1*. G, *BCL11B* (CTIP2). H, *FOXP2* expression although decrease failed to reach statistical difference at day 30, however *FOXP2* expression was significantly reduced in *ZDHHC8+/-* at day 60 and 80 when compared to the control. I, *CUTL1* (CUX1). J, *GAD1* (GAD67) expression in *ZDHHC8+/-* although similar to the control at day 10, 30 and 60, was found to be signicantly increased at day 80 in *ZDHHC8+/-*. K, *GRIN2A* was observed to be decreased at day 60 and 80 in *ZDHHC8+/-*. L, *SLC17A7* (VGLUT1) expression although it appeared reduced in the *ZDHHC8* mutant was not significant expect at day 60. M, *SLC17A6* (VGLUT2) was found to be reduced at day 60 in *ZDHHC8+/-* when compared to the control. N, *DLG4* (PSD-95). The data presented correspond to one experiment with n = 3 biological replicates. Data were normalised to the housekeeping gene β-actin and compared to day 0. Error bars represent +/-SEM. Statistical analysis was performed on the ΔCT value with a one-way ANOVA with Bonferroni post-hoc to compare whether for each differentiation (control and *ZDHHC8+/-*), the expression at each time point differs from day 0 (Control and *ZDHHC8+/-*). The significance is showed using * for the control and # for *ZDHHC8+/-*. The cell line used for the cortical neurons differentiation was iCas9 for the control and 541 for *ZDHHC8+/-*. *P<0.05, **P<0.01, ***P<0.001 and ****P<0.0001.

4.2.2.4. Motility defect in *ZDHHC8+/-* neuronal progenitors

Homozygous and heterozygous mouse model for *Zdhhc8+/-* showed alteration of axon growth and arborization in vitro due to a decrease of CDC42 palmitoylation by ZDHHC8.

In order to investigate whether ZDHHC8 is involved in the migration of excitatory neuronal progenitors, we investigated their motility using motility assay.

Excitatory neuronal progenitors at day 20 of differentiation from two independent experiments using the heterozygous mutant 541 and the control iCas9 were imaged over 12 hours and subsequently analysed. Different parameters were analysed such as the total distance, the displacement, the speed and the velocity (Figure 4-18). This analysis revealed that neuronal progenitors deficient for *ZDHHC8* migrated less when compared to the control progenitors (Figure 4-18A). The displacement was also significantly decreased in the mutants compared to the control (Figure 4-18B). It also appeared that mutant neural progenitors were significantly slower as shown by the speed and the velocity (Figures 4.18C and D).

This data suggests that *ZDHHC8+/-* impairs migration and motility of the excitatory neuronal progenitors. Because cells were too close from each other we were unable to trace neurons in order to determine their length and branching number.

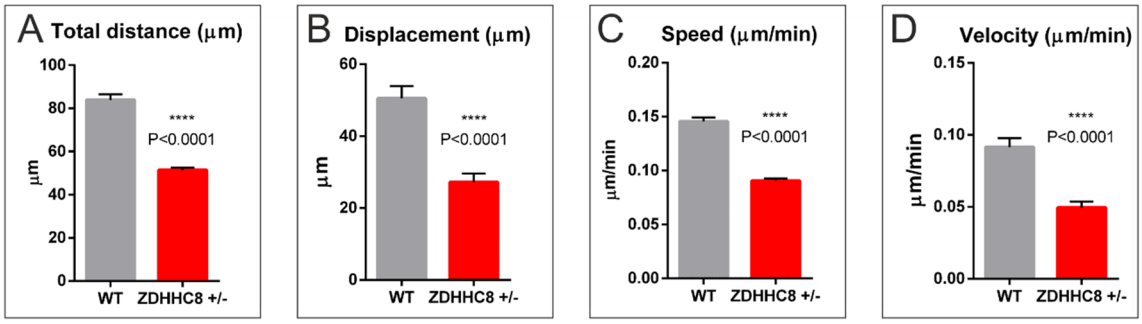

Figure 4-19 Glutamatergic progenitor cells motility. Cells were recorded for 12h in a recording chamber (Temperature, CO_2 and humidity monitored) under a light microscope. Images were acquired every 5min with a 10x objective at different location. Data were analysed and visualized using a bar plot which represent mean ± SEM. A, total migration in µm. of the WT and the KO *ZDHHC8*. Control = 83.92 ± 2.645 µm; KO = 51.42 ± 1.228 µm, P < 0.0001. B, displacement in µm, WT = 50.50 ± 3.428 µm; KO = 27.22 ± 2.411 µm, P < 0.0001. C, Migration speed in µm/min, WT = 0.1456 ±0.003627 µm/min; KO = 0.09055 ± 0.001964 µm/min, P < 0.0001. D, Velocity in µm/min, WT = 0.09155 ± 0.006285 µm/min; KO = 0.04955 ± 0.004178 µm/min, P < 0.0001. Statistical analysis was performed using a Mann-Whitney U test. N = 2 WT with 218 values and 2 KO with 180 values.

4.2.2.5. Calcium activity is enhanced in *ZDHHC8+/-*

Due to the important role of palmitoylation at the synapses (Figure 4-1). We investigated whether *ZDHHC8* deficiency had an impact on spontaneous neuronal calcium activity in excitatory projection neurons. Indeed, as explained in chapter 1, calcium activity is responsible of several signalling pathways in neurons amongst them the release of

neurotransmitter from the presynaptic neurons. Thereby we used the calcium indicator Fluo-4AM in order to evaluate the calcium activity in vitro in neurons comparing *ZDHHC8+/-* with the control parental line. The calcium activity from excitatory projection neurons in a solution of aCSF was acquired using an inverted fluorescent microscope equipped with a LED setup. The questions we were interested were: 1) whether the calcium activity was different between the WT and ZDHHC8 mutant cultures; 2) how ZDHHC8 neural cells were maturing in the context of calcium activity during long time culture. Three different clones of *ZDHHC8* heterozygous cells (297, 541 and 510) and a control (iCas9) were used in this study with neurons recorded at different time points as presented in the table 12.

Table 4-1 Time point analysed for each cell line

Cell line	Time points in days
Control – iCas9	60, 70, 80, 110, 130, 150
ZDHHC8 +/- 541	60, 70, 80, 110, 130, 150
ZDHHC8 +/- 297	60, 70, 80, 110
ZDHHC8 +/- 510	60, 70

To determine the longitudinal calcium activity maturation, we first examined the calcium activity in the control cells line (iCas9) (Figure 4-19). The calcium amplitude represented the variation of the calcium intensity emitted by the Fluo-4 dye. The amplitude was represented as $\Delta F/F_0$ from which ΔF represents the variation in the calcium intensity at a given time while F_0 is representing the fluorescence calcium intensity at the beginning of the experiment. We observed that the calcium amplitude remained similar from day 60 to 80 with a value of $\Delta F/F_0$ around 0.06 in the control cell line. However, by day 110 the amplitude reached an average of 0.2438 ± 0.008220 but decreased by day 130 until day150 to be 0.06028 ± 0.002085 (Figure 4-19A).

The interspike interval (ISI) represented the interval between two spikes. Instead, the total number of events described the average number of spikes occurring at a given time point recorded from all the active cells in our different fields of view. During the course of the differentiation, an overall decrease of the ISI was observed in the control which was correlated by an increase number of spikes (Figure 4-19B and C). Except at day 110 which exhibited a high ISI and low number of spikes, the average ISI varied from 106 ± 5.926 seconds at day 60 to 41.64 ± 2.077 seconds at day 150 (Figure 4-19B). Similarly, the average number of events varied from 5.386 ±0.2636 at day 60 to 25.39 ± 0.785 at

day 150 (Figure 4-19 C). Thereby, when the ISI decreased, the number of events was instead increased.

The rise was defined as the time necessary to reach half of the maximal amplitude while the fall time corresponded to decay of the calcium event (Figures 4.19D and E). From day 60 to 80, the average control rise time was 1.30 ± 0.038 seconds. By day 110, it unexpectedly increased to reached 1.745 ± 0.017640 seconds however it decreased to reach 0.7563 ± 0.01207 seconds at day 150 (Figure 4-19D). Figure 4-19E illustrates the evolution of the calcium decay time. Overall, the average fall time in the control cell line kept increasing from 0.8093 ± 0.027410 seconds at day 60 to 1.56 ± 0.01349 seconds at day 150 (Figure 4-19E).

Therefore, we observed that despite the amplitude remained relatively similar during the course of the differentiation, the ISI and the number of events were observed to be decreased and increased respectively during the course of the differentiation. Therefore, these data demonstrated that in vitro excitatory projection neurons derived from embryonic stem cells have the ability to mature which was demonstrated by the increase in the number of events occurring during spontaneous calcium activity which was correlated with the decrease in the ISI.

Next, we decided to investigate whether the *ZDHHC8* mutation altered the calcium activity in neurons and also compared its activity with the control neurons. Strikingly, the *ZDHHC8* KO neurons exhibited an overall higher amplitude compared to the control from day 60 to 80 (day 70 $P_{297} < 0.0001$, $P_{510} < 0.0001$, $P_{541} < 0.0001$). Although the amplitude was higher in the control at day 110 and 130, at day 150 it was higher in the mutant clone 541.

The ISI in the mutant *ZDHHC8* was observed to constantly decrease at each recording time. In the mutant, except at day 70 at which two mutant clones exhibited similar value of ISI than the control, all remaining recording time points displayed a significant decrease of the ISI in the mutant (day 80, $P_{297} = 0.0002$, $P_{541} < 0.0001$; d150, $P_{541} < 0.0001$). The total number of calcium events appeared to also constantly increase while *ZDHHC8+/-* neurons mature. At day 60 they were on average 9.5 ± 0.2813 events during the recording while it increased to reach 86.01 ± 1.343 events at day 150 in the mutant clone 541.

The rise time in the mutant *ZDHHC8* was very heterogenous from day 60 to 80. While the rise time was significantly slower (higher values, day 60 $P_{541} = 0.0015$, day 70 $P_{541} = 0.0008$) than the control for clone 541 at day 60 and 80, we observed that it was faster (lower values) than the control in the clone 297 and 510 (day 60, $P_{297} < 0.0001$, $P_{510} = 0.0001$; d70 $P_{297} < 0.0001$, $P_{510} = 0.0017$). From day 110 and onwards, the mutant *ZDHHC8+/-* had values of rise time that were significantly lower than the control therefore the rise time were faster in the mutant neurons. Similarly to the control, the decay time of the calcium transient in the mutant kept increasing at each recording time point. From 0.8217 ± 0.01373 seconds at day 60 it was 1.763 ± 0.01396 seconds at day 150 for the clone 541. When compared to the control, we observed that the fall time was significantly higher in the mutant *ZDHHC8.*

Table 13 depicts the number of cells analysed per cell lineages and time point.

Table 4-2 Number of cells analysed per cell lineages and time point

Cell lineages	D60	D70	D80	D110	D130	D150
iCas9	210	155	166	816	476	778
541	549	363	228	581	1347	768
297	301	334	212	639	/	/
510	267	104	/	/	/	/

To conclude, the control cells demonstrated a maturation of the neurons which was demonstrated by a decrease of ISI and increased of the number of events. A similar trend was also observed for the different KO for *ZDHHC8*. However, the data suggested that the neurons heterozygous for *ZDHHC8* mature faster than the control. Although we observed some variability between the different KO, the difference was usually in the same direction especially for day 110. However, while maturing, although the rise time of the calcium amplitude appeared to be faster, the fall time was observed to be slower.

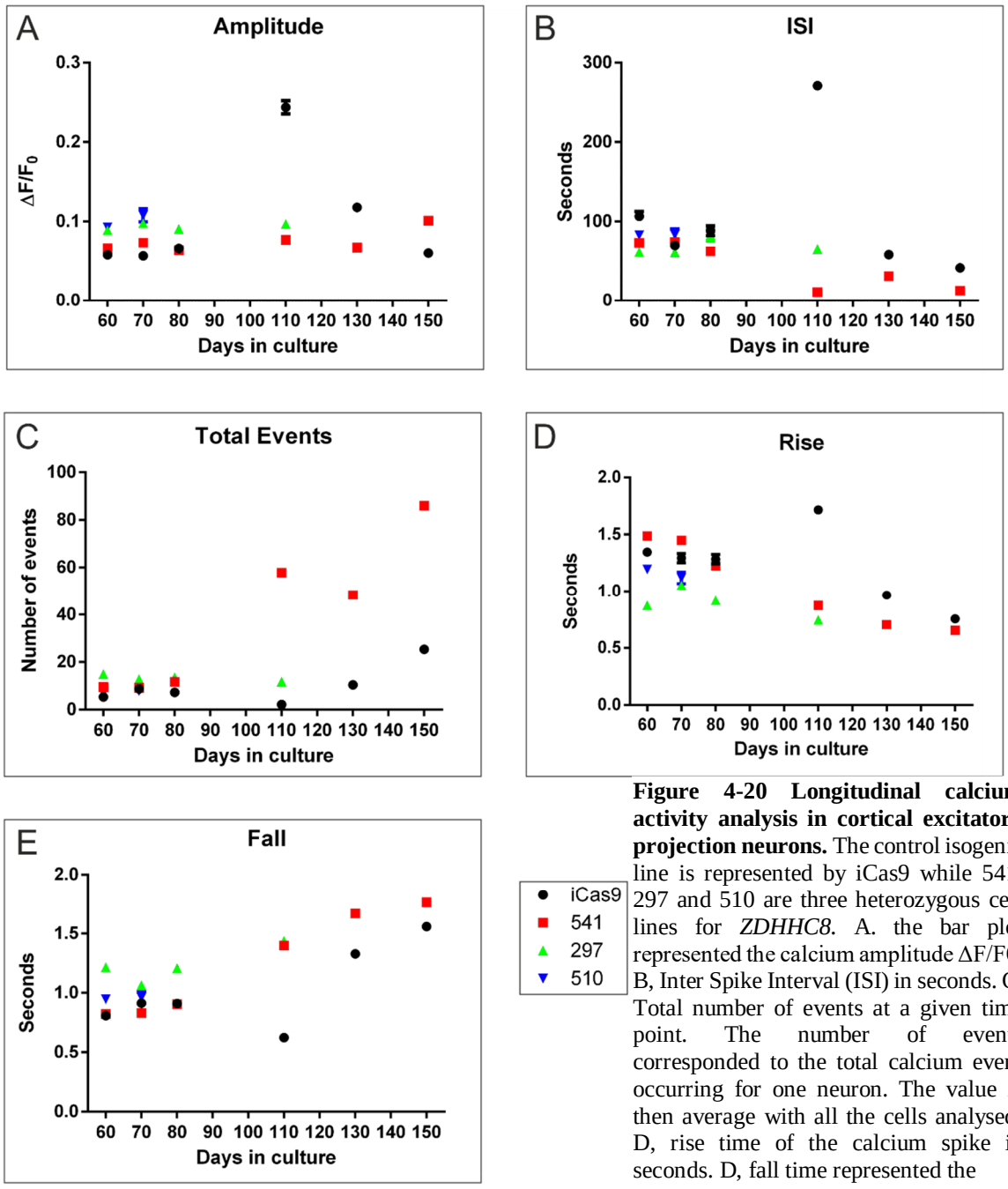

Figure 4-20 Longitudinal calcium activity analysis in cortical excitatory projection neurons. The control isogenic line is represented by iCas9 while 541, 297 and 510 are three heterozygous cell lines for *ZDHHC8*. A. the bar plot represented the calcium amplitude ΔF/F0. B, Inter Spike Interval (ISI) in seconds. C, Total number of events at a given time point. The number of events corresponded to the total calcium event occurring for one neuron. The value is then average with all the cells analysed. D, rise time of the calcium spike in seconds. D, fall time represented the decay of the calcium spike. The data presented in the graphics are the results of the recordings of hundred of neurons across different field of view. Data are presented as the mean +/-SEM, howver, they are very small therefore not visible. Statistical analysis was performed using a two-tailed unpaired Student's t-test comparing each condition to the control. Calcium activity was analysed in Matlab, using the FluoroSNNAP package.

Figure 4-20 illustrated calcium traces recorded and their respective temporal raster plot from the control cell Cas9, KO 541 and 297 at day 110 and 150 for the control and the KO 541.

We observed that the control cells only displayed two calcium events (Figure 4-20A). However, while analysing different neurons, a similar pattern was observed (Figure 4-20B). Indeed, the raster plot of six random cell displayed similar spontaneous calcium events

Although the number of events was significantly higher for the KO 541, we observed a similar phenomenon than the control in the KO 541 and 297 (Figure 4-20A-B). Therefore, by day 110, we start to observe that the spontaneous calcium activity become synchronizes across our recordings. Furthermore, this synchronicity was also observed at day 130 (data not shown) and 150 (Figure 4-20C-D). It was noteworthy that the number of events also increased from day 110 to 150 (Figures 4-19C, 4-20C-D). Figure 4-20D represented the calcium activity of six cells randomly selected. Similar than day 110, most neurons were active together as a network.

While calcium is important for the physiology of the cells, in a preliminary experiment (data not shown), we examined whether the incubation of specific drugs would block the calcium signalling. The main purpose was to determine whether the signal we acquired was due to calcium activity mediated by action potential or by the movement of calcium from the different internal storage of the cells. We observed that upon incubation of the neurons in a solution of aCSF containing Tetrodotoxin (sodium channel blocker), AP5 and CNQX, the calcium signalling activity of the neurons become quiet. Therefore, we conclude that the calcium signal was mediated by synaptic activity as otherwise cells would have remained active.

To conclude, we found that is possible to assess neuronal maturation using calcium imaging. Furthermore, while maturing the spontaneous calcium transient evolve from an asynchronous to a synchronized activity.

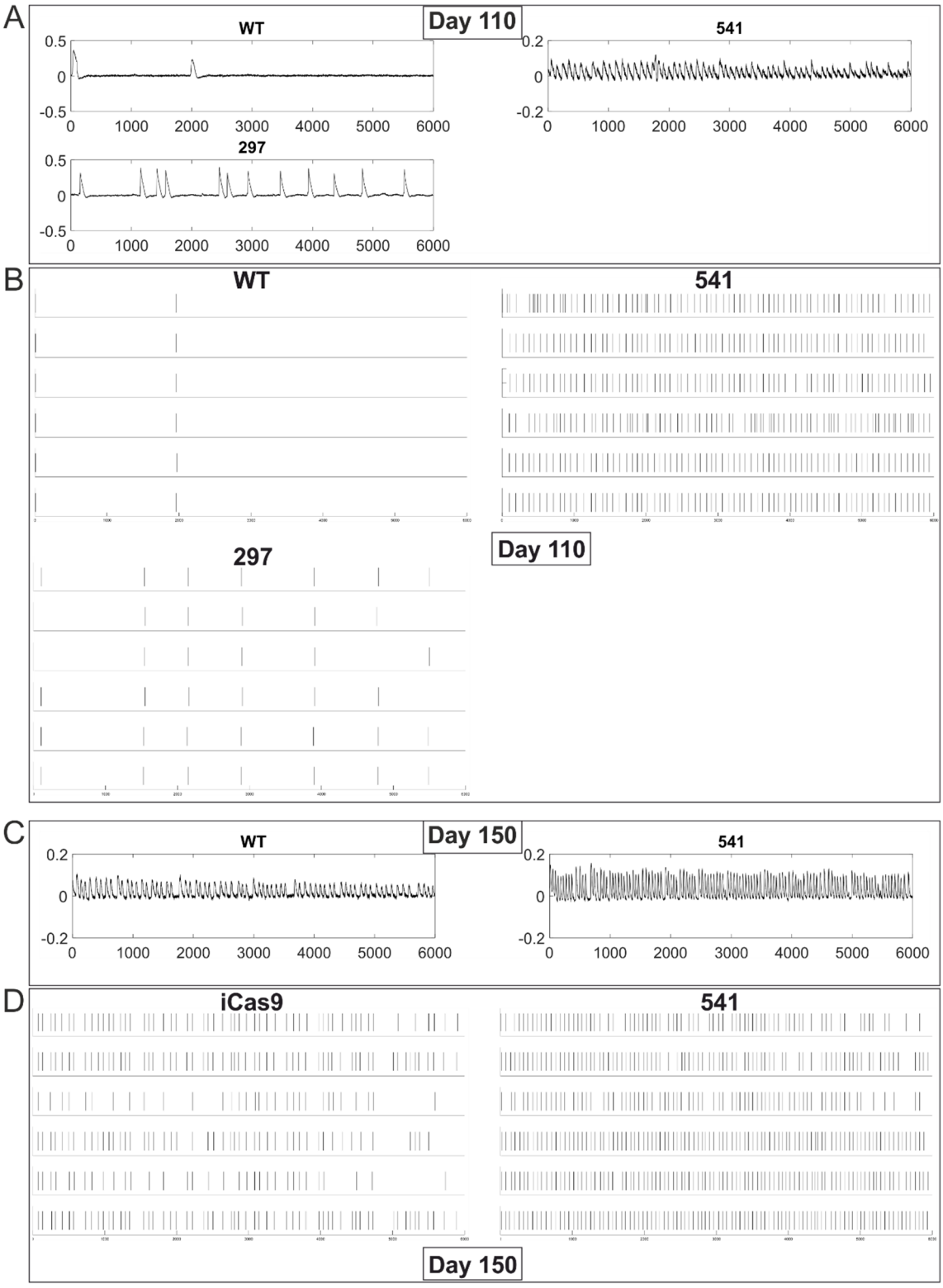

Figure 4-21 Calcium trace and raster plot of control and *ZDHHC8*+/- glutamatergic neurons. 541 and 297 are two heterozygous line for *ZDHHC8* which were differentiated into glutamatergic excitatory neurons. A and C represented the calcium trace recorded with their respective spikes recorded for 10min or 6000s. Each traces represented a single cells. B and D, raster plot of couple of cells at day 110 and 150 respectively. Each bar on the raster plot represented a calcium event. The X-axis represents the time in milli-seconds.

4.3. Discussion

While animals carrying either heterozygous or homozygous *Zdhhc8* deletions were previously generated, investigations of its role in hESCs derived excitatory projection neurons has yet to be reported. This study therefore aimed to investigate whether *ZDHHC8* influenced human cortical projection neuron development.

While we successfully generated lines carrying a heterozygous deletion using the CRIPSR/Cas9 technique, the different clones were genetically the same with disruption that occurred in the middle of exon 3 and 4. It resulted to the deletion of the intron 3 and the fusion of the upstream and downstream sequence of exon 3 and 4 respectively (Figure 4-7).

In order to understand why only gRNA 2 and 3 were able to cut the gDNA sequence, it would be interesting to sequence the plasmid used for the generation of our heterozygous line. Indeed, although we observed the integration of 4gRNA, it still remains possible that we had ligated two gRNA 2 and 3 instead of one of each gRNA.

Although the heterozygosity of these clones was confirmed by sequencing at the gDNA level, we were unable to confirm a change at the protein level. Several ZDHHC8 antibodies tested yield multiple bands in western blot in the control. Even if all these antibodies were expected to detect regions of the protein that is deleted in our heterozygous, we were unable to detect the wild-type protein in our control condition. Despite several attempts were made using a blocking peptide in order to determine which bands corresponded to the wild-type ZDHHC8 protein, it failed to give satisfactory result. Other attempts should be made aiming at varying the different incubation time during the western blot process, such as the blocking step or else the antibody incubation.

Several attempts were also made in order to generate a homozygous hESCs line for *ZDHHC8*. We used the same gRNAs that were shown to be efficient and anticipated that it would target the second allele. To overcome this issue, we decided to design a multiplex lentiviral vector (Alessandra Sperandeo) which was based on the publication from Kabadi et *al.*2014 (Kabadi et *al.* 2014). Although we successfully managed to generate the lentiviral vector, at the moment we did not start the lentivirus production yet. Due to the overall higher efficiency of lentivirus compared to conventional plasmids, we would expect to generate a homozygous line based on the hemizygous deletion. Although 22q11.2DS is a hemizygous deletion, using a homozygous will allow us to study in more depth the function of *ZDHHC8* during neuronal differentiation.

Study reporting a decrease of neural stem cells proliferation in patients with schizophrenia are thought to result in decrease of the cortical thickness in several brain areas in schizophrenic individuals, interestingly such observation was also found in 22q11.2DS carriers (Jalbrzikowski et *al*. 2013; Reif et *al*. 2006). Interestingly, our data suggested the opposite, we observed an increase in proliferation of the neural progenitor cells (Figure 4-13). As the area of the rosettes was also observed to be increase in *ZDHHC8+/-* (Figure 4-12). We suggested that the increase of neural rosettes area and the proliferation of the progenitors might be related. Thus, it would be interested to determine first the identity of the cells which displayed an increase proliferation, then determine whether these cells survived over the course of the differentiation.

Apart from Nissl staining which were used to evaluate the mouse brain morphology, which moreover appeared to be normal in both *Zdhhc8+/-* and *Zdhhc8-/-* no extensive analysis was performed (Mukai et *al.* 2004). Overall, although they were slight fluctuation in the temporal expression profile of *ZDHHC8* in the control condition, the temporal profile was considered as being constant along the course of differentiation in both control and *ZDHHC8+/-* (Figure 4-16).

The temporal expression of key markers of neuronal differentiation was used to examine the kinetics of differentiation of the *ZDHHC8+/-* neurons, therefore to assess whether *ZDHHC8+/-* alter the process of differentiation. Our analysis did not reveal an alteration of the kinetics of differentiation in the *ZDHHC8* KO neurons. On the other hand, we observed that several genes in *ZDHHC8+/-* are differentially expressed when compared to the control. Examination of the relative mRNA expression of crucial developmental and synaptic genes in *ZDHHC8+/-* differentiation revealed a significant downregulation of *PAX6* mRNA at day 10 and 30 which corresponded to the peak of its expression (Figure 4-17B). Therefore, it would be interesting to examine whether we also observed a decrease of PAX6 protein by quantifying the protein in western blot.

We observed an overall significant downregulation of the mRNA expression of *EMX1*, *EOMES* and *FOXP2*. *Emx1* is part of the EMX family, in mouse study, this gene was shown to be restricted to the dorsal telencephalon while *Emx2* is expressed in the dorsal and ventral telencephalon. Our data suggested a downregulation of 55% of *EMX1*. Interestingly, while studies using homozygous knockout for *Emx1* provide evidence regarding its role in cortical aeralization, others showed that *Emx1* knockout reduced the migratory capacity of the neural stem cells (Kobeissy et *al.* 2016; Muzio et *al.* 2003). It would be interested to determine if this decrease at the mRNA level would result to a

decrease at the protein level using western blot. We could also perform immunocytochemistry to examine whether the proportion of cells positive for EMX1 are also decreased in *ZDHHC8+/-*. Similarly, *Eomes* is important for neurogenesis as it promotes the generation and proliferation of IPCs in vivo. Thereby, TBR2 depletion in the mouse cortex was demonstrated to decrease the proliferation of cells from the SVZ but also decrease the proportion of IPCs which overall led to a decrease of the cortical plate (Sessa et *al.* 2008). While we observed an increase in cell proliferation at day 15, it would be interested to examine whether this alteration in proliferation still occurs at later time point when cells that express TBR2 are generated. *FOXP2* encodes a protein which is mainly expressed by deep layer neurons in the cortex. Loss of *FOXP2* has been associated with severe speech and language disorders. As patients with 22q11.2DS were also observed to have delay in the emergence of speech it would therefore be interested to investigate whether it could be due to *ZDHHC8* (Solot et *al.* 2001). Therefore, immunocytochemistry that would examine the proportion of cells positive for EMX1, FOXP2 and TBR2 but also the quantification of these proteins by western blot would enable us to determine whether these alterations at the mRNA level are associated with a difference at the protein level between *ZDHHC8+/-* and the control condition.

Interestingly, we observed an upregulation of *GAD1* (Figure 4-17J). This gene is known to be enriched in inhibitory neurons and is responsible of the decarboxylation of glutamate to GABA (Erlander et *al.* 1991; Fenalti et *al.* 2007). Although small proportion of inhibitory neurons are always found in our excitatory projection neurons protocol, we observed an upregulation of *GAD1* expression by day 80 in the KO for *ZDHHC8* which might suggest a higher propensity of the remaining mitotic cells to differentiate towards inhibitory neurons. However, two genes are responsible of the decarboxylation of GABA, while *GAD1* is localized throughout the cell, *GAD2* (GAD65) was instead observed to be mostly localized at the synapses (Soghomonian et *al.* 1998). To determine if *ZDHHC8* heterozygous alters the proportion of GABAergic cells it would be interesting to derived hESCs deficient for *ZDHHC8* using a protocol of cortical interneurons. Furthermore, it would also be interested to evaluate the proportion of both GAD65 and GAD67 positive cells in our culture.

The proportion of the synaptic protein PSD-95 and VGLUT1 were shown to be impaired in *Zdhhc8+/-* and *Zdhhc8-/-* mouse model (Mukai et *al.* 2008). In this study, we showed that both *SLC17A7* and *SLC17A6* mRNA were downregulated. VGLUT1 and VGLUT2 are mainly expressed by glutamatergic neurons but not exclusively. These proteins are

responsible for glutamate uptake into synaptic vesicles, thus their alteration could affect the glutamatergic synaptic transmission (Vigneault et *al.* 2015; Zander et *al.* 2010). Studies investigating the role of VGLUT1 identified that mice homozygous knockout despite not showing phenotypic change at birth, presented severe coordination impairment, learning and memory deficits (Takamori 2006). On the other hand, VGLUT2 is predominantly expressed during embryonic development and homozygous knockout is lethal immediately after birth(Wallén-Mackenzie et *al.* 2010). Although we observed a downregulation of both *SLC17A7* and *SLC17A6*, we have no indication whether their reductions result in a decrease of their proteins level. It would therefore be interesting to address this question by quantifying the proportion of both VGLUT1 and VGLUT2 proteins in mature neurons but also to identify whether these proteins could be palmitoylated by ZDHHC8.

PSD-95 is a major scaffolding protein localized at the postsynaptic density of excitatory glutamatergic neurons (Gomperts 1996). It allows the clustering of the different synaptic proteins such as AMPA and NMDA receptors (Chen et *al.* 2015). PSD-95 alteration has been associated with neurodegenerative disorder but also psychiatric disorders such as schizophrenia and ASD (Catts et *al.* 2015; Shao et *al.* 2011; Xing et *al.* 2016). Despite our study did not reveal an alteration of the *DLG4* expression it did not indicate whether ZDHHC8+/- protein is altering PSD-95 protein. Indeed, several studies demonstrated that in order to be correctly addressed to the postsynaptic membrane, PSD-95 required to be palmitoylated (El-Husseini et *al.* 2000). Interestingly, the palmitoylation enzyme was shown to be ZDHHC8 which upon phosphorylation by the brain specific PKC isoform protein kinase Mζ (PKMζ) is able to palmitoylate PSD-95 (Yoshii et *al.* 2011; Yoshii et *al.* 2014). In addition, mouse model of 22q11.2DS demonstrated a decrease proportion of PSD-95, interestingly a similar phenotype was observed in mouse deficient for *Zdhhc8*. Therefore it was postulated that the decrease of PSD-95 in mouse model of 22q11.2DS could be attributed to the loss or the alteration of the palmitoyl activity of ZDHHC8 (Mukai et *al.* 2008). Using acyl-biotin exchange in our *ZDHHC8+/-* heterozygous, we could identify whether PSD-95 requires to be palmitoylated by ZDHHC8 furthermore it would allow us to identify additional proteins that are targeted by ZDHHC8.

Neuronal migration occurred in two distinct mechanism in the forebrain, by radial or tangential migration (Nadarajah et *al.* 2002). While radial migration is thought to be the principal mode of migration of cortical excitatory neurons, the cortical interneurons are migrating from the MGE and LGE through tangential migration. Thus, the correct

position of neurons within the brain is essential for the correct neuronal circuitry. Alteration can therefore be responsible of several disorders such as schizophrenia (Rehn et *al.* 2005). Migrating neurons are known to be highly polarized in the direction of their movement (Marín et *al.* 2010). Neuronal migration which is also called locomotion is composed of three steps. First, cells extend a leading process which then lead to the translocation of the nucleus and finally, the cell retracts all its processes. The leading process usually acts as a compass by migration toward or avoiding chemotactic cues. Migration is dependent on different mechanisms which involved adhesion molecule such as N-cadherin or SEMA3A receptor, both were shown to be important for the regulation and stability of the processes (Chen et *al.* 2008; Jossin et *al.* 2011). On the other hand, regulation of intracellular signalling involves proteins like slit-robo or GTPase activating protein (srGAP2) which stimulates branching and thus slows the migration (Guerrier et *al.* 2009). Our data identified that neuronal progenitor cells deficient for *ZDHHC8* showed indication of migration defect. Future work would be needed to identify which steps of the migration process was altered and also identified which genes/proteins is associated with this alteration. Neurons from primary neuronal culture of *Zdhhc8+/-* mice was shown to exhibit shorter axons and dendritic arborisation which were demonstrated to be due to a defect in CDC42 palmitoylation, a protein part of the Rho GTPase family. As Rho GTPases are a regulator of radial migration it might therefore be interesting to identify whether other members of this family are affected by *ZDHHC8* mutation such as Rac1 which is known to affects lamellipodia and therefore important for axonal growth (Ng et *al.* 2004; Woo et *al.* 2006).

In order to determine whether *ZDHHC8* mutation altered the physiology of the neurons, we decided to use calcium imaging as a readout for neuronal function. Here, we identified that glutamatergic neurons deficient for *ZDHHC8* exhibited an increased calcium activity compared to control. Indeed, these neurons have a higher amplitude as well as an increase in the number of spontaneous calcium transients. We also identified that the calcium activity was first asynchronous but over the course of differentiation gradually become synchronous, suggesting that these neurons form connexion. This switch in their activity might explain the strong decrease in spontaneous calcium events occurring in the control at day 110. Indeed, by day 130, control neurons exhibited a large increase in the number of events which kept increasing until day 150 therefore the pattern at day 110 is likely to be due to the switch from an asynchronous to a synchronous activity. In addition, these data also showed that this switch might happen earlier in the *ZDHHC8* heterozygous

mutant compared to control as we did not observe alteration of the number of calcium events in this population during our recordings. To determine whether synchronisation involves the appearance of more synaptic connexion, we could use the advantage of the modified rabies virus (Reardon et *al*. 2016). Indeed, this technique allow to map monosynaptic connexion through retrograde trans-synaptic transfer. Furthermore, during neuronal development, spontaneous calcium activity regulates many processes including neuronal migration, axonal outgrowth, dendritic patterning and synaptic receptors maturation (Komuro et *al.* 1998; Spitzer 2006; Wong et *al.* 2002). Calcium concentration is characterized by the balance between influx and efflux (Grienberger et *al.* 2012). Therefore, several studies focused on identifying the compartment or receptors from which the calcium activity arise (Kirwan et *al.* 2015). It would therefore be interesting to identify in a similar way which synaptic receptors are responsible of the spontaneous calcium activity. This could be achieved by using drugs which are known to block specifically a receptor and then record the subsequent calcium activity. Furthermore, it was demonstrated that ion channels as well as voltage gated calcium channels required to be palmitoylated to be correctly addressed to the pre and post-synaptic membrane (Shipston 2011). Furthermore, study have suggested that palmitoylation might regulate calcium channel inactivation (Hurley et *al.* 2000). As in our study we observed an overall increase in spontaneous calcium activity it might suggest that one of these channels require palmitoylation by ZDHHC8 and therefore might explain the increase in the calcium activity in *ZDHHC8+/-*.

Previous studies have demonstrated the utility of protein palmitoylation for their correct function and localization. While in this study we obtained a heterozygous mutant for *ZDHHC8,* we currently have no data assessing the resulting proteins level of potential target of ZDHHC8. However, the Figure below represents a schematic representation of what we should expect with our mutant *ZDHHC8* and therefore might explain our motility and calcium data. While in normal condition, PSD-95 proteins receive the addition of a palmitate by ZDHHC8 and therefore are properly targeted to the postsynaptic membrane. In *ZDHHC8+/-* due to the expected reduction in the palmitoyl activity, we suggest, that ZDHHC8 protein would be unable to palmitoylate all PSD-95 proteins therefore would result to a PSD-95 impairment at the postsynaptic membrane. It was noteworthy that this example is expected to apply for other proteins than PSD-95. Indeed, the impaired motility observed in our NPCs heterozygous for *ZDHHC8+/-* could result from impaired

CDC42 palmitoylation which are thought to be a protein involved actin cytoskeleton. In addition, we also suggest that the increase of calcium activity in *ZDHHC8*+/- could result from either a decrease palmitoylation of a protein responsible of calcium channel inactivation or else the decrease of a specific channel or voltage gated channel at the surface of neurons.

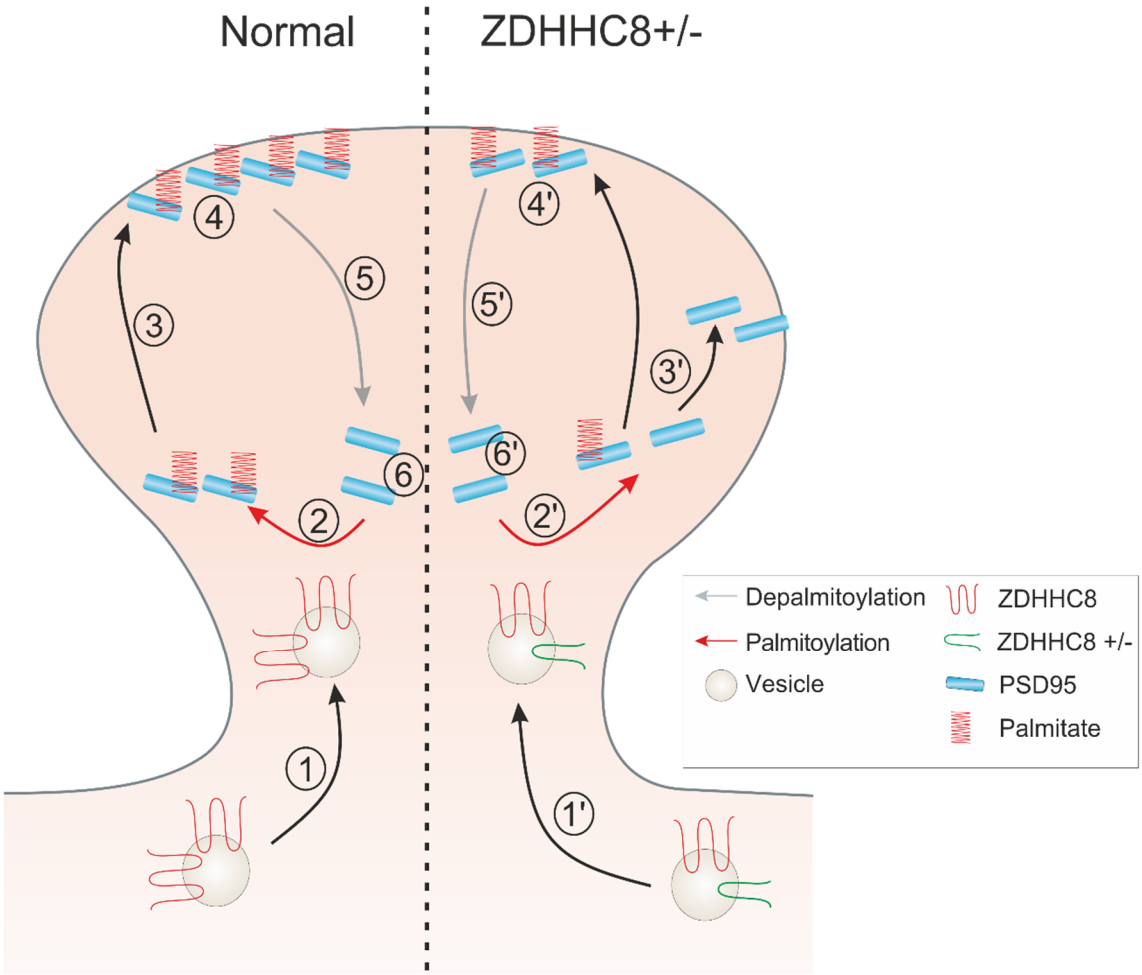

Figure 4-22 Putative PSD-95 protein palmitoylation defect at the postsynaptic membrane. In normal condition, vesicle carrying ZDHHC8 protein are transported towards the dendritic spine (1). The palmitoyltransferase activity of ZDHHC8 will result to the addition of a 16C fatty acid onto the protein (2) which will enable its targeting and insertion to the postsynaptic membrane (3 and 4). PSD-95 will then be depalmitoylated (5, 6). In ZDHHC8+/-, while the protein is expected to still be able to be transported to the spine (1'), the palmitoyltransferase activity which is expected to be reduced by half (2') would result to only a fraction of the proteins to be palmitoylated which imply that only proteins with the palmitate will be able to be properly adressed to the membrane (3' and 4'). The protein will similar to control be depalmitoylated (5' and 6').

To summarize our data from this chapter, it is the first time a hESC line heterozygous for *ZDHHC8* was generated. While no defect was observed at the embryonic stem cells level, we identified several genes (Figure below) whose expression was suggested to be downregulated in red and upregulated in green by the *ZDHHC8* heterozygous mutation.

Furthermore, phenotypic characteristic of the motility and spontaneous calcium activity respectively identified decrease (red) and increase (green) in NPCs and neurons deficient for *ZDHHC8.*

While motility defect has been observed in 22q11.2 carriers, it's too early to conclude whether the increase in spontaneous calcium activity resulted with an increase in neurotransmitter release as demonstrated in patient carrying a 22q11.2 deletion (Earls et *al.* 2010), however further study should consider to identify the proteins targeted by ZDHHC8 in order to elucidate its role during these processes.

5. Transcriptomic analysis of neural progenitors derived from *ZDHHC8* +/- hESCs and 22q11.2DS iPSCs

5.1. Introduction

Individuals with 22q11.2DS have higher probability to develop psychiatric disorders such as schizophrenia. Whereas the 22q11.2 pathology has already been intensively studied using engineered animal model, the possibility of reprogramming fibroblast into iPSCs allows investigations into 22q11.2DS in a human setting. Several studies already reported the successful reprogramming fibroblasts from 22q11.2 patients into iPSCs which were subsequently differentiated into neuronal fate (M. Lin et *al.* 2016; Pedrosa et *al.* 2011).

Lin et *al.* has previously performed a RNA sequencing (RNA-seq) study using iPSCs lines derived from eight 22q11.2 patients and seven control subjects (M. Lin et *al.* 2016). IPSCs were differentiated to a mix population of glutamatergic and GABAergic cortical neurons (Marchetto et *al.* 2010). The study revealed a 2-fold reduction of almost all of the transcripts from genes of the 22q11.2 region except *CLDN5* and *TBX1*. Amongst the 12981-proteins coding transcripts identified, 782 were differentially expressed between the controls and 22q11.2 neurons. Gene ontology (GO) terms enrichment analysis identified dysregulated genes related to apoptosis as well as immune response while GO terms related to cell cycle, glutamate metabolic process and synaptic transmission were upregulated.

Despite the generation of mouse model homozygous and heterozygous for *zdhhc8*, the transcriptome of these mice remains unknown. In the previous chapter, we showed that hESCs heterozygous for *ZDHHC8* had an increase neuronal rosette area. Neuronal rosettes express several markers of neurectoderm and form columnar structure that mimic the formation of the neural tube in vivo. Cells within the rosettes are capable of symmetrical division to constitute the pool of cells which will become neurons.

Furthermore, our study on neurons derived from hESC heterozygous for *ZDHHC8* revealed an increase in cells proliferation which was assessed by Ki67 immunostaining. In addition, we discovered that excitatory neuronal progenitors were migrating slower and less when compared to neuronal progenitors from an isogenic control. Finally, evaluation of the neuronal calcium activity revealed alterations in neurons mutant for *ZDHHC8*. As several aspects of the development of neuronal progenitor was suggested

to be affected in *ZDHHC8*+/- progenitor cells, we decided to investigate whether specific neuronal pathways were affected in our model. To our knowledge, how ZDHHC8 deficiency affects gene expression has not been reported. Therefore, transcriptomic analysis would be able to shed light on molecular pathways regulated by *ZDHHC8*.

Due to the availably of fibroblasts from carrier of a 22q11.2DS, we generated our own 22q11.2 iPSCs. In a pilot experiment performed by Alessandro Sperandeo, both control and 22q11.2 iPSCs were differentiated using a protocol of cortical excitatory projection neurons. During neuronal rosettes formation that usually occurs at the NPCs stage, we observed an alteration of their morphologies exhibiting various shapes (unpublished data). While, immunofluorescences examination of the developing forebrain marker FOXG1 and the neuroectodermal marker PAX6 suggest that both cells line correctly convert to neuronal fate, the proportion of cells positive to PAX6 was observed to be significantly decreased in 22q11.2 NPCs. In addition, the proportion of SOX2 positive cells, was observed to be decreased in 22q11.2 NPCs. SOX2 is a transcriptional factor crucial for stem cells regulation, furthermore, this protein is also important for the proliferation and maintenance of dorsal telencephalic neuronal progenitor cells (Zappone et *al.* 2000).

Therefore, in this chapter we performed a genome wide transcriptomic analysis using excitatory neuronal progenitors at day 15 derived from a line of 22q11.2 iPSCs (E11), a line of control iPSCs (900), a hESCs line heterozygous for *ZDHHC8* (541) and its isogenic control (cas9).

Aims

- To differentiation hESCs and iPSCs (iCas9'control', 541'*ZDHHC8*+/-', 900'control' and E11'22q11.2') in a protocol of excitatory projection neurons.
- To compare the transcriptome of *ZDHHC8* mutant with the control
- To determine whether genes overlap between *ZDHHC8*+/- and 22q11.2 neuronal progenitors

5.2. Results

5.2.1. Experimental design and quality control of RNA samples

Four different cell lines were used for the purpose of this experiment a *ZDHHC8* heterozygous line (541) and its isogenic control (iCas9), a control iPSCs from a healthy subject (900) and a 22q11.2 line. All four-cell line were differentiated using a protocol of cortical excitatory projection neurons (Chambers et *al.* 2009; Espuny-Camacho et *al.* 2013). The experimental procedure for neuronal differentiation was illustrated in Figure 5.1. At day 15 of differentiation, RNA samples from 6 biological replicates per cells line were extracted.

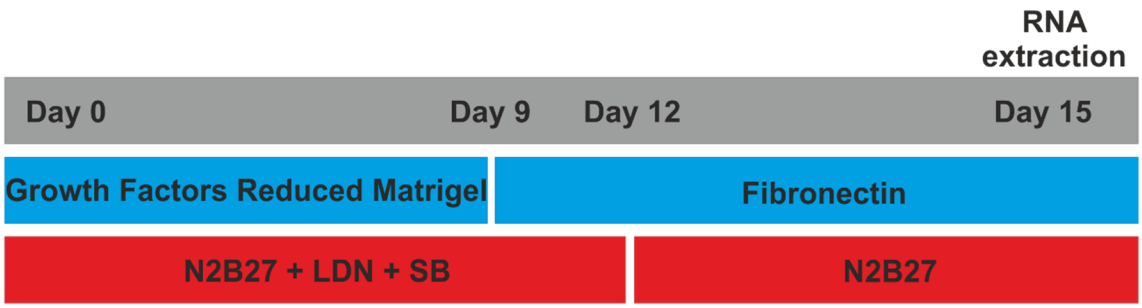

Figure 5-1 Glutamatergic neurons differentiation. Schematic of the cortical excitatory neuronal progenitor's differentiation. The grey area is representing the timeline; the blue area represents the different coating composition while the red area is the media composition. At day 15 all RNA samples were extracted, 6 biological replicates per cell line. The concentration of LDN and SB are described in 2.2.3.1

5.2.1.1. Immunofluorescence of glutamatergic progenitors

To verify whether our different cells line properly commit to neural fate, we stained our cultures of cortical progenitors which were fixed on the same day of the RNA extraction at day 15 (Figure 5.2). PAX6 and FOXG1 antibody were used as markers of neuroepithelial and telencephalic cell markers respectively. A high proportion of PAX6 and FOXG1 positive cells were observed in all four lines which suggest a proper induction into cortical progenitors.

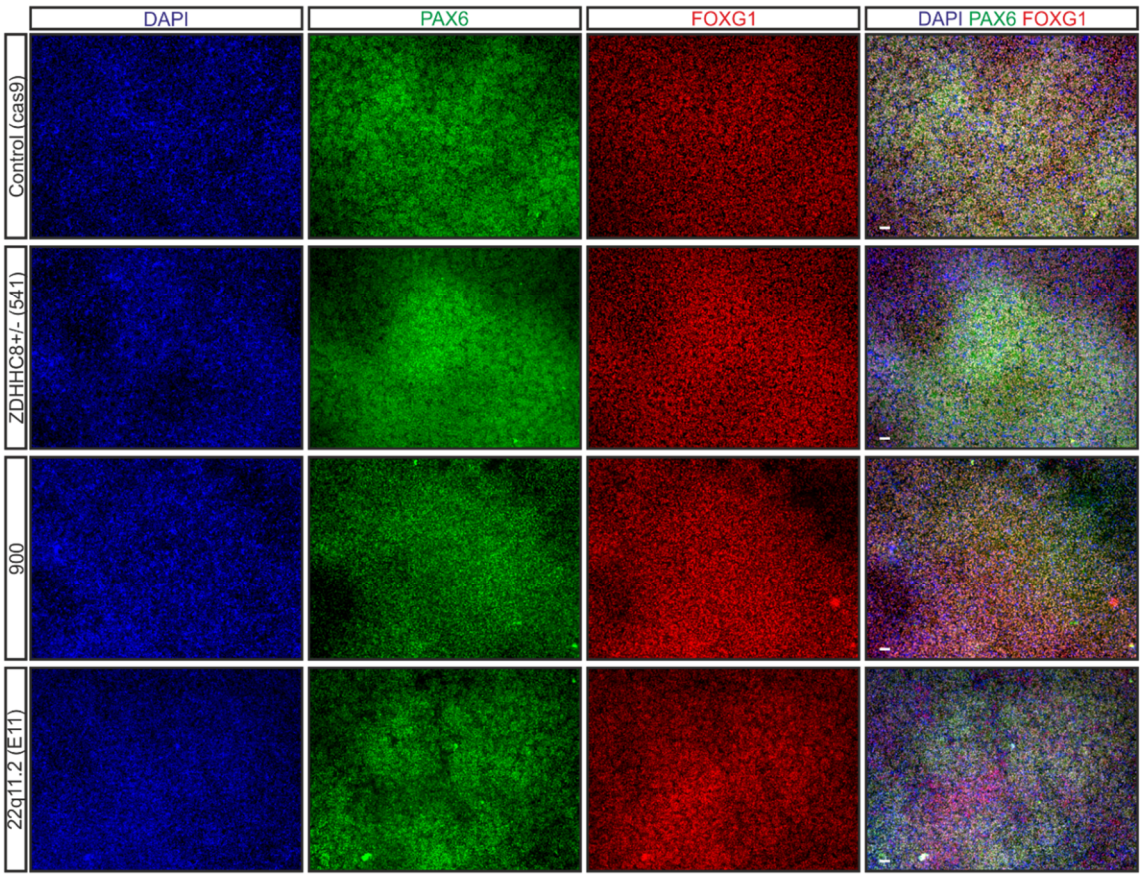

Figure 5-2 Glutamatergic neurons progenitors. NPC at day 15 were fixed and subsequently stained with antibodies against PAX6 (green) and FOXG1 (red). Cells were counterstained with the nuclear marker DAPI (blue). A, NPCs control Cas9. B, NPCs deficient for *ZDHHC8*. C, control NPCs derived from iPSCs 900. D, 22q11.2 NPCs derived iPSCs from 22q11.2 patient. Scale = 50µm.

5.2.1.2. RNA and cDNA quality control

RNA samples were run on a bioanalyzer in order to control for the purity of the RNA. This technique allows to determine whether the two ribosomal RNA subunits 28S and 18S are intact. Over the 24 samples (6 biological replicate per cell line), all had a RNA integrity Number (RIN) over 8.70.

Samples were further processed for the library preparation and subsequently the quality of the cDNA was examined using the Qubit DNA High Sensitivity Kit (life technologies) while the size was controlled with the DNA High Sensitivity Kits (Agilent) The results indicated that all cDNA samples achieved an appropriate purity for being processed on the sequencer (HiSeq 4000, Illumina).

5.2.2. Analysis of the heterozygous *ZDHHC8* transcriptome

To analyse the data collected by the Illumina HiSeq4000, the reads were first aligned on the human genome, hg38. To perform this step, the Spliced Transcripts Alignment to a Reference (STAR) protocol was used in Unix (Dobin et *al.* 2013). The outcome of the STAR analysis was a text file which contained all the different genes with their respective number of reads per samples. To determine the differentially expressed genes, data were processed using DESeq2 package in R (Love et *al.* 2014).

Genome wide RNA-Seq coverage of the *ZDHHC8* sequences were visualized using IGV (Integrative Genomic viewer). Figure 5.3A illustrates an image encompassing the region of exon 3 and 4 of *ZDHHC8* from 6 biological replicates for the mutants and controls. There was a decrease in the number of reads in the *ZDHHC8* mutation region compared to the controls. It was noteworthy that IGV only displayed a random number of samples on the alignment, thereby, region with high reads were downsampled. Therefore, exons count would be more suitable to evaluate whether the number of reads in the region of *ZDHHC8* deletion is reduced.

The Principal Component Analysis (PCA) is a useful tool to visualize genetic distance between populations and reveals which components of the data cause variability in the data set (Figure 5.3B). PC1 captures the direction with the most variation in gene expression while PC2 captures the direction with the second most variation in gene expression. Thereby, Figure 5.3B displayed that all samples for cas9 and 541 respectively controls and mutants are located on the left and right of the PCA. This graphic therefore indicated that 70% of the variation, which is the biggest variation in our samples, is attributed to the deletion. On the other hand,13% of the variation which corresponded to the PC2 was attributed to the variation between our biological replicates.

DESeq2 analysis identified 23421 genes in total (Figure 5.3C). Of which, 64.24% of the genes (15046 genes) are protein coding. By applying a specific cut-off for the pvalue adjusted below 0.01, we found that 0.86% (130 genes) of the genes were downregulated while 0.41% (62 genes) were upregulated of an absolute FC superior to 1.5. As a result, the transcript of 98.73% (14854) of the genes did not show statistical significance between ZDHHC8 mutants and controls.

Together, these data demonstrated that a total of 192 genes were found to be differentially expressed in *ZDHHC8*+/-.

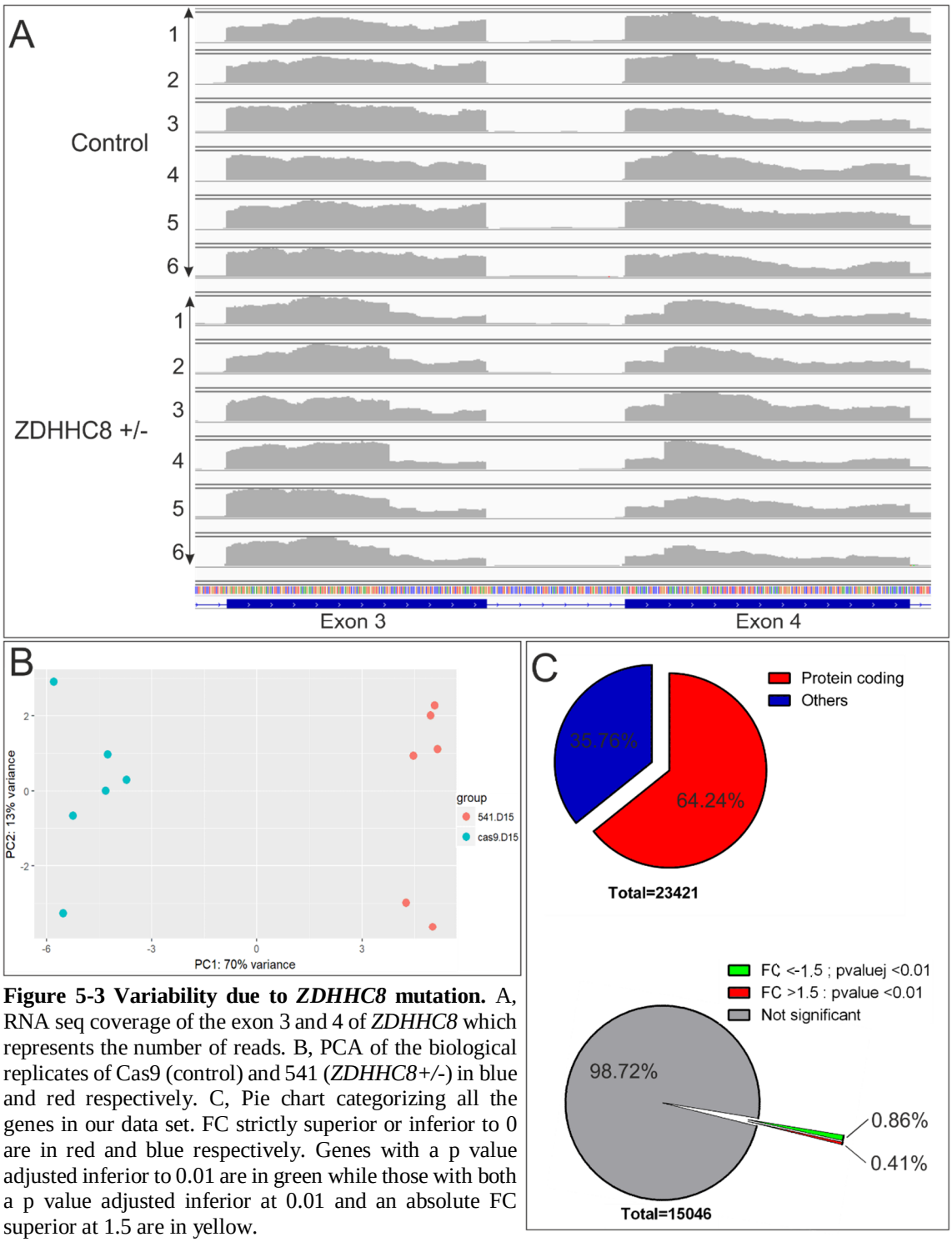

Figure 5-3 Variability due to *ZDHHC8* mutation. A, RNA seq coverage of the exon 3 and 4 of *ZDHHC8* which represents the number of reads. B, PCA of the biological replicates of Cas9 (control) and 541 (*ZDHHC8*+/-) in blue and red respectively. C, Pie chart categorizing all the genes in our data set. FC strictly superior or inferior to 0 are in red and blue respectively. Genes with a p value adjusted inferior to 0.01 are in green while those with both a p value adjusted inferior at 0.01 and an absolute FC superior at 1.5 are in yellow.

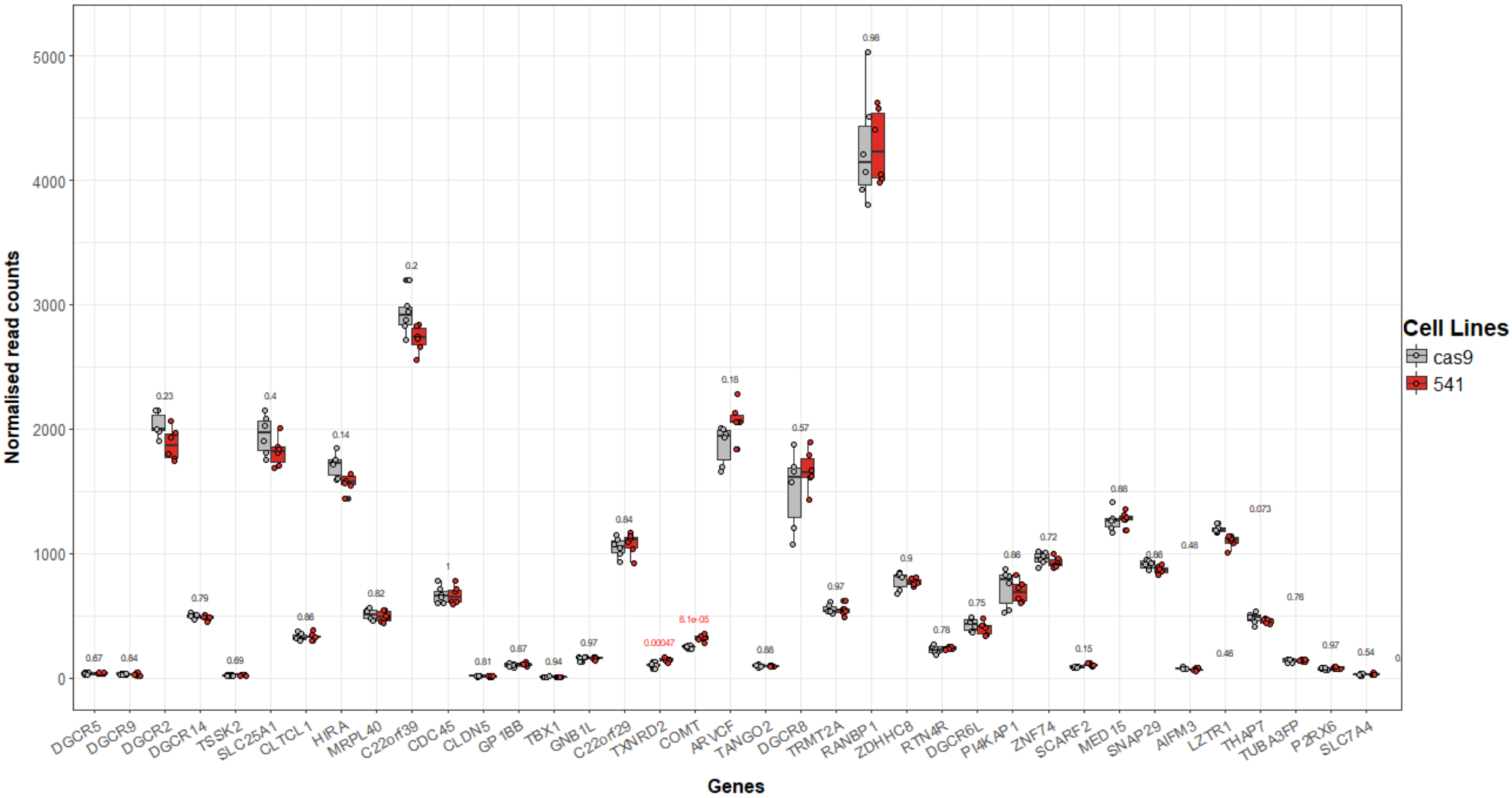

Figure 5-4 Gene expression of the 22q11.2DS genes. All genes from the 3Mb deletion were displayed on this plot. Control samples (cas9) were represented in grey while the mutant ZDHHC8+/- (541) were in red. The pvalue for each gene was written above each boxplot. Only significant pvalue was written in red. Data for each gene represented the normalized count. Data are represented as the median ± SD

5.2.2.1. Expression of 22q11.2 genes in ZDHHC8-deficient cells

The expression of the 22q11.2 genes in *ZDHHC8* heterozygous knockout cells were analysed (Figure 5.4). Only 37 out of 48 genes in the 22q11DS region between LCRA and D were detected in our analysis. Amongst them only TXNRD2 and COMT exhibited statistical difference between the control and *ZDHHC8*+/- (P_{TXNRD2} = 0.00048, P_{COMT} = 0.000081). Indeed, these two genes were observed to be upregulated in *ZDHHC8*+/- NPCs. However, it was noteworthy that we had very low reads for these two genes in the control condition therefore only a small change could result in a significant change in the mutant condition.

5.2.2.2. Cross comparison of GO terms and KEGG pathways altered in ZDHHC8+/-

5.2.2.2.1. GO terms analysis

Gene ontology analysis revealed a total of 318 GO terms enriched in our data from which the top genes related to neuronal development are displayed in Table 5-1. Interestingly, the majority of the GO terms are related to neurons. The top four GO terms with the smallest p value relates to synaptic transmission. Furthermore, 18 of the top 30 GO terms directly relates to the brain suggesting that *ZDHHC8* function is mostly involved in brain development and/or its physiology.

Table 5-1 Gene Ontology enrichment analysis

ID	Description	p.adjust	Gene ratio
GO:0007268	Chemical synaptic transmission	1.97E-12	122/1597
GO:0098916	Anterograde trans-synaptic signalling	1.97E-12	122/1597
GO:0099536	Synaptic signalling	1.97E-12	122/1597
GO:0099537	Trans-synaptic signalling	1.97E-12	122/1597
GO:0005578	Proteinaceous extracellular matrix	2.12E-12	82/1682
GO:0061564	Axon development	3.92E-12	106/1597
GO:0003002	Regionalization	1.26E-11	75/1597
GO:0007411	Axon guidance	1.26E-11	65/1597
GO:0045596	Negative regulation of cell differentiation	1.26E-11	1181597
GO:0097485	Neuron projection guidance	1.34E-11	65/1597
GO:0007409	Axonogenesis	1.41E-11	98/1597
GO:0007389	pattern specification process	1.52E-11	91/1597
GO:0030900	forebrain development	1.57e-11	86/1597
GO:0048667	cell morphogenesis involved in neuron differentiation	3.97E-11	112/1597
GO:0048812	neuron projection morphogenesis	4.07E-11	119/1597
GO:0010721	negative regulation of cell development	8.02E-11	72/1597
GO:0001655	urogenital system development	2.48E-10	
GO:0072001	renal system development	4.54E-10	

GO:0051961	negative regulation of nervous system development	6.85E-10	68/1597
GO:0050768	negative regulation of neurogenesis	1.12E-09	64/1597
GO:0001822	kidney development	1.26E-09	
GO:0035295	tube development	2.04E-09	11/1597
GO:0045165	cell fate commitment	2.45E-09	55/1597
GO:0021953	central nervous system neuron differentiation	1.33E-08	47/1597
GO:0031012	extracellular matrix	3.10E-08	96/1682
GO:0042330	taxis	4.05E-08	94/1597
GO:0001764	neuron migration	5.27E-08	41/1597
GO:0048589	developmental growth	5.93E-08	106/1597
GO:0006935	chemotaxis	7.16E-08	93/1597
GO:0072073	kidney epithelium development	1.35E-07	

Genes from three GO terms, axon development/migration, neurogenesis/brain development and synaptic signalling were identified (Figure 5.5A, B and C). Thereby, we investigated amongst the 192 differentially expressed genes those belonging to one of these categories ($p < 0.001$; $-1.5 < FC > 1.5$). Interestingly, when analysing the other genes from the different GO terms present in table 5-1, we found that it was the same gene. Therefore, we can say that the genes presented below are representative of the genes identified by GO terms.

Interestingly, most of the genes involved in axon development were upregulated. This include three members of the SLIT family, *SLIT1*, *SLIT2* and *SLIT3*. Conversely, *LRRC4C*, *SEMA5A* and *SLITRK3* are three of the top downregulated genes (Figure 5.5A).

Likewise, several genes involved in neurogenesis/brain development were upregulated in our data set (Figure 5.5B). Three genes from of the Wnt family were identified, *WNT8B*, *WNT7B* and *WNT2A* were shown to be upregulated in *ZDHHC8+/-*. On the other hand, *FOXG1* expression was shown to be downregulated. Two members of the Wnt receptors family Frizzled, *FZD5* and *FZD8* were shown to be also downregulated.

Although, we were not expecting genes whose expression are only expressed in mature cells to be expressed in NPCs, we found, eleven differentially expressed genes part of GO terms related to synaptic signalling (Figure 5.5C). *CHRM3* gene which encodes for the cholinergic/acetylcholine receptor M_3 was shown to be downregulated. *DRD2* and *DRD4* which are dopaminergic receptors were also upregulated. In addition, *GRIA2*, a subunit of the AMPA receptor was also upregulated in *ZDHHC8+/-*.

To conclude, GO terms analysis revealed that several genes belonging to the brain development and its physiology were altered in *ZDHHC8+/-*.

Neurogenesis/Brain development			
Gene Name	Normalised counts		Fold change
	ZDHHC8+/-	Control	
BARHL1	543.14	118.32	3.26
CBLN1	95.94	21.50	2.75
WNT8B	4159.32	1597.19	2.41
WNT7B	8521.96	4197.0	1.98
RSPO2	199.16	86.63	1.93
FZD10	49.05	13.57	1.90
WLS	9699.55	4782.76	1.89
HES3	40.61	12.35	1.84
S1PR8	82.46	36.15	1.81
SPOCK1	1589.43	886.97	1.73
SOX10	160.22	83.11	1.72
OLIG3	39.78	14.14	1.67
VTN	99.02	46.53	1.66
1ERBB4	87.83	38.88	1.62
ONECUT2	389.15	223.48	1.61
BOK	129.31	71.12	1.60
SALL3	1111.51	659.30	1.57
WNT2B	1206.41	739.34	1.56
MSX1	38.88	16.61	1.56
ETS1	171.11	100.76	1.55
NGEF	211.38	126.90	1.54
TBR1	668.06	395.27	1.54
CNTN1	77.75	41.50	1.54
HEY2	40.68	19.56	1.52
DLC1	285.33	171.91	-1.50
FOXG1	4497.42	7680.20	-1.66
POU3F3	551.25	988.73	-1.71
FZD8	377.38	710.10	-1.75
ID2	333.86	654.00	-1.82
DIOD3	19.01	86.60	-2.27
FZD5	1579.45	4687.94	-2.34

Axon development			
Gene Name	Normalised counts		Fold change
	ZDHHC8+/-	Control	
GDF7	102.34	15.87	2.78
SLIT2	2679.68	924.35	2.69
BAHRL2	63.86	19.45	2.03
LHX1	267.12	119.93	1.97
SLIT3	441.94	216.94	1.90
FGFR2	4775.62	2725.93	1.71
POU4F1	35.83	12.17	1.69
LMX1A	20.17	3.70	1.65
SLIT1	606.88	357.36	1.59
NEFM	1723.37	1053.78	1.58
CNTN4	196.07	114.47	1.56
OLFM1	557.97	349.15	1.55
GAP43	246.12	149.04	1.54
PTPRM	2174.16	1392.57	1.52
FOXB1	40.66	19.78	1.51
CNTN2	2208.58	1393.68	1.51
GFRA1	1773.55	1151.02	-1.50
INPP5F	6102.45	9585.42	-1.55
LRRC4C	523.64	836.52	-1.55
GFRA2	178.83	294.44	-1.57
SEMA5A	1113.25	1901.92	-1.60
SLITRK3	57.33	124.83	-1.80
VAX1	26.75	85.50	-1.95

Synaptic signalling			
Gene Name	Normalised counts		Fold Change
	ZDHHC8+/-	Control	
CBLN1	95.94	21.50	2.75
DRD2	74.18	28.43	1.93
P2RX3	702.31	360.70	1.81
DRD4	668.43	379.90	1.70
GRIA2	195.57	90.70	1.66
PCDHB5	353.06	207.13	1.60
SYT5	82.01	42.55	1.59
SLC6A1	54.39	27.33	1.56
PDYN	16.99	4.25	1.54
GJD2	21.79	5.52	1.50
CHRM3	63.93	110.85	-1.55

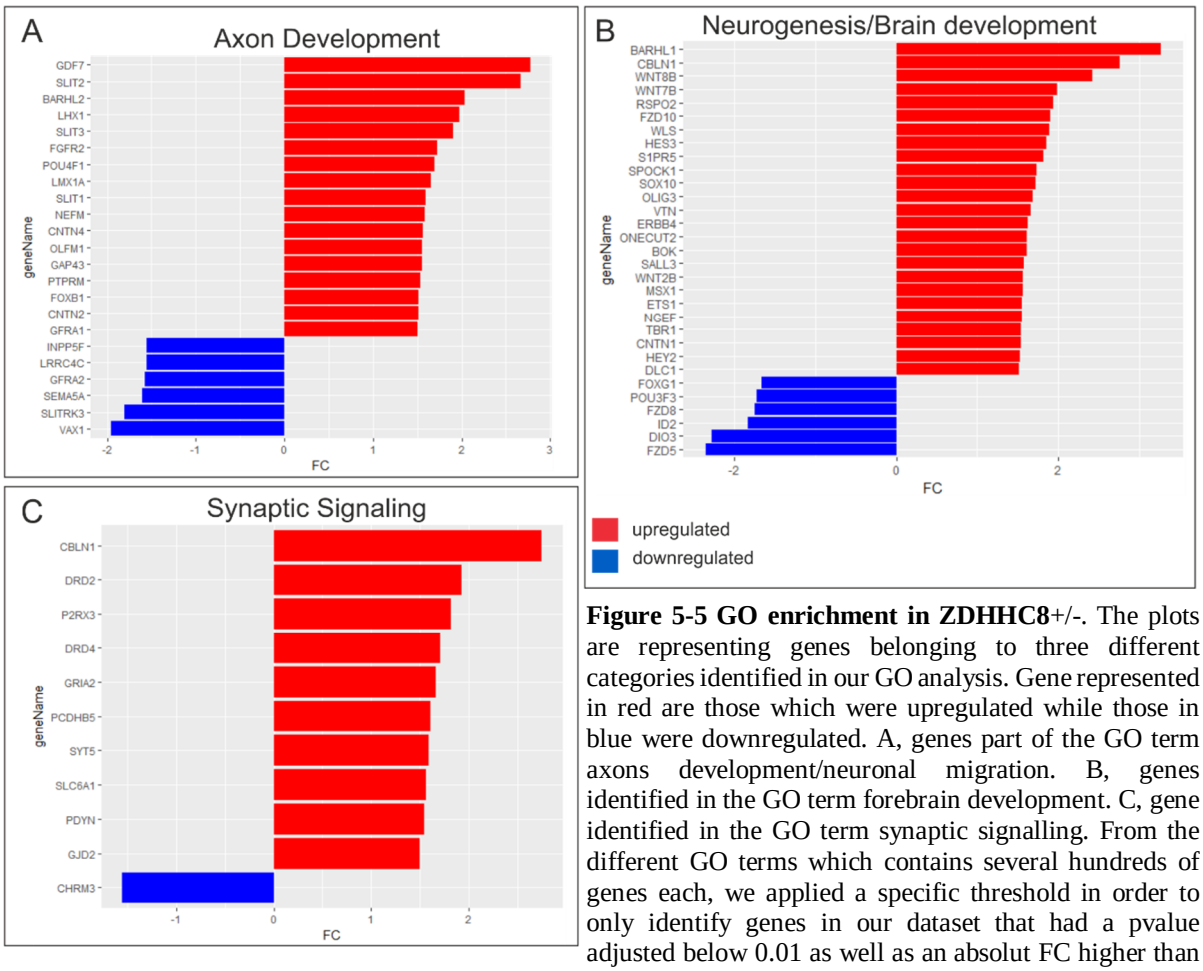

Figure 5-5 GO enrichment in ZDHHC8+/-. The plots are representing genes belonging to three different categories identified in our GO analysis. Gene represented in red are those which were upregulated while those in blue were downregulated. A, genes part of the GO term axons development/neuronal migration. B, genes identified in the GO term forebrain development. C, gene identified in the GO term synaptic signalling. From the different GO terms which contains several hundreds of genes each, we applied a specific threshold in order to only identify genes in our dataset that had a pvalue adjusted below 0.01 as well as an absolut FC higher than 1.5. The X-axis represents the fold change (FC) difference.

5.2.2.2.2. KEGG pathways analysis

In addition to GO enrichment analysis, data were processed to examine the Kyoto Encyclopedia of Genes and Genomes (KEGG) pathway enrichment which are predicted to be altered in *ZDHHC8+/-*. A total of 18 pathways were shown to be altered by *ZDHHC8* mutation with several relating to the brain and heart pathologies (Table 15). For the purpose of this thesis, only pathways related to the brain will be presented. These pathways were associated to neuronal receptors, calcium signalling and axon guidance.

Table 5-2 KEGG pathway enrichment analysis in ZDHHC8+/-

KEGG ID	Description	p.adjust
hsa04080	Neuroactive ligand receptor interaction	0.00074532
hsa04020	Calcium signalling pathway	0.00074532
hsa05410	Hypertrophic cardiomyopathy (HCM)	0.00074532
hsa04512	ECM-receptor interaction	0.00074532

hsa03010	Ribosome	0.00074532
hsa04514	Cell adhesion molecules (CAMs)	0.000929825
hsa05414	Dilated cardiomyopathy (DCM)	0.000929825
hsa05412	Arrhymogenic right ventricular cardiomyopathy (ARVC)	0.002446221
hsa04713	Circadian entrainment	0.007926987
hsa04060	Cytokine-cytokine receptor interaction	0.008085623
hsa03040	Spliceosome	0.014207723
hsa04974	Protein digestion and absorption	0.016332156
has04213	Longevity regulating pathway – multiple species	0.034047458
has04670	Leukocyte transendothelial migration	0.034047458
has04360	Axon guidance	0.037029985
has04120	Ubiquitin mediated proteolysis	0.048523161
hsa04510	Focal Adhesion	0.048523161
hsa04141	Protein processing in endoplasmic reticulum	0.048523161

Figures 5.6 and 5.7 illustrate three neuronal pathways altered by *ZDHHC8* mutation.

Pathway involved in synaptic receptors Figure 5.6A. This pathway represents a map of the different neuronal receptors together with their ligands altered in *ZDHHC8*+/-. The analysis identified that mRNA expression of genes coding for Epinephrine and Norepinephrine receptor (ADR) were upregulated. as well as the family of the dopamine receptor (DRD). Conversely, the expression of genes coding for the 5-hydroxytryptamin (5-HT) also known as serotonin receptor were found to be downregulated. In addition, it also appeared that the expression of genes coding for NMDA (*GRIN*), GABA (*GABR*) and AMPA (*GRIA*) receptors were also upregulated in *ZDHHC8*+/-. On the other hand, the expression of the *CHRN* genes family which encoded for the acetylcholine receptors were downregulated. However, it was noteworthy that these data did not indicate which subunits of these receptors were affected.

Pathway involved in calcium signalling (Figure 5.6B). As presented in the general introduction, extracellular calcium is the main source of Ca2+ for the cells and is involved in a multitude of physiological functions even in young NPCs. Many genes coding for receptors responsible of calcium uptake were upregulated, which include the voltage gate calcium channel CaV2 and CaV3 and also the receptor operated channels (ROC) which comprised most of the ionotropic receptors such as AMPA and NMDA. GPCR were also observed to be downregulated, upon activation by an extracellular signal which can be a neurotransmitter, theses receptors are involved in signal transduction either through cAMP or phosphatidylinositol signalling pathway. We also observed that genes such as the gene coding for the inositol 1,4,5-trisphosphate receptor, type 1 (*ITPR1*) and the calmodulin are also upregulated by *ZDHHC8*+/-.

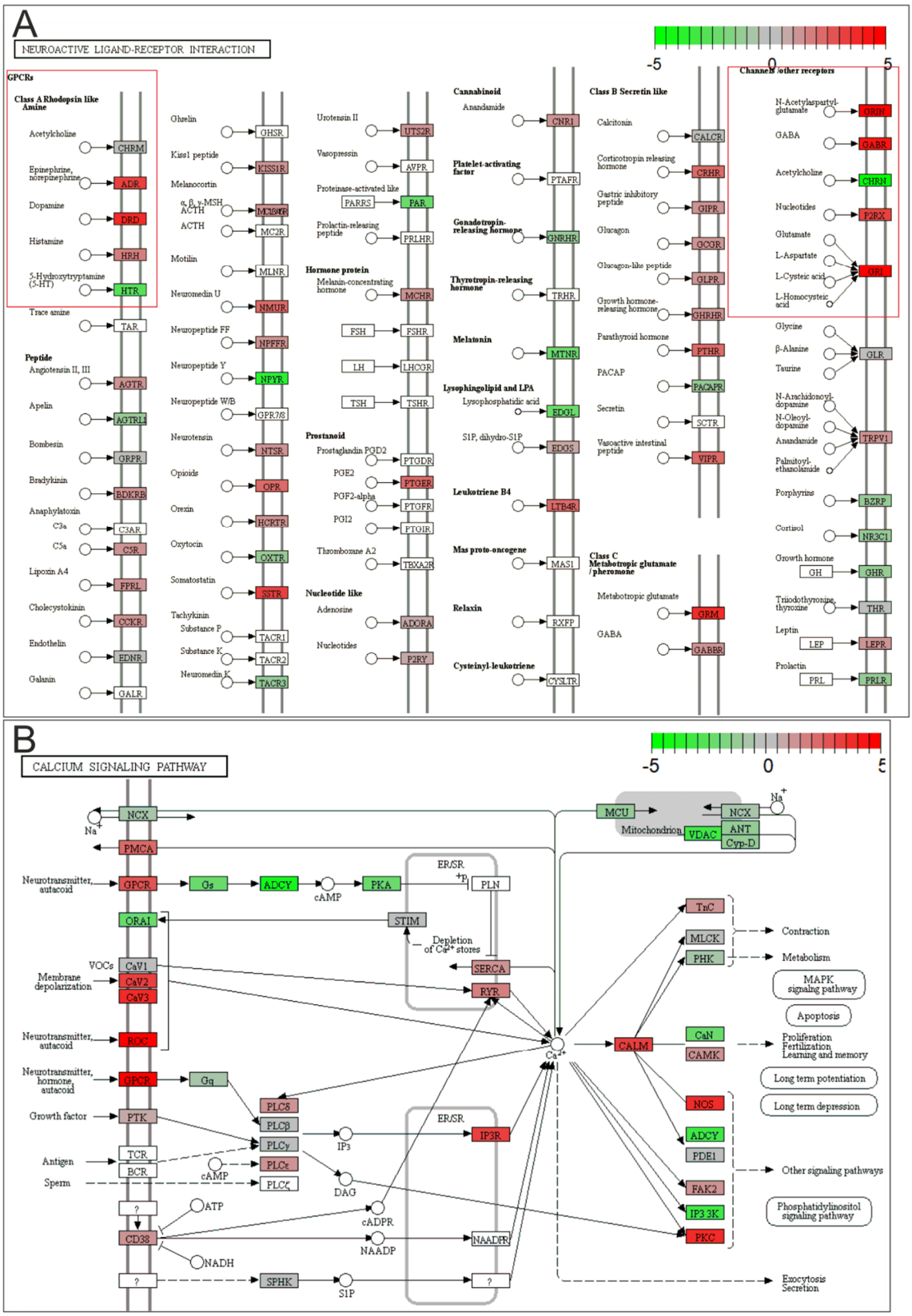

Figure 5-6 KEGG enrichment pathways. A-B, the intensity which is represented in the top right corner of each schematic shows the FC of each gene, from green and red respectively a FC of -5 and 5. A, Neuroactive ligand receptor interaction. B, Calcium signalling pathway. The analysis had as parameter a p value cut off of 0.05. Figure can be found at higher magnification in annexe

Pathway involved in axon guidance (Figure 5.7). In addition to be one of the top GO term enriched in our analysis, the axon guidance pathway was also revealed by KEGG enrichment analysis. This pathway is primordial for the proper growth of axons which ultimately lead to novel synaptic connexion. As shown in Figure 5.7, the expression of genes of the SLIT family were upregulated. It also appeared that the expression of *ROBO* which encodes for the SLIT receptors are likewise upregulated. Similarly, Plexin B, a receptor of semaphorins and EphA, a ephrin receptor, were both upregulated in *ZDHHC8+/-*. Conversely, a strong downregulation was observed for *TRPC* (Transient Receptor Potential Channel), which is responsible for axons attraction and outgrowth. Finally, *NGL-1* also known as *LRRC4C*, was also downregulated. Together, KEGG pathways analysis established that several signalling pathways were found to be altered by heterozygous knockout of *ZDHHC8*.

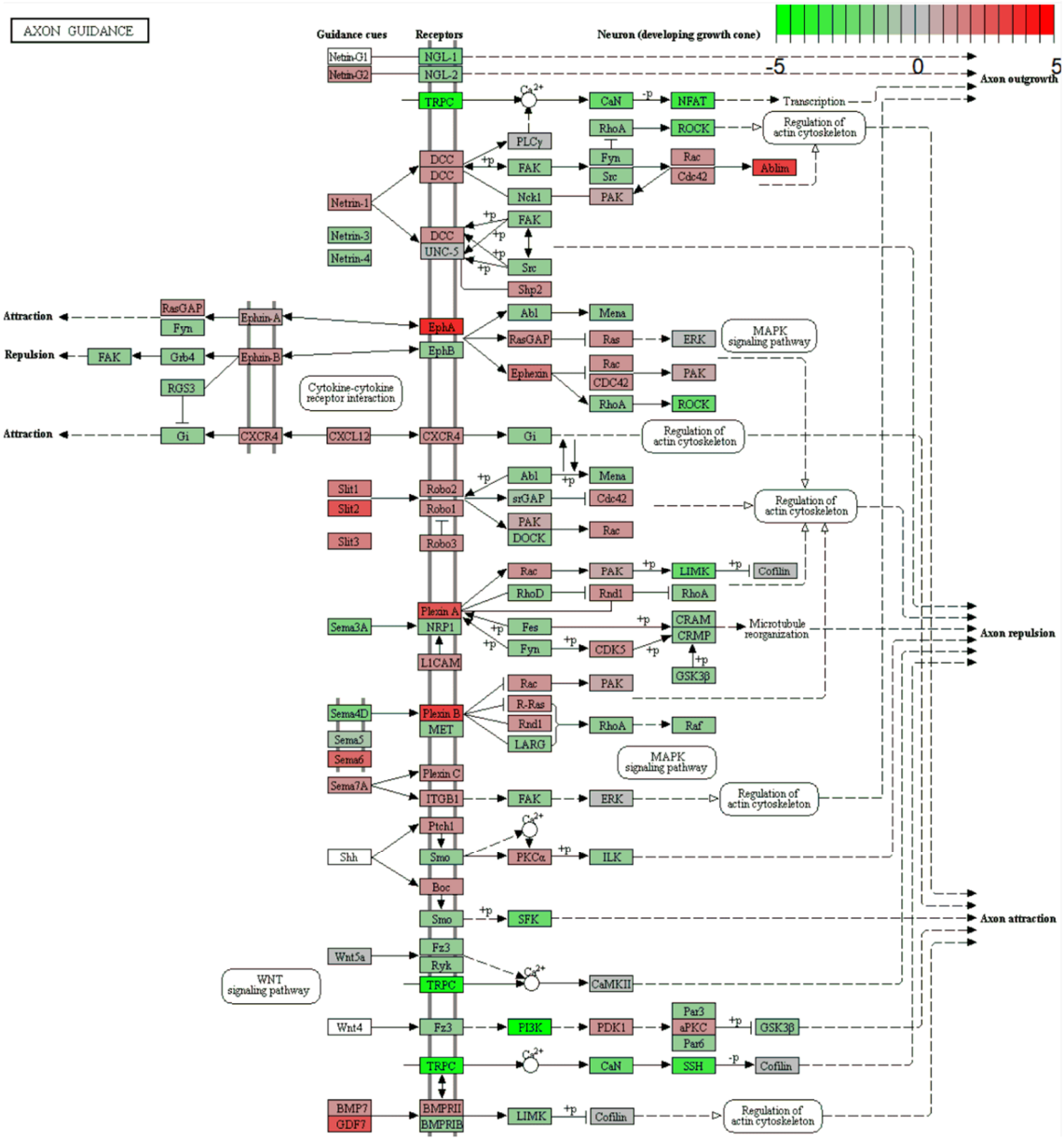

Figure 5-7 Axon guidance pathway is altered in *ZDHHC8*+/-. The intensity of red and green represents either an upregulation or downregulation of the mRNA relative expression. A, Axonal guidance pathway. The analysis had as parameter a p value cut off of 0.05. Picture can be found at higher magnification in annexe

5.2.3. Differentially expressed genes of a 22q11.2 hPSC derived NPCs

Analysis of the 22q11 iPSCs derived into excitatory NPCs revealed that a CNV might be located on the chromosome 17 in the iPSCs from 22q11.2 NPCs as 25 genes in the vicinity of *TP53* were observed to be half expressed when compared to the control cells. The function of this gene was suggested to impact the viability of cells (Amir et *al.* 2017). Therefore, we decided to only investigate the expression of the of the 3Mb deletion in the 22q11 iPSC derived NPCs (Figure 5.8).

We observed that 37 out of 40 genes were expressed in the 22q11.2 NPCs. However, it appeared that not the same genes were present in 22q11.2 and *ZDHHC8+/-* NPCs. The analysis revealed that 24 genes were significantly different in 22q11.2 NPCs when compared to the control NPCs. In contrast to the assumption that these genes would show reduced expression, many (*DGCR6, PRODH, CLTCL1, C22ORF39, C22ORF29, RTN4R, MEP15, AIFM3* and *HIC2)* were in fact upregulated in the 22q11.2 iPSCs when compared to the control.

While other studies did observe a reduction in the expression of the genes of the 22q11 mutation, our analysis were unable to find similar result. Therefore, it would be interested to examine the number of reads per exons which should provide us with more information regarding the expression of these genes.

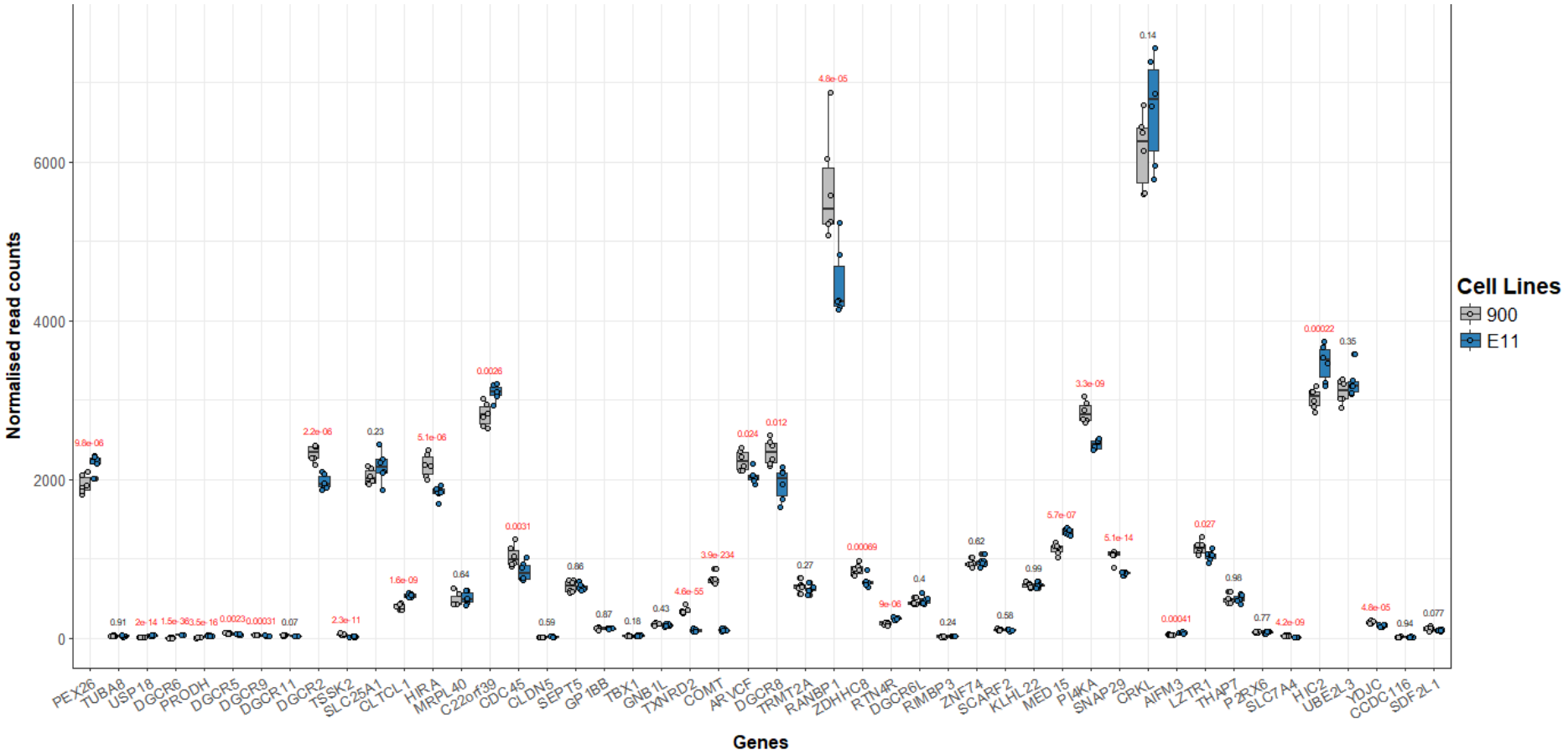

Figure 5-8 Gene expression of the 22q11.2DS genes in the iPS cells carrying the 3Mb 22q11.2 deletion. All genes from the 3Mb deletion were displayed on this plot. Control samples from the cell line 900 were represented in grey while the mutant E11 (22q11.2 deletion) were in blue. The pvalue for each gene was written above each boxplot. Only significant pvalue was written in red. Data for each gene represented the normalized count. The box plot allows to visualize the spread of the data as each point is representing a biological replicate.

5.2.4. Comparison of the differentially expressed genes in 22q11.2 and *ZDHHC8+/-*.

To investigate whether ZDHHC8 deficiency and 22q11.2 deletion leads to the alteration of similar genes, we compared the overlap between the genes differentially expressed in *ZDHHC8+/-* and 22q11.2 iPSCs derived NPCs.

Instead of comparing the transcriptome of control and mutant as performed in 5.2.2 and 5.2.3, the DEseq2 analysis compared the transcriptome of the two mutants (22q11.2 and *ZDHHC8+/-*) and the two controls (900 and iCas9) with each other's. In total, the analysis identified 24748 genes from which we performed a Venn diagram to identify the genes coding proteins overlapping between *ZDHHC8+/-* and 22q11 derived NPCs (Figure 5.9).

Figure 5.9A illustrates the number of significant genes (pvalue < 0.01) overlapping between *ZDHHC8+/-* and 22q11.2 NPCs. We observed that each group is composed of 7080 and 1176 for 22q11.2 and ZDHHC8 respectively. From these genes, it appeared that 978 overlapped. Figures 5.9B and C illustrate the number of genes with a pvalue inferior to 0.01 and either a FC higher or below 1.5 or -1.5 respectively. We observed that 36 genes with a FC superior to 1.5 appeared to overlap while only 15 genes with a FC below -1.5 overlapped between ZDHHC8 and 22q11.2 derived NPCs.

Using similar cut off than in **5.2.2.2.1**, we examined whether amongst the genes significant in 22q11.2 derived NPCs, we found overlap with significant genes identified in *ZDHHC8+/-*. Table 17 presents the genes identified in the GO terms neurogenesis and synaptic signalling that were significant in *ZDHHC8+/-* and 22q11.2 derived NPCs. While no genes from the axon development appeared to overlap, several genes from the neurogenesis and synaptic signalling GO terms was found in both populations.

Table 5-3 List of genes identified by GO terms in *ZDHHC8*+/- transcriptome analysis that overlap with 22q11.2

Neurogenesis	FC		Average normalised counts	
	541 (ZDHHC8)	22q11.2	541 (ZDHHC8+/-)	22q11.2
HES3	2.74	1.72	41.67041321	77.54539634
S1PR5	2.19	11.80	84.5717733	180.5516844
SOX10	1.90	2.13	164.3187092	92.4346293
FOXB1	1.84	1.67	41.70039398	89.3692161
SPOCK1	1.65	1.65	1629.890056	2086.111991
ATP8B1	1.83	1.84	38.07521853	48.45993288
GBX2	1.66	3.08	40.87800978	172.0529326
MMD2	1.66	2.00	22.21205691	36.49503382
IRX3	1.62	1.52	88.57409616	236.1496279
RELN	1.54	2.02	680.0307409	577.2294353
Synaptic signalling				
GLRA4	1.70	2.33	29.22057558	41.04416266
PCDHB5	1.64	11.27	362.0848839	1437.218139

To conclude, despite 978 genes overlapped between 22q11.2 and *ZDHHC8* when we apply a cut off for those with a pvalue below 0.01. This number drastically decreased when they were also classified depending on their FC.

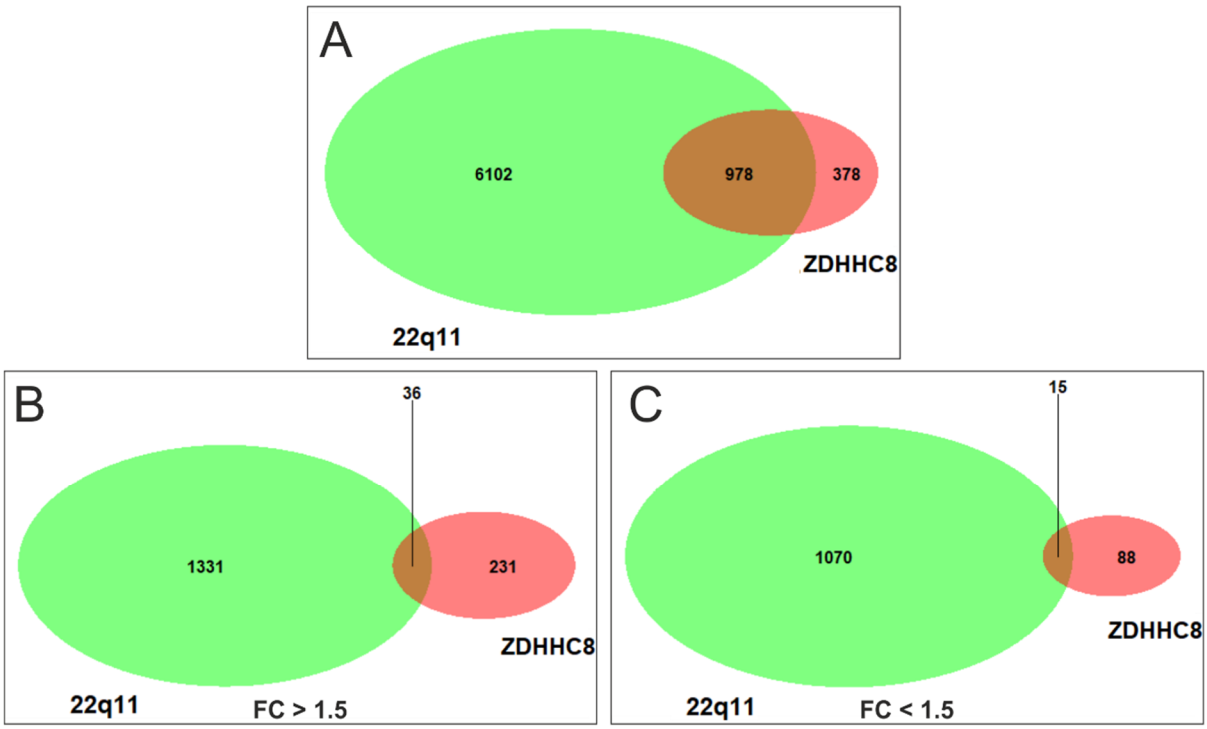

Figure 5-9 Venn diagramm illustrating the overlap between *ZDHHC8*+/- and 22q11.2 derived NPCs. This vendiagram is illustrating the number of significant genes (A) p < 0.01 in both condition while it illustates the number of significant genes p < 0.01 with -1.5 < FC > 1.5 in C and B.Green and red circle are respectivelly repsenting the number of genes in 22q11.2 and *ZDHHC8*+/- while both circle crossed correspond to the overlap between the22q11 and ZDHHC8. A, The 22q11 population is composed of 7080 genes while it is 1356 for ZDHHC8. Therefore, 978 genes were found to be similar. B, genes with a FC superior to 1.5. 22q11 and ZDHHC8 are composed respetively of 1367 and 267 genes. In this condition, 36 genes overlapped between 22q11 and ZDHHC8. C, genes with a FC < -1.5. We found 1085 genes in 22q11, 103 genes in ZDHHC8 and 15 genes overlapped between the two.

5.3. Discussion

In this study, we performed a whole transcriptome shotgun sequencing (also known as RNA-seq) analysis of *ZDHHC8*+/- glutamatergic progenitor cells with the aim 1) to analyse the transcriptome of *ZDHHC8*+/- derived NPCs, 2) to determine whether similar group of genes overlapped between 22q11.2 and *ZDHHC8*+/-.

The first part of the study investigates if the 22q11.2 genes located in the region of the 3Mb deletion were altered by *ZDHHC8*+/-. Apart from *COMT* and *TXNRD2*, the expression of the remaining 22q11.2 genes were similar when compared to the control. *COMT* expression was observed to be altered in individual with schizophrenia. The function of COMT was demonstrated to be responsible of the inactivation of dopamine neurotransmitter following its releases in the synaptic cleft. Individuals with schizophrenia were reported to have an increase mRNA level of *COMT* in the dorsolateral prefrontal cortex which was shown to be detrimental for the dopaminergic innervation (Matsumoto et *al.* 2003). Therefore, we suggest that *ZDHHC8*+/- might be responsible

of the increase in *COMT* expression, which therefore could result in decrease dopaminergic innervation in individuals with 22q11.2DS. Further studies should consider investigating whether these two genes interact.

TXNRD2 is important for the development and function of the heart. Mice deficient for *Txnrd2* die around E13.5 due to severe anaemia which resulted in part to an increase apoptosis in the liver that alter haematopoiesis but also due to a thinner ventricular walls of the heart and decrease of cardiomyocyte proliferation (Conrad et *al.* 2004; Kiermayer et al. 2015; Soerensen et *al.* 2008). Conversely, *TXNRD2* overexpression was found to be associated with an increase lifespan in female *Drosophila melanogaster*, in addition overexpression of this gene was also found decrease the therapeutic effect of bortezomib, a proteasome inhibitor in multiple myeloma cells (Fink et al. 2016; Pickering et *al.* 2017). Although we identified several GO terms and KEGG pathways enrichment related to cardiac function such as Dilated cardiomyopathy (DCM), the relation between *TXNRD2* and *ZDHHC8* if one remains largely unknown.

The *ZDHHC8*+/- transcriptomic analysis identified 1203 proteins coding genes whose expression were significantly different between *ZDHHC8*+/- and its isogenic control (pvalue < 0.01), from which 192 genes had an absolute FC higher than 1.5. Interestingly, most of the GO terms identified were related to neurons development and physiology emphasising the role of *ZDHHC8* during brain development.

Axon development was identified as a top GO enriched term. Several genes related to axon development were demonstrated to be upregulated in *ZDHHC8* +/-, such as the SLIT family (*SLIT1*, *SLIT2* and *SLIT3*), *LRRC4C*, *SEMA5A* and *SLITRK3*. Interestingly, KEGG pathway enrichment analysis also identified the axonal guidance pathway as altered in *ZDHHC8*+/-. While axonal guidance defect was demonstrated to be responsible for neuronal migration disorder (NMD) such as lissencephaly, polymicrogyria or micropolygyria. Neuronal migration was also linked to schizophrenia and Parkinson disease (Gilman et *al.* 2012; Lesnick et *al.* 2007).

The *SLIT1*, *SLIT2* and *SLIT3* genes was observed to be upregulated in *ZDHHC8*+/-. The SLITs proteins are implicated in a multitude of different physiological processes such as axon pathfinding as well as axonal and dendritic branching (Bagri et *al.* 2002; Wang et *al.* 1999; Whitford et *al.* 2002). While SLITs homozygous knockout are lethal, the data presented in this chapter indicate an upregulation of these three genes with a FC of at least 1.5. In drosophila, *Slit* overexpression appears to have a similar phenotype than

Roundabout (*Robo)* loss of function, the receptor of slit. Once crossing midline, high level of ROBO are expressed by commissural axons to avoid them to cross again. In the vertebrate brain, neurons require to cross the floor plate or midline (drosophila) in order to innervate the other part of the brain. Thus *ZDHHC8*+/- might alter this process resulting in an abnormal axons guidance which might result in abnormal axonal connexion. While the Slit family is shown to be upregulated in our study, previous report by Mukai et al. 2008, 2015 using heterozygous mouse model for *Zdhhc8* demonstrated an alteration of the palmitoylation of CDC42 (Mukai et *al.* 2008, 2015). This protein is an actin cytoskeleton regulator, whose palmitoylation alteration resulted in shorter axons arborisation (Tapon et *al.* 1997). The *SLIT* genes are located in the same signalling pathway than *CDC42* (Figure 5.7) (Huber et *al.* 2003). It was demonstrated that Slit increases the complex of Robo1-srGAP which in turn inactivate CDC42 (Huber et *al.* 2003). Although our data suggest that the expression of *SLITs* genes as well as their receptors *ROBOs* are increased, an increase in the expression of srGAP was not detected. Thus, it is possible that this overall upregulation of the *SLIT/ROBO* might have no effect on the expression of *CDC42*. Therefore, it would be interesting to evaluate the level of these proteins by western blot analysis in order to estimate if they influence the SLIT/ROBO/CDC42 pathway.

LRRC4C also known as *NGL-1* is the receptor of the guidance cue netrin-G1 which is part of the netrin family and was shown to be downregulated in *ZDHHC8*+/-. NGL-1 is thought to be highly expressed in the striatum and cerebral cortex (Lin et *al.* 2003). While its role was suggested to promote thalamic axons outgrowth, it was also demonstrated to interact with PSD-95 at the postsynaptic membrane (Lin et *al.* 2003; Ricciardi et *al.* 2012). While our data suggested a downregulation of the *NGL-1*, knockout experiment of this gene revealed that the signalling cue netrin-G1 was also significantly reduced (Matsukawa et *al.* 2014) therefore resulting to a decrease in synaptogenesis and disruption of the growth of thalamic axons. As thalamic reduction was also observed in children with 22q11.2DS, this phenotype could be attributed to the reduction of *LRRC4C* (Bish et *al.* 2004) due in part by *ZDHHC8.*

In addition, we also observed a downregulation of *SEMA5A*. Semaphorins are a group of proteins that were identified as axon guidance molecules. In the central nervous system, this class of proteins acts as both chemoattractant and chemorepellent for the growth of axons (Raper 2000). Interestingly, a *de novo* deletion of *SEMA5A* was recently identified as contributing to ASD and intellectual disability which are pathologies that also arise in

patients with 22q11.2DS (Angkustsiri et *al.* 2014; Radoeva et *al.* 2014; Subramanian et *al.* 2015).

SLITRK3 was also found to be downregulated in *ZDHHC8+/-*. This molecule was discovered as a synaptogenesis molecule responsible for inhibitory synapse development. Indeed, *slitrk3-/-* mice was observed to increase the risk for spontaneous epileptic seizure due to an unbalance between excitatory and inhibitory synapses (H. Takahashi et *al.* 2012). As patients with 22q11.2DS also exhibit spontaneous epileptic seizure it would be interested to investigate whether alteration of this gene is also present in 22q11.2DS which could therefore be due to *ZDHHC8* (Kao et *al.* 2004; Strehlow et *al.* 2016).

While this study revealed migration defect due to *ZDHHC8+/-*, several studies in individuals with 22q11.2DS were also observed to have migration defect such as polymicrogyria or reduced corpus callosum volume (Castro et *al.* 2011; Robin et *al.* 2006). However, it is currently not known which genes or groups of genes are associated with this pathology in 22q11.2DS. Finally, to determine the implication of the gene listed above, it would be interested to perform experiment aiming to identify whether the proportion of these different proteins is altered at the growth cone of *ZDHHC8+/-* NPCs.

Amongst the other GO enrichment identified was the one related to neurogenesis/brain development. Three members of the WNT family, *WNT8B*, *WNT7B* and *WNT2B* were shown to be upregulated. The WNT family constitutes a major signalling pathway involved in neural development. These three genes were shown to be expressed in the forebrain during development suggesting their importance for this process (Abu-Khalil et *al.* 2004; Lako et *al.* 1998). *Wnt7b* was observed to be highly express throughout the cortex but more specifically in the cortical plate while absent from the ventricular zone during cortical neurogenesis (Chenn 2008; Funatsu et *al.* 2004). *Wnt8b* was shown to be mostly expressed in the cortical hem and hippocampus, similarly the expression of *Wnt2b* was shown to be restricted to the cortical hem (Harrison-Uy et *al.* 2012). While *Wnt8b* knockout was observed to be responsible of decrease *Wnt2b* expression , the expression of *Wnt7b* was unchanged (Fotaki et *al.* 2010). In addition, alteration of *Wnt2b* and *Wnt7b* was shown to affect neuronal development by altering the neural tube formation (Bai et *al.* 2016). Despite their implication in many others signalling pathways apart from the brain, these genes should be further investigated, such as quantifying their proteins level in *ZDHHC8+/-* neurons differentiation.

FOXG1 is a gene which was demonstrated to be associated with development of Rett syndrome. In addition, this gene is also crucial for the development of the telencephalon during embryonic development. Indeed, experiments in which mice were deficient for *Foxg1* were demonstrated to exhibit telencephalon and brain size defects. Instead *Foxg1* overexpression resulted in telencephalon and mesencephalon overgrowth (Ahlgren et *al.* 2003). In chapter 4, we observed no difference in the proportion of FOXG1 positive cells in *ZDHHC8+/-* when compared to the control. Also, mice deficient for *Zdhhc8+/-* or *Zdhhc8-/-* did not have obvious brain morphological defect. Therefore, this decrease in the transcript of *FOXG1* might not be correlated to a decrease of the subsequent FOXG1 protein in vitro.

FZD5 and *FZD8* are two genes part of the frizzled family of G-protein coupled receptors (Schulte et *al.* 2007). Interestingly, it was demonstrated that the sequence of both FZD5 and FZD8 shared 70% identity (Huang et *al.* 2004). While *Fzd8* was shown to be expressed throughout the ventricular zone in the dorsal and ventral telencephalon, the expression of *Fzd5* was observed to be restricted to the ventral telencephalon (Fischer et *al.* 2007; Harrison-Uy et *al. 2012*). Knockdown of *Fzd5* was shown to result in loss of neuronal polarity (Slater et *al*. 2013). While mice heterozygous knockout for *Fzd5* are viable, homozygous knockout die in utero due to angiogenic defect (Fischer et *al*. 2007). Considering that we observed a decreased expression of both *FZD5* and *FZD8* it would therefore be interested to investigate the resulting phenotype to such a decrease by examining their respective proteins.

To conclude, in addition to the three WNT genes upregulated, we also found that *ZDHHC8+/-* had a decrease of the expression of two WNT receptors *FZD5* and *FZD8*.

Alteration of signalling pathway related to synaptic receptors. KEGG pathway enrichment analysis identified that the “neuroactive ligand receptor interaction” pathways were altered in *ZDHHC8+/-*. While we might not expect these types of genes to have an important impact on young neurons, it might demonstrate that their alteration at early stage could result to alteration of their expression when expressed in mature neurons. Therefore, we decided to present these data in the present thesis. Amongst these genes, the DRD and GRI family, respectively dopaminergic and glutamatergic AMPA receptors. The dopamine receptor D2 was recently identified as being palmitoylated by ZDHHC8 (Ebersole et *al.* 2015). Furthermore, ZDHHC8 was demonstrated to palmitoylate PICK1 (protein interacting with C-kinase) and GRIP1 (glutamate receptor interacting protein), two proteins known to bind the GRIA2 receptors (Thomas et *al.* 2012, 2013). However,

our data are suggesting an upregulation of the GRIA2 receptor which might suggest a novel role for *ZDHHC8* other than its implication at the protein levels. Thereby it would be interested to assess the protein level of GRIA2 to determine whether this upregulation is correlated with an increase of the protein translation. Similarly, to *GRIA2*, the *DRD2* and *DRD4* were upregulated. Antipsychotics medication are known to increase the level of DRD2 and DRD4 proteins. However it is noteworthy that an elevated level of DRD2 receptor was observed in patients with schizophrenia prior their psychotic medication (Seeman et *al.* 2000). Whereas it was not previously observed with the DRD4 protein. These data are thereby suggesting that *ZDHHC8* might alter the expression level *DRD2* and *DRD4* thereby we would need to determine if this increase results to an increase translation of their respective proteins.

Lastly, the calcium signalling pathway was shown to be enriched by KEGG pathway analysis. Calcium signalling is particularly important for neurons (chapter 1). It was previously demonstrated that calcium signalling was altered in two different mouse models of 22q11.2DS, the *Df(16)A/+* and the *Df(16)5* (P Devaraju et al. 2017; Earls et al. 2010) as well as in schizophrenia patients. Although no report described calcium alteration with *ZDHHC8*, the data presented in this study are suggesting otherwise. Indeed, Figure 5.6B showed an increase of the voltage dependent calcium channel which might suggest an increase in calcium uptake within the neuron which would thereby result in an alteration of the neuronal calcium signalling. Furthermore, we observed a slight upregulation of *SERCA* which was observed to be associated with an alteration of calcium signalling through increase neurotransmitter release at the presynaptic neurons (Earls et *al.* 2010). Although more than one gene within the 22q11.2DS might be responsible of the calcium signalling alteration, our data suggested that *ZDHHC8* might be an important contributor to this signalling pathway.

This study investigated for the first time the role of *ZDHHC8* at the transcriptional level in excitatory neuronal progenitor cells. Therefore, these data will give valuable insight on the genes and pathways affected by *ZDHHC8* mutation.

The second aim of this study was to examine whether similar genes in *ZDHHC8+/-* and 22q11 derived NPCs were found to overlap. Although we aimed to compare the RNA-seq data from 22q11.2 and *ZDHHC8+/-* derived NPCs, however, due to issue regarding

a potential CNV on the chromosome 17 we did not perform gene enrichment analysis on the 22q11.2 NPCs.

Genomic instabilities in ESCs have already identified several mutations which were observed to be mostly located on the chromosome 1, 12 and 17 and X (Lamm et *al.* 2016). Surprisingly, these mutations often correspond to observation made with embryo carcinoma (Nouspikel 2013). These observations also note a higher number of CNV in iPSCs than hESCs (Hussein et *al.* 2011; Laurent et *al.* 2011; Martins-Taylor et *al.* 2011). Thus, in order to avoid similar outcome for future experiments, it would be advised to test all new cells lines on SNP arrays. Furthermore, regular SNP array might be useful to check for spontaneous deletion or duplication that might be due to the culture condition as well as the number of passages.

Furthermore, it was noteworthy that the iPSCs from the 22q11.2 individual was a female while the control iPSCs (900) was a male. Therefore, we could not exclude that several genes overlapping between 22q11.2 and *ZDHHC8+/-* might be influenced by genes located on sexual chromosome.

However, our comparison of the genes overlapping between *ZDHHC8+/-* and 22q11.2 NPCs suggested that *ZDHHC8* might only have small impact on the pathophysiology of 22q11.2DS. Indeed, only 36 and 15 genes were significantly different ($p < 0.01$) with a FC superior to 1.5 or below -1.5 respectively. However, because we only had one line for *ZDHHC8+/-* and one line for 22q11.2, it would be interested to test with more line.

To summarize, this chapter allowed us to identify that the expression of the region deleted in *ZDHHC8+/-* was reduced by half when compared to the control. In addition, the transcriptomic analysis of *ZDHHC8+/-* allowed us to identify that several genes/pathways involved in neurons development and function appeared to be altered by the mutation such as axonal guidance as well as calcium signalling. While it was already demonstrated that the function of *ZDHHC8* was link to neuronal and axonal arborisation, it is the first time that its relation with neurons was shown at the transcriptomic level. The study also identified that only few genes deleted in the 22q11.2 mutation overlapped with gene deleted in *ZDHHC8+/-*.

Chapter 6. General discussion

This thesis was divided into two main part, the first part investigates the temporal and cell specific expression profile of the genes from the 1.5Mb deletion of the 22q11.2 mutation into four different cell lineages while the second and third part was focusing on elucidating the function of *ZDHHC8* in cortical projection neurons and NPCs.

Many pathologies are associated with 22q11.2DS, several of which affect the central nervous system (Angkustsiri et al. 2014; Bassett et al. 2003; Cascella and Muzio 2015; Retnakaran et al. 2010). Although several mouse models have been generated to study either the full spectrum or individual genes (Gogos et al. 1998; Kimber et al. 1999; Mukai et al. 2008; Paronett et al. 2015; Paylor and Lindsay 2006), only few studies have been performed in a human setting. In addition, due to the number of genes present in this CNV, the role of individual genes and their relative contribution to multiple pathologies remains largely unknown.

The study from Meechan et al. 2003 performed a comprehensive analysis of the 22q11.2 genes, they found that most genes were expressed in the developing and adult mouse brain, however, the study lacks temporal and spatial resolution (Maynard et al. 2003). On the other hand, our study allows to address when and in which cell lineages cells the gene present in the 1.5Mb deletion of the 22q11.2 mutation are expressed. Our study identified genes with higher expression during period of neuronal progenitors proliferation which appears to be in accordance with previous report (D. W. Meechan et al. 2006). Amongst them , the loss of *Ranbp1* has recently been studied in a mouse model which revealed a decrease of the cortical layer II/III due to alteration in the proportion of neuronal progenitors (Paronett et al. 2015). Interestingly, our study demonstrated consistent findings, indeed *RANBP1* was found to be mostly expressed when neuronal progenitors are proliferating therefore suggesting similar function in vitro and in vivo. In vitro mouse model of 22q11.2DS also reveals that *Cdc45* mRNA expression happen to follow the one of *Ranbp1*, however *cdc45* appears to exhibit an even higher expression than *Ranbp1* during cortical neurogenesis. Therefore, a loss of *Cdc45* might be responsible to a greater loss of progenitor cells than in mouse model of *Ranbp1-/-*. Interestingly, we also identified potential genes involved in neuronal maturation such as *SEPT5*. This gene has a role in neurotransmitters release and vesicular trafficking, as well as being a substrate of PARKIN. While knockout model of *Septin5* did not reveal strong phenotypic alteration of the synaptic signalling, its overexpression in dopaminergic neurons was observed to be toxic for the cells thus leading to cell death (Son et al. 2005; Tsang et al. 2008). In

addition, *Sept5* deficiency in mouse reveals behavioural deficit in social interaction but also increases of the prepulse inhibition therefore implying a potential underlying synaptic alteration that remain unknown. (Harper et al. 2012; Suzuki et al. 2009). Surprisingly, we identified novel genes that were not observed to be expressed by previous study such as *GP1BB*. Indeed, this gene is known for its role in platelet, however, because it increases over the course of the differentiation our data suggested that it might have a role in neuron maturation. While it was recently suggested that mechanisms responsible of granules exocytosis are conserved between different cell types (Goubau et al. 2013), it was noteworthy that the *SEPT5-GP1BB* locus can be transcribed due to an imperfect polyA signal in *SEPT5*. Although the resulting *SEPT5-GP1BB* transcript is candidate for nonsense-mediated mRNA decay, it might explain why we detect *GP1BB* in neurons and the reason why it follows similar profile than *SEPT5*.

While previous analysis from Maynard et *al*. in 2003 attempted to investigate the tissue specific expression of the 22q11.2 genes, their study 1) did not reveal specific candidates, 2) they used adult tissue 3) microdissected tissues contain different neuronal and non-neuronal population therefore is not specific. While the dopaminergic population is altered in both schizophrenia and Parkinson's disease, our study reveals enrichment of several genes in dopaminergic neurons. Therefore, this data suggests that the neuronal population in which the gene is studied should be taken into consideration.

In addition, to discover that several of these genes exhibit a specific temporal profile, our study also emphasized that neurons derived stem cells can mimic some aspects of the development in vivo.

The major part of this thesis then focused at the same time on the phenotypic and transcriptomic characteristic of *ZDHHC8* in cortical excitatory neurons development.

The fourth chapter is the first to report the generation of a hESCs line heterozygous for *ZDHHC8* using the CRIPSR/Cas9 technique. While most study on *ZDHHC8* used either brain primary culture from mouse model or cellular model (HEK cells), it is the first time that *ZDHHC8* is studied in the context of neuronal development in vitro. Despite the kinetics of differentiation appeared to be unaltered in *ZDHHC8+/-* when compared to control, the differential expression identified that several genes are altered in *ZDHHC8+/-*

.

While several studies reported that individual's carrier of 22q11.2DS and or affected with schizophrenia exhibited neuronal migration defect, a study from Mukai et *al.*, 2005 demonstrated that in vivo, ZDHHC8 was not essential for radial migration as neurons were able to reach the cortical plate in mice *Zdhhc8+/-* and *Zdhhc8-/-* (Mukai et al. 2015). Conversely, our study reveals that in vitro, *ZDHHC8+/-* neurons progenitors appear to migrate less and slower, therefore we suggest that although the ability of neurons to reach the cortical plate is unaltered their ability to populate the appropriate cortical layer might be altered. Furthermore, the axonal connexion to other cortical or brain region might also be impaired in these neurons.

Calcium activity is crucial for neurons as it allows the fusion and release of neurotransmitters from the presynaptic neurons but it is also involved in mechanisms such as synaptic plasticity. Mouse model of 22q11.2DS were shown to display an increase in the amplitude of calcium activity, while our data shows similar effect on the amplitude in *ZDHHC8+/-* we also observed an overall increase in the calcium activity resulting to an increase in the number of events that had not been reported in the past. It would be interesting to examine if this observation is due to an increase in neuronal receptors population or proportion or else due to an excessive release of glutamate which therefore can result to an hyperexcitability of the neurons. Hyperexcitability has been associated with pathology such as Alzheimer disease in which an excessive release of glutamate become toxic for the neurons due to an over excitation of extrasynaptic glutamate receptors (Hardingham and Bading 2010). It would therefore be interested to examine the proportion of synaptic versus extrasynaptic receptors. Furthermore, it would also be interested to investigate the population of metabotropic receptors such as CACNA1C or else potassium or sodium channel that could also be altered and therefore responsible of the underlying phenotype. Due to the function of ZDHHC8 as a palmitoyl transferase and the lack of knowledges about the substrates of this protein. It would be interested to perform proteomic analysis in order to determine which proteins are palmitoylated by ZDHHC8.

It was also interested to note that our preliminary result using *ZDHHC8+/-* derived neurons also identified an alteration of the dendritic morphology in late progenitors/young neurons. Overall, the total length was shorter and neurons appears to have less intersections. These results are in accordance with the previous work from Mukai et al.2008 which identified that these neurons appear to have a less complex dendritic arborization (Mukai et al. 2008)

Lastly, we investigated the transcriptome of neuronal progenitors heterozygous for *ZDHHC8*. The analysis reveals that pathways related to axon guidance and calcium signalling were altered in *ZDHHC8* mutant progenitors which therefore strengthen our findings in chapter 4. In addition, these results on axonal guidance complements studies performed in human reporting a disruption of the white matter in patient with 22q11.2DS which might be due to axon guidance alteration (Kikinis et al. 2012; Radoeva et al. 2012). Interestingly, *ZDHHC8* mutation appears to alter several pathways and genes related to neurons Although our comparison between *ZDHHC8+/-* and 22q11.2 iPSCs derived NPCs reveal that only a small proportion of genes overlap between the two lines, the study of *ZDHHC8* alone provide us with convincing information on its involvement for neurons development. Amongst the several genes associated with neuronal development, it was noteworthy that three genes from the WNT signalling pathway were upregulated while the two genes coding for the WNT receptors FZB were downregulated. Interestingly, *Wnt8b* overexpression was observed to promote hypothalamic markers. Additionally, *Wnt7b* overexpression was instead showed to impairs neuronal differentiation in neuronal progenitors and therefore forebrain development in mouse, interestingly, *Wnt7b* overexpression was also associated with a decrease in the expression of *Tbr2* and *Tbr1* without affecting *pax6* (Papachristou et al. 2014). *Wnt2b* overexpression was shown to inhibit differentiation therefore induces growth of tissue in retinal explants (Papachristou et al. 2014). While it would be interested to examine whether this gene affect early patterning of neurons development in our cellular models, the study would also would also benefit to investigate early neuronal patterning in vivo using the mice models for *Zdhhc8+/-* and *Zdhhc8-/-*(Mukai et al. 2004). Additionally, transcriptomic analysis identified that the *DRD2* and *DRD4* was upregulated in *ZDHHC8+/-* NPCs, as dopaminergic neurotransmission was observed to be disrupted in 22q11.2DS it would be interested to investigate whether we observed difference at the protein level between the control and the mutant (Boot et al. 2008). *ZDHHC8+/-* has been associated with downregulation of other genes coding synaptic receptors such as GRIA2 and CHRM3 or DRD4. Thus, it would be interesting to investigate whether this downregulation lead to a decrease expression of specific neuronal receptors at the protein levels.

Therefore, this thesis in addition to provide valuable information regarding the expression of the 22q11.2 genes, demonstrates by the study of *ZDHHC8* that a cellular model can be a valuable tool to unravel the function of genes and therefore can be used to generate

cellular model that would enable to decipher the function of other genes of the 22q11.2 mutation.

To summarize, our study identified that several genes of the 22q11.2DS have a specific expression profile during neuronal differentiation. In addition, some of these genes appeared to be preferentially expressed in dopaminergic neurons. The study of *ZDHHC8* heterozygous mutation in hESCs derived cortical projection neurons addressed that the kinetics of neuronal differentiation was similar to control. However, the motility/migration of the cells lacking *ZDHHC8* was abnormal compared to control. Furthermore, the calcium signalling activity of the neurons was also found to be altered by the lack of *ZDHHC8*. Lastly, transcriptomic analysis demonstrated that the role of *ZDHHC8* appeared to be associated with the development of neurons and its physiology. Finally, although only few genes appeared to overlap with a hiPSCs derived from 22q11.2 patients, our study strongly suggest the importance of *ZDHHC8* for neuronal development.

Limitations and future directions

Limitations

Although my RT-PCR analysis (Chapter 3) on 22q11.2DS genes offer potentially valuable insight on their temporal profile, the study remains preliminary and requires repeat with independent sets of samples. I had similar issues regarding the differential expression between *ZDHHC8*+/- and control neurons. Therefore, future experiments should consider having more samples to solve this issue.

Genome editing using CRISPR/Cas technique successfully allowed the generation of several cell lines heterozygous for *ZDHHC8*. Despite confirmation of heterozygosity by sequencing, we were unable to verify a change of protein expression. Despite being used in previous studies to evaluate the ZDHHC8 protein in human cells, I observed multiple unspecific bands in western blot and therefore were unable to evaluate the protein expression of ZDHHC8.

My preliminary phenotypic analysis of ZDHHC8 KO cells revealed an increase in cortical neural progenitor proliferation, accompanied by a decrease in the number of CTIP2 positive deep layer neurons. However, further investigation will be necessary to assess whether this increase in progenitor proliferation leads to a subsequent alteration in the

number of neurons expressing cortical layer-specific markers, such as CUX1, TBR1, TBR2.

The transcriptomic analysis of the 22q11.2 iPSCs revealed the presence of a potential CNV on chromosome 17. Therefore, we did not carry on with gene enrichment analysis as well as KEGG pathways enrichment. My observation points to the importance of performing SNP array on all PSC lines to detect spontaneous mutation that may accumulate.

Future Experiments

As already mentioned in chapter 3, in addition to the temporal expression performed using control cells, we aimed to investigate the temporal profile of the 22q11.2 genes using iPSCs from individual carrier of a 22q11.2 mutation.

Although we have identified some deficits using heterozygous *ZDHHC8* cells, a ZDHHC8-null mutant model would provide a better model to decipher the functional role of ZDHHC8 in neurons. Towards this goal, we have constructed a lentiviral vector expressing ZDHHC8 gRNAs. Future work is needed to produce the virus in HEK cells, which can then be used to transduce either the *ZDHHC8+/-* or wildtype hESCs. In addition, the temporal expression analysis identified that *ZDHHC8* is preferentially expressed in dopaminergic neurons, therefore future experiments will investigate the function of *ZDHHC8* in this neuronal population.

My calcium activity assay suggests that heterozygous neurons for *ZDHHC8* exhibit more spontaneous calcium events but also appear to mature faster than the control neurons. Future experiments should aim to investigate whether blocking synaptic receptors with specific antagonist alter spontaneous calcium activity differently in the *ZDHHC8+/-* compared to the control neurons. The drugs could be used for such studies include 2R-amino-5-phosphonovaleric acid (AP5), a selective NMDA antagonist and 6-cyano-7-nitroquinoxaline-2,3-dione (CNQX), a competitive AMPA antagonist. In addition, the administration of these drugs during calcium recording could determine whether mutant cells are maturing in a similar fashion to the controls. Other drugs targeting GABAergic receptors could also be tested such as bicuculine or picrotoxin which are a GABAa antagonist.

To further investigate whether the synaptic activity and electrical activity of neurons heterozygous for ZDHHC8 is altered we thought to use MEA. Indeed, our institute has the expertise and the equipment necessary for such experiment. MEA allows to study the network activity in group of neurons. We previously observed an increase calcium spontaneous activity in *ZDHHC8* KO therefore we are interesting to determine if it also results in an increase of the electrical activity but also if it affects the overall network activity.

Finally, a rescue experiment in which we reintroduce ZDHHC8 back into our *ZDHHC8+/-* line would be interested to determine whether we can reverse the phenotype due to heterozygous loss of *ZDHHC8*. In addition, due to the availability of 22q11.2 iPSCs, it would also be interested to perform similar experiment in which we would reintroduction the ZDHHC8 in 22q11.2 iPSCs. Therefore, it would enable us to determine whether the phenotype we would observe in 22q11.2 derived neurons can be rescue by ZDHHC8.

7. References

Abu-Khalil, A et al. 2004. “Wnt Genes Define Distinct Boundaries in the Developing Human Brain: Implications for Human Forebrain Patterning.” *The Journal of comparative neurology* 474(2): 276–88. http://www.ncbi.nlm.nih.gov/pubmed/15164427.

Ahlgren, Sara, Peter Vogt, and Marianne Bronner-Fraser. 2003. “Excess FoxG1 Causes Overgrowth of the Neural Tube.” *Journal of neurobiology* 57(3): 337–49. http://www.ncbi.nlm.nih.gov/pubmed/14608667.

Alifragis, Pavlos, Anastasia Liapi, and John G Parnavelas. 2004. “Lhx6 Regulates the Migration of Cortical Interneurons from the Ventral Telencephalon but Does Not Specify Their GABA Phenotype.” *The Journal of neuroscience : the official journal of the Society for Neuroscience* 24(24): 5643–48. http://www.jneurosci.org/cgi/doi/10.1523/JNEUROSCI.1245-04.2004.

Alvarez-Medina, Roberto et al. 2008. “Wnt Canonical Pathway Restricts Graded Shh/Gli Patterning Activity through the Regulation of Gli3 Expression.” *Development (Cambridge, England)* 135(2): 237–47. http://dev.biologists.org/cgi/doi/10.1242/dev.012054.

Amir, Hadar et al. 2017. “Spontaneous Single-Copy Loss of TP53 in Human Embryonic Stem Cells Markedly Increases Cell Proliferation and Survival.” *Stem cells (Dayton, Ohio)* 35(4): 872–85. http://www.ncbi.nlm.nih.gov/pubmed/27888558.

Angkustsiri, Kathleen et al. 2014. “Social Impairments in Chromosome 22q11.2 Deletion Syndrome (22q11.2DS): Autism Spectrum Disorder or a Different Endophenotype?” *Journal of autism and developmental disorders* 44(4): 739–46. http://www.ncbi.nlm.nih.gov/pubmed/24045981.

Arber, Charles et al. 2015. “Activin A Directs Striatal Projection Neuron Differentiation of Human Pluripotent Stem Cells.” *Development (Cambridge, England)* 142(7): 1375–86. http://dev.biologists.org/cgi/doi/10.1242/dev.117093.

Arenas, Ernest, Mark Denham, and J. Carlos Villaescusa. 2015. “How to Make a Midbrain Dopaminergic Neuron.” *Development (Cambridge, England)* 142(11): 1918–36. http://dev.biologists.org/cgi/doi/10.1242/dev.097394.

Asada, Akiko et al. 2010. “Neuronal Expression of Two Isoforms of Mouse Septin 5.” *Journal of neuroscience research* 88(6): 1309–16. http://www.ncbi.nlm.nih.gov/pubmed/19937814.

Aubry, Laetitia et al. 2008. “Striatal Progenitors Derived from Human ES Cells Mature into DARPP32 Neurons in Vitro and in Quinolinic Acid-Lesioned Rats.” *Proceedings of the National Academy of Sciences of the United States of America* 105(43): 16707–12.

http://www.pubmedcentral.nih.gov/articlerender.fcgi?artid=2575484&tool=pmcentrez&rendertype=abstract.

Azim, Eiman, Denis Jabaudon, Ryann M Fame, and Jeffrey D Macklis. 2009. "SOX6 Controls Dorsal Progenitor Identity and Interneuron Diversity during Neocortical Development." *Nature neuroscience* 12(10): 1238–47. http://www.nature.com/doifinder/10.1038/nn.2387.

Backman, Mattias et al. 2005. "Effects of Canonical Wnt Signaling on Dorso-Ventral Specification of the Mouse Telencephalon." *Developmental biology* 279(1): 155–68. http://www.ncbi.nlm.nih.gov/pubmed/15708565.

Bagri, Anil et al. 2002. "Slit Proteins Prevent Midline Crossing and Determine the Dorsoventral Position of Major Axonal Pathways in the Mammalian Forebrain." *Neuron* 33(2): 233–48. http://www.ncbi.nlm.nih.gov/pubmed/11804571.

Bai, Baoling et al. 2016. "Abnormal Epigenetic Regulation of the Gene Expression Levels of Wnt2b and Wnt7b: Implications for Neural Tube Defects." *Molecular medicine reports* 13(1): 99–106. http://www.ncbi.nlm.nih.gov/pubmed/26548512.

Bassett, Anne S. et al. 2003. "The Schizophrenia Phenotype in 22q11 Deletion Syndrome." *The American journal of psychiatry* 160(9): 1580–86. http://psychiatryonline.org/doi/abs/10.1176/appi.ajp.160.9.1580.

Bassett, Anne S et *al*. 2017. "Rare Genome-Wide Copy Number Variation and Expression of Schizophrenia in 22q11.2 Deletion Syndrome." *American Journal of Psychiatry* 174(11): 1054–63. http://ajp.psychiatryonline.org/doi/10.1176/appi.ajp.2017.16121417.

Bassett, Anne S., and E W Chow. 1999. "22q11 Deletion Syndrome: A Genetic Subtype of Schizophrenia." *Biological psychiatry* 46(7): 882–91. http://www.ncbi.nlm.nih.gov/pubmed/10509171.

Batista-Brito, Renata et al. 2009. "The Cell-Intrinsic Requirement of Sox6 for Cortical Interneuron Development." *Neuron* 63(4): 466–81. http://www.ncbi.nlm.nih.gov/pubmed/19709629.

Beites, C L, H Xie, R Bowser, and W S Trimble. 1999. "The Septin CDCrel-1 Binds Syntaxin and Inhibits Exocytosis." *Nature neuroscience* 2(5): 434–39. http://dx.doi.org/10.1038/8100.

Bellone, C., C. Lüscher, and M. Mameli. 2008. "Mechanisms of Synaptic Depression Triggered by Metabotropic Glutamate Receptors." *Cellular and molecular life sciences : CMLS* 65(18): 2913–23. http://www.ncbi.nlm.nih.gov/pubmed/18712277.

Benarroch, Eduardo E. 2010. "Neuronal Voltage-Gated Calcium Channels: Brief Overview of

Their Function and Clinical Implications in Neurology." *Neurology* 74(16): 1310–15. https://www.scopus.com/inward/record.uri?eid=2-s2.0-77951467323&partnerID=40&md5=d41394b856952e938e883fa05bb4eb47.

Bender, Hans-Ulrich et al. 2005. "Functional Consequences of PRODH Missense Mutations." *American journal of human genetics* 76(3): 409–20. http://www.ncbi.nlm.nih.gov/pubmed/15662599.

Berridge, Michael J, Peter Lipp, and Martin D Bootman. 2000. "The Versatility and Universality of Calcium Signalling." *Nature reviews. Molecular cell biology* 1(1): 11–21. http://www.ncbi.nlm.nih.gov/pubmed/11413485.

Bish, Joel P. et al. 2004. "Thalamic Reductions in Children with Chromosome 22q11.2 Deletion Syndrome." *Neuroreport* 15(9): 1413–15. http://www.ncbi.nlm.nih.gov/pubmed/16517069.

Bish, Joel P., Renee Chiodo, Victoria Mattei, and Tony J. Simon. 2007. "Domain Specific Attentional Impairments in Children with Chromosome 22q11.2 Deletion Syndrome." *Brain and cognition* 64(3): 265–73. http://www.ncbi.nlm.nih.gov/pubmed/17499412.

Bolger, Anthony M., Marc Lohse, and Bjoern Usadel. 2014. "Trimmomatic: A Flexible Trimmer for Illumina Sequence Data." *Bioinformatics (Oxford, England)* 30(15): 2114–20. http://www.ncbi.nlm.nih.gov/pubmed/24695404.

Boot, Erik et al. 2008. "Disrupted Dopaminergic Neurotransmission in 22q11 Deletion Syndrome." *Neuropsychopharmacology* 33(6): 1252–58. http://www.nature.com/doifinder/10.1038/sj.npp.1301508.

Brennand, Kristen J et al. 2011. "Modelling Schizophrenia Using Human Induced Pluripotent Stem Cells." *Nature* 473(7346): 221–25. http://dx.doi.org/10.1038/nature09915.

Brini, Marisa, Tito Calì, Denis Ottolini, and Ernesto Carafoli. 2014. "Neuronal Calcium Signaling: Function and Dysfunction." *Cellular and molecular life sciences : CMLS* 71(15): 2787–2814. http://www.ncbi.nlm.nih.gov/pubmed/24442513.

Brocki, Karin C.;, and Gunilla Bohlin. 2004. "Executive Functions in Children Aged 6 to 13: A Dimensional and Developmental Study." *Developmental neuropsychology* 26(2): 571–93. http://www.ncbi.nlm.nih.gov/pubmed/15456685.

Burk, Raymond F. et al. 2007. "Deletion of Apolipoprotein E Receptor-2 in Mice Lowers Brain Selenium and Causes Severe Neurological Dysfunction and Death When a Low-Selenium Diet Is Fed." *The Journal of neuroscience : the official journal of the Society for Neuroscience* 27(23): 6207–11. http://www.jneurosci.org/cgi/doi/10.1523/JNEUROSCI.1153-07.2007.

Carlson, C et al. 1997. “Molecular Definition of 22q11 Deletions in 151 Velo-Cardio-Facial Syndrome Patients.” *American journal of human genetics* 61(3): 620–29. http://www.ncbi.nlm.nih.gov/pubmed/9326327%5Cnhttp://www.pubmedcentral.nih.gov/articlerender.fcgi?artid=PMC1715959.

Cascella, Marco, and Maria Rosaria Muzio. 2015. “Early Onset Intellectual Disability in Chromosome 22q11.2 Deletion Syndrome.” *Revista chilena de pediatria* 86(4): 283–86. http://dx.doi.org/10.1016/j.rchipe.2015.06.019.

Castro, Ana, Nadia Rodrigues, Marco Pereira, and Claudia Goncalves. 2011. “Bilateral Polymicrogyria: Always Think in Chromosome 22q11.2 Deletion Syndromes.” *BMJ case reports* 2011: 10–12.

Catterall, William a. 2000. “Structure and Regulation of Voltage-Gated Ca2+ Channels.” *Annual review of cell and developmental biology* 16(521): 521–55. http://www.ncbi.nlm.nih.gov/pubmed/11031246.

Catts, Vibeke Sørensen, Dominique Suzanne Derminio, Chang-Gyu Hahn, and Cynthia Shannon Weickert. 2015. “Postsynaptic Density Levels of the NMDA Receptor NR1 Subunit and PSD-95 Protein in Prefrontal Cortex from People with Schizophrenia.” *NPJ schizophrenia* 1(April): 15037. http://www.nature.com/articles/npjschz201537.

Das Chakraborty, R et al. 2012. “Dysregulation of DGCR6 and DGCR6L: Psychopathological Outcomes in Chromosome 22q11.2 Deletion Syndrome.” *Translational psychiatry* 2(5): e105. http://www.ncbi.nlm.nih.gov/pubmed/22832905.

Chamberlain, Luke H, and Michael J Shipston. 2015. “The Physiology of Protein S-Acylation.” *Physiological reviews* 95(2): 341–76. http://physrev.physiology.org/content/95/2/341.

Chambers, Stuart M et al. 2009. “Highly Efficient Neural Conversion of Human ES and iPS Cells by Dual Inhibition of SMAD Signaling.” *Nature biotechnology* 27(3): 275–80.

Chaouch, Amina et al. 2014. “Mutations in the Mitochondrial Citrate Carrier SLC25A1 Are Associated with Impaired Neuromuscular Transmission.” *Journal of neuromuscular diseases* 1(1): 75–90. http://iospress.metapress.com/index/L36500736V3R4132.pdf.

Chen, Gang et al. 2008. “Semaphorin-3A Guides Radial Migration of Cortical Neurons during Development.” *Nature neuroscience* 11(1): 36–44. http://www.nature.com/doifinder/10.1038/nn2018.

Chen, Jingshan et al. 2004. “Functional Analysis of Genetic Variation in Catechol-O-Methyltransferase (COMT): Effects on mRNA, Protein, and Enzyme Activity in Postmortem Human Brain.” *American journal of human genetics* 75(5): 807–21. http://www.sciencedirect.com/science/article/pii/S0002929707637860.

Chen, Wu-Yan et al. 2004. “Case-Control Study and Transmission Disequilibrium Test Provide Consistent Evidence for Association between Schizophrenia and Genetic Variation in the 22q11 Gene ZDHHC8.” *Human molecular genetics* 13(23): 2991–95. http://www.ncbi.nlm.nih.gov/pubmed/15489219.

Chen, Xiaobing et al. 2015. “PSD-95 Family MAGUKs Are Essential for Anchoring AMPA and NMDA Receptor Complexes at the Postsynaptic Density.” *Proceedings of the National Academy of Sciences of the United States of America* 112(50): E6983-92. http://www.pnas.org/lookup/doi/10.1073/pnas.1517045112.

Chenn, Anjen. 2008. “Wnt/beta-Catenin Signaling in Cerebral Cortical Development.” *Organogenesis* 4(2): 76–80. http://www.ncbi.nlm.nih.gov/pubmed/19279718%5Cnhttp://www.pubmedcentral.nih.gov/articlerender.fcgi?artid=PMC2634251.

Cheour, M et al. 1997. “The First Neurophysiological Evidence for Cognitive Brain Dysfunctions in Children with CATCH.” *Neuroreport* 8(7): 1785–87. http://www.ncbi.nlm.nih.gov/entrez/query.fcgi?cmd=Retrieve&db=PubMed&dopt=Citation&list_uids=9189933%5Cnhttp://graphics.tx.ovid.com.turing.library.northwestern.edu/ovftpdfs/FPDDNCDCBHEAHH00/fs025/ovft/live/gv015/00001756/00001756-199705060-00043.pdf.

Chieffo, C et al. 1997. “Isolation and Characterization of a Gene from the DiGeorge Chromosomal Region Homologous to the Mouse Tbx1 Gene.” *Genomics* 43(3): 267–77.

Choi, P. et al. 2003. “SEPT5_v2 Is a Parkin-Binding Protein.” *Brain research. Molecular brain research* 117(2): 179–89. http://www.ncbi.nlm.nih.gov/pubmed/14559152.

Chow, Eva W C et al. 2011. “Association of Schizophrenia in 22q11.2 Deletion Syndrome and Gray Matter Volumetric Deficits in the Superior Temporal Gyrus.” *The American journal of psychiatry* 168(5): 522–29.

Chung, Chee Yeun et al. 2013. “Identification and Rescue of α-Synuclein Toxicity in Parkinson Patient-Derived Neurons.” *Science (New York, N.Y.)* 342(6161): 983–87. http://www.sciencemag.org/cgi/doi/10.1126/science.1245296.

Cohen, Susan M., and J. Victor Nadler. 1997. “Proline-Induced Potentiation of Glutamate Transmission.” *Brain research* 761(2): 271–82. http://www.ncbi.nlm.nih.gov/pubmed/9252026.

Colnaghi, Rita, Gillian Carpenter, Marcel Volker, and Mark O’Driscoll. 2011. “The Consequences of Structural Genomic Alterations in Humans: Genomic Disorders, Genomic Instability and Cancer.” *Seminars in cell & developmental biology* 22(8): 875–

85. http://dx.doi.org/10.1016/j.semcdb.2011.07.010.

Conrad, Marcus et al. 2004. “Essential Role for Mitochondrial Thioredoxin Reductase in Hematopoiesis, Heart Development, and Heart Function.” *Molecular and cellular biology* 24(21): 9414–23. http://mcbasm.academyofeating.com/content/24/21/9414.short.

Corbetta, Maurizio, and Gordon L. Shulman. 2002. “Control of Goal-Directed and Stimulus-Driven Attention in the Brain.” *Nature reviews. Neuroscience* 3(3): 201–15. http://www.nature.com/doifinder/10.1038/nrn755.

Coyle, Joseph T. 2004. “The GABA-Glutamate Connection in Schizophrenia: Which Is the Proximate Cause?” *Biochemical Pharmacology* 68(8): 1507–14.

Craddock, N, M J Owen, and M C O’Donovan. 2006. “The Catechol-O-Methyl Transferase (COMT) Gene as a Candidate for Psychiatric Phenotypes: Evidence and Lessons.” *Molecular psychiatry* 11(5): 446–58. http://www.nature.com/doifinder/10.1038/sj.mp.4001808.

De Decker, H P, and J B Lawrenson. 2001. “The 22q11.2 Deletion: From Diversity to a Single Gene Theory.” *Genetics in medicine : official journal of the American College of Medical Genetics* 3(1): 2–5. http://www.ncbi.nlm.nih.gov/pubmed/11339372.

Delli Carri, Alessia et al. 2013. “Developmentally Coordinated Extrinsic Signals Drive Human Pluripotent Stem Cell Differentiation toward Authentic DARPP-32+ Medium-Sized Spiny Neurons.” *Development (Cambridge, England)* 140(2): 301–12. http://dev.biologists.org/cgi/doi/10.1242/dev.084608.

Demily, C. et al. 2015. “[Neurocognitive and Psychiatric Management of the 22q11.2 Deletion Syndrome].” *L’Encephale* 41(3): 266–73. http://dx.doi.org/10.1016/j.encep.2014.10.005.

Demily, Caroline et al. 2007. “ZDHHC8 Single Nucleotide Polymorphism rs175174 Is Not Associated with Psychiatric Features of the 22q11 Deletion Syndrome or Schizophrenia.” *Psychiatric genetics* 17(5): 311–12. http://content.wkhealth.com/linkback/openurl?sid=WKPTLP:landingpage&an=00041444-200710000-00010.

Derynck, Rik, and Ying E Zhang. 2003. “Smad-Dependent and Smad-Independent Pathways in TGF-Beta Family Signalling.” *Nature* 425(6958): 577–84. http://www.ncbi.nlm.nih.gov/pubmed/14534577.

Devaraju, P et al. 2017. “Haploinsufficiency of the 22q11.2 Microdeletion Gene Mrpl40 Disrupts Short-Term Synaptic Plasticity and Working Memory through Dysregulation of Mitochondrial Calcium.” *Molecular psychiatry* 22(9): 1313–26. http://www.nature.com/doifinder/10.1038/mp.2016.75.

Devaraju, Prakash, and Stanislav S. Zakharenko. 2017. “Mitochondria in Complex Psychiatric Disorders: Lessons from Mouse Models of 22q11.2 Deletion Syndrome: Hemizygous Deletion of Several Mitochondrial Genes in the 22q11.2 Genomic Region Can Lead to Symptoms Associated with Neuropsychiatric Disease.” *BioEssays : news and reviews in molecular, cellular and developmental biology* 39(2): 1600177. http://doi.wiley.com/10.1002/bies.201600177.

Digilio, Mc, B Marino, R Capolino, and B Dallapiccola. 2005. “Clinical Manifestations of Deletion 22q11.2 Syndrome (DiGeorge/Velo-Cardio-Facial Syndrome).” *Images in paediatric cardiology* 7(2): 23–34. http://www.ncbi.nlm.nih.gov/pubmed/22368650%5Cnhttp://www.pubmedcentral.nih.gov/articlerender.fcgi?artid=PMC3232571.

Dobin, Alexander et al. 2013. “STAR: Ultrafast Universal RNA-Seq Aligner.” *Bioinformatics (Oxford, England)* 29(1): 15–21. http://www.ncbi.nlm.nih.gov/pubmed/23104886.

Le Dréau, Gwenvael, and Elisa Martí. 2012. “Dorsal-Ventral Patterning of the Neural Tube: A Tale of Three Signals.” *Developmental neurobiology* 72(12): 1471–81. http://www.ncbi.nlm.nih.gov/pubmed/22821665.

Driscoll, D a et al. 1993. “Prevalence of 22q11 Microdeletions in DiGeorge and Velocardiofacial Syndromes: Implications for Genetic Counselling and Prenatal Diagnosis.” *Journal of medical genetics* 30(10): 813–17.

Dufournet, B. et al. 2017. “Parkinson’s Disease Associated with 22q11.2 Deletion: Clinical Characteristics and Response to Treatment.” *Revue neurologique* 173(6): 406–10. http://dx.doi.org/10.1016/j.neurol.2017.03.021.

Earls, Laurie R et al. 2010. “Dysregulation of Presynaptic Calcium and Synaptic Plasticity in a Mouse Model of 22q11 Deletion Syndrome.” *J. Neurosci.* 30(47): 15843–55. http://www.pubmedcentral.nih.gov/articlerender.fcgi?artid=3073555%5C&tool=pmcentrez%5C&rendertype=abstract%5Cnhttp://www.pubmedcentral.nih.gov/articlerender.fcgi?artid=3073555$%5C$%7B&%7Dtool=pmcentrez$%5C$%7B&%7Drendertype=abstract.

Ebersole, Brittany et al. 2015. “Effect of C-Terminal S-Palmitoylation on D2 Dopamine Receptor Trafficking and Stability.” *PloS one* 10(11): e0140661. http://dx.plos.org/10.1371/journal.pone.0140661.

Edelmann, L, R Pandita, and B Morrow. 1999. “Low-Copy Repeats Mediate the Common 3-Mb Deletion in Patients with Velo-Cardio-Facial Syndrome.” *American Journal of Human Genetics* 64: 1076–86.

Edelmann, Lisa et al. 2001. “Two Functional Copies of the DGCR6 Gene Are Present on

Human Chromosome 22q11 due to a Duplication of an Ancestral Locus." *Genome research* 11(2): 208–17. http://www.ncbi.nlm.nih.gov/pubmed/11157784.

Edvardson, Simon et al. 2013. "Agenesis of Corpus Callosum and Optic Nerve Hypoplasia due to Mutations in SLC25A1 Encoding the Mitochondrial Citrate Transporter." *Journal of medical genetics* 50: 240–45. http://www.ncbi.nlm.nih.gov/pubmed/23393310.

El-Husseini, A E et al. 2000. "PSD-95 Involvement in Maturation of Excitatory Synapses." *Science (New York, N.Y.)* 290(5495): 1364–68. http://www.ncbi.nlm.nih.gov/pubmed/11082065.

El-Husseini, Alaa E. et al. 2000. "Dual Palmitoylation of PSD-95 Mediates Its Vesiculotubular Sorting, Postsynaptic Targeting, and Ion Channel Clustering." *The Journal of cell biology* 148(1): 159–72. http://www.ncbi.nlm.nih.gov/pubmed/10629226.

El-Husseini, Alaa el-Din, and David S Bredt. 2002. "Protein Palmitoylation: A Regulator of Neuronal Development and Function." *Nature reviews. Neuroscience* 3(10): 791–802.

Ellegood, J et al. 2014. "Neuroanatomical Phenotypes in a Mouse Model of the 22q11.2 Microdeletion." *Molecular Psychiatry* 19(April 2013): 99–107. http://www.pubmedcentral.nih.gov/articlerender.fcgi?artid=3872255&tool=pmcentrez&rendertype=abstract.

Ensenauer, Regina E et al. 2003. "Microduplication 22q11.2, an Emerging Syndrome: Clinical, Cytogenetic, and Molecular Analysis of Thirteen Patients." *American journal of human genetics* 73(5): 1027–40. http://www.mendeley.com/c/6678083321/p/122340771/ensenauer-2003-microduplication-22q11--2--an-emerging-syndrome--clinical--cytogenetic--and-molecular-analysis-of-thirteen-patients/.

Erlander, Mark G. et al. 1991. "Two Genes Encode Distinct Glutamate Decarboxylases." *Neuron* 7(1): 91–100. http://linkinghub.elsevier.com/retrieve/pii/089662739190077D.

Esk, Christopher, Chih-Ying Chen, Ludger Johannes, and Frances M. Brodsky. 2010. "The Clathrin Heavy Chain Isoform CHC22 Functions in a Novel Endosomal Sorting Step." *The Journal of cell biology* 188(1): 131–44. http://www.ncbi.nlm.nih.gov/pubmed/20065094.

Espuny-Camacho, Ira et al. 2013. "Pyramidal Neurons Derived from Human Pluripotent Stem Cells Integrate Efficiently into Mouse Brain Circuits in Vivo." *Neuron* 77(3): 440–56. http://www.ncbi.nlm.nih.gov/pubmed/23395372.

Fenalti, Gustavo et al. 2007. "GABA Production by Glutamic Acid Decarboxylase Is Regulated by a Dynamic Catalytic Loop." *Nature structural & molecular biology* 14(4): 280–86.

http://www.nature.com/doifinder/10.1038/nsmb1228.

Fénelon, Karine et al. 2011. “Deficiency of Dgcr8, a Gene Disrupted by the 22q11.2 Microdeletion, Results in Altered Short-Term Plasticity in the Prefrontal Cortex.” *Proceedings of the National Academy of Sciences of the United States of America* 108(11): 4447–52. http://www.pnas.org/cgi/doi/10.1073/pnas.1101219108.

Fink, E E et al. 2016. “Mitochondrial Thioredoxin Reductase Regulates Major Cytotoxicity Pathways of Proteasome Inhibitors in Multiple Myeloma Cells.” *Leukemia* 30(1): 104–11. http://dx.doi.org/10.1038/leu.2015.190.

Fischer, T., J. Guimera, W. Wurst, and N. Prakash. 2007. “Distinct but Redundant Expression of the Frizzled Wnt Receptor Genes at Signaling Centers of the Developing Mouse Brain.” *Neuroscience* 147(3): 693–711. http://www.ncbi.nlm.nih.gov/pubmed/17582687.

Fotaki, Vassiliki et al. 2010. “Loss of Wnt8b Has No Overt Effect on Hippocampus Development but Leads to Altered Wnt Gene Expression Levels in Dorsomedial Telencephalon.” *Developmental dynamics : an official publication of the American Association of Anatomists* 239(1): 284–96. http://www.ncbi.nlm.nih.gov/pubmed/19890917.

Funato, Hiromasa et al. 2010. “Loss of Goosecoid-like and DiGeorge Syndrome Critical Region 14 in Interpeduncular Nucleus Results in Altered Regulation of Rapid Eye Movement Sleep.” *Proceedings of the National Academy of Sciences of the United States of America* 107(42): 18155–60. http://www.pnas.org/cgi/doi/10.1073/pnas.1012764107.

Funatsu, Nobuo, Takayoshi Inoue, and Shun Nakamura. 2004. “Gene Expression Analysis of the Late Embryonic Mouse Cerebral Cortex Using DNA Microarray: Identification of Several Region- and Layer-Specific Genes.” *Cerebral cortex (New York, N.Y. : 1991)* 14(9): 1031–44. http://www.ncbi.nlm.nih.gov/pubmed/15142957.

Gaiano, Nicholas, Jhumku D Kohtz, Daniel H Turnbull, and Gord Fishell. 1999. “A Method for Rapid Gain-of-Function Studies in the Mouse Embryonic Nervous System.” *Nature Neuroscience* 2(9): 812–19. http://www.ncbi.nlm.nih.gov/pubmed/10461220.

Gambini, Orsola. 2016. “Psychiatric Disorders Associated with 22q11.2 Deletion Syndrome.” *Mental illness* 8(1): 6590. http://www.ncbi.nlm.nih.gov/pubmed/27403278.

Gao, Wenming et al. 2015. “DGCR6 at the Proximal Part of the DiGeorge Critical Region Is Involved in Conotruncal Heart Defects.” *Human genome variation* 2(November 2014): 15004. http://dx.doi.org/10.1038/hgv.2015.4.

Garg, V et al. 2001. “Tbx1, a DiGeorge Syndrome Candidate Gene, Is Regulated by Sonic Hedgehog during Pharyngeal Arch Development.” *Developmental biology* 235(1): 62–73.

http://www.sciencedirect.com/science/article/pii/S0012160601902830.

Gauthier-Campbell, Catherine, David S Bredt, Timothy H Murphy, and Alaa El-Din El-Husseini. 2004. “Regulation of Dendritic Branching and Filopodia Formation in Hippocampal Neurons by Specific Acylated Protein Motifs.” *Molecular biology of the cell* 15(5): 2205–17. http://www.ncbi.nlm.nih.gov/pubmed/14978216.

Gerdes, Marsha et al. 1999. “Cognitive and Behavior Profile of Preschool Children with Chromosome 22q11.2 Deletion.” *American journal of medical genetics* 85(2): 127–33. http://www.ncbi.nlm.nih.gov/pubmed/10406665.

Ghosh, T.K., J.D. Brook, and A. Wilsdon. 2017. “T-Box Genes in Human Development and Disease.” In *T-Box Genes in Development and Disease*, Elsevier Inc., 383–415. http://linkinghub.elsevier.com/retrieve/pii/S0070215316301739.

Gilman, Sarah R et al. 2012. “Diverse Types of Genetic Variation Converge on Functional Gene Networks Involved in Schizophrenia.” *Nature neuroscience* 15(12): 1723–28. http://www.pubmedcentral.nih.gov/articlerender.fcgi?artid=3689007&tool=pmcentrez&rendertype=abstract.

Glaser, Beate et al. 2006. “Analysis of ProDH, COMT and ZDHHC8 Risk Variants Does Not Support Individual or Interactive Effects on Schizophrenia Susceptibility.” *Schizophrenia research* 87(1–3): 21–27. http://www.ncbi.nlm.nih.gov/pubmed/16860541.

Globa, Andrea K, and Shernaz X Bamji. 2017. “Protein Palmitoylation in the Development and Plasticity of Neuronal Connections.” *Current opinion in neurobiology* 45(Table 1): 210–20. http://linkinghub.elsevier.com/retrieve/pii/S0959438816302379.

Gogos, J. A. et al. 1998. “Catechol-O-Methyltransferase-Deficient Mice Exhibit Sexually Dimorphic Changes in Catecholamine Levels and Behavior.” *Proceedings of the National Academy of Sciences of the United States of America* 95(17): 9991–96. http://www.pnas.org/cgi/doi/10.1073/pnas.95.17.9991.

Gogos, J A et al. 1999. “The Gene Encoding Proline Dehydrogenase Modulates Sensorimotor Gating in Mice.” *Nature genetics* 21(4): 434–39. http://www.nature.com.libproxy.ucl.ac.uk/ng/journal/v21/n4/full/ng0499_434.html.

Gomperts, Stephen N. 1996. “Clustering Membrane Proteins: It’s All Coming Together with the PSD-95/SAP90 Protein Family.” *Cell* 84(5): 659–62. http://www.ncbi.nlm.nih.gov/pubmed/8625403.

Goodship, J, I Cross, J LiLing, and C Wren. 1998. “A Population Study of Chromosome 22q11 Deletions in Infancy.” *Archives of disease in childhood* 79(4): 348–51.

Goubau, Christophe et al. 2013. “Regulated Granule Trafficking in Platelets and Neurons: A Common Molecular Machinery.” *European journal of paediatric neurology : EJPN : official journal of the European Paediatric Neurology Society* 17(2): 117–25. http://dx.doi.org/10.1016/j.ejpn.2012.08.005.

Grienberger, Christine, and Arthur Konnerth. 2012. “Imaging Calcium in Neurons.” *Neuron* 73(5): 862–85. http://dx.doi.org/10.1016/j.neuron.2012.02.011.

Guerrier, Sabrice et al. 2009. “The F-BAR Domain of srGAP2 Induces Membrane Protrusions Required for Neuronal Migration and Morphogenesis.” *Cell* 138(5): 990–1004. http://www.ncbi.nlm.nih.gov/pubmed/19737524.

Gunhaga, Lena et al. 2003. “Specification of Dorsal Telencephalic Character by Sequential Wnt and FGF Signaling.” *Nature neuroscience* 6(7): 701–7. http://www.ncbi.nlm.nih.gov/pubmed/12766771.

Günzel, Dorothee, and Alan S L Yu. 2013. 93 Physiological reviews *Claudins and the Modulation of Tight Junction Permeability.* http://physrev.physiology.org/content/93/2/525.

Habas, Raymond, Igor B. Dawid, and Xi He. 2003. “Coactivation of Rac and Rho by Wnt/Frizzled Signaling Is Required for Vertebrate Gastrulation.” *Genes & development* 17(2): 295–309. http://www.ncbi.nlm.nih.gov/pubmed/12533515.

Hansen, David V, Jan H Lui, Philip R L Parker, and Arnold R Kriegstein. 2010. “Neurogenic Radial Glia in the Outer Subventricular Zone of Human Neocortex.” *Nature* 464(7288): 554–61. http://dx.doi.org/10.1038/nature08845.

Hao, Zhonglin et al. 2004. “Expression Analysis of the Human Testis-Specific Serine/threonine Kinase (TSSK) Homologues. A TSSK Member Is Present in the Equatorial Segment of Human Sperm.” *Molecular human reproduction* 10(6): 433–44. http://www.ncbi.nlm.nih.gov/pubmed/15044604.

Hardingham, Giles E., and Hilmar Bading. 2010. “Synaptic versus Extrasynaptic NMDA Receptor Signalling: Implications for Neurodegenerative Disorders.” *Nature reviews. Neuroscience* 11(10): 682–96. http://www.nature.com/doifinder/10.1038/nrn2911.

Harper, Kathryn M. et al. 2012. “Alterations of Social Interaction through Genetic and Environmental Manipulation of the 22q11.2 Gene Sept5 in the Mouse Brain.” *Human molecular genetics* 21(15): 3489–99. http://www.ncbi.nlm.nih.gov/pubmed/22589251.

Harrison-Uy, Susan J., and Samuel J. Pleasure. 2012. “Wnt Signaling and Forebrain Development.” *Cold Spring Harbor perspectives in biology* 4(7): a008094. http://www.ncbi.nlm.nih.gov/pubmed/22621768.

Harrison, Paul J, and Elizabeth M Tunbridge. 2008. “Catechol-O-Methyltransferase (COMT): A Gene Contributing to Sex Differences in Brain Function, and to Sexual Dimorphism in the Predisposition to Psychiatric Disorders.” *Neuropsychopharmacology : official publication of the American College of Neuropsychopharmacology* 33(13): 3037–45.

Hatakeyama, Jun et al. 2004. “Hes Genes Regulate Size, Shape and Histogenesis of the Nervous System by Control of the Timing of Neural Stem Cell Differentiation.” *Development (Cambridge, England)* 131(22): 5539–50. http://www.ncbi.nlm.nih.gov/pubmed/15496443.

He, Meng, Khadar M. Abdi, and Vann Bennett. 2014. “Ankyrin-G Palmitoylation and βII-Spectrin Binding to Phosphoinositide Lipids Drive Lateral Membrane Assembly.” *The Journal of cell biology* 206(2): 273–88. http://www.ncbi.nlm.nih.gov/pubmed/25049274.

Hemmati-Brivanlou, Ali, Olivia G. Kelly, and Douglas A. Melton. 1994. “Follistatin, an Antagonist of Activin, Is Expressed in the Spemann Organizer and Displays Direct Neuralizing Activity.” *Cell* 77(2): 283–95. http://www.ncbi.nlm.nih.gov/pubmed/8168135.

Hicks, David G et al. 2010. “The Expression of TRMT2A, a Novel Cell Cycle Regulated Protein, Identifies a Subset of Breast Cancer Patients with HER2 over-Expression That Are at an Increased Risk of Recurrence.” *BMC cancer* 10: 108. http://www.pubmedcentral.nih.gov/articlerender.fcgi?artid=2859753&tool=pmcentrez&rendertype=abstract.

Hierck, Beerend P et al. 2004. “A Chicken Model for DGCR6 as a Modifier Gene in the DiGeorge Critical Region.” *Pediatric research* 56(3): 440–48. http://www.ncbi.nlm.nih.gov/pubmed/15333760.

Hille, Bertil. 1994. “Modulation of Ion-Channel Function by G-Protein-Coupled Receptors.” *Trends in neurosciences* 17(12): 531–36. http://www.ncbi.nlm.nih.gov/pubmed/7532338.

Holland, Sabrina M., and Gareth M. Thomas. 2017. “Roles of Palmitoylation in Axon Growth, Degeneration and Regeneration.” *Journal of neuroscience research* 95(8): 1528–39. http://doi.wiley.com/10.1002/jnr.24003.

Horii, Takuro et al. 2013. “Generation of an ICF Syndrome Model by Efficient Genome Editing of Human Induced Pluripotent Stem Cells Using the CRISPR System.” *International journal of molecular sciences* 14(10): 19774–81. http://www.ncbi.nlm.nih.gov/pubmed/24084724.

Hsu, Ruby et al. 2007. “Nogo Receptor 1 (RTN4R) as a Candidate Gene for Schizophrenia: Analysis Using Human and Mouse Genetic Approaches.” *PloS one* 2(11): e1234.

Huang, Hui-Chuan, and Peter S Klein. 2004. “The Frizzled Family: Receptors for Multiple

Signal Transduction Pathways." *Genome biology* 5(7): 234. http://www.ncbi.nlm.nih.gov/pubmed/15239825%5Cnhttp://www.pubmedcentral.nih.gov/articlerender.fcgi?artid=PMC463283.

Huang, Kun et al. 2009. "Neuronal Palmitoyl Acyl Transferases Exhibit Distinct Substrate Specificity." *FASEB journal : official publication of the Federation of American Societies for Experimental Biology* 23(8): 2605–15. http://www.fasebj.org/cgi/doi/10.1096/fj.08-127399.

Huang, Kun, and Alaa El-Husseini. 2005. "Modulation of Neuronal Protein Trafficking and Function by Palmitoylation." *Current opinion in neurobiology* 15(5): 527–35. http://www.ncbi.nlm.nih.gov/pubmed/16125924.

Huber, Andrea B, Alex L Kolodkin, David D Ginty, and Jean-François Cloutier. 2003. "Signaling at the Growth Cone: Ligand-Receptor Complexes and the Control of Axon Growth and Guidance." *Annual review of neuroscience* 26: 509–63. http://www.ncbi.nlm.nih.gov/pubmed/12677003.

Hunt, David et al. 2002. "Nogo Receptor mRNA Expression in Intact and Regenerating CNS Neurons." *Molecular and cellular neurosciences* 20(4): 537–52. http://linkinghub.elsevier.com/retrieve/pii/S104474310291153X.

Hurley, J H, A L Cahill, K P Currie, and A P Fox. 2000. "The Role of Dynamic Palmitoylation in Ca2+ Channel Inactivation." *Proceedings of the National Academy of Sciences of the United States of America* 97(16): 9293–98. http://www.pnas.org/cgi/doi/10.1073/pnas.160589697%5Cnpapers3://publication/doi/10.1073/pnas.160589697.

Hussein, Samer M et al. 2011. "Copy Number Variation and Selection during Reprogramming to Pluripotency." *Nature* 471(7336): 58–62. http://dx.doi.org/10.1038/nature09871.

Hynes, Mary et al. 1997. "Control of Cell Pattern in the Neural Tube by the Zinc Finger Transcription Factor and Oncogene Gli-1." *Neuron* 19(1): 15–26. http://www.ncbi.nlm.nih.gov/pubmed/9247260.

Iacovelli, L. et al. 2002. "Native Group-III Metabotropic Glutamate Receptors Are Coupled to the Mitogen-Activated Protein Kinase/phosphatidylinositol-3-Kinase Pathways." *Journal of neurochemistry* 82(2): 216–23. http://www.ncbi.nlm.nih.gov/pubmed/12124422.

Infantino, Vittoria et al. 2014. "A Key Role of the Mitochondrial Citrate Carrier (SLC25A1) in TNFα- and IFNγ-Triggered Inflammation." *Biochimica et biophysica acta* 1839(11): 1217–25. http://www.ncbi.nlm.nih.gov/pubmed/25072865.

Irie, M et al. 1997. "Binding of Neuroligins to PSD-95." *Science (New York, N.Y.)* 277(5331):

1511–15. http://www.sciencemag.org/cgi/doi/10.1126/science.277.5331.1511.

Irudayanathan, Flaviyan Jerome, John P. Trasatti, Pankaj Karande, and Shikha Nangia. 2016. "Molecular Architecture of the Blood Brain Barrier Tight Junction Proteins--A Synergistic Computational and In Vitro Approach." *The journal of physical chemistry. B* 120(1): 77–88. http://www.ncbi.nlm.nih.gov/pubmed/26654362.

Jacquet, Hélène et al. 2002. "PRODH Mutations and Hyperprolinemia in a Subset of Schizophrenic Patients." *Human molecular genetics* 11(19): 2243–49. http://www.ncbi.nlm.nih.gov/pubmed/12217952.

Jaeger, I. et al. 2011. "Temporally Controlled Modulation of FGF/ERK Signaling Directs Midbrain Dopaminergic Neural Progenitor Fate in Mouse and Human Pluripotent Stem Cells." *Development* 138(20): 4363–74. http://dev.biologists.org/cgi/doi/10.1242/dev.066746.

Jalbrzikowski, Maria et al. 2013. "Structural Abnormalities in Cortical Volume, Thickness, and Surface Area in 22q11.2 Microdeletion Syndrome: Relationship with Psychotic Symptoms." *NeuroImage. Clinical* 3: 405–15. http://dx.doi.org/10.1016/j.nicl.2013.09.013.

James, Daylon, Ariel J Levine, Daniel Besser, and Ali Hemmati-Brivanlou. 2005. "TGFbeta/activin/nodal Signaling Is Necessary for the Maintenance of Pluripotency in Human Embryonic Stem Cells." *Development (Cambridge, England)* 132(6): 1273–82. http://dev.biologists.org/cgi/doi/10.1242/dev.01706.

Jang, Min Jee, and Yoonkey Nam. 2015. "NeuroCa: Integrated Framework for Systematic Analysis of Spatiotemporal Neuronal Activity Patterns from Large-Scale Optical Recording Data." *Neurophotonics* 2(3): 35003. http://neurophotonics.spiedigitallibrary.org/article.aspx?articleid=2422279.

Johnson, R L, R D Riddle, E Laufer, and C Tabin. 1994. "Sonic Hedgehog: A Key Mediator of Anterior-Posterior Patterning of the Limb and Dorso-Ventral Patterning of Axial Embryonic Structures." *Biochemical Society transactions* 22(3): 569–74. http://www.ncbi.nlm.nih.gov/pubmed/7821639.

Johnston-Wilson, N L et al. 2000. "Disease-Specific Alterations in Frontal Cortex Brain Proteins in Schizophrenia, Bipolar Disorder, and Major Depressive Disorder. The Stanley Neuropathology Consortium." *Molecular psychiatry* 5(2): 142–49. http://www.ncbi.nlm.nih.gov/pubmed/10822341.

Jonas, Rachel K., Caroline a. Montojo, and Carrie E. Bearden. 2014. "The 22q11.2 Deletion Syndrome as a Window into Complex Neuropsychiatric Disorders over the Lifespan."

Biological psychiatry 75(5): 351–60. http://dx.doi.org/10.1016/j.biopsych.2013.07.019.

Josephson, Anna et al. 2002. "Nogo-Receptor Gene Activity: Cellular Localization and Developmental Regulation of mRNA in Mice and Humans." *The Journal of comparative neurology* 453(3): 292–304.

Jossin, Yves, and Jonathan A Cooper. 2011. "Reelin, Rap1 and N-Cadherin Orient the Migration of Multipolar Neurons in the Developing Neocortex." *Nature neuroscience* 14(6): 697–703. http://www.nature.com/doifinder/10.1038/nn.2816.

Kabadi, Ami M., David G. Ousterout, Isaac B. Hilton, and Charles a. Gersbach. 2014. "Multiplex CRISPR/Cas9-Based Genome Engineering from a Single Lentiviral Vector." *Nucleic acids research* 42(19): e147. http://nar.oxfordjournals.org/content/early/2014/08/13/nar.gku749.abstract.

Kajiwara, K et al. 1996. "Cloning of SEZ-12 Encoding Seizure-Related and Membrane-Bound Adhesion Protein." *Biochemical and biophysical research communications* 222(1): 144–48. http://www.ncbi.nlm.nih.gov/pubmed/8630060.

Kao, Amy et al. 2004. "Increased Prevalence of Unprovoked Seizures in Patients with a 22q11.2 Deletion." *American journal of medical genetics. Part A* 129A(January): 29–34.

Karayiorgou, M et al. 1995. "Schizophrenia Susceptibility Associated with Interstitial Deletions of Chromosome 22q11." *Proceedings of the National Academy of Sciences of the United States of America* 92(17): 7612–16.

Karayiorgou, Maria, and Joseph A. Gogos. 2004. "The Molecular Genetics of the 22q11-Associated Schizophrenia." *Brain research. Molecular brain research* 132(2): 95–104. http://www.ncbi.nlm.nih.gov/pubmed/15582150.

Karayiorgou, Maria, Tony J Simon, and Joseph a Gogos. 2010. "22q11.2 Microdeletions: Linking DNA Structural Variation to Brain Dysfunction and Schizophrenia." *Nature reviews. Neuroscience* 11(6): 402–16. http://dx.doi.org/10.1038/nrn2841.

Kausalya, P Jaya, Dominic C Y Phua, and Walter Hunziker. 2004. "Association of ARVCF with Zonula Occludens (ZO)-1 and ZO-2: Binding to PDZ-Domain Proteins and Cell-Cell Adhesion Regulate Plasma Membrane and Nuclear Localization of ARVCF." *Molecular biology of the cell* 15(12): 5503–15. http://www.ncbi.nlm.nih.gov/pubmed/15509653.

Kelsom, Corey, and Wange Lu. 2013. "Development and Specification of GABAergic Cortical Interneurons." *Cell & bioscience* 3(1): 19. http://cellandbioscience.biomedcentral.com/articles/10.1186/2045-3701-3-19.

Khosravani, Houman, and Gerald W Zamponi. 2006. "Voltage-Gated Calcium Channels and

Idiopathic Generalized Epilepsies." *Physiological reviews* 86(3): 941–66. http://www.ncbi.nlm.nih.gov/pubmed/16816142.

Kiermayer, Claudia et al. 2015. "Heart-Specific Knockout of the Mitochondrial Thioredoxin Reductase (Txnrd2) Induces Metabolic and Contractile Dysfunction in the Aging Myocardium." *Journal of the American Heart Association* 4(7): 1–21. http://www.ncbi.nlm.nih.gov/pubmed/26199228.

Kikinis, Z et al. 2012. "Reduced Fractional Anisotropy and Axial Diffusivity in White Matter in 22q11.2 Deletion Syndrome: A Pilot Study." *Schizophrenia research* 141(1): 35–39. http://linkinghub.elsevier.com/retrieve/pii/S0920996412003490.

Kim, Daesik et al. 2015. "Digenome-Seq: Genome-Wide Profiling of CRISPR-Cas9 off-Target Effects in Human Cells." *Nature methods* 12(3): 237–43, 1 p following 243. http://www.nature.com/doifinder/10.1038/nmeth.3284.

Kimber, Wendy L. et al. 1999. "Deletion of 150 Kb in the Minimal DiGeorge/velocardiofacial Syndrome Critical Region in Mouse." *Human molecular genetics* 8(12): 2229–37. http://www.ncbi.nlm.nih.gov/pubmed/10545603.

Kirwan, Peter et al. 2015. "Development and Function of Human Cerebral Cortex Neural Networks from Pluripotent Stem Cells in Vitro." *Development (Cambridge, England)* 142(18): 3178–87. http://dev.biologists.org/cgi/doi/10.1242/dev.123851.

Kispert, A. 2017. "T-Box Genes in the Kidney and Urinary Tract." In *T-Box Genes in Development and Disease*, Elsevier Inc., 245–78. http://linkinghub.elsevier.com/retrieve/pii/S0070215316301399.

Knable, Michael B. et al. 1994. "Quantitative Autoradiography of Dopamine-D1 Receptors, D2 Receptors, and Dopamine Uptake Sites in Postmortem Striatal Specimens from Schizophrenic Patients." *Biological psychiatry* 36(12): 827–35. http://www.ncbi.nlm.nih.gov/pubmed/7893846.

Kobeissy, Firas H. et al. 2016. "Deciphering the Role of Emx1 in Neurogenesis: A Neuroproteomics Approach." *Frontiers in molecular neuroscience* 9(October): 98. http://www.ncbi.nlm.nih.gov/pubmed/27799894%5Cnhttp://www.pubmedcentral.nih.gov/articlerender.fcgi?artid=PMC5065984%5Cnhttp://journal.frontiersin.org/article/10.3389/fnmol.2016.00098/full.

Kollmar, R et al. 1997. "Predominance of the alpha1D Subunit in L-Type Voltage-Gated Ca2+ Channels of Hair Cells in the Chicken's Cochlea." *Proceedings of the National Academy of Sciences of the United States of America* 94(26): 14883–88. http://www.pubmedcentral.nih.gov/articlerender.fcgi?artid=25132&tool=pmcentrez&rend

ertype=abstract.

Komuro, Hitoshi, and Pasko Rakic. 1998. “Orchestration of Neuronal Migration by Activity of Ion Channels, Neurotransmitter Receptors, and Intracellular Ca2+ Fluctuations.” *Journal of neurobiology* 37(1): 110–30. http://www.ncbi.nlm.nih.gov/pubmed/9777736.

Korycka, Justyna et al. 2012. “Human DHHC Proteins: A Spotlight on the Hidden Player of Palmitoylation.” *European journal of cell biology* 91(2): 107–17. http://linkinghub.elsevier.com/retrieve/pii/S0171933511001981.

Kremer, Laura S. et al. 2016. “Bi-Allelic Truncating Mutations in TANGO2 Cause Infancy-Onset Recurrent Metabolic Crises with Encephalocardiomyopathy.” *American journal of human genetics* 98(2): 358–62. http://www.ncbi.nlm.nih.gov/pubmed/26805782.

Kriaucionis, Skirmantas et al. 2006. “Gene Expression Analysis Exposes Mitochondrial Abnormalities in a Mouse Model of Rett Syndrome.” *Molecular and cellular biology* 26(13): 5033–42. http://mcb.asm.org/cgi/doi/10.1128/MCB.01665-05.

Kriegstein, Arnold, Stephen Noctor, and Verónica Martínez-Cerdeño. 2006. “Patterns of Neural Stem and Progenitor Cell Division May Underlie Evolutionary Cortical Expansion.” *Nature reviews. Neuroscience* 7(11): 883–90. http://www.ncbi.nlm.nih.gov/sites/entrez?Db=pubmed&DbFrom=pubmed&Cmd=Link&LinkName=pubmed_pubmed&LinkReadableName=Related Articles&IdsFromResult=17033683&ordinalpos=3&itool=EntrezSystem2.PEntrez.Pubmed.Pubmed_ResultsPanel.Pubmed_RVDocSum.

Kullmann, Dimitri M, and Karri Lamsa. 2008. “Roles of Distinct Glutamate Receptors in Induction of Anti-Hebbian Long-Term Potentiation.” *The Journal of physiology* 586(6): 1481–86.

Kunishima, Shinji et al. 2013. “Bernard-Soulier Syndrome Caused by a Hemizygous GPIbβ Mutation and 22q11.2 Deletion.” *Pediatrics international : official journal of the Japan Pediatric Society* 55(4): 434–37. http://www.ncbi.nlm.nih.gov/pubmed/23566026.

Lachman, H M et al. 1996. “Human Catechol-O-Methyltransferase Pharmacogenetics: Description of a Functional Polymorphism and Its Potential Application to Neuropsychiatric Disorders.” *Pharmacogenetics* 6(3): 243–50.

Lahti, Adrienne C., Bettylou Koffel, D LaPorte, and Carol A. Tamminga. 1995. “Subanesthetic Doses of Ketamine Stimulate Psychosis in Schizophrenia.” *Neuropsychopharmacology : official publication of the American College of Neuropsychopharmacology* 13(1): 9–19. http://www.ncbi.nlm.nih.gov/pubmed/8526975.

Lako, Majlinda et al. 1998. “A Novel Mammalian Wnt Gene, WNT8B, Shows Brain-Restricted

Expression in Early Development, with Sharply Delimited Expression Boundaries in the Developing Forebrain." *Human molecular genetics* 7(5): 813–22. http://www.ncbi.nlm.nih.gov/pubmed/9536085.

Lamm, Noa et al. 2016. "Genomic Instability in Human Pluripotent Stem Cells Arises from Replicative Stress and Chromosome Condensation Defects." *Cell stem cell* 18(2): 253–61. http://www.ncbi.nlm.nih.gov/pubmed/26669899.

Lang, Undine E et al. 2007. "Molecular Mechanisms of Schizophrenia." *Cellular physiology and biochemistry : international journal of experimental cellular physiology, biochemistry, and pharmacology* 20(6): 687–702. http://www.ncbi.nlm.nih.gov/pubmed/17982252.

Laping, N. J. et al. 2002. "Inhibition of Transforming Growth Factor (TGF)-beta1-Induced Extracellular Matrix with a Novel Inhibitor of the TGF-Beta Type I Receptor Kinase Activity: SB-431542." *Molecular pharmacology* 62(1): 58–64. http://molpharm.aspetjournals.org/cgi/doi/10.1124/mol.62.1.58.

Laurent, Louise C. et al. 2011. "Dynamic Changes in the Copy Number of Pluripotency and Cell Proliferation Genes in Human ESCs and iPSCs during Reprogramming and Time in Culture." *Cell stem cell* 8(1): 106–18. http://dx.doi.org/10.1016/j.stem.2010.12.003.

Lesnick, Timothy G. et al. 2007. "A Genomic Pathway Approach to a Complex Disease: Axon Guidance and Parkinson Disease." *PLoS genetics* 3(6): e98. http://www.ncbi.nlm.nih.gov/pubmed/17571925.

Leyns, Luc et al. 1997. "Frzb-1 Is a Secreted Antagonist of Wnt Signaling Expressed in the Spemann Organizer." *Cell* 88(6): 747–56. http://www.ncbi.nlm.nih.gov/pubmed/9118218.

Li, Yahui et al. 2011. "Expression and Localization of Five Members of the Testis-Specific Serine Kinase (Tssk) Family in Mouse and Human Sperm and Testis." *Molecular human reproduction* 17(1): 42–56. http://www.ncbi.nlm.nih.gov/pubmed/20729278.

Li, Yanxin, and Jianwei Jiao. 2017. "Histone Chaperone HIRA Regulates Neural Progenitor Cell Proliferation and Neurogenesis via β-Catenin." *The Journal of cell biology* 216(7): 1975–92. http://www.ncbi.nlm.nih.gov/pubmed/28515277.

Li, You et al. 2011. "Association Study between GNB1L and Three Major Mental Disorders in Chinese Han Populations." *Psychiatry research* 187(3): 457–59. http://dx.doi.org/10.1016/j.psychres.2010.04.019.

Lin, Amy et al. 2017. "Mapping 22q11.2 Gene Dosage Effects on Brain Morphometry." *The Journal of neuroscience : the official journal of the Society for Neuroscience* 37(26): 6183–99. http://www.jneurosci.org/content/early/2017/05/23/JNEUROSCI.3759-16.2017.

Lin, John C, Wei-Hsien Ho, Austin Gurney, and Arnon Rosenthal. 2003. “The Netrin-G1 Ligand NGL-1 Promotes the Outgrowth of Thalamocortical Axons.” *Nature neuroscience* 6(12): 1270–76. http://www.ncbi.nlm.nih.gov/pubmed/14595443.

Lin, Mingyan et al. 2016. “Integrative Transcriptome Network Analysis of iPSC-Derived Neurons from Schizophrenia and Schizoaffective Disorder Patients with 22q11.2 Deletion.” *BMC systems biology* 10(1): 105. http://bmcsystbiol.biomedcentral.com/articles/10.1186/s12918-016-0366-0.

Lindsay, E a et al. 2001. “Tbx1 Haploinsufficieny in the DiGeorge Syndrome Region Causes Aortic Arch Defects in Mice.” *Nature* 410(6824): 97–101.

Lindsay, E A, and A. Baldini. 1997. “A Mouse Gene (Dgcr6) Related to the Drosophila Gonadal Gene Is Expressed in Early Embryogenesis and Is the Homolog of a Human Gene Deleted in DiGeorge Syndrome.” *Cytogenetics and cell genetics* 79(3–4): 243–47. http://www.karger.com/doi/10.1159/000134736.

Lindsay, Elizabeth A et al. 1999. “Congenital Heart Disease in Mice Deficient for the DiGeorge Syndrome Region.” *Nature* 401(6751): 379–83. http://www.ncbi.nlm.nih.gov/pubmed/10517636.

Lindsay, Elizabeth A., Emma L. Harvey, Peter J. Scambler, and Antonio Baldini. 1998. “ES2, a Gene Deleted in DiGeorge Syndrome, Encodes a Nuclear Protein and Is Expressed during Early Mouse Development, Where It Shares an Expression Domain with a Goosecoid-like Gene.” *Human molecular genetics* 7(4): 629–35. http://www.ncbi.nlm.nih.gov/pubmed/9499415.

Lisman, John E. et al. 2008. “Circuit-Based Framework for Understanding Neurotransmitter and Risk Gene Interactions in Schizophrenia.” *Trends in neurosciences* 31(5): 234–42. http://www.ncbi.nlm.nih.gov/pubmed/18395805.

Liu, Hui et al. 2002. “Genetic Variation in the 22q11 Locus and Susceptibility to Schizophrenia.” *Proceedings of the National Academy of Sciences of the United States of America* 99(26): 16859–64.

Liu, Siqiong June, and R. Suzanne Zukin. 2007. “Ca2+-Permeable AMPA Receptors in Synaptic Plasticity and Neuronal Death.” *Trends in neurosciences* 30(3): 126–34. http://www.ncbi.nlm.nih.gov/pubmed/17275103.

Love, Michael I, Wolfgang Huber, and Simon Anders. 2014. “Moderated Estimation of Fold Change and Dispersion for RNA-Seq Data with DESeq2.” *Genome biology* 15(12): 550. http://genomebiology.biomedcentral.com/articles/10.1186/s13059-014-0550-8.

Lu, Wei et al. 2009. “Subunit Composition of Synaptic AMPA Receptors Revealed by a Single-

Cell Genetic Approach." *Neuron* 62(2): 254–68. http://dx.doi.org/10.1016/j.neuron.2009.02.027.

LUBY, E. D. et al. 1962. "Model Psychoses and Schizophrenia." *The American journal of psychiatry* 119: 61–67. http://www.ncbi.nlm.nih.gov/pubmed/14467063.

Ma, Lixiang et al. 2012. "Human Embryonic Stem Cell-Derived GABA Neurons Correct Locomotion Deficits in Quinolinic Acid-Lesioned Mice." *Cell stem cell* 10(4): 455–64. http://dx.doi.org/10.1016/j.stem.2012.01.021.

Magnaghi, P et al. 1998. "HIRA, a Mammalian Homologue of Saccharomyces Cerevisiae Transcriptional Co-Repressors, Interacts with Pax3." *Nature genetics* 20(september): 74–77.

Mangos, Steve et al. 2001. "Ran Binding Protein RanBP1 in Zebrafish Embryonic Development." *Molecular reproduction and development* 59(3): 235–48. http://www.ncbi.nlm.nih.gov/pubmed/11424209.

Marchetto, Maria C N Mcn et al. 2010. "A Model for Neural Development and Treatment of Rett Syndrome Using Human Induced Pluripotent Stem Cells." *Cell* 143(4): 527–39. http://www.pubmedcentral.nih.gov/articlerender.fcgi?artid=3003590&tool=pmcentrez&rendertype=abstract%5Cnhttp://www.sciencedirect.com/science/article/pii/S0092867410011864%5Cnhttp://www.pubmedcentral.nih.gov/articlerender.fcgi?artid=3003590&tool=pmcentrez&.

Marín, Oscar, Manuel Valiente, Xuecai Ge, and Li-Huei Tsai. 2010. "Guiding Neuronal Cell Migrations." *Cold Spring Harbor perspectives in biology* 2(2): a001834. http://www.ncbi.nlm.nih.gov/pubmed/20182622.

Mariner, D J, J Wang, and a B Reynolds. 2000. "ARVCF Localizes to the Nucleus and Adherens Junction and Is Mutually Exclusive with p120(ctn) in E-Cadherin Complexes." *Journal of cell science* 113 (Pt 8: 1481–90. http://www.ncbi.nlm.nih.gov/pubmed/10725230.

Maroof, Asif M et al. 2013. "Directed Differentiation and Functional Maturation of Cortical Interneurons from Human Embryonic Stem Cells." *Cell stem cell* 12(5): 559–72. http://www.sciencedirect.com/science/article/pii/S1934590913001446.

Martin, G R. 1981. "Isolation of a Pluripotent Cell Line from Early Mouse Embryos Cultured in Medium Conditioned by Teratocarcinoma Stem Cells." *Proceedings of the National Academy of Sciences of the United States of America* 78(12): 7634–38.

Martins-Taylor, Kristen et al. 2011. "Recurrent Copy Number Variations in Human Induced Pluripotent Stem Cells." *Nature biotechnology* 29(6): 488–91.

http://www.ncbi.nlm.nih.gov/pubmed/21654665.

Matsukawa, Hiroshi et al. 2014. “Netrin-G/NGL Complexes Encode Functional Synaptic Diversification.” *The Journal of neuroscience : the official journal of the Society for Neuroscience* 34(47): 15779–92. http://www.jneurosci.org/cgi/doi/10.1523/JNEUROSCI.1141-14.2014.

Matsumoto, Mitsuyuki et al. 2003. “Catechol O-Methyltransferase (COMT) mRNA Expression in the Dorsolateral Prefrontal Cortex of Patients with Schizophrenia.” *Neuropsychopharmacology : official publication of the American College of Neuropsychopharmacology* 28(8): 1521–30. http://www.ncbi.nlm.nih.gov/pubmed/12799619.

Maynard, T. M. et al. 2008. “Mitochondrial Localization and Function of a Subset of 22q11 Deletion Syndrome Candidate Genes.” *Molecular and cellular neurosciences* 39(3): 439–51. http://dx.doi.org/10.1016/j.mcn.2008.07.027.

Maynard, T M et al. 2003. “A Comprehensive Analysis of 22q11 Gene Expression in the Developing and Adult Brain.” *Proceedings of the National Academy of Sciences of the United States of America* 100(24): 14433–38.

McDonald-McGinn, Donna M. et al. 2015. “22q11.2 Deletion Syndrome.” *Nature reviews. Disease primers* 1(November): 15071. http://www.nature.com/articles/nrdp201571.

Meechan, D. W. et al. 2006. “Gene Dosage in the Developing and Adult Brain in a Mouse Model of 22q11 Deletion Syndrome.” *Molecular and cellular neurosciences* 33(4): 412–28. http://www.ncbi.nlm.nih.gov/pubmed/17097888.

Meechan, D. W., T. M. Maynard, E. S. Tucker, and a. S. LaMantia. 2011. “Three Phases of DiGeorge/22q11 Deletion Syndrome Pathogenesis during Brain Development: Patterning, Proliferation, and Mitochondrial Functions of 22q11 Genes.” *International Journal of Developmental Neuroscience* 29(3): 283–94. http://dx.doi.org/10.1016/j.ijdevneu.2010.08.005.

Meechan, Daniel W. et al. 2015. “Modeling a Model: Mouse Genetics, 22q11.2 Deletion Syndrome, and Disorders of Cortical Circuit Development.” *Progress in neurobiology* 130: 1–28. http://linkinghub.elsevier.com/retrieve/pii/S030100821500026X.

Meechan, Daniel W, Eric S Tucker, Thomas M Maynard, and Anthony-Samuel LaMantia. 2009. “Diminished Dosage of 22q11 Genes Disrupts Neurogenesis and Cortical Development in a Mouse Model of 22q11 deletion/DiGeorge Syndrome.” *Proceedings of the National Academy of Sciences of the United States of America* 106(38): 16434–45.

Merscher, Sandra et al. 2001. “TBX1 Is Responsible for Cardiovascular Defects in Velo-

Cardio-facial/DiGeorge Syndrome." *Cell* 104(4): 619–29. http://www.ncbi.nlm.nih.gov/pubmed/11239417.

Mohamed, Salah Ali et al. 2005. "Ubiquitin Fusion Degradation 1-like Gene Dysregulation in Bicuspid Aortic Valve." *The Journal of thoracic and cardiovascular surgery* 130(6): 1531–36. http://www.ncbi.nlm.nih.gov/pubmed/16307994.

Mohrmann, Ralf et al. 2013. "Synaptotagmin Interaction with SNAP-25 Governs Vesicle Docking, Priming, and Fusion Triggering." *The Journal of neuroscience : the official journal of the Society for Neuroscience* 33(36): 14417–30. http://www.jneurosci.org/cgi/doi/10.1523/JNEUROSCI.1236-13.2013.

Molyneaux, Bradley J, Paola Arlotta, Joao R L Menezes, and Jeffrey D Macklis. 2007. "Neuronal Subtype Specification in the Cerebral Cortex." *Nature reviews. Neuroscience* 8(6): 427–37.

Moreau, Michael P et al. 2011. "Altered microRNA Expression Profiles in Postmortem Brain Samples from Individuals with Schizophrenia and Bipolar Disorder." *Biological psychiatry* 69(2): 188–93. http://linkinghub.elsevier.com/retrieve/pii/S0006322310010085.

Moutin, E. et al. 2017. "Palmitoylation of cdc42 Promotes Spine Stabilization and Rescues Spine Density Deficit in a Mouse Model of 22q11.2 Deletion Syndrome." *Cerebral cortex (New York, N.Y. : 1991)* 27(7): 3618–29. http://www.cercor.oxfordjournals.org/lookup/doi/10.1093/cercor/bhw183.

Moyer, Caitlin E, Micah a Shelton, and Robert a Sweet. 2015. "Dendritic Spine Alterations in Schizophrenia." *Neuroscience letters* 601: 46–53. http://dx.doi.org/10.1016/j.neulet.2014.11.042.

Mukai, Jun et al. 2004. "Evidence That the Gene Encoding ZDHHC8 Contributes to the Risk of Schizophrenia." *Nature genetics* 36(7): 725–31.

Mukai, Jun et al. 2008. "Palmitoylation-Dependent Neurodevelopmental Deficits in a Mouse Model of 22q11 Microdeletion." *Nature neuroscience* 11(11): 1302–10.

Mukai, Jun et al.. 2015. "Molecular Substrates of Altered Axonal Growth and Brain Connectivity in a Mouse Model of Schizophrenia." *Neuron* 86(3): 680–95. http://linkinghub.elsevier.com/retrieve/pii/S0896627315003323.

Mukhopadhyay, Mahua et al. 2001. "Dickkopf1 Is Required for Embryonic Head Induction and Limb Morphogenesis in the Mouse." *Developmental cell* 1(3): 423–34. http://www.ncbi.nlm.nih.gov/pubmed/11702953.

Muly, E Chris, Irakli Mania, Ji-Dong Guo, and Donald G Rainnie. 2007. "Group II

Metabotropic Glutamate Receptors in Anxiety Circuitry: Correspondence of Physiological Response and Subcellular Distribution." *The Journal of comparative neurology* 505(6): 682–700. http://onlinelibrary.wiley.com/doi/10.1002/cne.21301/abstract?systemMessage=Due+to+scheduled+maintenance%2C+access+to+Wiley+Online+Library+will+be+disrupted+on+Saturday%2C+5th+Mar+between+10%3A00-12%3A00+GMT%5Cnhttp://onlinelibrary.wiley.com/doi/10.1002/c.

Muzio, Luca, and Antonello Mallamaci. 2003. "Emx1, emx2 and pax6 in Specification, Regionalization and Arealization of the Cerebral Cortex." *Cerebral cortex (New York, N.Y. : 1991)* 13(6): 641–47. http://cercor.oxfordjournals.org/content/13/6/641.long.

Nadarajah, B, P Alifragis, R O L Wong, and J G Parnavelas. 2003. "Neuronal Migration in the Developing Cerebral Cortex: Observations Based on Real-Time Imaging." *Cerebral cortex (New York, N.Y. : 1991)* 13(6): 607–11. http://www.ncbi.nlm.nih.gov/pubmed/12764035.

Nadarajah, Bagirathy, and John G Parnavelas. 2002. "Modes of Neuronal Migration in the Developing Cerebral Cortex." *Nature reviews. Neuroscience* 3(6): 423–32. http://www.ncbi.nlm.nih.gov/entrez/query.fcgi?cmd=Retrieve&db=PubMed&dopt=Citation&list_uids=12042877.

Nahorski, Michael S. et al. 2015. "A Novel Disorder Reveals Clathrin Heavy Chain-22 Is Essential for Human Pain and Touch Development." *Brain : a journal of neurology* 138(Pt 8): 2147–60. http://www.ncbi.nlm.nih.gov/pubmed/26068709.

Napoli, Eleonora et al. 2015. "Mitochondrial Citrate Transporter-Dependent Metabolic Signature in the 22q11.2 Deletion Syndrome." *The Journal of biological chemistry* 290(38): 23240–53. http://www.ncbi.nlm.nih.gov/pubmed/26221035.

Ng, Julian, and Liqun Luo. 2004. "Rho GTPases Regulate Axon Growth through Convergent and Divergent Signaling Pathways." *Neuron* 44(5): 779–93. http://www.ncbi.nlm.nih.gov/pubmed/15572110.

Niarchou, Maria et al. 2014. "Psychopathology and Cognition in Children with 22q11.2 Deletion Syndrome." *The British journal of psychiatry : the journal of mental science* 204(1): 46–54. http://www.ncbi.nlm.nih.gov/pubmed/24115343.

Nicoleau, Camille et al. 2013. "Embryonic Stem Cells Neural Differentiation Qualifies the Role of Wnt/β-Catenin Signals in Human Telencephalic Specification and Regionalization." *Stem cells (Dayton, Ohio)* 31(9): 1763–74. http://www.ncbi.nlm.nih.gov/pubmed/23818270.

Nishimura, Akiyuki, and Maurine E Linder. 2013. “Identification of a Novel Prenyl and Palmitoyl Modification at the CaaX Motif of Cdc42 That Regulates RhoGDI Binding.” *Molecular and cellular biology* 33(7): 1417–29. http://www.pubmedcentral.nih.gov/articlerender.fcgi?artid=3624279&tool=pmcentrez&rendertype=abstract.

Nitta, Takehiro et al. 2003. “Size-Selective Loosening of the Blood-Brain Barrier in Claudin-5-Deficient Mice.” *The Journal of cell biology* 161(3): 653–60. http://www.ncbi.nlm.nih.gov/pubmed/12743111.

Niwa, H, T Burdon, I Chambers, and A Smith. 1998. “Self-Renewal of Pluripotent Embryonic Stem Cells Is Mediated via Activation of STAT3.” *Genes & development* 12(13): 2048–60. http://www.pubmedcentral.nih.gov/articlerender.fcgi?artid=316954&tool=pmcentrez&rendertype=abstract.

Noctor, Stephen C, Verónica Martínez-Cerdeño, Lidija Ivic, and Arnold R Kriegstein. 2004. “Cortical Neurons Arise in Symmetric and Asymmetric Division Zones and Migrate through Specific Phases.” *Nature neuroscience* 7(2): 136–44. http://www.nature.com/doifinder/10.1038/nn1172.

Noritake, Jun et al. 2009. “Mobile DHHC Palmitoylating Enzyme Mediates Activity-Sensitive Synaptic Targeting of PSD-95.” *The Journal of cell biology* 186(1): 147–60. http://www.ncbi.nlm.nih.gov/pubmed/19596852.

Nouspikel, Thierry. 2013. “Genetic Instability in Human Embryonic Stem Cells: Prospects and Caveats.” *Future oncology (London, England)* 9(6): 867–77. http://www.ncbi.nlm.nih.gov/pubmed/23718307.

Omidinia, Eskandar et al. 2014. “Polymorphism of the CLDN5 Gene and Schizophrenia in an Iranian Population.” *Iranian journal of public health* 43(1): 79–83. http://www.ncbi.nlm.nih.gov/pubmed/26060683.

Otani, Kyohei et al. 2005. “The ZDHHC8 Gene Did Not Associate with Bipolar Disorder or Schizophrenia.” *Neuroscience letters* 390(3): 166–70. http://www.ncbi.nlm.nih.gov/pubmed/16150541.

Papachristou, Panagiotis et al. 2014. “Transgenic Increase of Wnt7b in Neural Progenitor Cells Decreases Expression of T-Domain Transcription Factors and Impairs Neuronal Differentiation.” *Brain research* 1576: 27–34. http://dx.doi.org/10.1016/j.brainres.2014.06.015.

Paronett, Elizabeth M. et al. 2015. “Ranbp1, Deleted in DiGeorge/22q11.2 Deletion Syndrome,

Is a Microcephaly Gene That Selectively Disrupts Layer 2/3 Cortical Projection Neuron Generation." *Cerebral cortex (New York, N.Y. : 1991)* 25(10): 3977–93. http://www.cercor.oxfordjournals.org/cgi/doi/10.1093/cercor/bhu285.

Patel, Tapan P., Karen Man, Bonnie L. Firestein, and David F. Meaney. 2015. "Automated Quantification of Neuronal Networks and Single-Cell Calcium Dynamics Using Calcium Imaging." *Journal of neuroscience methods* 243: 26–38. http://dx.doi.org/10.1016/j.jneumeth.2015.01.020.

Pathak, Gunja K et al. 2016. "Increases in Retrograde Injury Signaling Complex-Related Transcripts in Central Axons Following Injury." *Neural plasticity* 2016: 3572506. https://www.hindawi.com/journals/np/2016/3572506/.

Paylor, Richard, and Elizabeth Lindsay. 2006. "Mouse Models of 22q11 Deletion Syndrome." *Biological psychiatry* 59(12): 1172–79. http://www.ncbi.nlm.nih.gov/pubmed/16616724.

Pedrosa, Erika et al. 2011. "Development of Patient-Specific Neurons in Schizophrenia Using Induced Pluripotent Stem Cells." *Journal of neurogenetics* 25(3): 88–103.

Petri, Rebecca et al. 2014. "miRNAs in Brain Development." *Experimental cell research* 321(1): 84–89. http://dx.doi.org/10.1016/j.yexcr.2013.09.022.

Pfuhl, Thorsten et al. 2005. "Biochemical Characterisation of the Proteins Encoded by the DiGeorge Critical Region 6 (DGCR6) Genes." *Human genetics* 117(1): 70–80. http://www.ncbi.nlm.nih.gov/pubmed/15821931.

Piccolo, Stefano, Yoshiki Sasai, Bin Lu, and Eddy M. De Robertis. 1996. "Dorsoventral Patterning in Xenopus: Inhibition of Ventral Signals by Direct Binding of Chordin to BMP-4." *Cell* 86(4): 589–98. http://www.ncbi.nlm.nih.gov/pubmed/8752213.

Pickering, Andrew M. et al. 2017. "Mitochondrial Thioredoxin Reductase 2 Is Elevated in Long-Lived Primate as Well as Rodent Species and Extends Fly Mean Lifespan." *Aging cell* 16(4): 683–92. http://www.ncbi.nlm.nih.gov/pubmed/28474396.

Pierfelice, Tarran, Lavinia Alberi, and Nicholas Gaiano. 2011. "Notch in the Vertebrate Nervous System: An Old Dog with New Tricks." *Neuron* 69(5): 840–55. http://dx.doi.org/10.1016/j.neuron.2011.02.031.

Pillai, Roshan, Jane H. Uyehara-Lock, and Frederick P. Bellinger. 2014. "Selenium and Selenoprotein Function in Brain Disorders." *IUBMB life* 66(4): 229–39. http://www.ncbi.nlm.nih.gov/pubmed/24668686.

Placzek, Marysia et al. 1991. "Control of Dorsoventral Pattern in Vertebrate Neural Development: Induction and Polarizing Properties of the Floor Plate." *Development*

(Cambridge, England). Supplement Suppl 2(Supplement 2): 105–22. papers2://publication/uuid/F57D7100-7932-40F4-B130-E3860465BCC9%5Cnpapers2://publication/uuid/52B2E417-852E-4C59-A8C8-C793FA3AB369%5Cnhttp://eutils.ncbi.nlm.nih.gov/entrez/eutils/elink.fcgi?dbfrom=pubmed&id=1842349&retmode=ref&cmd=prlinks%5Cnpapers2://pub.

Prabakaran, S et al. 2004. "Mitochondrial Dysfunction in Schizophrenia: Evidence for Compromised Brain Metabolism and Oxidative Stress." *Molecular psychiatry* 9(7): 684–97, 643.

Puelles, Luis, and John L R Rubenstein. 2003. "Forebrain Gene Expression Domains and the Evolving Prosomeric Model." *Trends in neurosciences* 26(9): 469–76. http://www.ncbi.nlm.nih.gov/pubmed/12948657.

Radoeva, Petya D et al. 2012. "Atlas-Based White Matter Analysis in Individuals with Velo-Cardio-Facial Syndrome (22q11.2 Deletion Syndrome) and Unaffected Siblings." *Behavioral and brain functions : BBF* 8(1): 38. http://behavioralandbrainfunctions.biomedcentral.com/articles/10.1186/1744-9081-8-38.

Radoeva, Petya D et al. 2014. "Association between Autism Spectrum Disorder in Individuals with Velocardiofacial (22q11.2 Deletion) Syndrome and PRODH and COMT Genotypes." *Psychiatric genetics* 24(6): 269–72. http://www.ncbi.nlm.nih.gov/pubmed/25325218.

Rallu, Murielle et al. 2002. "Dorsoventral Patterning Is Established in the Telencephalon of Mutants Lacking Both Gli3 and Hedgehog Signaling." *Development (Cambridge, England)* 129(21): 4963–74.

Raper, J A. 2000. "Semaphorins and Their Receptors in Vertebrates and Invertebrates." *Current opinion in neurobiology* 10(1): 88–94. http://www.ncbi.nlm.nih.gov/pubmed/10679438.

Reardon, Thomas R. et al. 2016. "Rabies Virus CVS-N2c(ΔG) Strain Enhances Retrograde Synaptic Transfer and Neuronal Viability." *Neuron* 89(4): 711–24. http://dx.doi.org/10.1016/j.neuron.2016.01.004.

Rees, E et al. 2014. "Evidence That Duplications of 22q11.2 Protect against Schizophrenia." *Molecular psychiatry* 19(1): 37–40. http://www.pubmedcentral.nih.gov/articlerender.fcgi?artid=3873028&tool=pmcentrez&rendertype=abstract.

Rehn, Alexandra E, and Sandra M Rees. 2005. "Investigating the Neurodevelopmental Hypothesis of Schizophrenia." *Clinical and experimental pharmacology & physiology* 32(9): 687–96. http://www.ncbi.nlm.nih.gov/pubmed/16173923.

Reif, A et al. 2006. "Neural Stem Cell Proliferation Is Decreased in Schizophrenia, but Not in

Depression." *Molecular psychiatry* 11(5): 514–22. http://www.nature.com/doifinder/10.1038/sj.mp.4001791.

Rensen, Wilhelmina M, Rosamaria Mangiacasale, Marilena Ciciarello, and Patrizia Lavia. 2008. "The GTPase Ran: Regulation of Cell Life and Potential Roles in Cell Transformation." *Frontiers in bioscience : a journal and virtual library* 13: 4097–4121. http://www.ncbi.nlm.nih.gov/pubmed/18508502.

Retnakaran, Ravi et al. 2010. "Glucose Intolerance in Pregnancy and Postpartum Risk of Metabolic Syndrome in Young Women." *The Journal of clinical endocrinology and metabolism* 95(2): 670–77. http://archneur.jamanetwork.com/article.aspx?doi=10.1001/jamaneurol.2013.3646.

Reversade, Bruno, and E. M. De Robertis. 2005. "Regulation of ADMP and BMP2/4/7 at Opposite Embryonic Poles Generates a Self-Regulating Morphogenetic Field." *Cell* 123(6): 1147–60. http://www.ncbi.nlm.nih.gov/pubmed/16360041.

Ricciardi, Sara et al. 2012. "CDKL5 Ensures Excitatory Synapse Stability by Reinforcing NGL-1-PSD95 Interaction in the Postsynaptic Compartment and Is Impaired in Patient iPSC-Derived Neurons." *Nature cell biology* 14(9): 911–23. http://dx.doi.org/10.1038/ncb2566.

Roberts, Catherine et al. 2002. "Targeted Mutagenesis of the Hira Gene Results in Gastrulation Defects and Patterning Abnormalities of Mesoendodermal Derivatives prior to Early Embryonic Lethality." *Molecular and cellular biology* 22(7): 2318–28. http://www.pubmedcentral.nih.gov/articlerender.fcgi?artid=133693&tool=pmcentrez&rendertype=abstract.

Robin, Nathaniel H. et al. 2006. "Polymicrogyria and Deletion 22q11.2 Syndrome: Window to the Etiology of a Common Cortical Malformation." *American journal of medical genetics. Part A* 140(22): 2416–25. http://doi.wiley.com/10.1002/ajmg.a.31443.

Rump, Patrick et al. 2014. "Central 22q11.2 Deletions." *American journal of medical genetics. Part A* 164A(11): 2707–23. http://doi.wiley.com/10.1002/ajmg.a.36711.

Sahara, Setsuko, and Dennis D M O'Leary. 2009. "Fgf10 Regulates Transition Period of Cortical Stem Cell Differentiation to Radial Glia Controlling Generation of Neurons and Basal Progenitors." *Neuron* 63(1): 48–62. http://linkinghub.elsevier.com/retrieve/pii/S0896627309004590.

Saint-Jore, B et al. 1998. "Goosecoid-like (Gscl), a Candidate Gene for Velocardiofacial Syndrome, Is Not Essential for Normal Mouse Development." *Human molecular genetics* 7(12): 1841–49. http://www.ncbi.nlm.nih.gov/pubmed/9811927.

Sakuma, Tetsushi et al. 2014. "Multiplex Genome Engineering in Human Cells Using All-in-

One CRISPR/Cas9 Vector System." *Scientific reports* 4: 5400. http://www.pubmedcentral.nih.gov/articlerender.fcgi?artid=4066266&tool=pmcentrez&rendertype=abstract.

Sasai, Yoshiki et al. 1994. "Xenopus Chordin: A Novel Dorsalizing Factor Activated by Organizer-Specific Homeobox Genes." *Cell* 79(5): 779–90. http://www.ncbi.nlm.nih.gov/pubmed/8001117.

Scherer, N J, L L D'Antonio, and J H Kalbfleisch. 1999. "Early Speech and Language Development in Children with Velocardiofacial Syndrome." *American journal of medical genetics* 88(6): 714–23.

Schneider, Maude et al. 2014. "Psychiatric Disorders From Childhood to Adulthood in 22q11.2 Deletion Syndrome: Results From the International Consortium on Brain and Behavior in 22q11.2 Deletion Syndrome." *The American journal of psychiatry* 171(6): 627–39. http://www.ncbi.nlm.nih.gov/pubmed/24577245.

Schreiner, Matthew J., Maria T. Lazaro, Maria Jalbrzikowski, and Carrie E. Bearden. 2013. "Converging Levels of Analysis on a Genomic Hotspot for Psychosis: Insights from 22q11.2 Deletion Syndrome." *Neuropharmacology* 68: 157–73. http://dx.doi.org/10.1016/j.neuropharm.2012.09.012.

Schulte, Gunnar, and Vítezslav Bryja. 2007. "The Frizzled Family of Unconventional G-Protein-Coupled Receptors." *Trends in pharmacological sciences* 28(10): 518–25. http://www.ncbi.nlm.nih.gov/pubmed/17884187.

Seeman, P, and S Kapur. 2000. "Schizophrenia: More Dopamine, More D2 Receptors." *Proceedings of the National Academy of Sciences of the United States of America* 97(14): 7673–75. http://www.ncbi.nlm.nih.gov/pubmed/10884398%5Cnhttp://www.pubmedcentral.nih.gov/articlerender.fcgi?artid=PMC33999.

Sessa, Alessandro et al. 2008. "Tbr2 Directs Conversion of Radial Glia into Basal Precursors and Guides Neuronal Amplification by Indirect Neurogenesis in the Developing Neocortex." *Neuron* 60(1): 56–69. http://www.ncbi.nlm.nih.gov/pubmed/18940588.

Shaikh, T H et al. 2000. "Chromosome 22-Specific Low Copy Repeats and the 22q11.2 Deletion Syndrome: Genomic Organization and Deletion Endpoint Analysis." *Human molecular genetics* 9(4): 489–501. http://www.ncbi.nlm.nih.gov/pubmed/10699172.

Shao, Charles Y. et al. 2011. "Postsynaptic Degeneration as Revealed by PSD-95 Reduction Occurs after Advanced Aβ and Tau Pathology in Transgenic Mouse Models of Alzheimer's Disease." *Acta neuropathologica* 122(3): 285–92.

http://www.ncbi.nlm.nih.gov/pubmed/21630115.

Shawlot, W, J M Deng, and R R Behringer. 1998. “Expression of the Mouse Cerberus-Related Gene, Cerr1, Suggests a Role in Anterior Neural Induction and Somitogenesis.” *Proceedings of the National Academy of Sciences of the United States of America* 95(11): 6198–6203. http://www.ncbi.nlm.nih.gov/pubmed/9600941%5Cnhttps://www.ncbi.nlm.nih.gov/pmc/articles/PMC27625/pdf/pq006198.pdf.

Sheng, Morgan. 2001. “The Postsynaptic NMDA-Receptor--PSD-95 Signaling Complex in Excitatory Synapses of the Brain.” *Journal of cell science* 114(Pt 7): 1251. http://www.ncbi.nlm.nih.gov/pubmed/11256991.

Sheng, Morgan, and Eunjoon Kim. 2011. “The Postsynaptic Organization of Synapses.” *Cold Spring Harbor perspectives in biology* 3(12): a005678. http://www.ncbi.nlm.nih.gov/pubmed/22046028.

Shifman, Sagiv et al. 2006. “A Complete Genetic Association Scan of the 22q11 Deletion Region and Functional Evidence Reveal an Association between DGCR2 and Schizophrenia.” *Human genetics* 120(2): 160–70. http://www.ncbi.nlm.nih.gov/pubmed/16783572.

Shipston, Michael J. 2011. “Ion Channel Regulation by Protein Palmitoylation.” *The Journal of biological chemistry* 286(11): 8709–16. http://www.ncbi.nlm.nih.gov/pubmed/21216969.

Simon, Tony J. et al. 2005. “Volumetric, Connective, and Morphologic Changes in the Brains of Children with Chromosome 22q11.2 Deletion Syndrome: An Integrative Study.” *NeuroImage* 25(1): 169–80. http://www.ncbi.nlm.nih.gov/pubmed/15734353.

Sinibaldi, Lorenzo et al. 2004. “Mutations of the Nogo-66 Receptor (RTN4R) Gene in Schizophrenia.” *Human mutation* 24(6): 534–35. http://www.ncbi.nlm.nih.gov/pubmed/15532024.

Sirotkin, Howard et al. 1997. “Identification of a New Human Catenin Gene Family Member (ARVCF) from the Region Deleted in Velo-Cardio-Facial Syndrome.” *Genomics* 41(1): 75–83. http://www.sciencedirect.com/science/article/pii/S0888754397946279.

Skowronek, Markus H et al. 2006. “No Association between Genetic Variants at the ASCT1 Gene and Schizophrenia or Bipolar Disorder in a German Sample.” *Psychiatric genetics* 16(6): 233–34.

Slater, Paula G et al. 2013. “Frizzled-5 Receptor Is Involved in Neuronal Polarity and Morphogenesis of Hippocampal Neurons.” *PloS one* 8(10): e78892. http://www.pubmedcentral.nih.gov/articlerender.fcgi?artid=3800132&tool=pmcentrez&re

ndertype=abstract%5Cnhttp://www.ncbi.nlm.nih.gov/pubmed/24205342%5Cnhttp://www.pubmedcentral.nih.gov/articlerender.fcgi?artid=PMC3800132.

De Smedt, Bert et al. 2008. "Cognitive Correlates of Mathematical Disabilities in Children with Velo-Cardio-Facial Syndrome." *Genetic counseling (Geneva, Switzerland)* 19(1): 71–94. http://linkinghub.elsevier.com/retrieve/pii/S002839320600340X.

Smith, A G, and M L Hooper. 1987. "Buffalo Rat Liver Cells Produce a Diffusible Activity Which Inhibits the Differentiation of Murine Embryonal Carcinoma and Embryonic Stem Cells." *Developmental biology* 121(1): 1–9. http://www.ncbi.nlm.nih.gov/pubmed/3569655.

Smith, W C, and R M Harland. 1992. "Expression Cloning of Noggin, a New Dorsalizing Factor Localized to the Spemann Organizer in Xenopus Embryos." *Cell* 70(5): 829–40. http://www.ncbi.nlm.nih.gov/pubmed/1339313.

Sobin, Christina, Karen Kiley-Brabeck, and Maria Karayiorgou. 2005. "Lower Prepulse Inhibition in Children with the 22q11 Deletion Syndrome." *The American journal of psychiatry* 162(6): 1090–99. http://www.ncbi.nlm.nih.gov/pubmed/15930057.

Soerensen, Jonna et al. 2008. "The Role of Thioredoxin Reductases in Brain Development." *PloS one* 3(3): e1813. http://www.ncbi.nlm.nih.gov/pubmed/18350150.

Soghomonian, Jean Jacques, and David L. Martin. 1998. "Two Isoforms of Glutamate Decarboxylase: Why?" *Trends in pharmacological sciences* 19(12): 500–505. http://www.ncbi.nlm.nih.gov/pubmed/9871412.

Solot, Cynthia B et al. 2001. "Communication Issues in 22q11.2 Deletion Syndrome: Children at Risk." *Genetics in medicine : official journal of the American College of Medical Genetics* 3(1): 67–71. http://www.ncbi.nlm.nih.gov/pubmed/11339383.

Son, Jin H. et al. 2005. "Neurotoxicity and Behavioral Deficits Associated with Septin 5 Accumulation in Dopaminergic Neurons." *Journal of neurochemistry* 94(4): 1040–53. http://www.ncbi.nlm.nih.gov/pubmed/16092945.

Spemann, Hans, and Hilde Mangold. 1924. "Über Induktion von Embryonalen Durch Implantation Artfremder Organisatoren."

Spiegel, Ivo et al. 2006. "Identification of Novel Cell-Adhesion Molecules in Peripheral Nerves Using a Signal-Sequence Trap." *Neuron glia biology* 2(1): 27–38. http://www.ncbi.nlm.nih.gov/pubmed/16721426.

Spitzer, Nicholas C. 2006. "Electrical Activity in Early Neuronal Development." *Nature* 444(7120): 707–12. http://www.nature.com/doifinder/10.1038/nature05300.

Stark, Kimberly L et al. 2008. “Altered Brain microRNA Biogenesis Contributes to Phenotypic Deficits in a 22q11-Deletion Mouse Model.” *Nature genetics* 40(6): 751–60.

Strehlow, Vincent et al. 2016. “Generalized Epilepsy and Myoclonic Seizures in 22q11.2 Deletion Syndrome.” *Molecular syndromology* 7(4): 239–46. http://www.ncbi.nlm.nih.gov/pubmed/27781034.

Subramanian, Megha et al. 2015. “Characterizing Autism Spectrum Disorders by Key Biochemical Pathways.” *Frontiers in neuroscience* 9(SEP): 313. http://www.ncbi.nlm.nih.gov/pubmed/26483618.

Sudo, Hitomi et al. 2012. “ZDHHC8 Knockdown Enhances Radiosensitivity and Suppresses Tumor Growth in a Mesothelioma Mouse Model.” *Cancer science* 103(2): 203–9. http://www.ncbi.nlm.nih.gov/pubmed/22017350.

Sun, Yue, Yu Tao, Jian Wang, and David Saffen. 2015. “The Schizophrenia/bipolar Disorder Candidate Gene GNB1L Is Regulated in Human Temporal Cortex by a Cis-Acting Element Located within the 3’-region.” *Neuroscience bulletin* 31(1): 43–52. http://www.ncbi.nlm.nih.gov/pubmed/24831436.

Sun, Z-Y et al. 2004. “The CLDN5 Locus May Be Involved in the Vulnerability to Schizophrenia.” *European psychiatry : the journal of the Association of European Psychiatrists* 19(6): 354–57. http://www.ncbi.nlm.nih.gov/pubmed/15363474.

Surmacz, Beata et al. 2012. “Directing Differentiation of Human Embryonic Stem Cells toward Anterior Neural Ectoderm Using Small Molecules.” *Stem cells (Dayton, Ohio)* 30(9): 1875–84. http://www.ncbi.nlm.nih.gov/pubmed/22761025.

Suzuki, Go et al. 2009. “Sept5 Deficiency Exerts Pleiotropic Influence on Affective Behaviors and Cognitive Functions in Mice.” *Human molecular genetics* 18(9): 1652–60. http://www.ncbi.nlm.nih.gov/pubmed/19240081.

Swerdlow, Neal R. et al. 2008. “Realistic Expectations of Prepulse Inhibition in Translational Models for Schizophrenia Research.” *Psychopharmacology* 199(3): 331–88. http://link.springer.com/10.1007/s00213-008-1072-4.

Swillen, Ann, and Donna McDonald-McGinn. 2015. “Developmental Trajectories in 22q11.2 Deletion.” *American journal of medical genetics. Part C, Seminars in medical genetics* 169(2): 172–81. http://www.ncbi.nlm.nih.gov/pubmed/25989227.

Tai, Derek J C et al. 2016. “Engineering Microdeletions and Microduplications by Targeting Segmental Duplications with CRISPR.” *Nature neuroscience* 19(3): 517–22. http://www.ncbi.nlm.nih.gov/pubmed/26829649%5Cnhttp://www.nature.com/doifinder/10.1038/nn.4235.

Takahashi, Hideto et al. 2012. “Selective Control of Inhibitory Synapse Development by Slitrk3-PTPδ Trans-Synaptic Interaction.” *Nature neuroscience* 15(3): 389–98, S1-2. http://dx.doi.org/10.1038/nn.3040.

Takahashi, Kazutoshi et al. 2007. “Induction of Pluripotent Stem Cells from Adult Human Fibroblasts by Defined Factors.” *Cell* 131(5): 861–72. http://www.ncbi.nlm.nih.gov/pubmed/18035408.

Takahashi, Kazutoshi, and Shinya Yamanaka. 2006. “Induction of Pluripotent Stem Cells from Mouse Embryonic and Adult Fibroblast Cultures by Defined Factors.” *Cell* 126(4): 663–76. http://www.ncbi.nlm.nih.gov/pubmed/16904174.

Takamori, Shigeo. 2006. “VGLUTs: ‘Exciting’ Times for Glutamatergic Research?” *Neuroscience Research* 55(4): 343–51.

Tapon, Nicolas, and Alan Hall. 1997. “Rho, Rac and Cdc42 GTPases Regulate the Organization of the Actin Cytoskeleton.” *Current opinion in cell biology* 9(1): 86–92. http://www.ncbi.nlm.nih.gov/pubmed/9013670.

Telezhkin, Vsevolod et al. 2016. “Forced Cell Cycle Exit and Modulation of GABAA, CREB, and GSK3β Signaling Promote Functional Maturation of Induced Pluripotent Stem Cell-Derived Neurons.” *American journal of physiology. Cell physiology* 310(7): C520-41. http://www.ncbi.nlm.nih.gov/pubmed/26718628.

Thomas, Gareth M et al. 2012. “Palmitoylation by DHHC5/8 Targets GRIP1 to Dendritic Endosomes to Regulate AMPA-R Trafficking.” *Neuron* 73(3): 482–96. http://dx.doi.org/10.1016/j.neuron.2011.11.021.

Thomas, Gareth M., Takashi Hayashi, Richard L. Huganir, and David J. Linden. 2013. “DHHC8-Dependent PICK1 Palmitoylation Is Required for Induction of Cerebellar Long-Term Synaptic Depression.” *The Journal of neuroscience : the official journal of the Society for Neuroscience* 33(39): 15401–7. http://www.jneurosci.org/cgi/doi/10.1523/JNEUROSCI.1283-13.2013.

Tsang, Christopher W. et al. 2008. “Superfluous Role of Mammalian Septins 3 and 5 in Neuronal Development and Synaptic Transmission.” *Molecular and cellular biology* 28(23): 7012–29. http://mcb.asm.org/cgi/doi/10.1128/MCB.00035-08.

Tunbridge, Elizabeth M., Tracy A. Lane, and Paul J. Harrison. 2007. “Expression of Multiple Catechol-O-Methyltransferase (COMT) mRNA Variants in Human Brain.” *American journal of medical genetics. Part B, Neuropsychiatric genetics : the official publication of the International Society of Psychiatric Genetics* 144B(6): 834–39. http://www.ncbi.nlm.nih.gov/pubmed/17477346.

Ulfig, Norbert, and Wood Yee Chan. 2004. “Expression of ARVCF in the Human Ganglionic Eminence during Fetal Development.” *Developmental neuroscience* 26(1): 38–44. http://www.ncbi.nlm.nih.gov/pubmed/15509897.

Ungar, Anne R, Gregory M Kelly, and Randall T Moon. 1995. “Wnt4 Affects Morphogenesis When Misexpressed in the Zebrafish Embryo.” *Mechanisms of development* 52(2–3): 153–64. http://www.ncbi.nlm.nih.gov/pubmed/8541205.

Vallier, Ludovic et al. 2009. “Activin/Nodal Signalling Maintains Pluripotency by Controlling Nanog Expression.” *Development (Cambridge, England)* 136(8): 1339–49. http://dev.biologists.org/cgi/doi/10.1242/dev.033951.

Vigneault, Érika et al. 2015. “Distribution of Vesicular Glutamate Transporters in the Human Brain.” *Frontiers in neuroanatomy* 9(March): 23. http://www.pubmedcentral.nih.gov/articlerender.fcgi?artid=4350397&tool=pmcentrez&rendertype=abstract.

Wakamiya, Maki et al. 1998. “Functional Analysis of Gscl in the Pathogenesis of the DiGeorge and Velocardiofacial Syndromes.” *Human molecular genetics* 7(12): 1835–40. http://www.ncbi.nlm.nih.gov/pubmed/9811926.

Wallén-Mackenzie, Asa, Hanna Wootz, and Hillevi Englund. 2010. “Genetic Inactivation of the Vesicular Glutamate Transporter 2 (VGLUT2) in the Mouse: What Have We Learnt about Functional Glutamatergic Neurotransmission?” *Upsala journal of medical sciences* 115(1): 11–20. http://www.tandfonline.com/doi/full/10.3109/03009730903572073.

Walter, Henrik et al. 2009. “Altered Reward Functions in Patients on Atypical Antipsychotic Medication in Line with the Revised Dopamine Hypothesis of Schizophrenia.” *Psychopharmacology* 206(1): 121–32. http://www.ncbi.nlm.nih.gov/pubmed/19521678.

Wang, H et al. 2006. “Transmission Disequilibrium Test Provides Evidence of Association between Promoter Polymorphisms in 22q11 Gene DGCR14 and Schizophrenia.” *Journal of neural transmission (Vienna, Austria : 1996)* 113(10): 1551–61. http://www.ncbi.nlm.nih.gov/pubmed/16432632.

Wang, J, and J L Bixby. 1999. “Receptor Tyrosine Phosphatase-Delta Is a Homophilic, Neurite-Promoting Cell Adhesion Molecular for CNS Neurons.” *Molecular and cellular neurosciences* 14(4–5): 370–84.

Wang, Shouwen et al. 1997. “Frzb, a Secreted Protein Expressed in the Spemann Organizer, Binds and Inhibits Wnt-8.” *Cell* 88(6): 757–66. http://www.ncbi.nlm.nih.gov/pubmed/9118219.

Wang, Xingxing et al. 2002. “Localization of Nogo-A and Nogo-66 Receptor Proteins at Sites

of Axon-Myelin and Synaptic Contact." *The Journal of neuroscience : the official journal of the Society for Neuroscience* 22(13): 5505–15.

Wenger, Tara L. et al. 2016. "The Role of mGluR Copy Number Variation in Genetic and Environmental Forms of Syndromic Autism Spectrum Disorder." *Scientific Reports* 6(1): 19372. http://www.nature.com/articles/srep19372.

Whitford, Kristin L, Paul Dijkhuizen, Franck Polleux, and Anirvan Ghosh. 2002. "Molecular Control of Cortical Dendrite Development." *Annual review of neuroscience* 25(1): 127–49. http://www.annualreviews.org/doi/abs/10.1146/annurev.neuro.25.112701.142932%5Cnpapers3://publication/doi/10.1146/annurev.neuro.25.112701.142932.

Wickersham, Ian R. et al. 2007. "Monosynaptic Restriction of Transsynaptic Tracing from Single, Genetically Targeted Neurons." *Neuron* 53(5): 639–47. http://www.ncbi.nlm.nih.gov/pubmed/17329205.

Willert, Karl et al. 2003. "Wnt Proteins Are Lipid-Modified and Can Act as Stem Cell Growth Factors." *Nature* 423(6938): 448–52. http://www.nature.com/doifinder/10.1038/nature01611.

Williams, H J et al. 2003. "Association between PRODH and Schizophrenia Is Not Confirmed." *Molecular psychiatry* 8(7): 644–45. http://www.nature.com/doifinder/10.1038/sj.mp.4001276.

Williams, Hywel J. et al. 2013. "Schizophrenia Two-Hit Hypothesis in Velo-Cardio Facial Syndrome." *American journal of medical genetics. Part B, Neuropsychiatric genetics : the official publication of the International Society of Psychiatric Genetics* 162B(2): 177–82. http://www.ncbi.nlm.nih.gov/pubmed/23335482.

Williams, Nigel M et al. 2008. "Strong Evidence That GNB1L Is Associated with Schizophrenia." *Human molecular genetics* 17(4): 555–66. http://www.ncbi.nlm.nih.gov/pubmed/18003636.

Williams, Nigel M. 2011. "Molecular Mechanisms in 22q11 Deletion Syndrome." *Schizophrenia bulletin* 37(5): 882–89. http://www.ncbi.nlm.nih.gov/pubmed/21860033.

Willis, Alecia, Hans Uli Bender, Gary Steel, and David Valle. 2008. "PRODH Variants and Risk for Schizophrenia." *Amino acids* 35(4): 673–79. http://www.ncbi.nlm.nih.gov/pubmed/18528746.

Wirth, Alexander et al. 2013. "Dual Lipidation of the Brain-Specific Cdc42 Isoform Regulates Its Functional Properties." *The Biochemical journal* 456(3): 311–22. http://www.ncbi.nlm.nih.gov/pubmed/24059268.

Wong, Ling M. et al. 2014. “Children with Chromosome 22q11.2 Deletion Syndrome Exhibit Impaired Spatial Working Memory.” *American journal on intellectual and developmental disabilities* 119(2): 115–32. http://www.ncbi.nlm.nih.gov/pubmed/24679349.

Wong, Rachel O. L., and Anirvan Ghosh. 2002. “Activity-Dependent Regulation of Dendritic Growth and Patterning.” *Nature reviews. Neuroscience* 3(10): 803–12. http://www.nature.com/doifinder/10.1038/nrn941.

Woo, Stephanie, and Timothy M Gomez. 2006. “Rac1 and RhoA Promote Neurite Outgrowth through Formation and Stabilization of Growth Cone Point Contacts.” *The Journal of neuroscience : the official journal of the Society for Neuroscience* 26(5): 1418–28. http://www.jneurosci.org/cgi/doi/10.1523/JNEUROSCI.4209-05.2006.

Wu, Ning et al. 2010. “A Weak Association of the CLDN5 Locus with Schizophrenia in Chinese Case-Control Samples.” *Psychiatry research* 178(1): 223. http://dx.doi.org/10.1016/j.psychres.2009.11.019%5Cnhttp://linkinghub.elsevier.com/retrieve/pii/S0165178109004351.

Xing, Jingrui et al. 2016. “Resequencing and Association Analysis of Six PSD-95-Related Genes as Possible Susceptibility Genes for Schizophrenia and Autism Spectrum Disorders.” *Scientific reports* 6(1): 27491. http://www.nature.com/articles/srep27491.

Xu, Qing, Carl P Wonders, and Stewart A Anderson. 2005. “Sonic Hedgehog Maintains the Identity of Cortical Interneuron Progenitors in the Ventral Telencephalon.” *Development (Cambridge, England)* 132(22): 4987–98. http://www.ncbi.nlm.nih.gov/pubmed/16221724.

Xu, Xiaohong et al. 2017. “Reversal of Phenotypic Abnormalities by CRISPR/Cas9-Mediated Gene Correction in Huntington Disease Patient-Derived Induced Pluripotent Stem Cells.” *Stem cell reports* 8(3): 619–33. http://dx.doi.org/10.1016/j.stemcr.2017.01.022.

Yamagishi, Chihiro et al. 2003. “Functional Attenuation of UFD1l, a 22q11.2 Deletion Syndrome Candidate Gene, Leads to Cardiac Outflow Septation Defects in Chicken Embryos.” *Pediatric research* 53(4): 546–53. http://www.ncbi.nlm.nih.gov/pubmed/12612215.

Yamaguchi, Terry P. 2001. “Heads or Tails: Wnts and Anterior-Posterior Patterning.” *Current biology : CB* 11(17): R713-24. http://www.ncbi.nlm.nih.gov/pubmed/11553348.

Yobb, Twila M et al. 2005. “Microduplication and Triplication of 22q11.2: A Highly Variable Syndrome.” *American journal of human genetics* 76(5): 865–76. http://www.mendeley.com/c/6678083971/p/122340771/yobb-2005-microduplication-and-triplication-of-22q11--2--a-highly-variable-syndrome/.

Yoshii, Akira et al. 2011. “TrkB and Protein Kinase M {zeta} Regulate Synaptic Localization of PSD-95 in Developing Cortex.” *The Journal of neuroscience : the official journal of the Society for Neuroscience* 31(33): 11894–904.

Yoshii, Akira, and Martha Constantine-Paton. 2014. “Postsynaptic Localization of PSD-95 Is Regulated by All Three Pathways Downstream of TrkB Signaling.” *Frontiers in synaptic neuroscience* 6(MAR): 6. http://www.ncbi.nlm.nih.gov/pubmed/24744726.

Yudin, Dmitry et al. 2008. “Localized Regulation of Axonal RanGTPase Controls Retrograde Injury Signaling in Peripheral Nerve.” *Neuron* 59(2): 241–52. http://www.ncbi.nlm.nih.gov/pubmed/18667152.

Yun, K, S Potter, and J L Rubenstein. 2001. “Gsh2 and Pax6 Play Complementary Roles in Dorsoventral Patterning of the Mammalian Telencephalon.” *Development (Cambridge, England)* 128(2): 193–205.

Zander, Johannes-Friedrich et al. 2010. “Synaptic and Vesicular Coexistence of VGLUT and VGAT in Selected Excitatory and Inhibitory Synapses.” *The Journal of neuroscience : the official journal of the Society for Neuroscience* 30(22): 7634–45. http://www.jneurosci.org/cgi/doi/10.1523/JNEUROSCI.0141-10.2010.

Zappone, M V et al. 2000. “Sox2 Regulatory Sequences Direct Expression of a (Beta)-Geo Transgene to Telencephalic Neural Stem Cells and Precursors of the Mouse Embryo, Revealing Regionalization of Gene Expression in CNS Stem Cells.” *Development (Cambridge, England)* 127(11): 2367–82. http://www.ncbi.nlm.nih.gov/pubmed/10804179%5Cnhttp://dev.biologists.org/content/develop/127/11/2367.full.pdf.

Zhang, Hao et al. 2010. “Some Single-Nucleotide Polymorphisms of the TSSK2 Gene May Be Associated with Human Spermatogenesis Impairment.” *Journal of andrology* 31(4): 388–92. http://doi.wiley.com/10.2164/jandrol.109.008466.

Zhang, Michael Shaofei, Alexei Arnaoutov, and Mary Dasso. 2014. “RanBP1 Governs Spindle Assembly by Defining Mitotic Ran-GTP Production.” *Developmental cell* 31(4): 393–404. http://linkinghub.elsevier.com/retrieve/pii/S1534580714006807.

Zhou, Bin, Janet A Weigel, Amit Saxena, and Paul H Weigel. 2002. “Molecular Cloning and Functional Expression of the Rat 175-kDa Hyaluronan Receptor for Endocytosis.” ed. Mark J. Solomon. *Molecular biology of the cell* 13(8): 2853–68. http://www.ncbi.nlm.nih.gov/entrez/query.fcgi?cmd=Retrieve&db=PubMed&dopt=Citation&list_uids=12181351.

Zimmerman, Lyle B., José M. De Jesús-Escobar, and Richard M. Harland. 1996. “The Spemann

Organizer Signal Noggin Binds and Inactivates Bone Morphogenetic Protein 4." *Cell* 86(4): 599–606. http://www.ncbi.nlm.nih.gov/pubmed/8752214.

Zinkstok, J. et al. 2008. "Genetic Variation in COMT and PRODH Is Associated with Brain Anatomy in Patients with Schizophrenia." *Genes, brain, and behavior* 7(1): 61–69. http://www.ncbi.nlm.nih.gov/pubmed/17504246.

Zunner, Dagmar, Christina Deschermeier, and Hans-Christian Kornau. 2010. "GABA(B) Receptor Subunit 1 Binds to Proteins Affected in 22q11 Deletion Syndrome." *Biochemical and biophysical research communications* 393(2): 185–89. http://dx.doi.org/10.1016/j.bbrc.2009.12.120.

Zwarts, Liesbeth et al. 2017. "SlgA, Encoded by the Homolog of the Human Schizophrenia-Associated Gene PRODH, Acts in Clock Neurons to Regulate Drosophila Aggression." *Disease models & mechanisms* 10(6): 705–16. http://dmm.biologists.org/lookup/doi/10.1242/dmm.027151.

Annexes

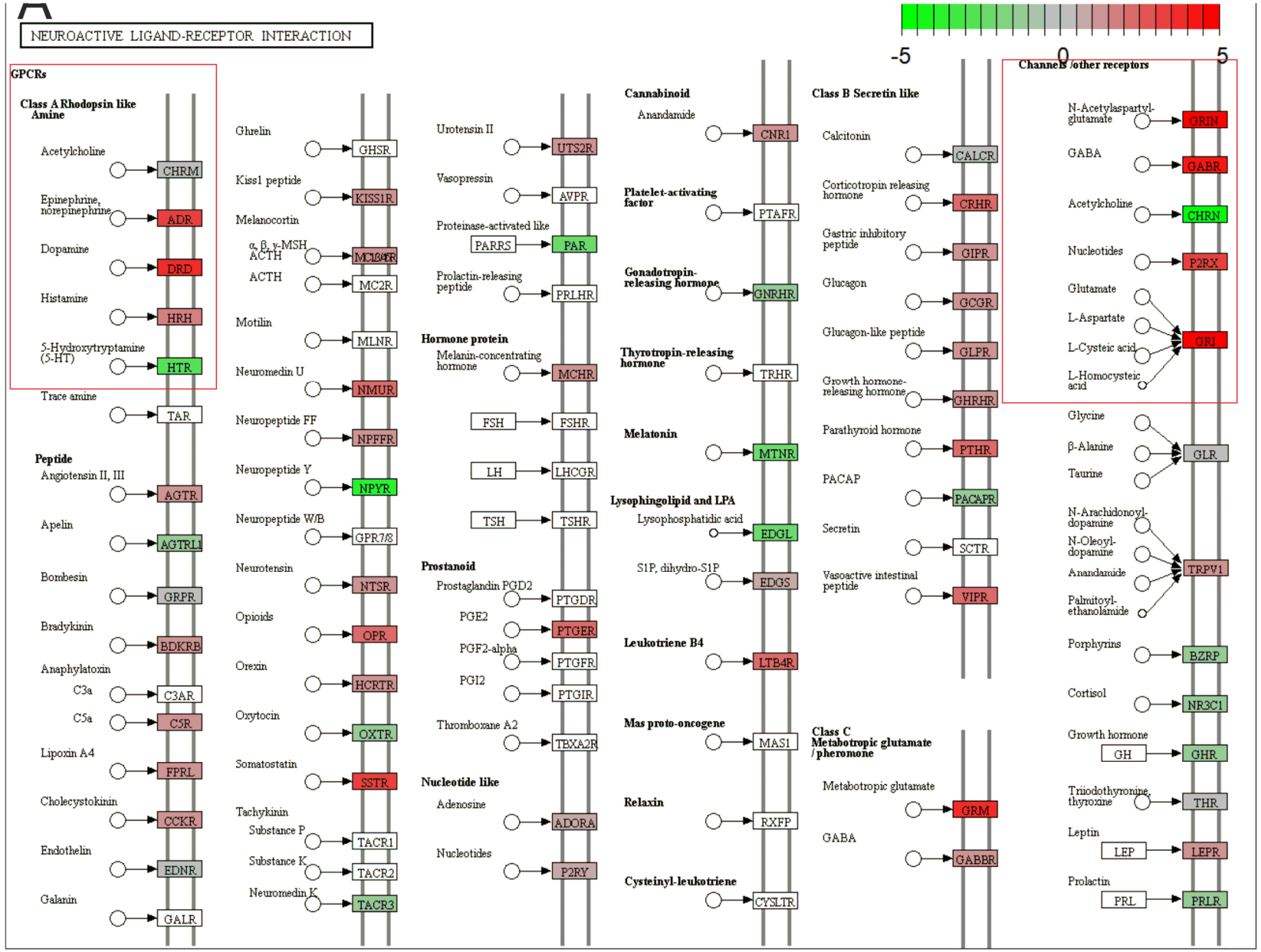

Supplementary Figure 1. Neuroactive ligand receptor interaction

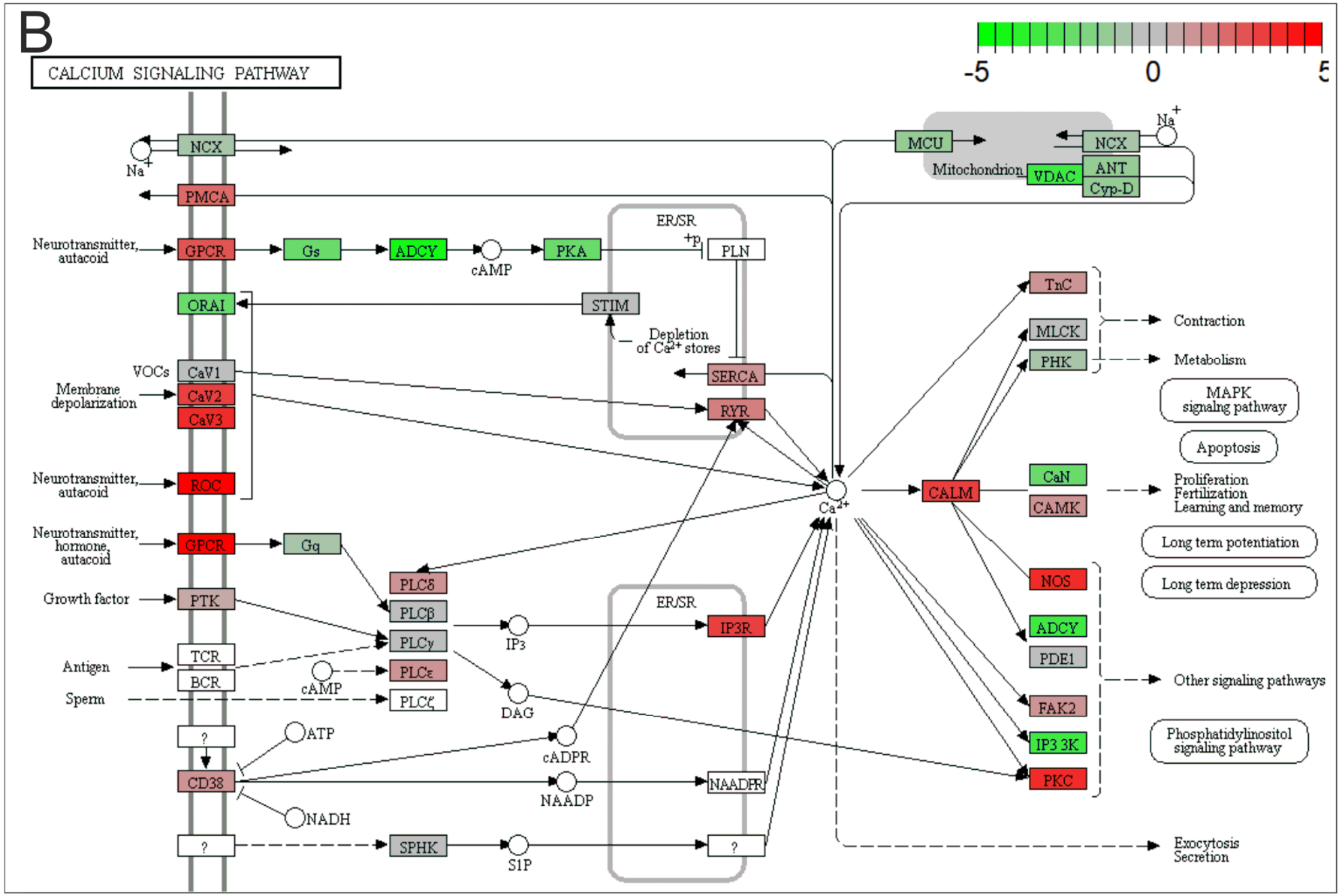

Supplementary Figure 2 Calcium Signalling pathway

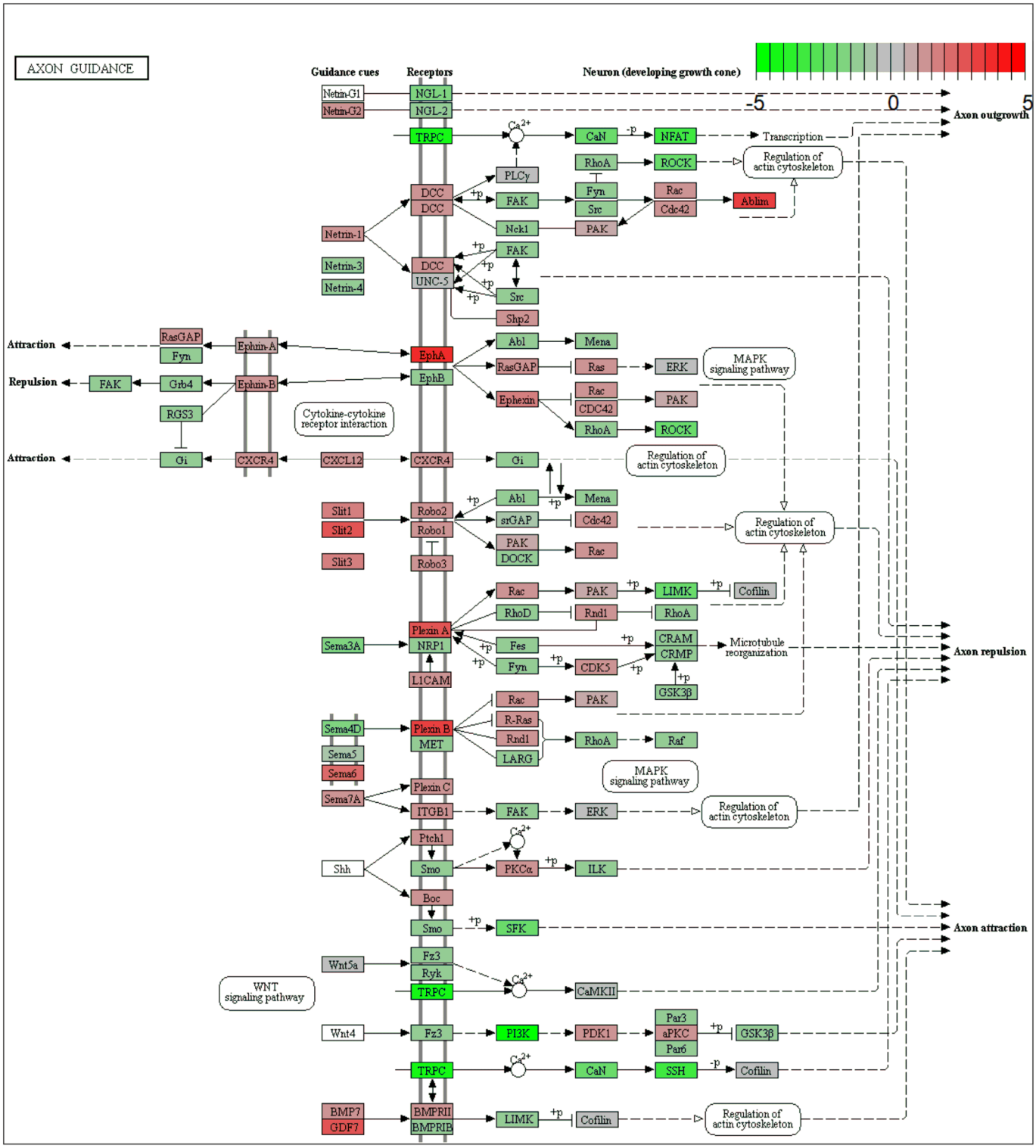

Supplementary Figure 3 Axon guidance